MEDDELELSER OM GRØNLAND

Carbon cycling in Arctic marine ecosystems: Case study Young Sound

Edited by
Søren Rysgaard & Ronnie N. Glud

BIOSCIENCE 58 • 2007

Carbon cycling in Arctic marine ecosystems: Case study Young Sound

Carbon cycling in Arctic marine ecosystems: Case study Young Sound

Edited by Søren Rysgaard & Ronnie N. Glud

Meddelelser om Grønland • Bioscience 58 • 2007

Rysgaard, S. & Glud, R. N. (Eds.), Carbon cycling in Arctic marine Ecosystems: Case study Young Sound. Meddelelser om Grønland, Bioscience Vol 58. Copenhagen, the Commission for Scientific Research in Greenland, 2007.

Publishing Editor: Kirsten Caning
Language revised by: Anna Haxen
Illustrations, layout and design: Tinna Christensen
Printed by: Nordjysk Tryk Snedsted

Front cover: Satellite image of the Young Sound study area.
Back cover: View of Clavering Ø and the Zackenberg mountains.
Photo: Mikael K. Sejr.

Scientific Editor:
Erik W. Born, Senior scientist, Greenland Institute of Natural Resources
P.O. Box 570, DK-3900 Nuuk, Greenland
Tel. +45 32880163, fax +45 32880101, e-mail: ewb@dpc.dk

About the monographic series Meddelelser om Grønland Bioscience
Meddelelser om Grønland, which is Danish for *Monographs on Greenland*, has published scientific results from all fields of research in Greenland since 1879. Bioscience invites papers that contribute significantly to studies of flora and fauna in Greenland and of ecological problems pertaining to all Greenland environments. Papers primarily concerned with other areas in the Arctic and Atlantic region may be accepted, if the work actually covers Greenland or is of direct importance to continued research in Greenland. Papers dealing with environmental problems and other borderline studies may be referred to any of the series *Geoscience*, *Bioscience* or *Man & Society* according to emphasis and editorial policy.

For more information and a list of publications, please visit the web site of the Danish Polar Center *http://www.dpc.dk*. An electronic version of this publication is available at *http://www.dpc.dk, http://www.natur.gl* and *http://www.zackenberg.dk*

All correspondence concerning this book or series *Meddelelser om Grønland* should be sent to:

Danish Polar Center
Strandgade 100H
DK-1401 Copenhagen
Denmark
Tel +45 3288 0100
Fax +45 3288 0101
Email dpc@dpc.dk
www.dpc.dk

Accepted January 2007
ISSN 0106-1054
ISBN 87-90369-90-4

Contents

Photo: Søren Rysgaard

Preface

Preface

This book synthesizes the marine research that has been conducted in Young Sound, a High Arctic fjord in Northeast Greenland since 1994. The reason our work started was the growing evidence of dramatic changes in sea ice cover as evident from satellite images (Parkinson, 1992), model predictions of a future dramatic temperature increase in the Arctic (Hansen et al., 1988; Manabe & Stouffer, 1994) and the possibility of shut-down of the thermohaline circulation (Rahmstorf, 1995). All this would have a profound influence on conditions in Greenland but would also greatly affect conditions in Northern Europe where the result might be a much colder future climate, despite the fact that it was becoming warmer globally. One of the areas where large changes in sea ice cover have occurred is off the coast of East Greenland. The area is difficult to work in due to the heavy sea ice conditions and ice drift. Here, large icebreakers are necessary platforms to perform measurements at sea. Even with icebreakers, however, it is often dif-

Preben Sørensen in our first "field laboratory" 1994.

Photo: Søren Rysgaard

ficult to obtain measurements on the inner parts of the shelf along East Greenland. The area is considered to be a sensitive indicator of climate change because of its contact with water masses from the Greenland Sea and direct meltwater flux from the Greenland Ice Sheet. Being a student, I did not have the means to hire an icebreaker. A childhood friend of mine was serving his military duty in Sirius, a Danish Military Division operating along East Greenland coast where it patrols the National Park area by dog sledge during winter. On one of his visits to Denmark, we discussed the possibility of a visit to the Daneborg area where the Patrol is located (74°N). Daneborg is situated close to a 100 km long fjord, Young Sound, which is in contact with the Greenland Ice Sheet and lies on the border between heavy sea ice conditions to the north and open-water conditions to the south, enabling supply by ship almost every year during the short summer season. Thus, this area was perfect for our studies – a relatively simple fjord in contact with the Ice Sheet and situated in a highly climate sensitive zone. In order to get up there I applied for financial support from the Carlsberg Foundation to cover the expenses for two persons and was granted the funds. We were lucky to get a lift with a military Twinotter plane and borrowed a small hut, "Sandodden" close to Daneborg during our stay in June–July 1994. We made a number of initial hydrographic, pelagic and benthic measurements in the area and had only brought a few boxes of equipment due to the limited space on the small plane. One of the surprising things was the high pelagic and benthic activity despite the sub-zero water temperatures. The oxygen penetration depth and oxygen consumption rates in the sediment were comparable with the temperate locality, Aarhus Bay, Denmark, and our initial work on designing special equipment for deeper profiling proved to be unnecessary. Staying in the area that summer, I realized that it would be the perfect place for integrated ecosystem studies and that we could greatly increase existing knowledge of High Arctic marine ecosystems by including diurnal, seasonal and interannual variability studies at a relatively low expense as compared with icebreaker activities. That summer, we also visited a former weather station "Kystens Perle" near Daneborg. It had served as weather station since World War II, but was closed down in 1975, as the new satellite system made many of these weather stations superfluous. As no one seemed to own the place, we started to clean it up and repair it and saw that it could accommodate a quite large research team.

On return to Denmark, I applied for a larger research grant from the Danish National Research Councils to start up seasonal studies in this High Arctic fjord. The project "Nutrient dynamics in northeast Greenland waters and sediment" was funded for three years and after one year of preparation 15 scientists from different scientific disciplines worked together in Young Sound during 1996–97. During this work, detailed information on the seasonal variation in pelagic and benthic compartments was obtained.

When this "baseline" study was accomplished, we applied for financial support from the Danish Natural Science Research Council for the continuation of our work in the project: "Changes in Arctic Marine Production" (CAMP). This project was focused on the coupling between climate and the marine ecosystem and involved 30 scientists. The project only received half of the money we needed to fulfil the three-year program. Despite this, we decided to continue our research and hoped we would find the financial support along the line. Over the next 3 years several applications were made and thanks to the Danish Natural Science Research Council, the Carlsberg Foundation, the Danish Environmental Protection Agency, the Commission for Scientific Research in Greenland, the Frimodt-Heineken Foundation, the Torben and Alice Frimodt Foundation, the Bodil Pedersen Foundation and the Prince Joachim and Princess Alexandra Foundation we managed to complete the project with great success.

Alongside the research activities we started to repair the station "Kystens Perle" more thoroughly. Initially, we received support from the Danish Polar Centre (DPC), the Danish National Research Institute and the Military Division Sirius. During the field campaigns, logistic members from DPC, a carpenter and scientists continued to repair and rebuild the station into laboratories, kitchen, bedrooms etc. whenever they had time in between experiments. There was a fantastic team spirit and everyone worked for weeks without much sleep.

The CAMP project showed the need for tighter coupling between research in the marine and terrestrial environments. In 1995 a long-term monitoring network called "Zackenberg Ecological Research Operations" (ZERO) was established further inside the fjord to monitor atmospheric, hydrologic and

Photo: Søren Rysgaard

The research team in front of the former weather station "Kystens Perle" in June 1999.

terrestrial parameters. For example, the suspended matter discharge from the Zackenberg River was quantified and it became evident that this terrestrial material could be detected in our marine sediment traps. Furthermore, the freshwater discharge from rivers had a profound impact on the circulation in the fjord and the exchange with the Greenland Sea. Thus, tight cooperation with the terrestrial program was initiated and eventually resulted in the implementation of a long-term marine monitoring program "MarineBasic" as an integrated part of the Zackenberg Basic monitoring program. MarineBasic has collected data since 2002. The work is financially supported by DANCEA (the Danish Cooperation for the Environment in the Arctic) under the Danish Ministry of the Environment. Furthermore, we received financial support from the Aage V. Jensen Charity Foundation to cover the expenses for a research boat and scientific equipment to start up the program. The latter foundation also donated new housing facilities in Zackenberg/Daneborg.

I am very pleased that our research projects in Young Sound have now resulted in the implementation of a long-term marine monitoring program. Together with the monitoring programs in the terrestrial environment, it will provide important data on this remote region, from which very few data existed before 1994. Furthermore, time will show if our current understanding of this High Arctic ecosystem is adequate and if our predictions of future changes in the ecosystem is correct. Finally, I thank the number of scientists who have reviewed the individual chapters as well as the Greenland Institute of Natural Resources for providing funds for this publication.

Søren Rysgaard, Nuuk, October 2006

References

Parkinson, C. L. 1992. Spatial patterns of increases and decreases in the length of the sea ice season in the north polar region, 1979-1986. J. Geophys. Res. 97: 14377-14388.

Hansen, J., Fung, I., Lacis, A., Rind, D., Lebedeff, S., Ruedy, R. & Russell, G. 1988. Global climate changes as forecast by Goddard Institute for space studies Three-dimensional model. J. Geophys. Res. 93: 9341-9364.

Manabe, S. & Stouffer, R. J. 1994. Multi-century response of a coupled ocean-atmosphere model to an increase of atmospheric carbon dioxide. J. Climate 7: 5-23.

Rahmstorf, S. 1995. Bifurcations of the Atlantic thermohaline circulation in response to changes in the hydrological cycle. Nature 378: 145-149.

Photo: Søren Rysgaard

1

Physical oceanography of the Greenland Sea

Physical oceanography of the Greenland Sea

Erik Buch

Danish Meteorological Institute, Centre for Ocean and Ice, Lyngbyvej 100, 2100 Copenhagen, Denmark

Cite as: Buch, E. 2007. Physical oceanography of the Greenland Sea. In: Rysgaard, S. & Glud, R. N. (Eds.), Carbon cycling in Arctic marine ecosystems: Case study Young Sound. Meddr. Grønland, Bioscience 58: 14-21.

Abstract

Ocean-atmosphere interactions in the North Atlantic are responsible for heat transports that keep the Nordic region and North Western Europe 5–10°C warmer than the average of the corresponding latitude belt. This is to a large extent due to the ocean's thermohaline circulation (THC). This circulation is driven by differences in water density, which is a function of temperature (thermo) and salinity (haline) and particularly by convection processes in the northern North Atlantic, especially the Labrador Sea and the Greenland Sea.

Therefore, the Greenland Sea has attracted much attention in the marine research community over the past decades. Scientific research in the Greenland Sea has been important to understand:

- The physical processes generating deep convection
- The role of sea ice in the deep convection process and biological production
- Uptake of carbon dioxide from the atmosphere and further transport into the ocean interior
- Variability in deep convection, especially the decrease in the Greenland Sea convection observed over the recent decades

The main incentive behind all these activities has been to understand the role of the Greenland Sea – and the rest of the Nordic Seas (Greenland, Norwegian and Iceland Seas) – in the climate system of the world.

1.1 General circulation

The large-scale circulation in the Nordic Seas is dominated by the warm northward-flowing Atlantic inflow, mainly on the eastern side of the Nordic Seas area, and the cold East Greenland Current flowing southward on the western side (Fig. 1.1). Atlantic Water enters the Norwegian Sea through the Faroe-Shetland Channel, following the Scottish slope, and between the Faroe Islands and Iceland, where modified North Atlantic Water feeds the Faroe Current, which flows eastward north of the Faroe Islands. The Atlantic Water flows northward along the west coast of Norway with some side branches entering the Greenland Sea area. Off Northern Norway the current splits into the North Cape Current and the West Spitsbergen Current, both entering the Arctic Ocean. The West Spitsbergen Current has several side branches feeding water into the East Greenland Current and the Greenland Sea.

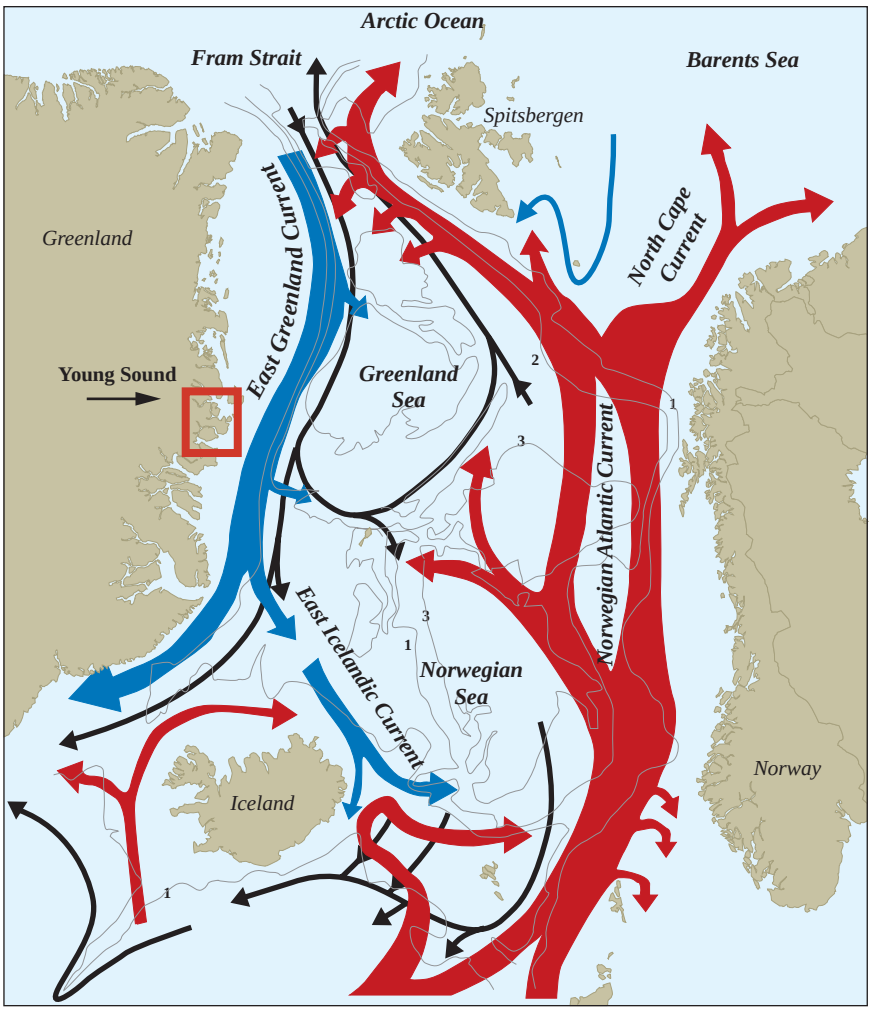

Figure 1.1 Ocean currents in the Nordic Seas. Blue arrows represent cold water masses and red arrows represent warm water masses.

In its upper layers, the southward-flowing East Greenland Current consists of cold Polar Water of low salinity, including large amounts of sea ice, from the Arctic Ocean (Aagaard & Carmack, 1989). In its deeper strata, there is also a transport of intermediate and deep water from the Arctic Ocean. A relatively warm intermediate layer with water of Atlantic origin returns from the West Spitsbergen Current and partly from the Arctic Ocean. Below, deep water formed in the Arctic Ocean, primarily Eurasian Basin Deep Water (Swift & Kolterman, 1988) can be traced all the way to the Denmark Strait (Buch et al., 1996) and constitutes an important contribution to the deep water in the Nordic Seas. The main side branches of the East Greenland Current are, firstly, the Jan Mayen Current, which brings all three water masses into the cyclonic circulation in the Greenland Sea Basin. Secondly, further south, the East Icelandic Current, which carries a somewhat varying combination of the same water masses from the East Greenland Current into the Iceland and Norwegian Seas (Buch et al., 1996). The remaining part of the East Greenland Current leaves the Nordic Seas through the Denmark Strait to supply fresh water to the sub-Arctic gyre in the North Atlantic as well as dense overflow water, which contributes to the deep western boundary current in the North Atlantic.

A distinct hydrographical regime lies between the regions dominated by the Polar and the Atlantic water masses (Fig. 1.2). In this hydrographical transition zone, the upper-layer water is warmer and more saline than that of the East Greenland Current, though still cooler and less saline than the Atlantic water. Helland-Hansen & Nansen (1909) used the general term ”Arctic Water” to distinguish the upper layer water of this transition region from those of more direct polar

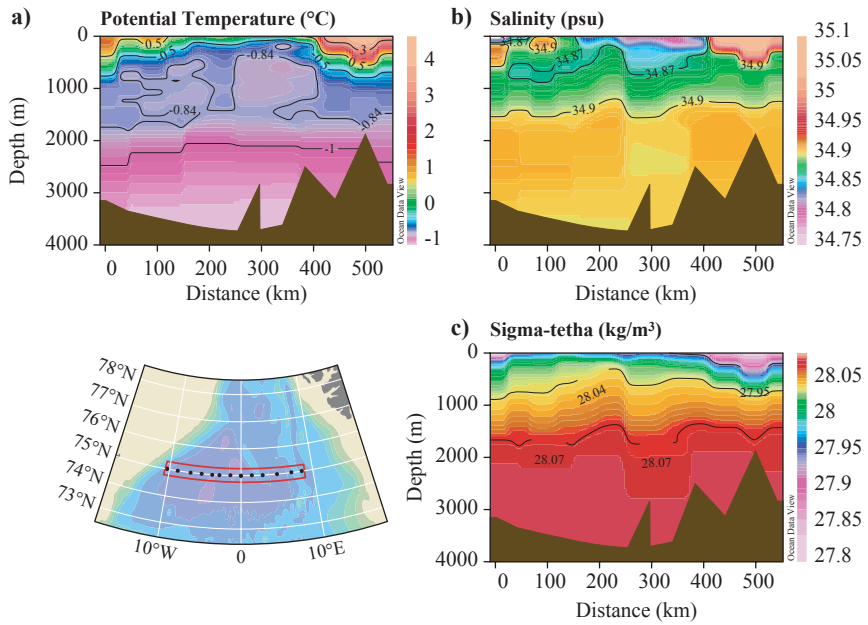

Figure 1.2 Vertical distribution of **(a)** potential temperature, **(b)** salinity and **(c)** density across the central Greenland Sea

or Atlantic origin. This Arctic domain is bounded to the east and west by regions of increased horizontal gradients in water properties, i.e. fronts. However, the temperature, salinity (T,S) property contrasts across these fronts vary seasonally and regionally. Both these boundary regions have by various authors been termed ”the Polar Front“, but Swift & Aagaard (1981) distinguished between the two by naming the front between the Polar and the Arctic domain ”the Polar Front“, while the front between the Arctic and the Atlantic domain is called ”the Arctic Front”.

Generally, it can be stressed that the Arctic domain is not simply the product of smooth transition between Atlantic and Polar influences, but rather an individual regime, locally modified, bounded by fronts, and only loosely connected to either of the bordering domains. In the Arctic domain a characteristic vertical progression of relatively dense water overlies the deep water.

In the vertical, the surface water of the Arctic domain is followed by a temperature minimum at 75–150 m, a temperature and salinity maximum at about 250 to 400 m, and, finally, the deep water. A crucial feature of the Arctic domain is that the vertical stability in the upper water stratum is lower than in the adjacent domains, while the density of the upper layer is overall quite high. Thus, winter cooling at the sea surface can produce very dense water, perhaps including deep water.

1.2 Water Masses

The dominant water masses in the Greenland Sea area are:

Atlantic Water (AW):
AW is traditionally defined as any water with salinity greater than 35.0. Upon entry into the Iceland and Norwegian Seas, AW has a temperature of 6–8°C and a salinity range of about 35.1–35.3. Because AW seldom, if ever, is cooler than 3°C and because a clear connection with AW can be observed in some water with salinities below the above-mentioned range, Swift & Aagaard (1981) expanded the traditional definition of AW to include all water warmer than 3°C and more saline than 34.9.

Polar Water (PW):
PW is defined as any water less saline than 34.4. Generally, the temperatures of this water are low, normally below 0°C, but because the layer is thin and strongly stratified, summer temperatures of 3 to 5°C in the surface are not unusual. Summer salinities as low as 29 have been observed in the western Greenland Sea. The Young Sound fjord is connected to the East Greenland Current and in direct contact with PW. Further details about water-column properties in the fjord are presented in Chapter 3.

Satellite image showing ice conditions late July in the surroundings of Young Sound.

Arctic Surface Water (ASW):
ASW is the water found at the surface in the Arctic domain during summer. The temperature is greater than 0°C for the salinity range 34.4 to 34.7 and greater than 2°C for the range 34.7 to 34.9.

Arctic Intermediate Water (AIW):
According to Swift & Aagaard (1981) AIW can be divided into upper AIW and lower AIW.

Upper AIW:
Temperatures are below 2°C and salinities from 34.7 to 34.9. This water mass is often found at the sea surface during winter.

Lower AIW:
Temperatures are in the range 0–3°C and the salinity is greater than 34.9 psu. This water mass is believed to be produced by the cooling and sinking of AW, especially in the northern Greenland Sea.

Greenland Sea Deep Water (GSDW):
GSDW is the densest water in the Greenland Sea. Its salinity is 34.895 and the temperature is -1.24°C. GSDW is found only in the central gyre of the Greenland Sea.

Norwegian Sea Deep Water (NSDW):
NSDW is the densest water mass in the Norwegian and Iceland Seas, but is also found around the periphery of the Greenland Sea. NSDW is slightly more saline than GSDW, namely 34.91 and has a temperature close to -1°C.

Arctic Ocean Deep Water:
Rudels & Quadfasel (1991) introduced three deep water masses of Arctic Ocean origin:

Upper Polar Deep Water:
$-0.5\,^{\circ}C < T < 0\,^{\circ}C$, $34.90 < S < 34.93$
Canadian Basin Deep Water:
$-0.8\,^{\circ}C < T < 0.5\,^{\circ}C$, $S > 34.92$
Eurasian Deep Water:
$T < -0.8\,^{\circ}C$, $S > 34.92$

These three water masses leave the Arctic Basin through the Fram Strait and flow southward in the western part of the Greenland Sea.

1.3 East Greenland Current

With respect to Greenland and the Young Sound Area, the part of the Greenland Sea attracting the greatest interest is the East Greenland Current, because of its effects on much of the Greenland coastline – especially due to the large amounts of sea ice it carries along with it. These concentrations of ice make great parts of the east coast of Greenland unnavigable, except for a couple of months a year.

The East Greenland Current is composed of three water masses. The upper 150–200 m is occupied by Polar Water (PW). The temperature varies between 0°C and the freezing point for sea water. During summer, there is usually a temperature minimum at about 50 m, while, in winter, the temperature is uniform from the surface to about 75 m with a value close to the freezing point of sea water. The salinity shows great variations within this region of PW. At the surface nearest to the Greenland coast salinities below 30.0 are found, while, at the bottom of the layer and close to the Polar Front (PF), salinities reach 34.5.

Underneath PW a body of both upper and lower AIW is found extending down to approximately 800 m. A temperature maximum can be observed throughout the year in the depth interval 200–400 m.

The third water mass is actually a combination of the different deep water masses mentioned above. Normally, the salinities observed are within the range 34.88–34.90, indicating that the water mass is GSDW, but occasionally salinities between 34.90–34.94 are observed, indicating the presence of NSDW and deep water masses of Arctic Ocean origin.

Current velocities

Estimation of current velocities can be made either by direct measurements or by dynamical calculations based on hydrographical observations; both kinds of observations are, however, hampered in the East Greenland Current system in the Greenland Sea area due to presence of sea ice throughout most of the year. During the Greenland Sea Project in 1987-1994, current meter moorings were deployed at 75°N; which is just north of Young Sound. Based on these observations the following conclusions can be drawn (Fahrbach et al, 1995):

- The long-term mean currents, determined as averages over the duration of the time series, are generally parallel to the depth contours. Cross-isobath flow was usually negligible.
- A current core with a maximum velocity of up to 0.30 m s^{-1} is found at a distance of approximately 45 km from the shelf break and extending to a depth of 2400 m (Fig.1.3).
- On the shelf, mean currents are 0.10 m s^{-1}.
- The time series reveal significant fluctuations of various timescales from tides to long-term trends, superimposed on the average currents. Variations of velocities on timescales of a week to a month, which represent current eddies and meanders, are up to 0.30 m s^{-1}. The fluctuations are most intense in the upper layer over the slope where maximum currents of 0.60 m s^{-1} were observed.
- Seasonal variations are displayed in most records. Normally, the currents are stronger in winter than in summer. In some years, the winter maximum split up into two well-separated maxima in autumn and spring. On the shelf, monthly mean currents attained minimum values of less than 0.05 m s^{-1} in August and a maximum of nearly 0.20 m s^{-1} in February.
- The tidal currents were dominated by the M2 (lunar-semidiurnal) constituent, with a magnitude of about 0.05 m s^{-1}. The S2 and K1 constituents were also significant. The semidiurnal (M2 and S2) constituents were significantly baroclinic and decreased with increasing depth. The diurnal (K1) constituent increased slightly with increasing depth.

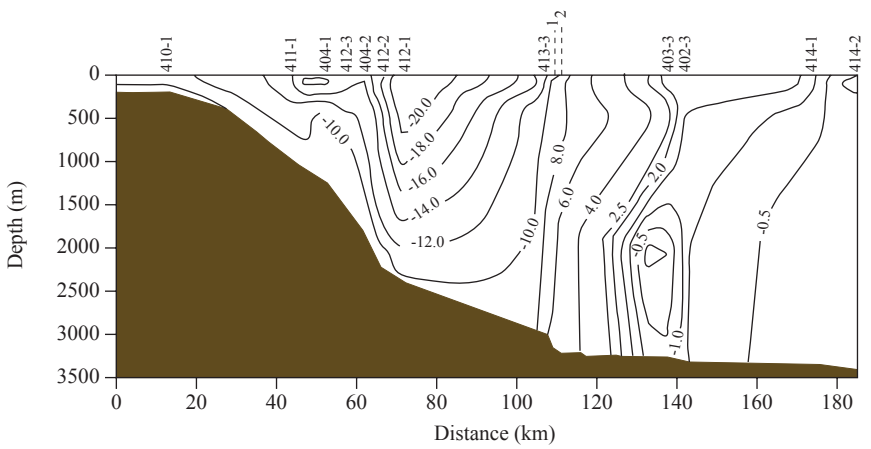

Figure1.3 Vertical distribution of current velocities at 75°N. From Fahrbach et al. (1995) Current velocities are in cm s^{-1}.

Photo: Søren Rysgaard

Pack ice in the Greenland Sea.

Sea Ice

The sea-ice cover along the east coast of Greenland can be divided into 4 zones, each with their own characteristic features and dynamics:

Landfast ice

Landfast ice is ice that grows seaward from a coast and stays in place throughout winter. Normally, it breaks up and drifts away or melts in spring, but may, under exceptional circumstances, stay in place all summer and thus survive into the second, or subsequent, years. The ice-free season grows rapidly shorter with increasing latitude, which is not surprising as the mean temperature in January falls from -4°C at Angmagssalik to below -18°C in North East Greenland. More details about sea ice in Young Sound are presented in Chapter 4.

Transition zone between coastal fast ice and the main body of pack ice

In many places within the Arctic, this zone is characterized by exceptionally heavy ridging, caused by the shoreward set of the polar pack as it circulates in the Beaufort Gyre (Wadhams, 1983). In the East Greenland Current there is no shear zone in this sense. The only area where it exists is the north coast of Greenland as far east as the Nordostrundingen. South of this point the East Greenland ice is in a state of almost free drift under wind and surface current, and an actual shear point, where internal stress integrated over a large area drives a consolidated ice field against the coast, never develop except locally around off-lying islands. Instead, a characteristic phenomenon of the winter and spring transition zone in East Greenland is the intermittent presence of open water, either as well-defined polynyas or as a continuous strip of open water seaward of the fast ice edge.

Pack ice

The drifting pack ice in the East Greenland Current is composed of ice floes originating from various places in the Arctic region. Three main types of pack ice have been defined (Wadhams, 1983):

- Paleocrystic ice is partly very old ice from the Beaufort Gyre, which has circulated for many years in the Canada Basin before crossing into the Trans Polar Drift Stream and exiting the Arctic Ocean with the East Greenland Current, and partly ice which has undergone heavy deformation in the

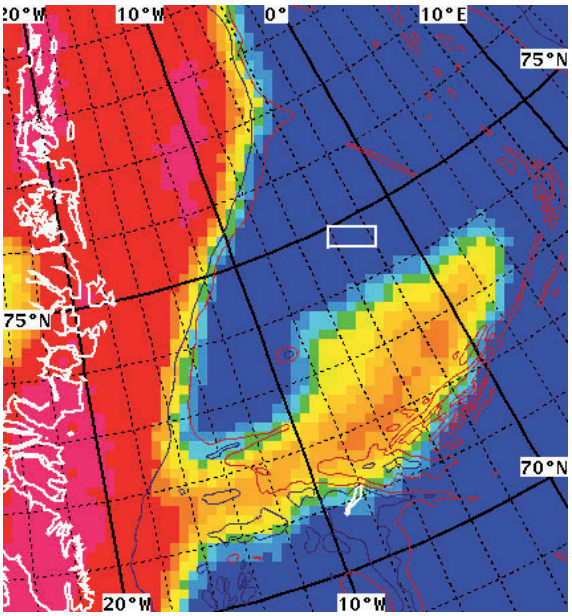

Figure 1.4 Odden Ice Tongue. Based on satellite observations analysed at the Danish Technical University (Leif Toudal).

North Greenland offshore zone before entering the Fram Strait via the Nordostrundingen.

- North Pole ice is ice of slightly more recent origin from both the Beaufort Gyre and the more distant parts of the Eurasian Basin (e.g. the northern part of the East Siberian Sea and the Chukchi Sea).
- Siberian ice is first- and second-year ice formed in the near-shore and shelf areas of the Soviet Arctic or in the region immediately north of the Fram Strait. In addition, young ice is found in the pack in winter, forming continuously in leads and polynyas, as they open up. Thus, the winter pack at the latitude of the Denmark Strait contains a significant portion of ice, which has formed south of the Fram Strait. Due to turbulence, which results in much churning and meandering of the ice, and the overall southward drift, ice of all types is mixed irretrievably together.

Marginal Ice Zone

The Marginal Ice Zone is the transition zone between the pack ice and the open ocean, which, due to the interaction between the ice and open ocean as well as the interaction between the water masses within and outside the East Greenland Current, has quite different physical properties than those found in the pack ice zone. Eddies of different sizes are a common phenomenon in the Marginal Ice Zone.

A special phenomenon regarding sea ice in the Greenland Sea is the Odden Ice Tongue. The Odden Ice Tongue is a winter ice cover phenomenon that occurs in the Greenland Sea. It is about 1300 km in length and may cover an area of as much as 330,000 square kilometres (Fig. 1.4). Within a very short

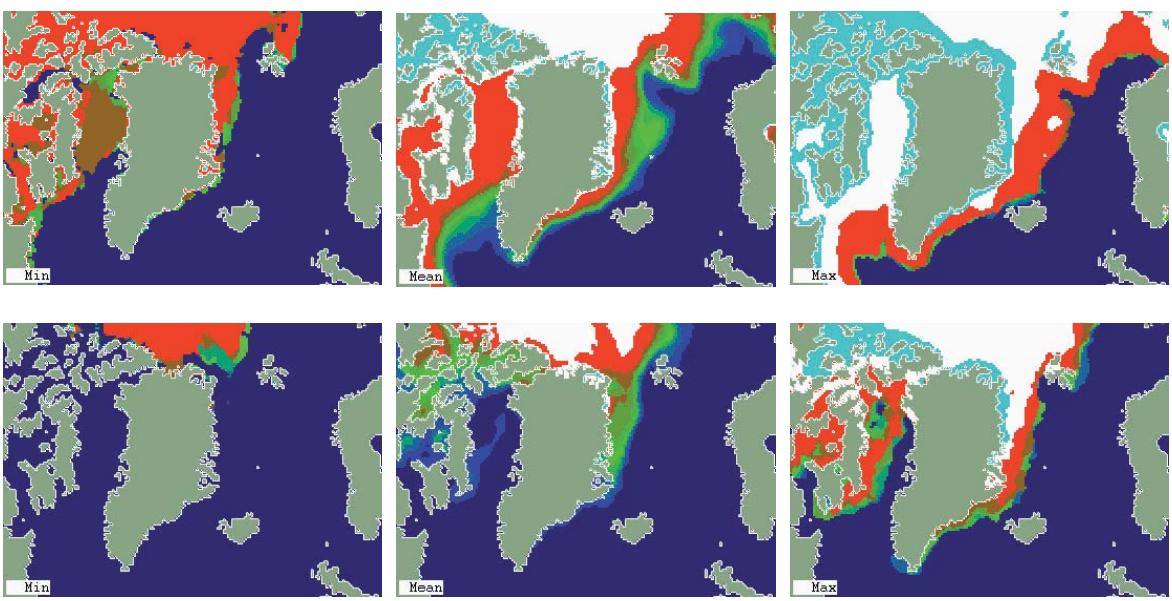

Figure 1.5 Minimum, mean and maximum distribution of sea ice in February (above) and September (below), representing months with maximum and minimum ice distribution, respectively.

period a great part of the ice cover disappears, leaving behind a large ice tongue advancing into the Greenland Sea. The ”Odden“ phenomenon has been known for more than a hundred years, and because it appears nearly every winter, it can also be traced in maps showing the mean ice distribution. The Odden Ice Tongue phenomenon is closely related to the convection processes taking place in the Greenland Sea.

Since the distribution of sea ice is coupled to the climatic conditions of the area, great seasonal and interannual fluctuations in the amount of sea ice are observed. Statistical analyses have shown that the portion of the Greenland Sea covered with ice in years with maximum distribution of sea ice is much larger than in years with minimum distribution. The increase amounts to more than 100%, i.e. the interannual variations in ice cover are comparable with the seasonal variations within a given year (Fig. 1.5). More details about the local sea ice variability in the Young Sound area are given in Chapter 4.

1.4 Acknowledgements

This work is a contribution to the Zackenberg Basic and Nuuk Basic Programs in Greenland.

1.5 References

Aagaard, K. & Carmack, E. 1989. The role of sea ice and other fresh water in the Arctic circulation. J. Geophys. Res. 94, C10: 14485-14498.

Buch, E., Malmberg, S. Aa. & Kristmannsson, S. S. 1996. Arctic Ocean Deep Water masses in the Western Iceland Sea. J. Geophys. Res. 101, C5: 11965-11973.

Fahrbach, E., Heintze, C., Rohardt, G. & Woodgate, R. A. 1995. Moored current meter measurements in the East Greenland Current. Paper presented at Nordic Seas Symposium, sponsored by Deutche Forschungsgemeinschaft and the US National Science Foundation, Hamburg, Germany.

Helland-Hansen, B. & Nansen, F. 1909. The Norwegian Sea. Its physical oceanography based upon the Norwegian researches 1900-1904. Report on Norwegian Fishery and Marine Investigations. 2 (12), 89 pp.

Rudels, B. & Quadfasel, D. 1991. The Arctic Ocean Component in the Greenland-Scotland Overflow. Publ. C.M.1991/C: 30, Int. counc. for exploration of the Sea, La Rochelle.

Swift, J. & Aagaard, K. 1981. Seasonal transitions and water mass formation in the Iceland and Greenland Seas. Deep Sea Res. 27A: 29-42.

Swift, J. & Kolterman, K. 1988. The origin of Norwegian Sea Deep Water. J. of Geophys. Res. 93, C4: 3563-3569.

Wadhams, P. 1983. The Ice Cover in the Greenland and Norwegian Seas. Rev. Geophys. Space Phys. 19, 3: 345-393.

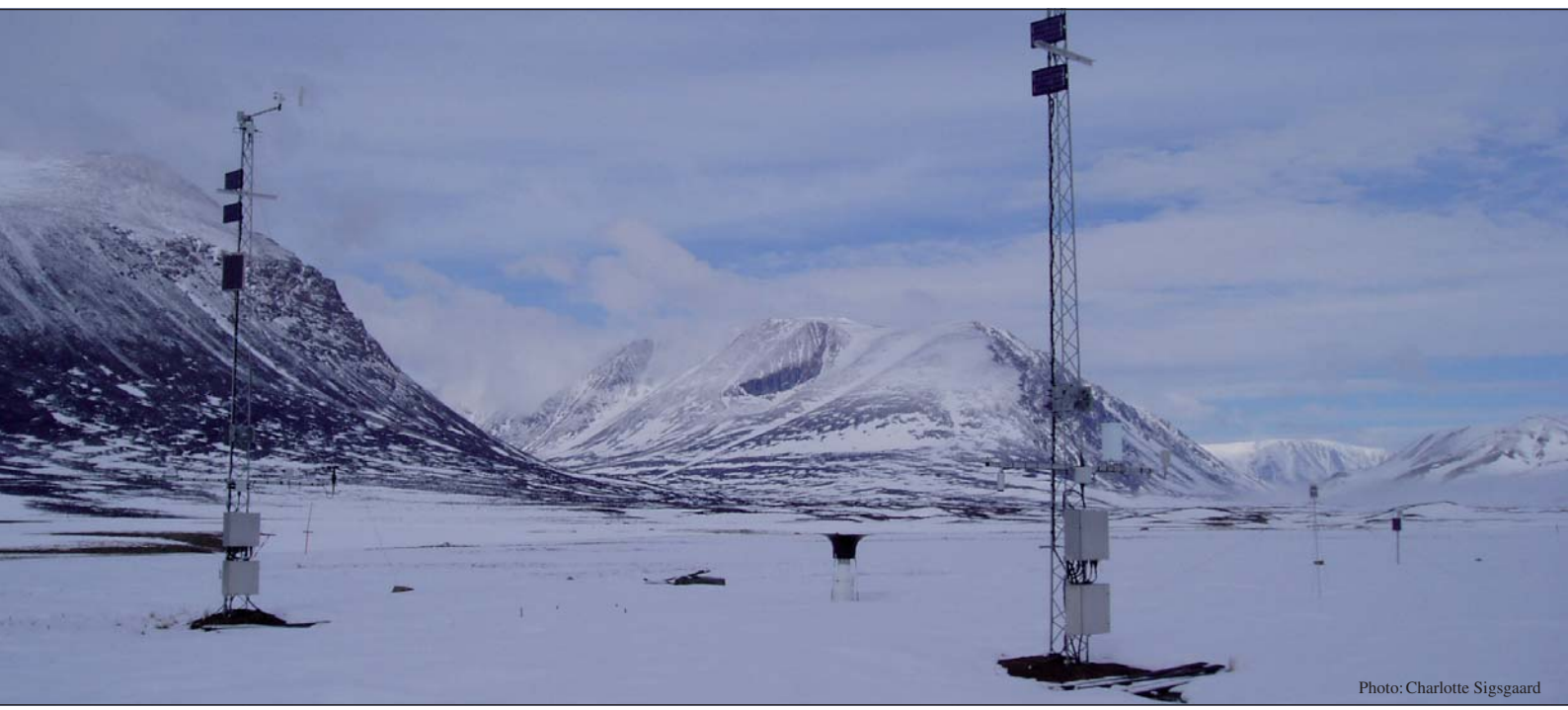

Photo: Charlotte Sigsgaard

2

Climate, river discharge and suspended sediment transport in the Zackenberg River drainage basin and Young Sound/Tyrolerfjord, Northeast Greenland, 1995–2003

Climate, river discharge and suspended sediment transport in the Zackenberg River drainage basin and Young Sound/ Tyrolerfjord, Northeast Greenland, 1995–2003

Sebastian H. Mernild[1], Charlotte Sigsgaard[1], Morten Rasch[2], Bent Hasholt[1], Birger U. Hansen[1], Michael Stjernholm[3] and Dorthe Petersen[4]

[1]Institute of Geography, University of Copenhagen, Øster Voldgade 10, DK-1350 Copenhagen, Denmark
[2]Danish Polar Center, Strandgade 102, DK-1401 Copenhagen, Denmark
[3]National Environmental Research Institute, Vejlsøvej 25, DK-8600 Silkeborg, Denmark
[4]ASIAQ, Greenland Survey, Qatserisut 8, Box 1003, DK-3900 Nuuk, Greenland

Cite as: Mernild, S. H., Sigsgaard, C., Rasch, M., Hasholt, B., Hansen, B. U., Stjernholm, M. & Pedersen, D. 2007. Climate, river discharge and suspended sediment transport in the Zackenberg River drainage basin and Young Sound/Tyrolerfjord, Northeast Greenland. In: Rysgaard, S. & Glud, R. N. (Eds.), Carbon cycling in Arctic marine ecosystems: Case study Young Sound. Meddr. Grønland, Bioscience 58: 24-43.

Abstract

Climate control on river discharge, suspended sediment transport and conductivity was investigated based on high-resolution time series (1995–2003) from a High Arctic drainage basin at Zackenberg, Northeast Greenland. Data from the Zackenberg River drainage basin (512 km^2) was extrapolated to estimate the total transport from land of freshwater, sediments and organic matter to the Young Sound/Tyrolerfjord system (3,016 km^2). During the investigation period, a 14-day increase in thawing period, a 50-day decrease in snow cover period, an increasing release of meltwater from exposed glacier surfaces and an increasing annual runoff were recorded. The total annual runoff from the Zackenberg River drainage basin ranges between 122 and 306 million m^3 (239–598 mm yr^{-1}), while the total annual runoff to the entire Young Sound/Tyrolerfjord system ranges between 630 and 1,570 million m^3 yr^{-1}. Suspended sediment discharges from the Zackenberg River drainage basin and the entire catchment area to Young Sound/Tyrolerfjord are 15,000–130,000 t yr^{-1} and 77,000–670,000 t yr^{-1}, respectively. For organic matter yield the ranges are, respectively, 1,100–11,500 t yr^{-1} and 6,000–59,000 t yr^{-1}. In 2003 the total transport of carbon was 1,180 t yr^{-1} and 6,000 t yr^{-1} and of nitrate 13 t yr^{-1} and 66 t yr^{-1}, respectively, for the Zackenberg River drainage basin and the entire catchment area to Young Sound/Tyrolerfjord.

2.1 Introduction

Over the last 100 years mean global surface air temperature has increased by 0.3 to 0.6°C (Maxwell, 1997; Kane, 1997). In this period, nine of the ten warmest years measured globally occurred between 1990 and 2001 (WHO, 2001), and it is likely that the 1990s was the warmest decade during the past 1,000 years (Crowley, 2000), the largest air temperature changes being seen in winter (Box, 2002; Sturm et al., 2005). Simulations of future climate by Global Circulation Models indicate an increase in global air temperature, and that warming will occur more intensively in northern latitudes than elsewhere (e.g. Maxwell, 1997; Flato & Boer, 2001; Rysgaard et al., 2003). For Northeast Greenland, atmosphere-ocean models indicate an air temperature increase of up to 6–8°C during this century (Rysgaard et al., 2003), with the largest changes occurring in autumn and winter (Sælthun & Barkved, 2003). As a result, the contribution of fresh water from Northeast Greenland to the Greenland Sea will increase during the next century. Combined with a pronounced reduction of sea ice within the Arctic Sea, including the Green-

land Sea (Serreze et al., 2002; Sturm et al., 2005), this might affect the density-driven sinking of cold surface water – the thermohaline circulation – in the sea off Northeast Greenland (e.g. Broecker et al., 1985; Broecker & Denton, 1990).

Information on climate and river discharge in Northeast Greenland was more or less non-existent before the establishment of the Zackenberg Research Station in 1995. The Zackenberg Research Station is situated near the fjord Young Sound/Tyrolerfjord in Northeast Greenland (74°28'N; 20°34'W). The station is maintained by the Danish Polar Center (DPC), and it runs an extensive monitoring programme, Zackenberg Basic, on ecological effects of climate change. The two sub-programmes, ClimateBasic and GeoBasic, provide information on the dynamics of the physical landscape processes, including climate and hydrology, in the Zackenberg River drainage basin. The ClimateBasic program is operated by ASIAQ (Greenland Survey), while the GeoBasic program is operated in cooperation between the Danish National Environmental Research Institute (NERI) and the Institute of Geography, University of Copenhagen. A third sub-programme, MarinBasic, focusing on the marine environment and operated by the Greenland Institute of Natural Resources and NERI, was implemented in 2002.

In this study, high-resolution climate and hydrology data from the first eight years (1995–2003) of measurements at Zackenberg are presented to describe the variation in meteorological conditions and its effects on river discharge, suspended sediment load, suspended organic matter load and on river water conductivity. Furthermore, the data from the Zackenberg River drainage basin is extrapolated to give an estimate of the river discharge, suspended sediment yield and dissolved yield from land to the Young Sound/Tyrolerfjord system.

2.2 Physical setting

The study area is the drainage basin to the Young Sound/Tyrolerfjord system in High Arctic (according to: Bliss & Matveyeva, 1992) Northeast Greenland (Fig. 2.1a). The low-lying valley floors in the drainage basin (e.g. the valley Zackenbergdalen, 'dalen' means 'valley' in Danish) are located at the borderline between the continental and oceanic parts of the bioclimate subzone C – the Middle Arctic climate zone – with a mean July air temperature of about 5.0–7.0°C (Bay, 1999; Walkers et al., 2002). The drainage basin is situated in the Northeast Greenland National Park. It has a total area of 3,016 km^2 (landcover only

Figure 2.1 **(a)** Location map showing the drainage basin of the Young Sound/Tyrolerfjord system (3,016 km^2) and the Zackenberg River drainage basin (512 km^2). **(b)** Location map showing the Zackenberg River drainage basin (512 km^2). H and C in the lower right-hand corner indicate the location of the hydrometric station and the meteorological station, respectively. The dashed line indicates the fault separating Caledonian gneiss and granite to the west (422 km^2) from Cretaceous and Tertiary sandstones and basalts to the east (90 km^2) (Modified from Rasch, 2000).

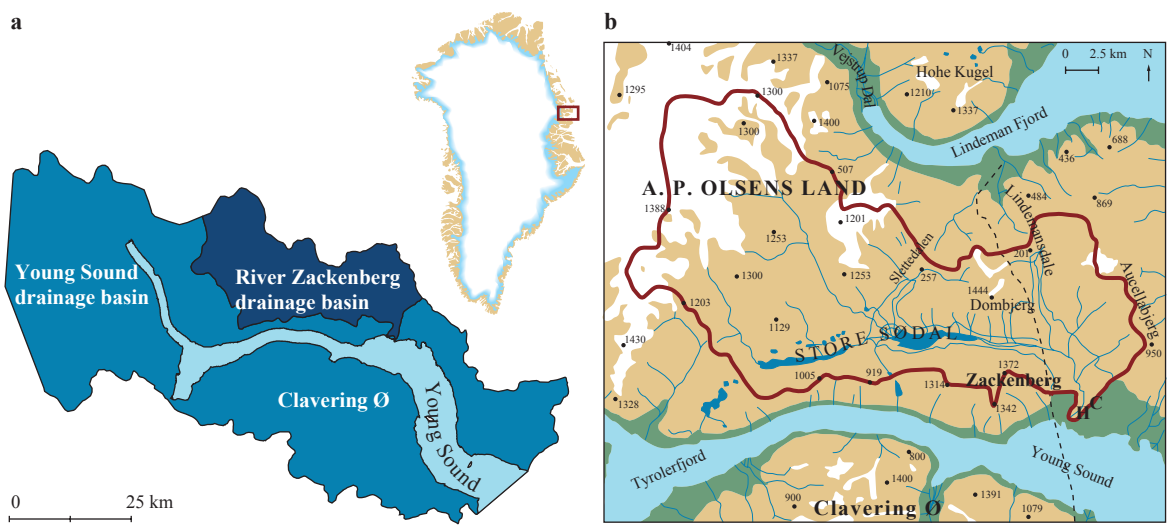

2,620 km^2) and drains into the more or less east-west oriented Young Sound/Tyrolerfjord with a total length of c. 90 km. The altitude of the drainage basin varies between 0 and 1,700 m above sea level (ASL), and lakes and glaciers cover 0.4% and 25%, respectively, of the drainage basin. Geologically the area mainly consists of Caledonian gneiss and granite to the west and Cretaceous and Tertiary sandstones and basalts to the east (Koch & Haller, 1971). The two settings are separated by a fault running through the valleys Zackenbergdalen and Lindemansdalen (Fig. 2.1b). Generally, the landscape is characterised by wide U-shaped valleys with gently sloping sides in the sandstone/basalt regions and narrow and deeper U-shaped valleys with steep valley sides in the gneiss regions. Quaternary deposits occur mainly in the lower part of the landscape as tills in various moraines and as marine/deltaic deposits in raised marine deltas below 70 m ASL.

Almost all data on meteorological conditions, river discharge and sediment yield from land to the Young Sound/Tyrolerfjord system has been collected in the Zackenberg River drainage basin, situated close to the Zackenberg Research Station. River discharge, sediment and solute discharge from the Zackenberg River are being measured approximately 2 km upstream from the mouth of the Zackenberg River. The Zackenberg River drainage basin has an area of 512 km^2 (1/6 of the Young Sound/Tyrolerfjord drainage basin) of which 101 km^2 (or approximately 20%) is glacierized by ice caps, valley glaciers, and cirques, mainly in the western part (Rasch et al., 2000; Rysgaard et al., 2003) (Fig. 2.1b). The Zackenberg River drainage basin is not connected to the Greenland Ice Sheet. The altitude of the drainage basin varies between 0 and 1,450 m ASL. (Fig. 2.1b), extensive plateaus with glaciers occur above c. 1,000 m ASL. (79% of the glacier cover), and wide U-shaped valleys carved out by glacial erosion occur below the plateaus (c. 200 m ASL) with extensive and nearly horizontal valley floors. Most of the lakes in the drainage basin are minor except for the lake Store Sø (4.9 km^2; c. 1%) occurring as a widening of Zackenberg River in Store Sødal. The aspect is almost homogeneous, with the majority (16.8%) of slopes facing SE and 8.3% of slopes facing NW.

The two different geological settings, i.e. Caledonian gneiss and granite to the west, Cretaceous, and Tertiary sandstones and basalts to the east constitute 422 and 90 km^2, respectively, of the drainage basin. Well-developed soils mainly occur in the lower part of the landscape as Inceptisols and weakly developed Spodosols (Soil Survey Staff, 1999). The vegetation in the lowland varies from wet *Eriophorum scheuchzeri-Carex atrofusca* meadows to well-drained heaths characterised by *Cassiope* and *Dryas* characteristic of the bioclimate subzone C (Bay, 1999; Walkers et al., 2002). Vegetation is almost absent on the high-lying plateaus. The river regime in the area is intermediate between the "Arctic nival regime" and the "proglacial regime" according to Church (1974) (Rasch et al., 2000).

The nearest town is Scoresbysund c. 450 km to the south, while the nearest settlements are Daneborg and Danmarkshavn situated c. 20 km southeast and c. 200 km north of Zackenberg Research Station, respectively. Meteorological stations are present at all three locations.

2.3 Methods

This study is based on meteorology and hydrology data from 1995–2003 measured by the Zackenberg Basic monitoring programme.

The meteorological station in Zackenberg (UTM Zone 27: 8264700 mN; 513400 mE, 43 m ASL.) on a dry *Cassiope* heath. Since 1995 continuous time series of air temperature, ground temperature, relative humidity, air pressure, radiation, wind velocity have been recorded (Table 2.1). The variation in snow depth has been logged since 1997 using a Campbell Scientific SR50 Sonic Range Sensor. Spatial variation in snow cover and snow depletion in the central part of the valley lowland has been monitored since 1997 using digital camera images from cameras mounted 477 m ASL on the Zackenberg Mountain (Table 2.1).

The solid precipitation is calculated from the rise in the accumulation curves of the recorded snow depth. When noise is removed, the rise in snow depth is multiplied by a variable density for snow (from 69.5 kg m^{-3} to 199.2 kg m^{-3}, average 81.4 kg m^{-3}) as a function of air temperature (Brown et al., 2003) and by an hourly settling rate for the snow pack (Anderson, 1976), to estimate the snow-water-equivalent precipitation (Table 2.2).

In Søgaard et al. (2001) basin evapotranspiration including sublimation for Zackenberg (1995/1996 to

Table 2.1 Parameters measured and sensors used for measurements of the meteorological conditions at the meteorological stations in the valley Zackenbergdalen.

Parameter	Unit	Period	Sensor type	Location	Above terrain	Frequency	Accuracy
Wind Direction	Deg.	Since 17 August 1995	Theodor Friedrichs & Co, 4121	8264700 mN, 513400 mE (43 m ASL)	7.5 m	10-min. intervals	± 5 deg.
Wind Speed	m s^{-1}	Since 17 August 1995	Theodor Friedrichs & Co, 4033	8264700 mN, 513400 mE (43 m ASL)	2.0 m	10-min. intervals	± 0.3 m s^{-1} for v > 15 m s^{-1}
Wind Speed	m s^{-1}	Since 17 August 1995	Theodor Friedrichs & Co, 4034	8264700 mN, 513400 mE (43 m ASL)	7.5 m	10-min. intervals	± 0.3 m s^{-1} for v > 15 m s^{-1}
Air Temperature	°C	Since 17 August 1995	Vaisala, HMP 35	8264700 mN, 513400 mE (43 m ASL)	2.0 m	1-hour intervals	± 0.3°C
Air Temperature	°C	Since 17 August 1995	Vaisala, HMP 35	8264700 mN, 513400 mE (43 m ASL)	7.5 m	1-hour intervals	± 0.3°C
Relative Humidity	%	Since 17 August 1995	Vaisala, HMP 35	8264700 mN, 513400 mE (43 m ASL)	2.0 m	1-hour intervals	±2% for 0-90% RH ±3% for 90-100% RH
Air Pressure	mbar	Since 17 August 1995	Vaisala, PTB200A	8264700 mN, 513400 mE (43 m ASL)	1.6 m	1-hour intervals	± 0.15 mbar
Incoming Shortwave Radiation	W m^{-2}	Since 17 August 1995	Kipp & Zonen, CM7B	8264700 mN, 513400 mE (43 m ASL)	2.0 m	1-hour intervals	± 1%
Outgoing Shortwave Radiation	W m^{-2}	Since 17 August 1995	Kipp & Zonen, CM7B	8264700 mN, 513400 mE (43 m ASL)	2.0 m	1-hour intervals	± 1%
Net Radiation	W m^{-2}	Since 17 August 1995	Kipp & Zonen	8264700 mN, 513400 mE (43 m ASL)	2.0 m	1-hour intervals	-----
Precipitation (Tipping bucket)	mm w.eq.	Since 17 August 1995	Belfort with Nipher (Universal Precipitation Gauge, serie no 5-780-4.8)	8264700 mN, 513400 mE (43 m ASL)	1.5 m	when bucket is full	0.5% (0.2 mm at one tip)
Snow depth	m	Since 26 June 1997	Campbell SR50	8264774 mN, 513480 mE (43 m ASL)	1.66 m	3-hour intervals	+/- 1 cm or 0.4% of distance to target (whichever is greatest)
Automatic Digital Camera:							
Camera 1		Since Summer 1999	Kodak DC-50	8265315 mN, 510992 mE (477 m ASL)	-----	Daily pictures at solar noon, 1.20 pm	756*504 pixels per inch (~20 m resolution)
Camera 2		Since Summer 1997	Kodak DC-50				
Camera 3		Since Summer 2001	Kodak DC-120				

Table 2.2 Parameters measured and sensors used for hydrological measurements, Zackenberg.

Parameter	Unit	Periode	Sensor type	Location	Frequency	Accuracy
Water level	m	Since August 1995 (automatic)	Campbell SR50	8264582 mN; 512538 mE (14 m ASL)	15-minute intervals	+/- 1 cm or 0.4% of distance to target (whichever is greatest)
Water discharge	m^3 s^{-1}	Summer season (manual)	Ott C31 current meter	8264582 mN; 512538 mE (14 m ASL)	10-15 per season	+/- 5-10%
Suspended sediment	g l^{-1}	Summer season (manual)	Nilssons depth-integrating sampler	8264582 mN; 512538 mE (14 m ASL)	Daily, 8 am	-----
Water conductivity	µS cm^{-1}	Summer season (manual)	YSI 30	8264582 mN; 512538 mE (14 m ASL)	Daily, 8 am	+/- 0.5% (full scale)

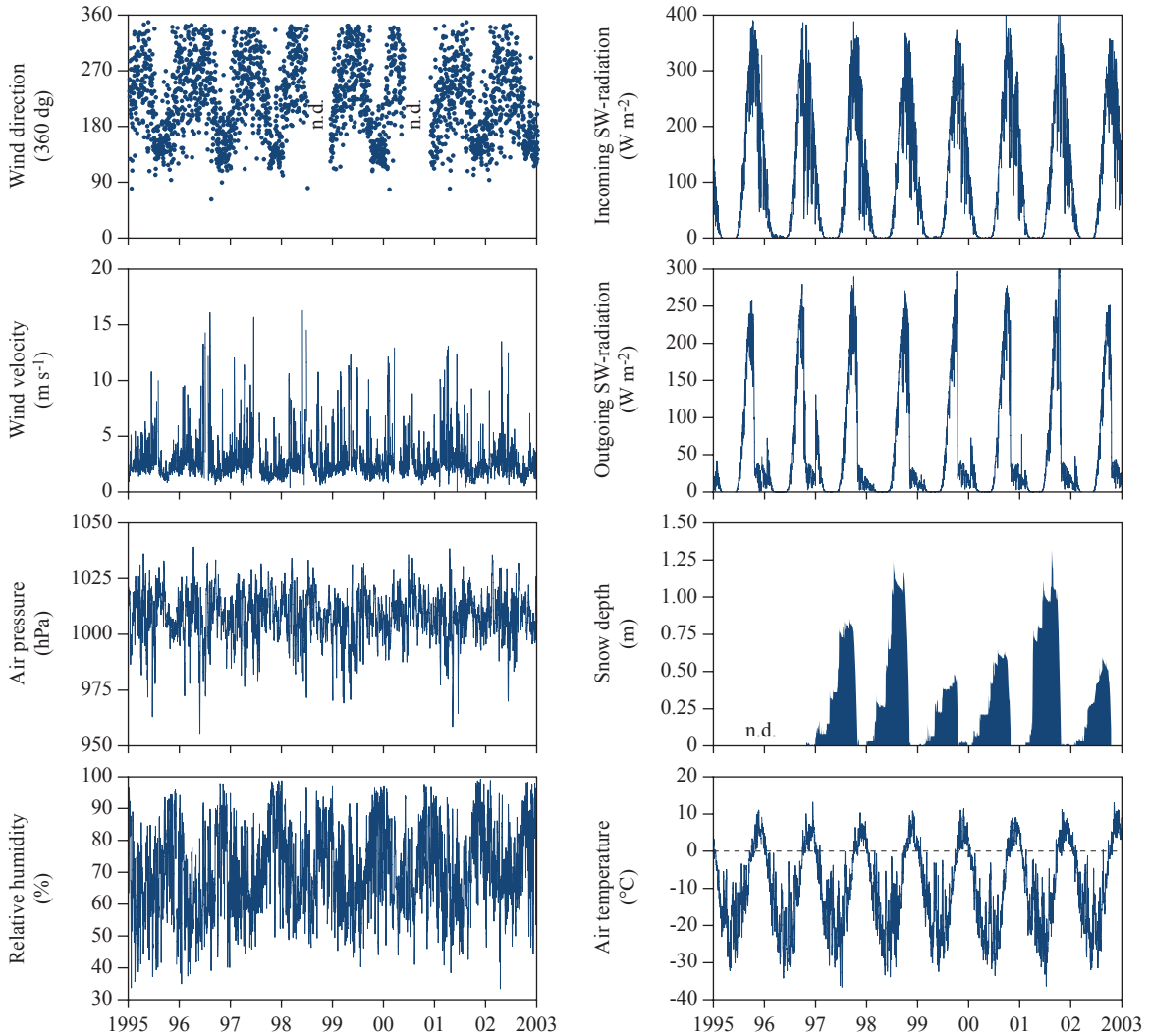

Figure 2.2 Daily mean values of meteorological parameters and snow cover at Zackenberg, 1995–2003. Note the difference in ordinate scale.

1997/1998) is calculated based on atmospheric fluxes measured by eddy correlation technique. High correlation exists (linear regression) between annual evapotranspiration and annual sum of Thawing Degree Days (TDD) (September to August) (see definition in section 2.4) for the seasons 1995/1996 to 1997/1998. Therefore, TDD is used to estimate evapotranspiration (ET) (Eq. 1):

$$ET\,(mm) = 0.44TDD - 77.5\ (R^2 = 0.98; p<0.01) \qquad (1)$$

from the Zackenberg drainage basin for the seasons 1998/1999 to 2002/2003. Evapotranspiration from a basin comes from snow and glacier surfaces, water surfaces and soil and vegetation surfaces. Therefore, ET as a function of TDD may to some extent be overestimated, because soils dry up during the summer.

In the lower part of the Zackenberg River, a hydrometric station (Fig. 2.1) has been measuring water level since 1995 and water conductivity since 2003. Water level is logged automatically once every 15 minutes throughout the year using a sonic range sensor (Campbell Scientific SR50) and water conductivity in runoff seasons, only, using a conductivity and temperature probe (Campbell Scientific 247). Manual river discharge measurements are carried out at the hydrometric station 8–10 times during the runoff season with an Ott C31 current meter to vali-

date the stage-discharge relation and to describe the runoff in the period when riverbanks and riverbed are still covered by snow and ice. During the first c. 1–2 weeks after river break-up, the river discharge measured automatically is probably unreliable, as the river bed and banks are partly covered by snow and ice, leading to changes in river bed cross profile, less friction at the river bed and raised water level due to snow at the river bed. The stage-discharge relation gradually becomes more and more valid as snow and ice melt. The stage-discharge relation is based on river discharge measurements from the period 1995–1998. Manual river discharge measurements in 1999–2003 indicate that the river cross profile has remained stable and that the stage-discharge relation is still valid. Total annual river discharge is quantified from the water level measurements and the stage-discharge relation. River water conductivity is measured manually in the field at 8 am using an YSI 30 incorporated conductivity meter.

Water samples have been collected every day at 8 am during the runoff season since 1997 using a Nilsson's depth-integrating sampler (Nilsson, 1969). In the summer of 1997, samples were collected at both 8 am and 6 pm. Suspended sediment concentrations are measured by filtering water samples (0.8 l) onto Whatmann GF/F filters (0.7µm) pre-weighed, and drying at 105°C and weighed again. Suspended organic matter concentration is estimated as LOI (Loss On Ignition), *i.e*. the difference between dry weight (105°C) and ash-free dry weight (520°C) (Sykes et al., 1999). An additional daily water sample is collected for chemical analyses. Major anions and cations are measured in filtered subsamples (0.45 µm). Analysis of dissolved organic carbon (DOC) is now incorporated in the monitoring programme but results in this paper are based on only nine DOC analyses on samples selected at regular intervals throughout the runoff season 2003. Dissolved inorganic carbon is based on daily alkalinity analyses.

Total annual transport of suspended sediment and suspended organic matter from the Zackenberg River to Young Sound/Tyrolerfjord is calculated by multiplying the concentrations measured in water samples at 8 am by average daily river discharge and summing these results up for the whole runoff season.

Since the geology and the glacier cover is almost the same in the Zackenberg River drainage basin (c. 20% glacier cover) as in the Young Sound/Tyrolerfjord drainage basin (c. 25%) this should probably not affect the rough upscaling of the suspended sediment transport to the entire Young Sound/Tyroler-fjord.

2.4 Indices and parameters

The following air temperature indices "degree day models" were calculated as estimates of the influence of the climate on the surrounding environment: (1) the accumulated Freezing Degree Days (FDD) is the sum of the numeric values of negative mean daily air temperatures and the number of Freezing Days (FD) is the sum of days with negative mean daily air temperatures per year; (2) the accumulated number of Thawing Degree Days (TDD) is the sum of values of positive mean daily air temperatures and the number of Thawing Days (TD) is the sum of days with mean positive daily air temperatures per year (Bay, 1992; Hinkler et al., 2002). TDD and TD are related to release of water from the annual snow pack and the exposed surfaces, when the annual snow cover has melted away. An increase of both will cause higher evaporation rates from wet surfaces and in particular cause increased runoff from the glaciated areas, and (3) the accumulated number of Growing Degree Days (GDD) is the sum of the values of mean daily air temperatures above 5°C and the number of Growing Days (GD) is the number of days with mean air temperatures above 5°C per year. Plant growth is more or less absent when daily mean air temperature is below 5°C. Therefore, GD and GDD are useful as threshold temperatures for defining the length and the intensity of the growing season (Hansen et al., 2003).

The elements of the water balance for a drainage basin depend on drainage basin characteristics and processes. The water balance equation (Eq. 2) is:

$$P - ET - R \pm \Delta S = 0 \pm \eta \quad (2)$$

Where P is the precipitation input from snow and rain (possible condensation); ET is the evapotranspiration (possibly sublimation); R is runoff throughout the entire period of flow; ΔS is change in surface storage (lake, wetlands, channels, etc.), subsurface storage of groundwater, storage in the unsaturated (vadose) zone, storage in glacier and storage in snow pack, (including snowdrifts) and η is the balance discrepancy (error).

The total runoff ($R_{surface} + R_{subsurface} + R_{rain} + R_{snow} + R_{glacier}$) is normally the most reliable component measured in the water balance if the stage-discharge relation is stable and valid. The runoff is an integrated response of the hydrological processes in the catchment, and contrary to most other parameters in the water balance it is therefore not affected by the representativity of the measuring station (Killingtveit et al., 2003).

2.5 Results

2.5.1 Meteorological conditions

Daily mean values of meteorological parameters and snow cover at Zackenberg, 1995-2003, is shown in Fig. 2.2.

The Mean Annual Air Temperature (MAAT) at the Zackenberg Meteorological Station was –9.6°C (2.0 m) for the period 1995–2003 (Table 2.3). The MAAT variation is between –10.1°C (1997) and –8.6°C (2002) (Fig. 2.3a) and the mean monthly air temperatures (MMAT) (1995–2003) for January and July were, respectively, –21.1°C and 5.5°C (Table 2.3). In general, air temperatures above 0°C occur from early June to mid September (Table 2.3; Fig. 2.3b). The lowest air temperature (–38.9°C) measured at Zackenberg occurred on 23 February 1998 (DOY 54), while the highest air temperature (21.3°C) was recorded on 12 August 1997 (DOY 224). The air temperature indicates an annual warming of c. 0.1°C yr^{-1} (1996–2002) (based on linear regression, non-significant), and a warming in all seasons except spring (March–May). In spring, the air temperature decreases 0.7°C yr^{-1} ($p<0.01$; root mean square (rms) = 0.05), while the highest air temperature increase (0.4°C yr-1) occurs in autumn (September–November; $p<0.05$; rms = 0.25; Fig. 2.3a). Fig. 2.3b and Table 2.6 illustrate the increasing autumn air temperature, indicated by a longer thawing period in autumn (16 days) and a decreasing thawing period in spring (2 days) and resulting in a net increase of the thawing period of 14 days yr^{-1} from 1996–2003. In the same period, TDD increased from 385 to 561 yr^{-1} (Fig. 3.b and Table 2.6).

The mean annual wind velocity (1995–2003) was 2.7 and 3.2 m s^{-1}, respectively, 2.0 m and 7.5 m above terrain (Table 2.3), with a maximum 10-minute mean of 29.5 m s^{-1} (14 February 1998, DOY 45) during a period with northerly winds. In general, the wind velocity was relatively high during autumn and winter and somewhat lower during summer (Table 2.3). Mean monthly air temperature in the outer parts of Young Sound is shown i Table 2.4. A high frequency (44.0%) of winds (7.5 m above terrain) coming from northerly directions (Table 2.5) typical during winter, while easterly and southerly winds are normal during summer (Fig. 2.2). The mean annual relative humidity was 72% (1995–2003) (Table 2.3), and the uncorrected mean liquid precipitation for June, July and August (1995–2003) was 44 mm (Table 2.3), which is lower than the highest monthly precipitation of 55 mm (August 1998). The highest precipitation rate recorded was slightly above 4.8 mm h^{-1} (16 August 2002, DOY 228). The annual precipitation (September to August) varies between 199 mm (1999/2000) and 403 mm (1998/1999), with an average of 273 mm (1997–2003) (Table 2.3). Approximately 75% of the precipitation falls as snow (Soegaard et al., 2001; Rasch & Caning, 2003). Continuous winter snow cover (1997–2003) is established each year between the beginning of September and the end of October, and lasts until mid-late June (Table 2.6). The length of the snow-cover period has decreased 50 days (10 days in spring and 40 days in autumn), from 304 days (1997/1998) to 253 days (2002/2003) (Table 2.6). This reduction is probably not caused by reduced snow precipitation but by increased thawing rates during summer and autumn (Table 2.6). The maximum annual snow depth varies between 0.48 m (1999/2000) and 1.32 m (2001/2002), and the average annual snow depth varies between 0.26 m (1999/2000) and 0.72 m (2001/2002) (Table 2.6).

In the period 1996–2003, the annual average FDD was –3,865 and the mean number of FD was 266, with an annual variation between –4,015 and –3,619 for FDD and 246 and 277 for FD (Table 2.6). The annual average (1996–2003) TDD was 408 and the number of TD was 100. From 1996 to 2003, TDD increased from 385 to 561 (46%) (Fig. 2.3b) indicating a higher thawing rate and a prolonged thawing period. The thawing period was prolonged 14 days (12%), indicating a longer thawing season in autumn (Table 2.6; Fig. 2.3b). For 1996–2003, the annual average GDD was 77 and the number of GD was 37. Since 1999, GD has increased from about 30 up to 49 yr^{-1} (a 63% increase) (Table 2.6).

Meteorological time series since 1961 exist for Daneborg, with an almost continuous gap betwee

Table 2.3 Monthly maximum, average and minimum values of air temperature, wind velocity, relative humidity, air pressure, shortwave radiation in and out, albedo, net radiation and uncorrected summer liquid precipitation based on Zackenberg data, 1995–2003. Winter precipitation (from September to June) is calculated from rise in the accumulation curves of recorded snow depth, 1997–2003. (*) indicates precipitation sum instead of average value.

	Jan.	Feb.	Mar.	Apr.	May	Jun.	Jul.	Aug.	Sept.	Oct.	Nov.	Dec.	Average
Air temperature 2.0 m (°C)													
Maximum	-2.9	-6.6	5.2	7.0	9.3	14.9	19.1	21.3	10.7	4.2	-3.1	6.8	-----
Average	-21.1	-20.0	-19.8	-14.5	-5.5	1.9	5.5	4.8	-1.5	-10.1	-15.8	-19.2	-9.6
Minimum	-36.7	-38.9	-38.4	-32.1	-21.8	-6.2	-2.6	-4.0	-13.0	-25.0	-27.8	-34.7	-----
Air temperature 7.5 m (°C)													
Maximum	-3.9	-0.3	-5.3	7.3	8.6	14.4	18.8	21.1	10.4	5.0	4.0	7.1	-----
Average	-19.9	-19.0	-12.6	-13.4	-5.3	1.8	5.2	4.7	-1.2	-9.3	-11.8	-18.0	-8.2
Minimum	-34.6	-37.0	-37.1	-30.8	-20.1	-5.6	-2.8	-3.5	-10.9	-23.7	-25.7	-33.0	-----
Wind velocity 2.0 m (m s^{-1})													
Maximum	20.7	25.6	22.3	22.6	17.6	13.1	13.0	12.3	16.9	25.6	20.1	21.6	-----
Average	3.1	3.9	2.8	2.4	2.2	1.7	2.4	2.3	2.5	3.1	3.0	3.0	2.7
Minimum	0.0	0.0	0.0	0.0	0.0	0.0	0.0	0.0	0.0	0.0	0.0	0.0	-----
Wind Velocity 7.5 m (m s^{-1})													
Maximum	29.5	22.5	17.1	24.5	19.9	15.1	15.9	14.9	15.6	20.1	24.2	25.4	-----
Average	3.7	4.7	3.5	2.7	2.6	1.9	2.7	2.6	2.9	3.7	3.5	3.7	3.2
Minimum	0.0	0.0	0.0	0.0	0.0	0.0	0.0	0.0	0.0	0.0	0.0	0.0	-----
Relative humidity 2.0 m (%)	96.7	98.9	95.1	97.6	98.5	99.9	100.0	100.0	99.3	99.4	96.3	97.1	-----
Maximum	63.7	69.3	68.1	69.2	77.3	82.7	82.3	79.5	73.5	69.3	66.0	63.8	72.0
Average	18.6	27.9	22.4	18.3	27.0	23.0	21.6	18.4	22.0	25.5	16.7	22.7	-----
Minimum													
Air Pressure (hPa)													
Maximum	1,036.9	1,042.0	1,066.3	1,034.9	1,35.4	1,023.3	1,026.4	1,028.6	1,037.9	1,035.6	1,035.6	1,042.5	-----
Average	1,004.5	1,003.1	1,009.6	1,013.3	1,013.0	1,009.8	1,006.2	1,005.9	1,007.4	1,008.7	1,008.6	1,007.6	1,008.1
Minimum	953.0	956.2	961.3	955.8	992.8	989.2	983.5	968.6	962.5	960.6	960.6	972.0	-----
Short-wave Rad In 2.0 m (W m^{-2})													
Maximum	15.7	166.2	469.2	730.9	833.0	920.0	863.0	748.0	537.3	281.5	24.2	11.9	-----
Average	0.6	6.8	61.8	172.1	270.5	292.9	218.9	148.9	78.0	16.0	0.7	0.3	105.6
Minimum	0.0	0.0	0.0	0.0	0.0	0.0	0.0	0.0	0.0	0.0	0.0	0.0	-----
Short-wave Rad Out 2.0 m (W m^{-2})													
Max	6.2	127.3	386.0	661.5	682.6	741.0	348.0	255.2	370.3	192.6	17.6	3.2	-----
Average	0.5	5.7	53.0	140.8	218.3	144.0	25.2	18.2	23.4	10.2	0.3	0.1	53.5
Minimum	0.0	0.0	0.0	0.0	0.0	0.0	0.0	0.0	0.0	0.0	0.0	0.0	-----
Albedo	81.8	83.2	85.6	81.7	80.8	49.6	11.5	12.2	29.9	64.0	61.0	88.4	60.8
Net Rad 2.0 m (W m^{-2})													
Maximum	17.4	34.2	73.8	106.1	172.7	633.6	609.4	537.5	328.8	124.8	12.3	16.8	-----
Average	-23.2	-19.5	-21.5	-20.1	-4.4	86.8	127.8	69.8	5.7	-26.5	-24.7	-17.3	11.1
Minimum	-92.8	-74.0	-101.5	-83.9	-165.4	-128.5	-60.9	-101.6	-123.7	-169.9	-198.9	-186.4	-----
Precipitation sum (mm w.eq.)	30.7	56.0	16.7	14.5	15.5	10.4	15.9	18.1	8.4	21.7	39.1	26.2	273.2(*)
Maximum summer intensity (mm/h)	-----	-----	-----	-----	-----	6.3	4.7	4.8	-----	-----	-----	-----	-----

Table 2.4 Mean monthly air temperature (MMAT)(°C) at Daneborg meteorological station approximately 20 km southeast of the Zackenberg River drainage basin, 1995–2002 (www.dmi.dk).

	Jan.	Feb.	Mar.	Apr.	May	Jun.	Jul.	Aug.	Sept.	Oct.	Nov.	Dec.	Average
Mean monthly air temperature,°C	-19.8	-19.9	-18.9	-13.3	-4.9	2.1	4.7	4.7	-1.5	-9.9	-14.7	-19.2	-9.2

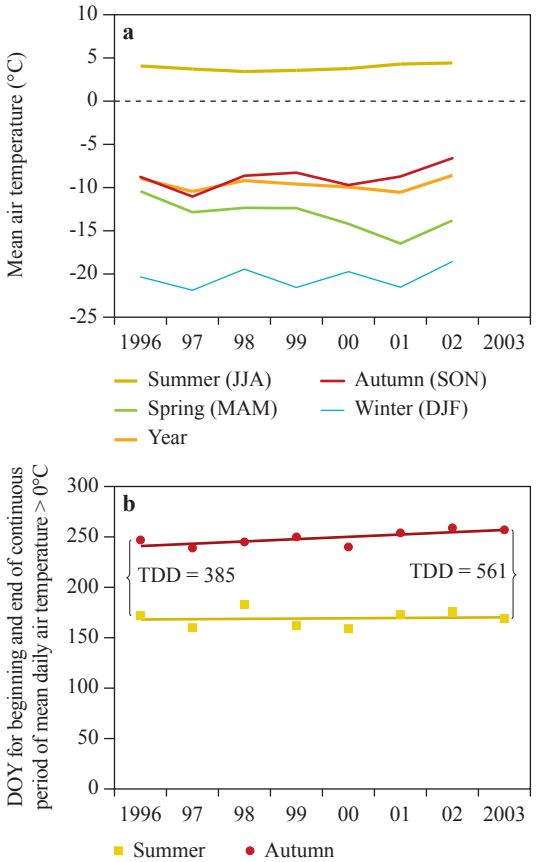

Figure 2.3 (a) Mean annual and seasonal air temperature at Zackenberg in the period 1996–2002. The abbreviations mean: DJF (December–January–February), MAM (March–April–May), JJA (June–July–August) and SON (September–October–November). **(b)** Day of year (DOY) for the beginning and the end of the continuous period of mean daily air temperatures above 0°C in Zackenbergdalen (1996–2003). The trend lines (linear regression) indicate lengthening of the thawing season in autumn (16 days) (1996–2003) and shortening in spring (2 days), indicating a net lengthening of the thawing season of 14 days. Furthermore, the increase in Thawing Degree Days (TDD) from 385 (1996) to 561 (2003) (46% increase) is illustrated.

AT at Zackenberg (–9.6°C) (1995–2003). A linear relation exists for MMAT between Zackenberg and Daneborg (1995–2002) (Eq. 3):

$$MMAT_{Zackenberg}(°C) = 1.03 MMAT_{Daneborg}(°C) + 0.24 \quad (R^2 = 0.99;\ p<0.01) \qquad (3)$$

where 1.03 indicates a more pronounced continental climate at Zackenberg. Between Zackenberg and Scoresbysund (1995–1999) (Eq. 4), and between Zackenberg and Danmarkshavn (1995–1999) (Eq. 5), the linear relations are, respectively:

$$MMAT_{Zackenberg}(°C) = 1.31 MMAT_{Scoresbysund}(°C) - 2.62 \quad (R^2 = 0.97;\ p<0.01) \qquad (4)$$

and

$$MMAT_{Zackenberg}(°C) = 0.97 MMAT_{Danmarkshavn}(°C) + 1.41 \quad (R^2 = 0.97;\ p<0.01) \qquad (5)$$

In the period 1968–99, the MAAT in Scoresbysund, Daneborg and Danmarkshavn increased c. 4°C ($p<0.01$), c. 2°C ($p<0.01$) and c. 1°C ($p<0.01$), respectively, (Cappelen et al., 2001). The highest changes in MMAT for the three locations between 1968 and 1999 are in autumn and winter, while spring and summer temperatures are quite stable.

2.5.2 Runoff

At Zackenberg, the date of river break-up at the hydrological measuring station has varied from year to year between 30 May (2003, DOY 150) and 10 June (1998, DOY 161) during the period 1996–2003 (Table 2.7). Approximately 10–20% of the snow pack in the valley Zackenbergdalen normally melts before the river breaks up (Table 2.6; Table 2.7). The river discharge varies between 122 million $m^3\ yr^{-1}$ (corresponding to a runoff of 239 mm yr^{-1}) for 1996 and 306 million $m^3\ yr^{-1}$ (corresponding to a runoff of 598 mm yr^{-1}) for 2002 (Table 2.7; Fig. 2.4). The mean annual river discharge for the period 1996–2003 was 188 million $m^3\ yr^{-1}$, corresponding to a runoff of 368 mm yr^{-1}. Annual runoff generally peaks in the beginning of the runoff season between DOY 161 and 190, and is caused mainly by melting of snow, except for 1998 (16 August, DOY 228) (Table 2.7; Fig. 2.4), when an extreme flood occurred (123.0 $m^3\ s^{-1}$) after 17 hours with rain (23.9 mm) and a 60-hour period with maximum and mean air temperatures of 8.8°C and 6.5°C, respectively. Maximum river discharge (158.9 $m^3\ s^{-1}$) was measured 10 June 2002 (DOY 161) after a warm period (thirty hours with a mean air temperature of 5.3°C) resulting in increased snow melt (Table 2.7; Fig. 2.4).

2.5.3 Suspended sediment load, suspended organic matter load, organic/inorganic carbon and water conductivity

Total annual transport of suspended sediment from the Zackenberg River to Young Sound/Tyrolerfjord (1997–2003) is in the range of 15,000 to 130,000 t yr^{-1}

Table 2.5 Wind statistics: Wind direction (7.5 m) and wind velocity (7.5 m) based on data from 1997, 1998, 2000 and 2002. Wind statistics for 1995, 1996, 1999, 2001 and 2003 are not included due to lack of complete time series.

	N	NNE	NE	ENE	E	ESE	SE	SSE	S	SSW	SW	WSW	W	WNW	NW	NNW	Calm
Wind direction, 7.5 m (%)	12.2	3.4	2.5	2.7	4.5	7.5	8.3	5.0	3.8	2.8	2.5	2.7	2.7	3.4	6.9	24.9	4.4
Mean wind velocity, 7.5 m ($m\ s^{-1}$)	4.2	2.7	2.6	2.3	2.1	2.2	2.4	2.4	2.4	2.3	2.1	2.4	2.4	2.7	3.7	5.1	
Maximum wind velocity, 7.5 m ($m\ s^{-1}$)	29.5	25.4	19.4	15.6	10.4	10.3	18.1	16.2	9.9	13.4	12.2	15.9	23.5	19.0	25.1	25.8	

	1995	1996	1997	1998	1999	2000	2001	2002
Mean annual wind velocity, 7.5 m ($m\ s^{-1}$)	No data	3.0	3.4	3.2	3.7	3.1	3.2	3.0
Maximum wind velocity ($m\ s^{-1}$) and wind direction (deg.), 7.5 m.	No data	23.1 (84 deg.)	26.2 (359 deg.)	29.5 (356 deg.)	22.0 (329 deg.)	23.5 (260 deg.)	25.0 (4 deg.)	24.5 (338 deg.)

Table 2.6 Air temperature (2.0 m), freezing degree days (FDD), freezing days (FD), thawing degree days (TDD), thawing days (TD), growing degree days (GDD), growing days (GD) and snow cover for Zackenberg (1996–2003). Snow depletion data for the valley Zackenbergdalen are from Hinkler et al. (2002, 2003). Data from 1995 is not included, due to lack of time series for the entire years.

Air Temperature, 2.0 m (C) and day of year (DOY)	1996	1997	1998	1999	2000	2001	2002	2003
Maximum (°C)	16.6 (203)	21.3 (224)	13.8 (197)	15.2 (220)	19.1 (189)	12.6 (213)	14.9 (179)	16.7 (198)
Average (°C)	-9.2	-10.1	-10.0	-9.5	-10.0	-9.7	-8.6	-9.2
Minimum (°C)	-33.7 (4)	-36.2 (15)	-38.9 (54)	-36.3 (88)	-36.7 (29)	-35.1 (63)	-37.7 (66)	-34.0 (27)
Continuous period of mean daily air temperature above 0°C, 2.0 m	DOY 172–247 (20 JUN – 3 SEP)	DOY 160–239 (9 JUN – 27 AUG)	DOY 183–245 (2 JUN – 2 AUG)	DOY 162–250 (11 JUN – 7 SEP)	DOY 159–240 (7 JUN – 27 AUG)	DOY 173–254 (22 JUN – 11 SEP)	DOY 176–259 (25 JUN – 16 SEP)	DOY 169–257 (18 JUN – 14 SEP)
Freezing degree days (FDD) and Freezing days (FD) (air temperature < 0°C)	-3,646 (271 days)	-4,015 (271 days)	-3,855 (276 days)	-3,833 (263 days)	-4,045 (277 days)	-3,984 (263 days)	-3,619 (246 days)	-3,924 (259 days)
Thawing degree days (TDD) and Thawing days (TD) (air temperature > 0°C)	385 (95 days)	354 (94 days)	333 (89 days)	358 (102 days)	370 (89 days)	433 (102 days)	471 (119 days)	561 (106 days)
Growing degree days (GDD) and Growing days (GD) (air temperature > 5 °C)	72 (32 days)	54 (31 days)	44 (30 days)	65 (27 days)	80 (35 days)	78 (43 days)	77 (44 days)	147 (49 days)

	1996-1997	1997-1998	1998-1999	1999-2000	2000-2001	2001-2002	2002-2003
Continuous snow cover at the climate station.		0.87	1.23	0.48	0.65	1.32	0.60
Maximum snow depth (m)	No data	0.43	0.56	0.26	0.35	0.72	0.20
Average snow depth (m)		DOY 241–180	DOY 244–187	DOY 303–168	DOY 266–176	DOY 287–172	DOY 280–168
Period with snow cover (days)		(304 days)	(308 days)	(230 days)	(275 days)	(250 days)	(253 days)
10% snow depletion in Zackenbergdalen (DOY)	163	158	175	-----	152	157	-----
20% snow depletion in Zackenbergdalen (DOY)	169	166	179	159	156	162	152
50% snow depletion in Zackenbergdalen (DOY)	176	182	186	164	167	170	163
75% snow depletion in Zackenbergdalen (DOY)	183	192	195	169	177	179	166
90% snow depletion in Zackenbergdalen (DOY)	195	198	214	175	186	189	173
100% snow depletion in Zackenbergdalen (DOY)	-----	-----	-----	238	238	-----	221

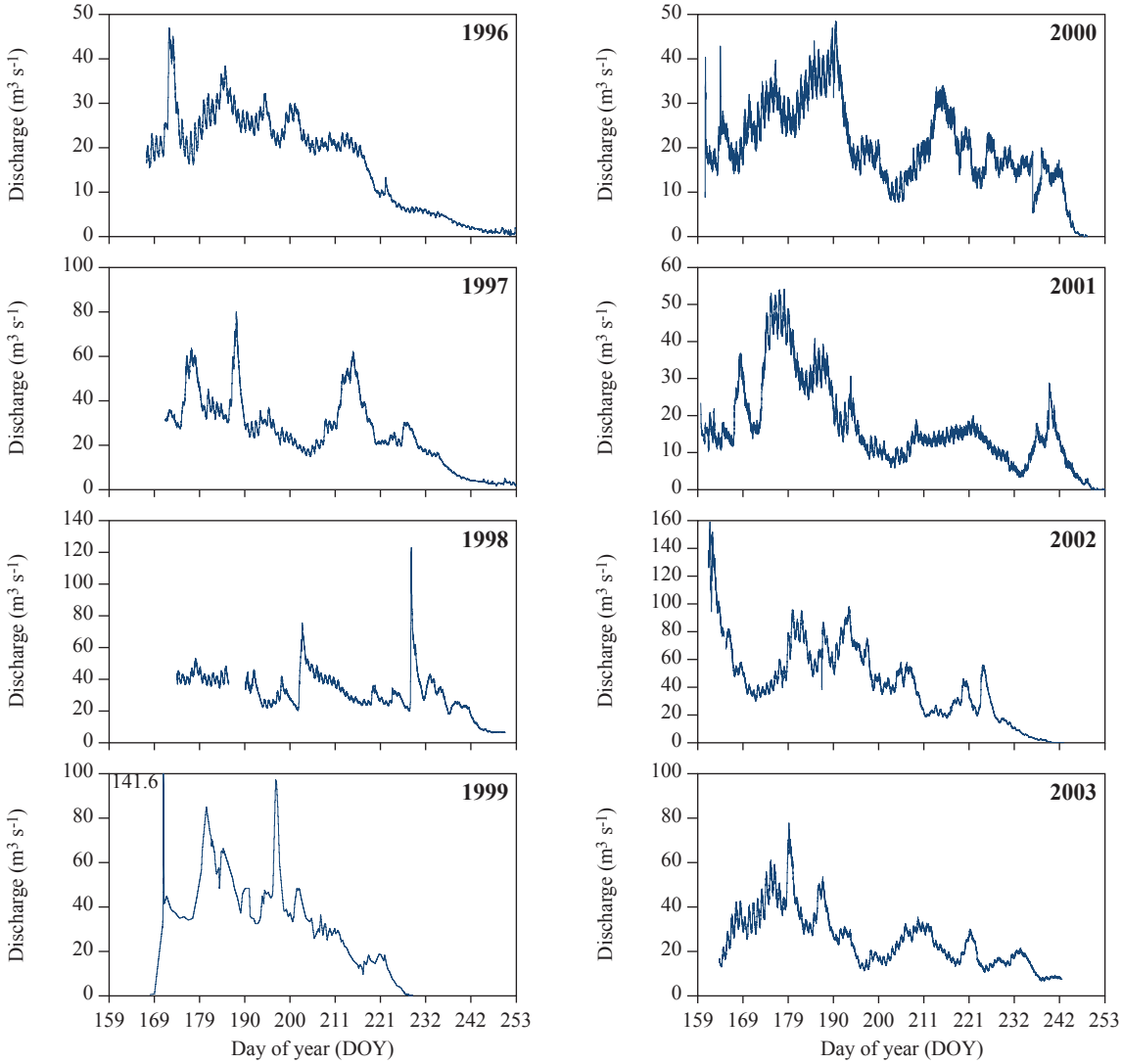

Figure 2.4 River discharge from the Zackenberg River based on 15-minute values from DOY 159–262 (1996–2003). Discharge curve for 1999 is based on manual readings, as the hydrometric station was flushed away during a violent break-up flood. Note the difference in ordinate scale.

(Table 2.8). This corresponds to a specific annual suspended sediment load between 29 and 253 t km^{-2} yr^{-1} for the Zackenberg River drainage basin. The average concentration of suspended sediment in the Zackenberg River is between 0.1 and 0.2 g l^{-1} (Table 2.8; Fig. 2.5). Peaks in suspended sediment transport are often observed during periods with high river discharge following precipitation events and high melting rates. Maximum concentration of suspended sediment (46.9 g l^{-1}) was measured in 1998 (DOY 228) during/after the 17-hour rainstorm. During this "extreme event", c. 105,000 t of suspended sediment was transported through Zackenberg River. The total suspended sediment transport during this event (c. 3 days) was 1.7 to 7.0 times larger than the total annual transport in the remaining years of the period 1997–2003 (Table 2.8).

Suspended organic matter constitutes 5–12% of the suspended sediment on an annual basis (Table 2.8). Total annual transport of suspended organic matter from Zackenberg River to Young Sound/Tyrolerfjord (1997–2003) is in the range of 1,100 to 11,500 t yr^{-1} (Table 2.8). This corresponds to a specific annual suspended organic matter load between 2 and 22 t km^{-2} yr^{-1} for the Zackenberg River drainage basin. The average concentration of suspended organic matter in the Zackenberg River is between 0.01 and 0.21 g l^{-1} (Table

Table 2.7 Date of break-up, period of measured river discharge and monthly and annual river discharge in the Zackenberg River measured at the hydrometric station (1996–2003).

	1996	1997	1998	1999	2000	2001	2002	2003
Break-up of river (DOY)	154	155	161	160	160	159	155	150
Period of measured river discharge (DOY)	167-252	172-252	174-246	168-229	160-249	159-251	161-242	164-243
Peak river discharge ($m^3 s^{-1}$)	47.0	80.1	123.0	141.6	48.5	54.1	158.9	77.8
Date of peak river discharge (DOY)	172	188	228	171	190	178	161	180
Total measured river discharge June, million m^3 and (mm w.eq.)	32.74 (64)	44.64 (87)	50.09 (98)	41.14 (80)	47.10 (92)	52.79 (103)	110.39 (216)	71.03 (139)
Total measured river discharge July, million m^3 and (mm w.eq.)	67.30 (131)	80.22 (157)	98.50 (192)	122.82 (240)	61.32 (120)	47.40 (93)	149.73 (292)	71.16 (139)
Total measured river discharge August, million m^3 and (mm w.eq.)	21.43 (42)	60.66 (118)	78.48 (153)	16.96 (33)	46.64 (91)	33.90 (66)	46.07 (90)	42.77 (84)
Total measured river discharge September, million m^3 and (mm w.eq.)	0.73 (1)	2.43 (5)	4.28 (8)	No Data	0.37 (1)	3.17 (6)	No Data	No Data
Annual measured river discharge, million m^3 and (mm w.eq.)	122.18 (239)	187.95 (367)	231.37 (452)	180.93 (353)	155.42 (304)	137.26 (268)	306.19 (598)	185.20 (361)

Table 2.8 Suspended sediment yield, suspended organic matter yield, organic/inorganic carbon and water conductivity in the Zackenberg River measured at the hydrometric station at 8 am (1997–2003).

	1997	1998	1999	2000	2001	2002	2003
Suspended sediment transport (t) and specific suspended sediment load (t km^{-2} yr^{-1})	29,444 (57.52)	130,133 (254.17)	18,761 (36.64)	14,958 (29.22)	16,906 (33.02)	60,667 (118.49)	18,245 (35.64)
Suspended sediment (g l^{-1})							
Maximum	1.914	46.925	0.444	0.248	0.816	2.994	0.319
Average	0.112	2.587	0.089	0.160	0.119	0.132	0.096
Minimum	0.004	0.007	0.002	0.006	0.018	0.039	0.041
Suspended organic matter transport (t)	1.643	11.551	2.297	1.340	1.101	3.299	1.353
Suspended organic matter (g l^{-1})							
Maximum	0.027	3.845	0.040	0.297	0.083	0.026	0.046
Average	0.009	0.213	0.007	0.012	0.007	0.009	0.007
Minimum	0.003	0.003	0.002	0.002	0.002	0.003	0.004
Carbon (t)							
Particulate organic carbon (POC)							416
Dissolved organic carbon (DOC)	No data	No data	No data	No data	No data	No data	421
Dissolved inorganic carbon (DIC)							342
Total transport of carbon							1,179
Water conductivity (µS cm^{-1})							
Maximum	66	302	104	101	118	67	58
Average	29	100	43	31	28	24	16
Minimum	18	23	25	19	11	11	11

2.8), with a maximum concentration of 3.8 g l^{-1} measured during the extreme event in 1998.

Organic carbon is transported through the fluvial system in both dissolved (DOC) and particulate form (POC). Results from 2003 show that the suspended organic matter determined by LOI contains 35% C (POC) (Table 2.9). The total fluvial transport of carbon also includes dissolved inorganic carbon (DIC) from dissolution of soil carbonate minerals. Based on data from the 2003 runoff season the three different forms of carbon are almost equal in amount: POC (416 t yr^{-1}), DOC (421 t yr^{-1}) and DIC (342 t yr^{-1}). The total carbon transport for 2003 is accordingly estimated at approximately 1,179 t yr^{-1} (Table 2.9). Peaks in POC are observed during periods with high river discharge, and the relation between suspended sediment concentration (Cs) and POC concentration is linear (Eq. 6):

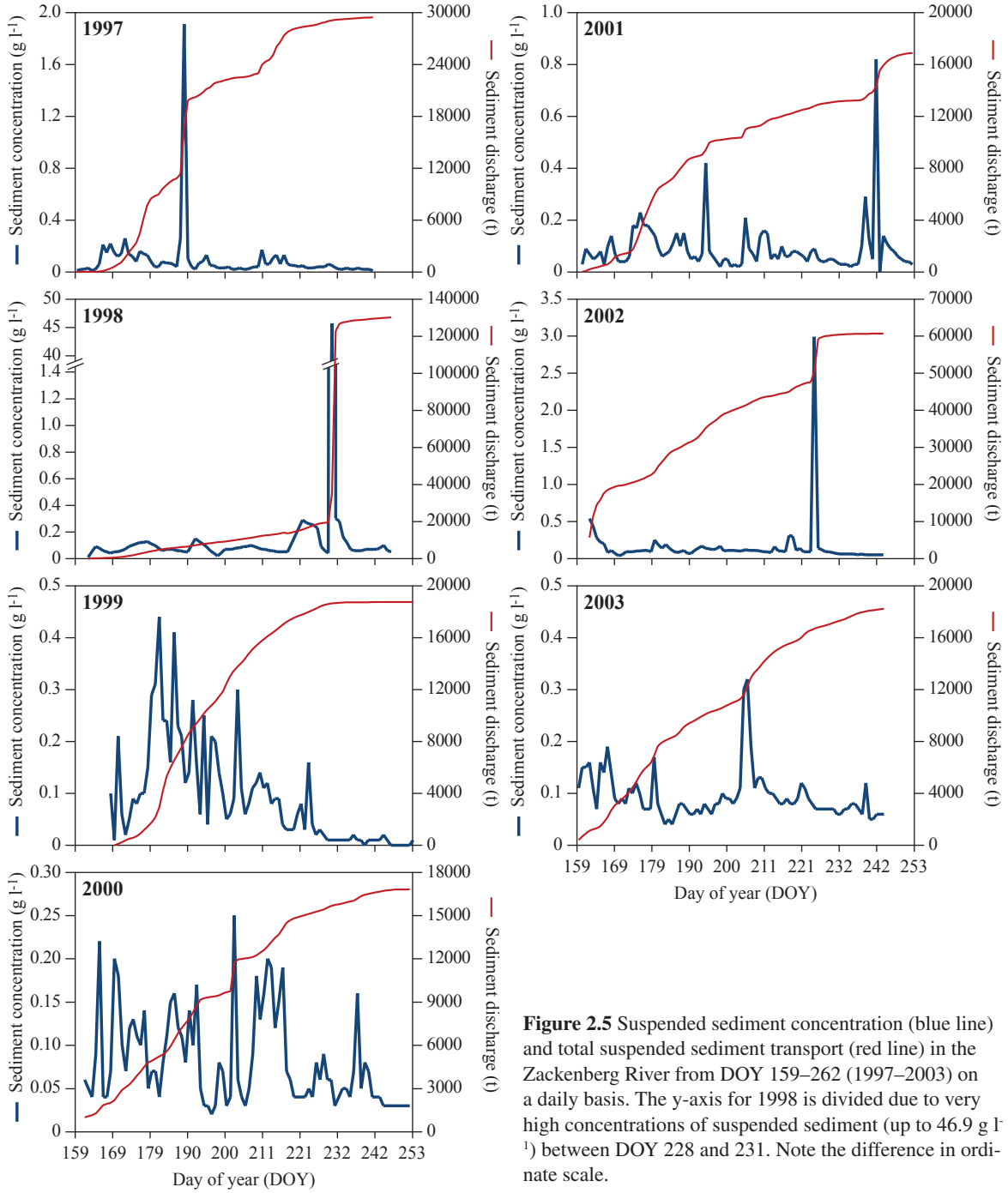

Figure 2.5 Suspended sediment concentration (blue line) and total suspended sediment transport (red line) in the Zackenberg River from DOY 159–262 (1997–2003) on a daily basis. The y-axis for 1998 is divided due to very high concentrations of suspended sediment (up to 46.9 g l^{-1}) between DOY 228 and 231. Note the difference in ordinate scale.

$$POC\ (mg\ l^{-1}) = 0.02Cs\ (mg\ l^{-1}) + 0.37 \quad (R^2 = 0.60;\ p<0.01) \qquad (6)$$

Average water conductivity in the Zackenberg River ranges between 16 and 100 µS cm^{-1} (1997–2003), with a maximum conductivity at 302 µS cm^{-1} measured in 1998 during the 17-hour rainstorm (Table 2.8).

Average concentration values for different anions and cations are given in Table 2.9. The input of nitrate (NO_3^-) from the Zackenberg River to Young Sound is estimated at 13 t yr^{-1} in 2003 based on the NO_3^- concentrations in the river water at 8 am. Nitrate concentrations generally vary during the runoff season between 0.08 mg l^{-1} and 0.36 mg l^{-1} (1997–2003;

Table 2.9 Chemical characteristics of the Zackenberg River water. Maximum, average and minimum values for anions and cations measured in water samples collected at 8 am during 1997–2003. Values from the extreme event in 1998 (DOY 288) are not included.

	Cl-	NO_3^{2-}	SO_4	Na^+	Mg^{2+}	K^+	Ca^{2+}	Fe^{2+}	Al^{3+}
Anions and cations (mg l^{-1})									
Maximum	3,02	0,36	29,98	3,73	14,71	0,75	13,31	0,74	0,87
Average	0,59	0,16	6,17	0,80	0,92	0,42	3,51	0,23	0,28
Minimum	0,14	0,08	1,56	0,31	0,40	0,22	1,38	0,06	0,07

Table 2.9). Peak concentrations are found during the first weeks (2–3 weeks) after river break up, reflecting high river discharge. This results in a peak input of NO_3^- to Young Sound in June.

2.5.4 Total river discharge, suspended sediment yield, suspended organic matter yield and organic/inorganic carbon to Young Sound/Tyrolerfjord

The annual river discharge from the Zackenberg River (Zackenberg River drainage basin), varies between 122 million m^3 yr^{-1} (239 mm yr^{-1}) and 306 million m^3 yr^{-1} (598 mm yr^{-1}) (Table 2.7). To estimate the river discharge from the total Young Sound/Tyrolerfjord drainage basin it seemed reasonable to upscale from the Zackenberg River drainage basin (512 km^2) to the Young Sound/Tyrolerfjord drainage basin (2,620 km^2), because the Zackenberg River drainage basin, due to its intermediate position in the east-west running drainage basin of Young Sound/Tyrolerfjord, probably represents an average in terms of climate. Consequently, the contribution of river discharge to the Young Sound/Tyrolerfjord system is estimated to vary between 630 and 1,570 million m^3 yr^{-1} with an average of 970 million m^3 yr^{-1} (1996–2003; Table 2.10).

Based on the same assumptions it is suggested that the annual contribution of suspended sediment to the Young Sound/Tyrolerfjord system varies between 77,000 and 670,000 t yr^{-1} with an average of 210,000 t yr^{-1} (1997–2003; Table 2.10). The annual contribution of suspended organic matter is estimated to vary between 6,000 and 59,000 t yr^{-1} with an average of 17,000 t yr^{-1} (1997–2003). The total carbon discharge (POC, DOC and DIC) is 6,033 t yr^{-1} (2003) and the total NO_3^- discharge is 66.5 t yr^{-1} (2003; Table 2.10).

2.6 Discussion

Early in the runoff season, runoff is controlled mainly by the Zackenberg lowland snow melt (R_{snow}) (phase change from solids to liquids) (Rasch et al., 2000), which in turn depends on (1) the amount of available energy fluxes for melting, and (2) the available snow cover in the lowland, quantified by snow depth and snow depletion (Fig. 2.2; Table 2.6). Table 2.6 shows the snow depth and the snow depletion for the valley Zackenbergdalen (lowland), indicating that 10–20% of the snow cover melts before river break-up, which occurs within the first 10 days of June. The meltwater is probably stored as internal accumulation in the remaining snow before the river breaks up. From mid June to the end of June (2–3 weeks) 50% of the lowland snow melts, and by the end of July at least 90% of the snow cover disappeared. This results in a year-

Table 2.10 Rough estimate of the river discharge, suspended sediment yield, organic matter yield and organic/inorganic carbon from the Young Sound/Tyrolerfjord drainage basin.

	1996	1997	1998	1999	2000	2001	2002	2003	Average
Rough estimate of annual river discharge from the Young Sound/Tyrolerfjord drainage basin (million m^3)	630	960	1,180	930	800	700	1,570	950	970
Rough estimate of annual suspended sediment yield from the Young Sound/Tyrolerfjord drainage basin (thousand t)	No data	150	670	100	80	90	310	90	210
Rough estimate of annual organic matter yield from the Young Sound/Tyrolerfjord drainage basin (thousand t)	No data	8	59	12	7	6	17	7	17
Rough estimate of annual carbon yield from the Young Sound/Tyrolerfjord drainage basin (thousand t)	No data	No data	No data	No data	No data	No data	No data	6	6

Photo: Charlotte Sigsgaard

View from the digital camera set up 477 m ASL (16 July 2005). Looking SE at the Zackenberg river delta and Young Sound.

to-year variation in runoff variability through June and July (Fig. 2.4), controlled mainly by snow melt in the lowland, and in part by precipitation events. Multiple regression shows significant correlation (R^2 = 0.84; p<0.01) between the total June-July discharge and winter average snow depth, and a less significant correlation (R^2 = 0.33; p<0.10) between the total June-July discharge and the total June-July precipitation, confirming the effect of snow melt in the early part of the runoff season. Maximum peak discharge (47–159 $m^3 s^{-1}$) is observed in June during the first 1/3 of the runoff period due to the lowland snow melt, except for the extreme 17-hour rainstorm in August 1998 (Fig. 2.4; Table 2.7).

In years with relatively high average snow depth 1999 (0.56 m) and 2002 (0.72 m) snow depletion is delayed compared with other years with lower average snow depth. The date for river break-up does not, however, change significantly in relation to average snow depth (no trend observed). River break-up occurs from DOY 154 to 161 (1996–2003; Table 2.7), approximately 16 to 20 days after the first continuous melting of snow has started at the Zackenberg Meteorological Station (Fig. 2.2; Table 2.6). In the investigation period 1996–2003 the two highest runoff peaks, 141.6 $m^3 s^{-1}$ (1999) and 158.9 $m^3 s^{-1}$ (2002), both in the early part of the melt season, correlate strongly with the lowland snow melt and the average snow depth.

Later in the runoff season when drainage from the lowland areas ceases, the runoff distribution is controlled by melting of the active layer (R_{ground}), by rainfall (R_{rain}), by melting of glaciers ($R_{glacier}$) and snow patches (R_{snow}) on the high-lying plateaus, above 1,000 m ASL (Rasch et al., 2000). Glaciers cover approximately 20% (101 km^2) of the drainage basin and, therefore, glacier meltwater will probably constitute an increasing part of the discharge throughout the runoff season as the snow cover decreases in the drainage basin, causing a more pronounced glacier runoff regime due to the melt rate from the glaciers located in the western part of the drainage basin (Fig. 2.1b). The form and size of the pronounced glacier runoff regime will probably be diminished and delayed through lake Store Sø on its way to Young Sound/Tyrolerfjord. This indicates a meltwater travel time of minimum 12 hours through the catchment (Rasch, 1999).

During the investigation period from 1996–2003, Thawing Degree Days (TDD) increased 46% while Thawing Days (TD) increased 12% (Table 2.6; Fig. 2.3b) mainly due to the increasing air temperature in autumn (0.4°C yr^{-1}; p<0.05) (Fig. 2.3a). This results in an intensified thawing rate, a prolonged thawing period in autumn (16 days) and a shorter snow cover period in spring (12 days) and autumn (39 days) (Table 2.6). This probably does not result in better growing conditions for vegetation due to the limited

Table 2.11 Annual water balance estimates (from September to August) from the Zackenberg drainage basin (1997–2003). Precipitation (P): winter precipitation is calculated from rise in the accumulation curves of recorded snow depth and summer precipitation from tipping-bucket measurements. Evapotranspiration (ET) (1998/1999 to 2002/2003) is calculated from linear regression based on evapotranspiration (ET) (1995/1996 to 1997/1998) and Thawing Degree Days (TDD) (1995/1996 to 1997/1998). Sublimation from snow is included in ET. Runoff (R) is measured at the hydrometric station, and storage (ΔS) is calculated as a residual term ($\Delta S = P - ET - R$) in the water balance. Snow drifting within the catchment and from nearby catchments is not included in the water balance.

	Precipitation (P) (mm w.eq.)	Evaporation (ET) (mm w.eq.)	Runoff (R) (mm w.eq.)	Storage (ΔS) (mm w.eq.)
1997–1998	259	68	448	-277
1998–1999	403	80	361	-58
1999–2000	199	85	304	-210
2000–2001	225	113	263	-171
2001–2002	370	129	604	-383
2002–2003	183	169	361	-367
Average	273	107	390	-244

amount of solar radiation in the beginning of October (Table 2.4). The longer autumn thawing period and the shorter autumn snow cover period indicate a longer period of meltwater release from exposed glacier surfaces, and, furthermore, an increase in runoff during the investigation period (Table 2.7). Precipitation (P) in the investigation period (1997–2003) is almost constant, 180–260 mm, except for two outliers 370 mm (2001/2002) and 403 mm (1998/1999) (Table 2.10) and the evapotranspiration (ET) during the investigation period varies between 68 mm (1997/1998) and 169 mm (2002/2003) (Table 2.11). Therefore, the increasing trend in annual runoff during the period (1996–2003) is likely not controlled by changes in precipitation or evapotranspiration but rather by increasing meltwater release from glacier storage (ΔS) (Table 2.11). This suggests a negative glacier mass balance.

Extensive glacier cover occurs in the western part of the Zackenberg River drainage basin (Fig. 2.1b). Subglacial erosion, which depends on the bedrock and the glacier dynamics, is probably a significant sediment contributor to the Zackenberg River. On the other hand, the lake Store Sø (Fig. 2.1b) acts as a reservoir where bed load and suspended sediment from the western part of the drainage basin is trapped. The retained sediment depends on the volume of the lake relative to the inflow (Hasholt, 2003). The trap efficiency of Store Sø has not been measured, but the lake undoubtedly lowers the suspended sediment transport from the Zackenberg drainage basin.

For the entire Zackenberg River drainage basin (512 km^2), the specific annual suspended sediment load is 29 to 253 t km^{-2} yr^{-1} (1997–2003; Table 2.8) during the investigation period. Results from reconnaissance along the Zackenberg River indicate that a major part of the suspended sediment in the river originates from the areas with Cretaceous and Tertiary sandstone in the eastern part of the catchment (Fig. 2.1b), indicating that the main contribution area is less than 512 km^2, and, furthermore, that specific yields are higher than 253 t km^{-2} yr^{-1}. River water from this part of the drainage basin does not pass through Lake Store Sø.

Recent studies on sediment transport to the Arctic Oceans (e.g. Borgen, 1996; Hasholt, 1996; Hasholt, 2003; Borgen & Bønsnes, 2003; pers. comm. Hasholt, 2005) suggest a specific sediment transport from glaciated basins in Greenland of c. 1,000 t km^{-2} yr^{-1} while non-glaciated basins have specific yields of c. 5 t km^{-2} yr^{-1}, and, in Svalbard, 586 t km^{-2} yr^{-1} from glaciated basins and 82.5 t km^{-2} yr^{-1} from non-glaciated basins. The lower values of specific annual suspended sediment load in the Zackenberg River drainage basin (29 to 253 t km^{-2} yr^{-1}) compared with other Arctic drainage basins might be due to the physical settings in Zackenberg, where glaciers are located in less erodable bedrock of Caledonian gneiss

Photo: Charlotte Sigsgaard

Water discharge measurement in the Zackenberg River.

and granite, resulting in a smaller suspended sediment load compared with other Arctic catchments. It might also be a result of the method used in Zackenberg, where sediment transport is based on the sediment concentration in water sampled at 8 am. In order to evaluate how representative the concentration at 8 am is compared with the average diurnal concentration, fluctuations in sediment concentrations throughout the day must be obtained. In periods with no significant rainfall events, a regular diurnal variation in discharge is observed, with a maximum discharge close to midnight and a minimum discharge around midday. Consequently, a similar diurnal variation in suspended matter is to be expected. Corresponding discharge and sediment concentrations at 8 am and 6 pm measured in 1997, show that the correlation in samples collected at 8 am and samples collected at 6 pm is not the same. There is a tendency towards the river carrying more sediment in the evening than in the morning at equal discharges, presumably due to differences in the river's capacity for carrying suspended material in the rising and falling stages. This indicates that the total sediment concentration based on the 8 am concentrations may be underestimated to some extent.

The variation in dissolved load is reflected in the conductivity of the water. Maximum conductivity in Zackenberg River (66–118 µS cm^{-1}) (1997–2003; Table 2.8) is usually measured during the first days of water discharge. This phenomenon has been ascribed to solutes being washed out of the snow during the first snowmelt (Rasch et al., 2000). After a runoff period of 3–5 days, the conductivity decreases to a level of c. 10–25 µS cm^{-1}, and remains fairly constant over the season, except for a peak observed after a period with rain, e.g. 302 µS cm^{-1} after the extreme event in 1998 (DOY 228; Table 2.8). During and after rain, active layer interflow contributes soil water to the river, and soil water is relatively rich in solutes compared with other sources. An estimate of the dissolved load based on the conductivity measurements is approximately 5,000 t yr^{-1} for the Zackenberg River drainage basin, suggesting that the suspended sediment load constitutes approximately 80% of the total load while bed load and dissolved load constitute the remaining load. This seems reasonable, as the river bed and banks at the cross section near the hydrometric station consist mainly of coarse material like cobbles and boulders, resulting in a stable profile without significant bed-load transport. A rough estimate of the dissolved yield to Young Sound/Tyrolerfjord based on conductivity measurements from Zackenberg River gives approximately 26,000 t yr^{-1}.

2.7 Conclusions

The study explored the meteorological conditions, river discharge, suspended sediment transport, suspended organic matter transport and river water conductivity in the Zackenberg River drainage basin (1995–2003). The data set indicates:

- An increase in mean annual air temperature of c. 0.1°C yr^{-1} (non-significant), and a seasonal warming in all seasons (highest in autumn; 0.4°C yr^{-1} ;$p<0.05$, except in spring, when air temperature decreased 0.7°C yr^{-1} ($p<0.01$).
- An increase in thawing period in autumn (16 days longer) and a decreasing thawing period in spring (2 days shorter), corresponding to a net increase in the thawing period of 14 days (1996–2003).
- A decrease in number of days (approximately 50 days less) with continuous snow cover from 304 days in season 1997/1998 to 253 days in 2002/2003, due to an increasing number of thawing degree days.
- An increasing annual trend in river discharge from Zackenberg River in the range of 122–306 million m^3 yr^{-1} and a river discharge (roughly estimated) from the entire catchment area of the Young Sound/Tyrolerfjord system in the range of 630–1,570 million m^3 yr^{-1}.
- Annual transport of suspended sediment from the Zackenberg River in the range of 15,000 to 130,000 t yr^{-1}, corresponding to a specific load between 29 and 253 t km^{-2} yr^{-1}.
- Annual transport of carbon and nitrate, respectively, from the Zackenberg River of 1,179 t yr^{-1} and 13 t yr^{-1} in 2003.
- Roughly estimated total annual suspended sediment yield from the entire catchment area of Young Sound/Tyrolerfjord to the sea of between 77,000 and 670,000 t yr^{-1}.
- Annual transport of suspended organic matter from the Zackenberg River in the range of 1,100 to 11,500 t yr^{-1}, corresponding to a specific load between 2 and 22 t km^{-2} yr^{-1}.
- Roughly estimated total annual suspended organic matter yield from the entire catchment of the Young Sound/Tyrolerfjord system of between 6,000 and 59,000 t yr^{-1}.
- Roughly estimated total annual carbon yield (POC, DOC and DIC) from the entire catchment of the Young Sound/Tyrolerfjord system of 6,033 t yr^{-1} and a nitrate yield of 66.5 t yr^{-1} for 2003.
- Maximum water conductivity (c. 100 µS cm^{-1}) during the first days of water discharge, indicating high dissolved load concentrations in the first meltwater being washed out of the snow. After a runoff period of 3–5 days the conductivity decreases to a level of c. 10–25 µS cm^{-1}, and stays more or less constant during the rest of the season. Based on conductivity measurements, the dissolved load from the Zackenberg River is c. 5,000 t yr^{-1}. A roughly estimated annual dissolved yield from the entire catchment of the Young Sound/Tyrolerfjord system gives c. 26,000 t yr^{-1}.

2.8 Acknowledgements

The Zackenberg Ecological Research Operations is acknowledged for providing access to ecosystem monitoring data from the Zackenberg Station. Ph.D. Student Jørgen Hinkler, Institute of Geography, University of Copenhagen, is acknowledged for quality control of data sets and for establishing the applied climate database. Furthermore, ASIAQ (Greenland

The hydrometric station where water level is measured every 15 min.

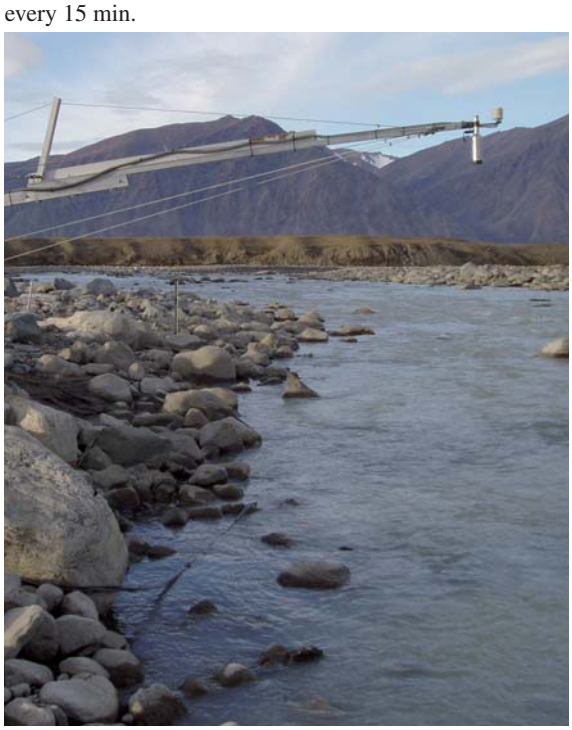

Photo: Charlotte Sigsgaard

Field Investigations) is acknowledged for quality control of data sets. Professor Søren Rysgaard, Greenland Institute of Natural Resources, is thanked for a critical review of the manuscript. We thank the two anonymous referees for their valuable comments.

2.9 References

Anderson, E. A. 1976. A point energy balance model of a snow cover. Office of Hydrology, National Weather Service, NOAA Tech. Rep. NWS 19, 150 pp.

Bay, C. 1992. A phytogeographical study of the vascular plants of northern Greenland – north of 74° northern latitude. Meddr. Grønland, Biosci., 36, 52 pp.

Bay, C. 1999. Teknisk rapport 27. Pinngortitaleriffik, Grønlands Naturinstitut: 23–27. (In Danish).

Bogen, J. 1996. Erosion and Sediment yield in Norwegian rivers. In: Walling, D. E. & Webb, B. W., (eds.). Erosion and Sediment Yield: Global and regional perspectives. Proc. of the Exeter Symposium, July. IAHS Publ. 236: 73–84.

Bogen, J. & Bønsnes, T. E. 2003. Erosion and sediment transport in High Arctic rivers, Svalbard. Polar Res. 22(2): 175–189.

Box, J. E. 2002. Survey of Greenland instrumental temperature records: 1973–2001. Int. J. Clim. 22: 1829–1847.

Broecker, W.S., Peteet, D.M. & Rind, D. 1985. Does the ocean-atmosphere system have more than one stable mode of operation. Nature 315: 21–26.

Broecker, W.S. & Denton, G.H. 1990. The role of ocean-atmosphere reorganization in glacial cycles. Quat. Sci. Rev. 9: 305–341.

Brown, R. D., Brasnett, B. & Robinson, D. 2003. Gridded North American monthly snow depth and snow water equivalent for GCM evaluation. Atm.-Ocean 41(1): 1–14.

Cappelen, J., Jørgensen, B. V., Laursen, E. V., Stannius, L. S. & Thomsen, R. S. 2001. The Observed Climate of Greenland, 1958–99 – with Climatological Standard Normals, 1961–90. Technical Report 00–18, Danish Meteorological Institute, Ministry of Transport, Copenhagen, 150 pp.

Church, M. 1974. Hydrology and permafrost with reference to northern North America. Proceedings, Workshop on Permafrost Hydrology, Canadian National Committee for IHD. Ottawa: 7–20.

Crowely, T. J. 2000. Causes of climate change over the past 1000 years. Science 289: 270–277.

Flato, G. M. & Boer, G. J. 2001. Warming asymmetry in climate change simulations. Geophys. Res. Lett. 28: 195–198.

Hansen, B. U., Humlum, O. & Nielsen, N. 2003. Meteorological Observations 2002 at the Arctic Station, Quqertarsuaq (69°15'N), Central West Greenland. Geografisk Tidsskrift/Danish J. Geogr. 103(2): 93–97.

Hasholt, B. 1996. Sediment transport in Greenland. In: Walling, D. E. & Webb, B. W., (eds.). Erosion and Sediment Yield: Global and regional perspectives. Proc. of the Exeter Symposium, July. IAHS Publ. 236: 105–114.

Hasholt, B. 2003. Method for estimation of the delivery of sediments and solutes from Greenland to the ocean. IAHS publication no. 279. Erosion Prediction in ungauged basins: Integrating Methods and Techniques. Proceedings of symposium HS01, IUGG 2003 at Sapporo: 84–92.

Hinkler. J., Pedersen, S. B., Rasch, M. & Hansen, B. U. 2002. Automatic snow cover monitoring at high temporal and spatial resolution, using images taken by a standard digital camera. Int. J. Rem. Sens. 23: 4669–4682.

Hinkler. J., Hansen, B. U. & Tamstorf, M. 2003. Sea-ice and snow accumulation in High Arctic Greenland. Proceedings of Northern Research Basins 14th International Symposium and Workshop, 25-29th August 2003. Kangerlussuaq/Sdr. Strømfjord, Greenland: 59–66.

Kane, D. 1997. The impact of hydrologic perturbation on Arctic ecosystems induced by climate change. In: Oechel, W.C., Callaghan, T., Gilmanov, T., Holten, J.I., Maxwell, B., Molau, U. & Sveinbjörnsson, B. (eds.). Global Change and Arctic Terrestrial Ecosystems. Ecological Studies 124: 63–81. Springer, New York.

Killingtveit, Å., Pettersson, L-E. & Sand, K. 2003. Water balance investigations in Svalbard. Polar Res. 22: 161–174.

Koch, L. & Haller, J. 1971. Geological map of East Greenland 72°-76° N. Lat. (1:250.000). Meddr. Grønland, 183: Plate 2.

Maxwell, B. 1997. Recent climate patterns in the Arctic. In: Oechel, W.C., Callaghan, T., Gilmanov, T., Holten, J.I., Maxwell, B., Molau, U. & Sveinbjörnsson, B. (eds.). Global Change and Arctic Terrestrial Ecosystems. Ecological Studies 124: 21–47. Springer, New York.

Meltofte, H. & Thing, H. (eds.) 1996. ZERO – Zackenberg Ecological Research Operations. 1st Annual Report, 1995. Danish Polar Center. Ministry of research and information technology, Copenhagen. 64 pp.

Meltofte, H. & Thing, H. (eds.) 1997. ZERO – Zackenberg Ecological Research Operations. 2nd Annual Report, 1996, Danish Polar Center. Ministry of research and information technology. 80 pp.

Meltofte, H. & Rasch, M. (eds.) 1998. ZERO – Zackenberg Ecological Research Operations. 3rd Annual Report, 1997. Danish Polar Center. Ministry of Research and Information Technology, Copenhagen. 68 pp.

Nielsson, B. 1969. Development of a depth-integrating water sampler, UNGI Report 2, Uppsala University, Sweden. 74 pp.

Rasch, M. (eds.) 1999. ZERO – Zackenberg Ecological Research Operations. 4th Annual report, 1998. Danish Polar Center. Ministry of Research and Information Technology. 62 pp.

Rasch, M. (ed.) 2000. Zackenberg Station – en platform for højarktisk økologisk forskning i Nordøstgrønland. Kaskelot 127. 32 pp. (In Danish).

Rasch, M. & Caning, K. (eds.) 2003. ZERO – Zackenberg Ecological Research Operations. 9th Annual report, 2003. Danish Polar Center. Ministry of research and information technology, Copenhagen. 91 pp.

Rasch, M., Elberling, B., Jakobsen, B. H. & Hasholt, B. 2000. High-resolution measurements of water discharge, sediment, and solute transport in the River Zackenbergelven, Northeast Greenland. Arct. Antarct. Alp. Res. 32: 336–345.

Rysgaard, S., Vang, T., Stjernholm, M., Rasmussen, B., Windelin, A. & Kiilsholm, S. 2003. Physical conditions, carbon transport, and climate change impacts in a Northeast Greenland fjord. Arct. Anarct. Alp. Res. 35: 301–312.

Serreze, M.C., Maslanik,J., Scambos, T. A., Fetterer F., Stroeve, J., Knowles, K., Fowler, C., Drobot, S., Barry, R. & Haran, T. M. 2002. A record minimum Arctic sea ice extent and area in 2002. Geophys. Res. Lett. 30(3): 1110, doi:10.1029/2002GL016406.

Soegaard, H., Hasholt, B., Friborg, T. & Nordstroem, C. 2001. Surface energy- and water balance in a High-Arctic environment in NE Greenland. Theor. Appl. Climatol. 70: 35–51.

Soil Survey Staff 1999. Soil Taxonomy. U.S. Government Printing Office, Washington D.C. 869 pp.

Sturm, M., Schimel, J., Michaelson, G., Welker, J. M., Oberbauer, S. F., Liston, G. E., Fahnestock, J. & Romanovsky, V. E. 2005. Winter biological processes could help convert Arctic tundra to shrubland. BioScience, 55: 17–26.

Sykes, J. M., Lane, A. M. J. & George, D. G. 1999. The United Kingdom environmental change network: Protocols for standard measurements at freshwater sites. Center for Ecology and Hydrology, Dorset, 131 pp.

Sælthun, N. R. & Barkved, L. J. 2003. Climate changes scenarios for the SCANNET region. Norwegian Institute for Water Research, Report no. 4663–2003: 1–70.

Walkers, D. A., Gould, H. A., Maier, H. A. & Reynolds, M. K. 2002. The circumpolar Arctic vegetation map: AVHRR-derived base map, environmental controls and integrated mapping procedures. Int. J. Rem. Sens. 23: 2552–2570.

WHO, 2001. WHO statement on the status of the global climate in 2001. WHO#670. World Meteorological Organization, Geneva, Switzerland, 84 pp.

Photo: Søren Rysgaard

3

Physical conditions, dynamics and model simulations during the ice-free period of the Young Sound/Tyrolerfjord system

Physical conditions, dynamics and model simulations during the ice-free period of the Young Sound/Tyrolerfjord system

Jørgen Bendtsen[1], Karin E. Gustafsson[1], Søren Rysgaard[2] and Torben Vang[3]

[1]National Environmental Research Institute, Department of Marine Ecology, Frederiksborgvej 399, P. O. Box 358, DK-4000 Roskilde, Denmark
[2]Greenland Institute of Natural Resources, Kivioq 2, Box 570, DK-3900, Greenland
[3]Council of Vejle, Damhaven 12, DK-7100 Vejle, Denmark

Cite as: Bendtsen, J., Gustafsson, K. E., Rysgaard, S. & Vang, T., 2007. Physical conditions, dynamics and model simulations during the ice-free period of the Young Sound/Tyrolerfjord system. In: Rysgaard, S. & Glud, R. N. (Eds.), Carbon cycling in Arctic marine ecosystems: Case study Young Sound. Meddr. Grønland, Bioscience 58: 46-59.

Abstract

The Young Sound/Tyrolerfjord system is a 90 km long and 2–7 km wide sill fjord in northeast Greenland, with a mean depth of 100 m. Observations of the bottom topography are presented from different sections of the fjord system, which has a total volume of 40 km^3 and a surface area of 390 km^2. Hydrographic observations from the summer period show the large influence from the freshwater discharge on the mixed layer depth in the fjord, which, during summer, is less than 5 m, with surface salinity increasing from values below 10 in the inner part of Young Sound to about 30 above the sill in the outer part of the fjord. The deep and intermediate water in the fjord is characterized by a temperature of -1.7 °C and a salinity of 33.1, corresponding to $\sigma_t < 26.5$. The maximum tidal amplitude is 0.8 m and 0.4 m during flood and neap tide, respectively, and is dominated by the lunar semi-diurnal M2 tidal constituent. New model simulations show the evolution of the mixed layer during the summer season. A sensitivity study based on this model is presented, showing that the mixed layer thickness will decrease by about 20 % if the runoff is increased by a factor of two, and the implications for the hydrographic conditions in relation to a global warming scenario are discussed.

3.1 Introduction

The Young Sound/Tyrolerfjord system is a c. 90 km long sill fjord in Northeast Greenland, which has been monitored regularly since 1995 from the research station ZERO (Zackenberg Ecological Research Operations). Outside the fjord (the inner part of the East Greenland Current system) water masses are characterized by relatively low salinity. The East Greenland Current is the major coastal-shelf current system in the Nordic Seas, transporting relatively fresh water from the Arctic Ocean together with "recirculating" Atlantic water from the Fram Strait towards the Denmark Strait (i.e. Rudels et al., 2002 ; Chapter 1). Thus, remote changes in the hydrographic conditions in this area will be reflected in the water masses outside Young Sound. For example, due to its role as a major pathway for fresh water from various sources in the Arctic Mediterranean, such as runoff and melted sea ice, a change in the strength and characteristics of the East Greenland Current can be an indicator, or potentially a measure, of large-scale climatic changes in the polar seas. Such changes have been simulated in several coupled ocean-atmosphere models, which

have shown the climate in the polar regions to be sensitive to changes in atmospheric greenhouse gas concentrations (Roeckner et al., 1999; Houghton et al., 2001). Analyses of long time series of sea ice cover in the Arctic region also indicate significant changes in the climatic conditions (Vinnikov et al., 1999). Decreasing sea ice cover in the Arctic Ocean could change the freshwater content of the East Greenland Current. Such changes would also influence hydrographic conditions inside Young Sound, and, therefore, a description of present hydrographic conditions and an understanding of the dynamics in the fjord is a prerequisite for assessing future changes and the possible impact of climate change in the area.

Large transport of sea ice and frequent calving of icebergs make investigation of the East Greenland Current difficult, which is why the existing dataset of the hydrographic conditions in this region is relatively limited. In particular, coastal observations are nonexistent in many areas, and, consequently, the dynamics here are basically unknown. Observations in the Young Sound provide the first time series of hydrographic conditions from a fjord in this region.

A complete description of the exchange to the open sea from the fjord requires more data on the hydrographic conditions outside the sill than are currently available. However, the fjord represents a typical deep sill fjord and, therefore, the dynamics and hydrography in the fjord can be related to the general dynamics of this type of fjord system (Stigebrandt, 2001). In such systems the water exchange to the open sea is a combination of several circulation processes: (1) The tidally driven barotropic exchange caused by sea level variations outside the fjord, (2) the baroclinic exchange caused by density variations of the coastal waters outside the fjord or due to up- or downwelling inside the fjord due to wind forcing, and (3) the baroclinic estuarine circulation driven by freshwater supply and mixing inside the fjord. The relatively shallow sill at the fjord mouth inhibits the exchange of deeper waters, and the water is therefore generally characterized by (1) a surface layer resulting from the local river discharge and sea ice melt kept well mixed by the wind down to a few meters depth, where a primary pycnocline can be observed, (2) an intermediary layer down to about sill depth with a stratification more or less imported from the coastal water outside the fjord, and (3) dense basin water trapped below sill level. The sill acts as an efficient barrier to ventilation of the deepest water mass and a secondary pycnocline usually develops in the fjord at about or below sill level. Between renewals of deep water the density of the basin water decreases slowly due to turbulent diffusion. Internal waves on the secondary pycnocline may provide energy for turbulent diffusion in the deeper layers of the fjord. In the cold season, cooling and ice formation may create dense water at the surface, resulting in convection, increased vertical mixing and formation of a dense winter water mass contributing to the intermediate and deep waters. These general characteristics are in accordance with the observed conditions in the fjord as shown below.

Photo: Søren Rysgaard

Launching CTD moorings in Young Sound during August 2001.

Results from moorings and synoptic transects are presented together with measurements of the bathymetry of the fjord. These provide the input data for a numerical study of the physical conditions during the summer season in the fjord, where the importance of interannual variability of runoff for the formation of the surface mixed layer is quantified through a model sensitivity study. Finally, the implications of increased runoff due to a warmer climate for the surface conditions in the fjord and the exchange between the fjord and the East Greenland Current are discussed.

3.2 Methods

3.2.1 Physical conditions

The bottom topography of the fjord system was surveyed along predefined transects using a dual-frequency echo sounder and a GPS receiver mounted on a rubber dinghy. A total distance of 850 km was covered and about 200,000 data points were collected (Rysgaard et al., 2003). The data was subsequently interpolated on a regular UTM grid using a method based on triangulation.

CTD measurements were made in the fjord during August 2003 and March 2005. Continuous temperature, salinity and water level measurements were taken from August 2003–July 2004 from a SBE 37 instrument (Sea-Bird Electronics, Inc.) placed at a depth of 63 m near the island Sandøen. The water level record was analyzed for amplitudes and phases for the dominant tidal constituents by the method described in Pawlowicz et al. (2002).

3.2.2 Numerical simulations

A three-dimensional primitive equation model based on the COHERENS model (Luyten et al., 1999) was used for quantifying transports and mixing in the fjord system. The model solves the hydrodynamic equations on a vertical sigma coordinate system. This implies a fixed number of vertical grid levels in the entire model domain, with a logarithmic increase of the grid resolution towards the surface. Mixing processes in the surface boundary layer are parameterized by a k-epsilon turbulence closure scheme, so that the mixing intensity is explicitly described as a function of turbulent diffusive momentum and energy transports across the air/sea interface. The model has a free surface, allowing an explicit description of the tides. The model is driven by hourly meteorological fields of wind, temperature, cloudiness, air pressure and relative humidity generated by an operational weatherforecast model (Brandt et al., 2001). The model is forced with the 8 most significant tidal constituents at the open-sea boundaries. River runoff is based on annual measurements of the Zackenberg River discharge during 2003 (Chapter 2). Furthermore, river runoff from the Zackenberg River, Djævlekløften, Lerbugten and the inner part of the fjord (Tyrolerdal) was quantified during 2005 by monitoring the water level (h) in these rivers every 15 min during the summer thaw by use of automatic diver systems. At each of the localities the amount of discharge (Q) was measured on several occasions during summer of 2005 to ensure that the absolute amount of fresh water from the terrestrial to the marine environment could be quantified from Q/h relations for each specific river. These 4 rivers contribute up to 90 % of the total freshwater runoff to the fjord and the ratio of the discharge from each of them relative to the Zackenberg River is: Zackenberg River 100 %, Djævlekløften 100 %, Lerbugten 100 % and the river in Tyrolerdal 310 %. These ratios cause the total runoff to the fjord to be a factor of 6.1 larger than the runoff from the Zackenberg River, corresponding to the ratio of the total drainage area to the drainage area of the Zackenberg River. The fresh water is assumed to enter the fjord in the upper 5 m of the water column at the river mouth. The bathymetry of the model is based on the gridded data set described above, and these data are averaged on a 1×1-km horizontal grid in the model domain. Outside the fjord, the bathymetry is based on the global 2-minute-gridded elevation data ETOPO2 (ETOPO2, 2001) and the landmask is based on the GLOBE data set (Hastings & Dunbarr, 1999). The model has 15 vertical grid levels and it is integrated during the period from 1 March to 1 September 2003. The model is initialised with temperature and salinity fields obtained in the deepest part of Tyrolerfjord in March 2005 (at the station "Dybet"). The open-sea boundary conditions of temperature and salinity are linearly interpolated in time between observed profiles of T and S from March to August. The horizontal diffusion is increased to 500 $m^2\ s^{-1}$ in a diffusive buffer layer 8 km wide along the open-sea boundaries, outside which it is zero. This buffer zone smoothes the temperature and salinity gradients close to the open boundaries but its influence on the conditions inside the fjord is limited. The formulation and assumptions of the open-sea boundary conditions are discussed further below.

3.3 Results & discussion

3.3.1 Bathymetry

The Young Sound/Tyrolerfjord system is a sill fjord located in Northeast Greenland between 22 °W–20 °W and 75.2 °N–74.6 °N. The Tyrolerfjord constitutes the narrow innermost part of the fjord system and Young Sound the wider outer part towards the open sea and

the East Greenland Current system (Fig. 3.1). The fjord system is about 90 km long and 2–7 km wide and covers an area of 390 km^2. The volume of the fjord system is 40 km^3 corresponding to a mean depth of 100 m (Tables 3.1 and 3.2). The sill depth in Young Sound is only 45 m and, therefore, more than 60% of the water volume in the system is located below the sill. The deepest part of the fjord system is located in Tyrolerfjord, with a maximum depth of 360 m. The Young Sound (areas 1, 2 and 3, Fig. 3.1) and outer part of the Tyrolerfjord (area 4) constitute 44 % and 30 % of the total volume, corresponding to a mean depth of 91 m and 183 m, respectively. The inner part of the fjord (areas 5 and 6) has a mean depth of 80 m.

3.3.2 Hydrography and tides

The hydrographic conditions in the fjord system are affected by estuarine circulation during the ice-free period because of the large freshwater input from the melting of snow and ice in the drainage area. The shallow sill reduces the exchange with the open sea, disconnecting the deepest part of the fjord from the East Greenland Current during most of the year. During winter, the fjord is covered with sea ice, which typically starts to melt in May-June when the surface air temperature increases, and complete breakup of the sea ice then takes place during mid-summer (see Chapter 4). The total drainage area to the fjord system is 3109 km^2 and the runoff typically starts in June and ends in August–September. The Zackenberg River drainage area is 512 km^2 and runs into Young Sound. Measurements show a large interannual variability of the discharge into Young Sound with a total runoff during the summer period ranging between 174 and 256 million m^3 for the years 1997–1999 (Chapter 2; Rysgaard et al., 2003).

The hydrographic conditions during August 2003 along a transect from the inner part of the fjord to the East Greenland Current shows the separation between the upper water masses above the sill depth and the deeper part of the fjord (Fig. 3.2). The deepest water mass below 300 m depth in the fjord is characterized by a temperature below -1.7 °C and a relatively high salinity – above 33.15 – corresponding to a density, σ_t, of 26.68. Between the sill depth and 300 m depth the salinity increases gradually from 33.1 to 33.15 and the temperature is about -1.7 °C. The bottom water masses near the sill are modified by water entering from the

Figure 3.1 (a) Relief model of Young Sound. **(b)** Cross-section at the sill in the outer part of Young Sound. **(c)** The Young Sound/Tyrolerfjord system is divided into 7 regions (see Table 3.1). The Tyrolerfjord covers regions 4–6 and Young Sound covers region 1–3. **(d)** Length section of the fjord with marking of regions. Figure adapted from Rysgaard et al. (2003).

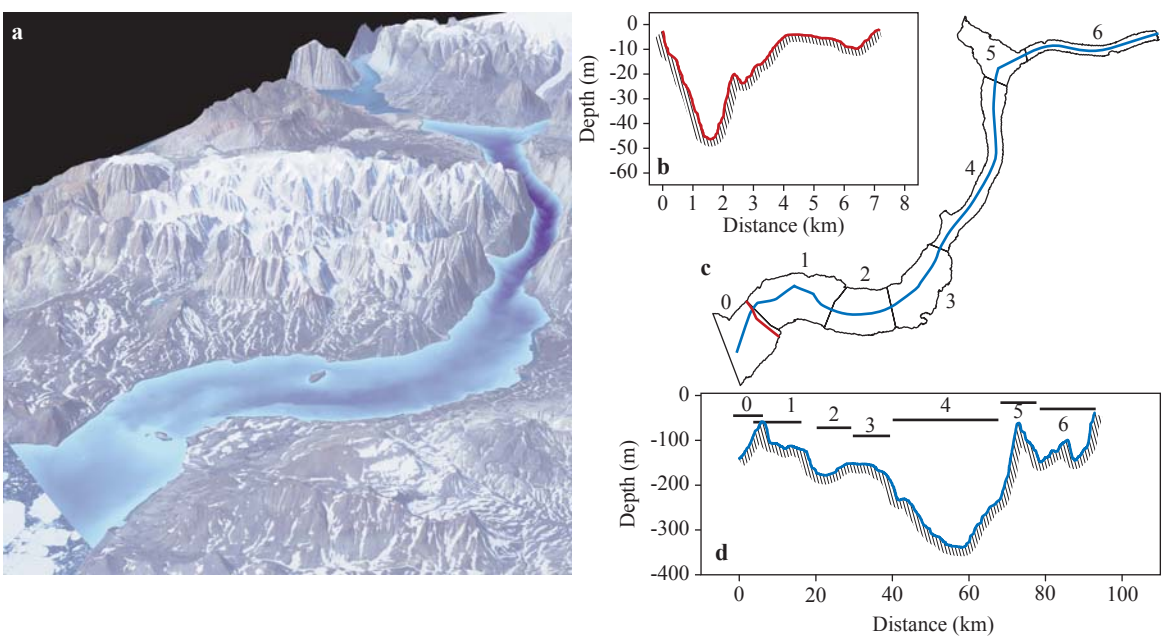

Table 3.1 Hypsometric data from each region of the fjord system. The sea-floor area in the depth intervals is in units of km^2. The table is adapted from Rysgaard et al. (2003).

Depth interval (m)	Region 0	Region 1	Region 2	Region 3	Region 4	Region 5	Region 6	Total (0–6)
0–10	9.827	5.324	1.479	3.521	1.913	3.512	1.473	27.049
10–20	3.958	3.136	1.610	2.578	1.741	2.407	1.424	16.853
20–30	3.427	3.405	1.757	2.465	1.677	2.281	1.469	16.480
30–40	3.288	3.630	1.800	2.509	1.682	2.228	1.528	16.664
40–50	3.828	3.863	1.917	2.558	1.641	2.271	1.585	17.661
50–60	4.668	4.776	2.328	2.308	1.642	2.803	1.680	20.204
60–70	3.868	5.456	2.813	2.452	1.547	2.361	2.063	20.559
70–80	4.078	7.678	3.349	2.770	1.506	1.988	2.098	23.465
80–90	4.139	10.111	5.404	3.036	1.539	1.688	2.052	27.968
90–100	4.214	8.888	3.979	3.425	1.495	1.601	2.320	25.921
100–120	8.263	13.036	6.323	7.574	2.984	2.878	5.083	46.141
120–140	5.274	2.782	7.338	8.724	3.106	3.114	3.761	34.100
140–160	0.929	2.452	7.012	12.600	3.331	3.735	1.299	31.358
160–180	0.000	1.609	6.057	5.026	3.609	2.694	0.172	19.167
180–200	0.000	0.000	0.343	1.706	3.999	2.005	0.010	8.062
200–250	0.000	0.000	0.000	0.305	13.754	4.204	0.000	18.263
250–300	0.000	0.000	0.000	0.000	11.813	0.000	0.000	11.813
300–360	0.000	0.000	0.000	0.000	7.637	0.000	0.000	7.637
Total area	**59.759**	**76.144**	**53.508**	**63.556**	**66.615**	**41.767**	**28.016**	**389.366**

Table 3.2 Volume (km^3) in depth intervals in the Young Sound/Tyrolerfjord system. Table adapted from Rysgaard et al. (2003).

Depth interval (m)	Region 0	Region 1	Region 2	Region 3	Region 4	Region 5	Region 6	Total (0–6)
0–10	0.556	0.734	0.529	0.616	0.657	0.399	0.273	3.764
10–20	0.484	0.694	0.513	0.589	0.639	0.372	0.259	3.550
20–30	0.448	0.662	0.496	0.563	0.622	0.348	0.245	3.385
30–40	0.414	0.627	0.479	0.539	0.605	0.326	0.230	3.219
40–50	0.380	0.590	0.460	0.513	0.589	0.303	0.214	3.048
50–60	0.338	0.548	0.440	0.489	0.572	0.278	0.198	2.863
60–70	0.294	0.496	0.414	0.465	0.556	0.252	0.180	2.657
70–80	0.255	0.433	0.384	0.440	0.541	0.230	0.158	2.440
80–90	0.214	0.346	0.342	0.411	0.526	0.211	0.138	2.187
90–100	0.172	0.245	0.291	0.378	0.511	0.195	0.116	1.909
100–120	0.219	0.266	0.478	0.650	0.977	0.345	0.155	3.089
120–140	0.072	0.104	0.349	0.489	0.916	0.288	0.064	2.281
140–160	0.004	0.061	0.196	0.269	0.851	0.214	0.013	1.608
160–180	0.000	0.010	0.066	0.084	0.783	0.151	0.002	1.095
180–200	0.000	0.000	0.001	0.020	0.707	0.104	0.000	0.832
200–250	0.000	0.000	0.000	0.002	1.341	0.079	0.000	1.422
250–300	0.000	0.000	0.000	0.000	0.679	0.000	0.000	0.679
300–360	0.000	0.000	0.000	0.000	0.169	0.000	0.000	0.169
Total volume	**3.849**	**5.816**	**5.437**	**6.517**	**12.240**	**4.095**	**2.245**	**40.199**

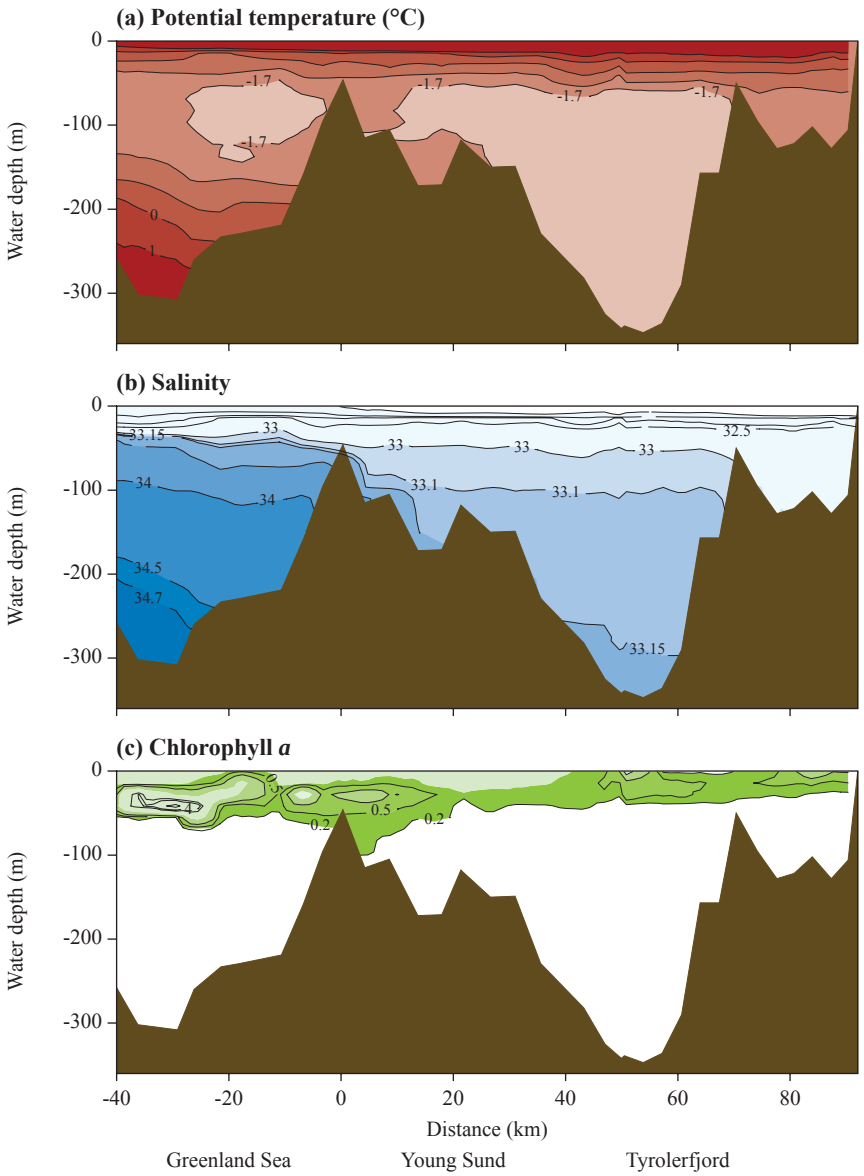

Figure 3.2 (a) Temperature, **(b)** salinity and **(c)** chlorophyll *a* in central Young Sound/Tyrolerfjord and in the inner part of the East Greenland Current system. The distance to the sill (0 km) of Young Sound is shown at the abscissa. Figure adapted from Rysgaard et al. (2005).

East Greenland Current and, therefore, temperatures and salinities are higher here than in the interior of the fjord. The salinity decreases towards the surface to about 30 and the temperature reaches about 2 °C at 5 m depth, corresponding to a σ_t of about 24 (Fig. 3.3). The mixed layer is only about 5 m deep in the fjord and is separated from the underlying water by a strong halocline. In the upper 5 m salinity and temperature change significantly from the inner to the outer part of the fjord, with temperature decreasing from 9 to 2 °C and salinity increasing from about 8 to 30 (Fig. 3.4). Due to the action of the Coriolis force the plume of relatively fresh water is concentrated in the southern part of the fjord, and this causes a slight deepening of the mixed layer of about 1 m in the outer part of Young Sound (Fig. 3.4a, c). The large horizontal variations seen in temperature and salinity distribution in the interior indicate the presence of internal waves in Young Sound between Zackenberg and the sill, with an internal wave amplitude of about 5 m (Fig. 3.4b, d). At present, no time series exist that confirm the frequency of these waves, so it cannot be determined whether they are progressive or not. Progressive components dissipate in the fjord, whereby they contribute to the mixing in the fjord.

The tidal amplitude has a maximum of about 0.8

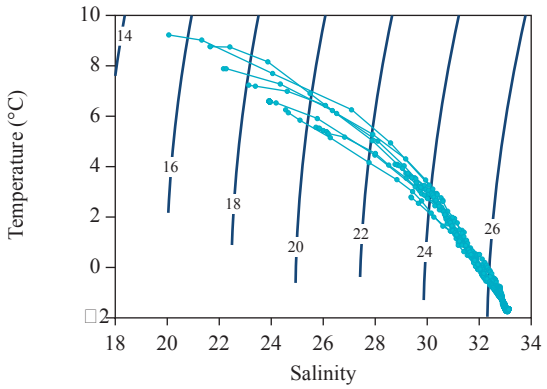

Figure 3.3 T-S plot of CTD profiles taken from a transect from the inner to the outer part of the fjord during August 2004. Contour lines of σ_t are shown.

m during spring flood at the entrance to the fjord and a minimum during neap tide of about 0.3 m (Fig. 3.5). The dominant constituent is the semi-diurnal lunar component M2 with amplitude 0.48 m, and the second and third most important constituents are S2 and K1 with amplitudes 0.18 m and 0.10 m, respectively (Table 3.3). This is in accordance with observations from current-meter moorings in the East Greenland Current system at 75 °N where analysis of currents in the water column showed a similar relative importance of the tidal constituents (Woodgate et al., 1999). Surface currents near Sandøen during August have been observed to reach a maximum value of 1.20 m s^{-1} and have a mean of 0.45 m^{-1} (Rysgaard et al., 2003). The long wave phase speed of the tidal wave gives a time lag of about 48 minutes

Figure 3.4 (a) Salinity and **(b)** temperature (°C) across the sill in the outer part of the fjord. **(c)** Salinity and **(d)** temperature along the centre of Young Sound. The horizontal resolution of measurements are 0.5 km in (**a,b**) and 2 km in (**c,d**), respectively, and 20 cm in the vertical. Figure adapted from Rysgaard et al. (2003).

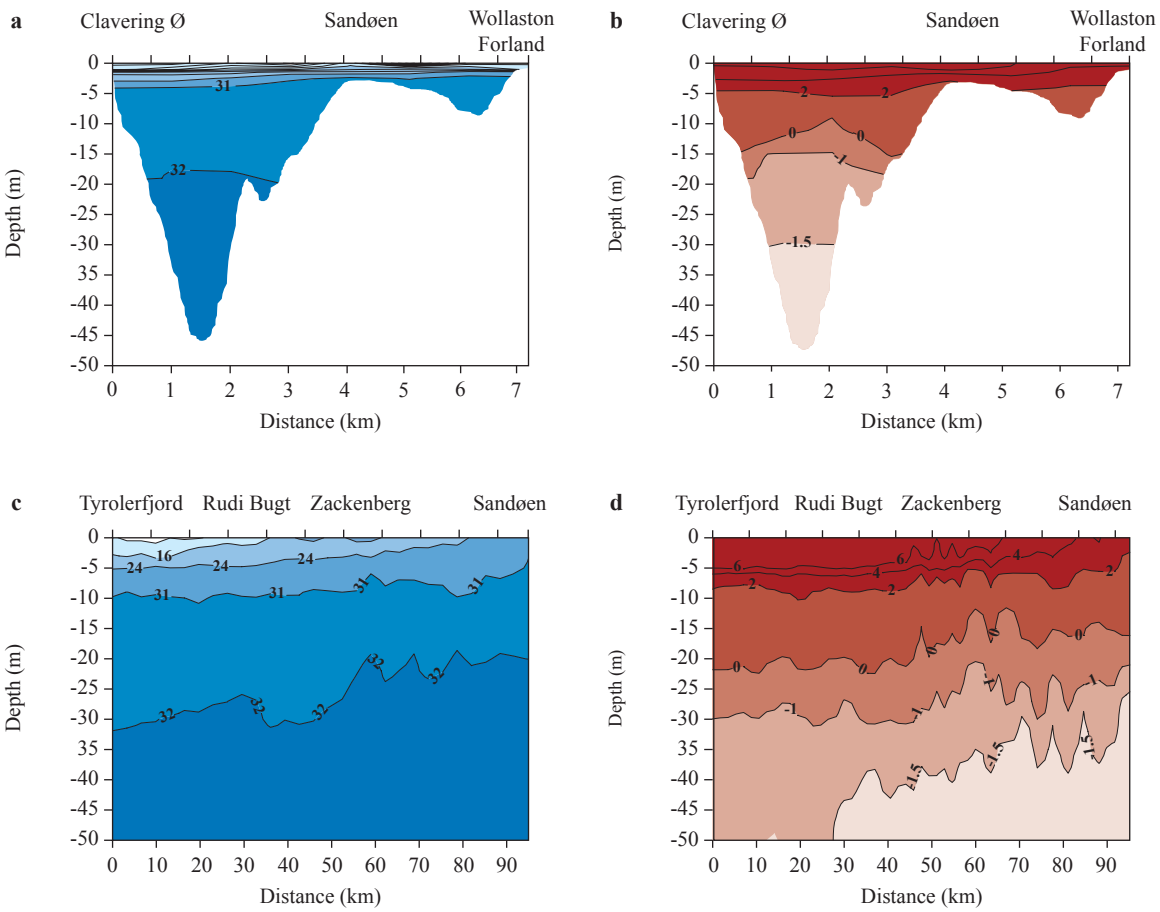

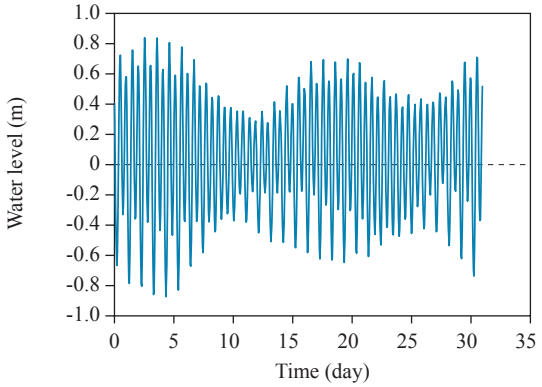

Figure 3.5 Water level measured near the island Sandøen in Young Sound in the period 1–31 July 2004.

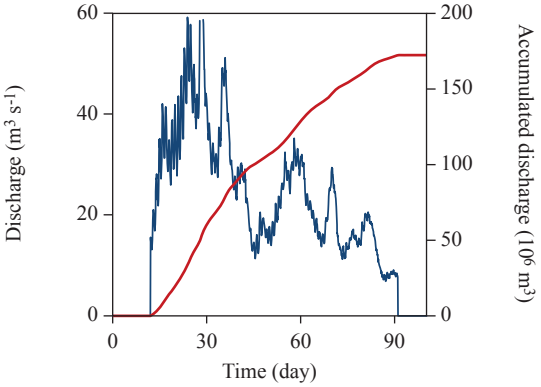

Figure 3.6 Freshwater discharge from the Zackenberg River in 2003 (blue line) and the accumulated discharge (red line). The time axis starts 1 June, and the discharge begins 13 June and ends 21 August.

Table 3.3 Tidal components and amplitudes for the 9 most important tidal constituents, based on data from an SBE-logger during August 2003–August 2004.

Tidal component	Period (hours)	Amplitude
SSA Solar semi-annual	4382.1	0.0386
MF Lunar fortnightly	327.8	0.0232
O1 Principal lunar diurnal	25.82	0.0802
P1 Principal solar diurnal	24.07	0.0319
K1 Luni-solar diurnal	23.93	0.0958
N2 Larger lunar elliptic	12.66	0.0936
M2 Principal lunar	12.42	0.4786
S2 Principal solar	12.00	0.1824
K2 Luni-solar semi-diurnal	11.97	0.0515

between the sill and the inner part of the fjord, and only about 17 minutes at the Zackenberg Station, which is located approximately 30 km from the sill, in accordance with the observed phase lag there.

3.3.3 Simulation of summer conditions

Numerical simulation of the hydrographic conditions during the ice-free summer period described the evolution of the three-dimensional distribution of temperature, salinity and currents together with the two-dimensional field of the water level in the fjord. The existing data set of the hydrographic conditions outside the fjord is very limited, so a detailed description of the time-varying density field in the water column is not yet possible even on a seasonal basis. The boundary conditions outside the fjord are therefore prescribed from a profile of temperature and salinity taken inside the fjord in mid-March and linearly interpolated in time to a profile taken outside the fjord in August. The coarse time resolution of the boundary conditions exclude processes potentially important for the exchange between the fjord and the East Greenland Current system such as short-term changes in the density field due to traveling waves along the Greenland coast or coastal wind surge effects on the water level. The temporal and spatial distribution of sea ice is likewise poorly described through the spring and summer season and, in particular, estimates of sea ice import or export from the fjord are not available, meaning that the influence of these processes on the surface salinity can not be determined. Therefore, the effect of sea ice is disregarded in the analysis below.

Within these limitations the model describes the conditions during the summer season. During this period, the salinity distribution is largely controlled by the freshwater runoff. The runoff is based on the observed river discharge from the Zackenberg River in 2003, which starts on 13 June and ends on 30 August, giving a total accumulated discharge of 172 million m^3 (Fig. 3.6).

In June, the monthly averaged model solution of surface salinity has decreased from the early spring value of about 33 to between 20 and 30 in the inner part of the fjord due to the large river discharge and limited exchange with the rest of Tyrolerfjord,

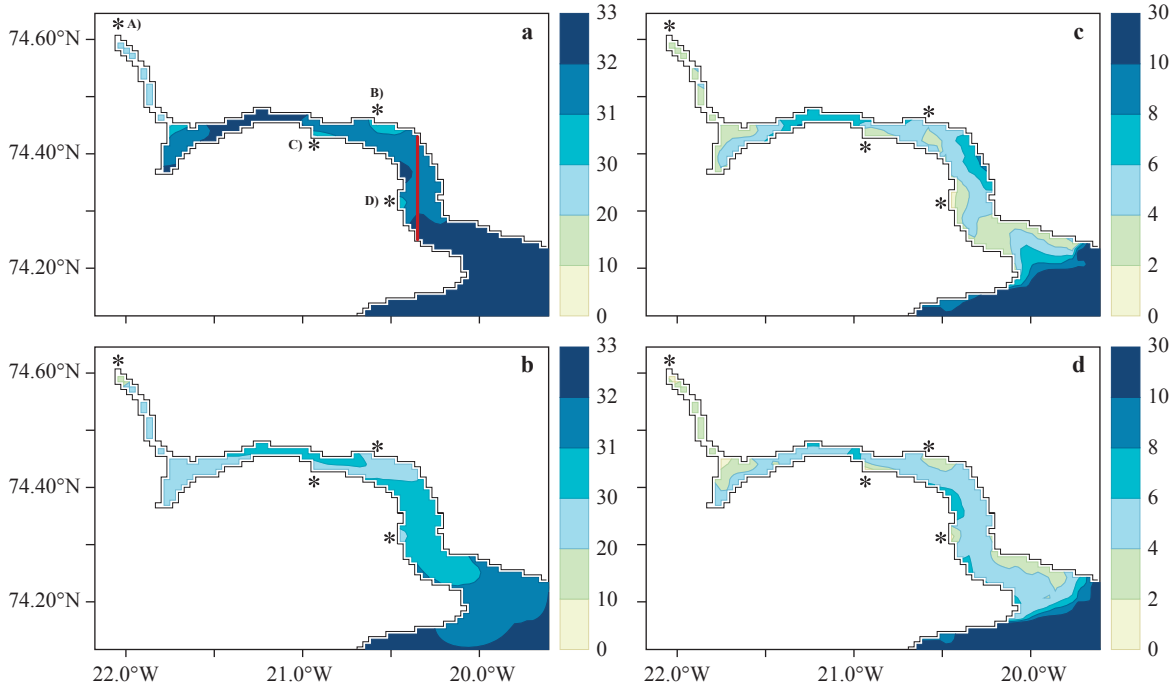

Figure 3.7 Model solutions of monthly averaged surface salinity in June **(a)** and August **(b)** in 2003. The mixed layer depth (m), defined by the depth level with the steepest density gradient in June **(c)** and August **(d)**. The locations of the four rivers are indicated by stars and shown in **(a)** as A) river in Tyrolerdal, (B) Zackenberg, (C) Lerbugten and (D) Djævlekløften. The red line along 20.35 °W in **(a)** shows the transect shown in Figure 3.9. Note that the model solution for June disregards the influence from sea ice.

whereas the salinity distribution in Tyrolerfjord and in Young Sound still exhibits salinities above 31 (Fig. 3.7). In August, the surface salinity has decreased to 30-31 in Young Sound, and decreases gradually towards the inner Tyrolerfjord. The river discharge creates a strong pycnocline in the upper 5-10 m, referred to below as the mixed layer. Already in June the monthly averaged mixed layer depth, defined by the depth having the largest vertical density gradient, is significantly influenced by the freshwater discharge, the mixed layer depth being less than 4 m in the inner Tyrolerfjord and between 4 and 8 m in the central Tyrolerfjord and Young Sound. In August, the mixed layer depth has decreased to 4-6 m in Young Sound and Tyrolerfjord and between 2 and 4 m in the inner part of the fjord. The salinity distribution on a transect across Young Sound shows the deepening of the shallow low-salinity surface layer toward the

Figure 3.8 Model solutions of monthly averaged temperature (°C, red color) and salinity (contour) in a transect across Young Sound at 74.29 °N as a function of depth (m) in July 2003.

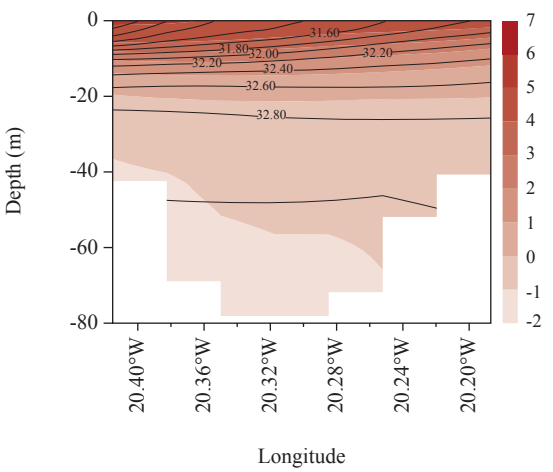

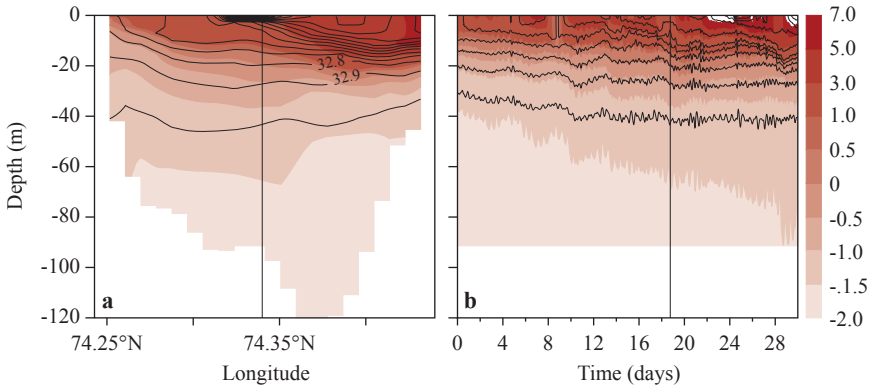

Figure 3.9 (a) Model solutions of temperature (°C, red color) and salinity (contour) along a transect at 20.35 °W on 18 June 2003, covering the central part of Young Sound. **(b)** Time series of the vertical distribution of temperature and salinity (contour) at 74.34 °N and 20.35 °W. The vertical line in **(a)** corresponds to the location used in **(b)**, and the vertical line in **(b)** corresponds to the time for the section shown in **(a)**. Contour intervals are 0.1.

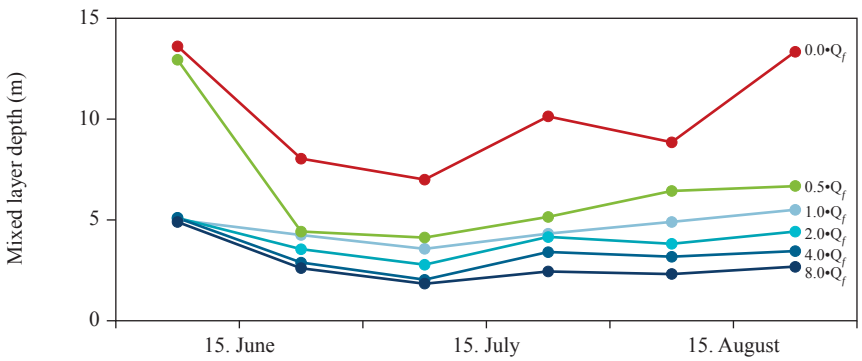

Figure 3.10 Model solutions from the sensitivity study of the relation between the mixed layer depth and the freshwater discharge (Q_f) for 2003 scaled with a constant in each model run. The mixed layer depth is averaged in 14-day intervals from June–August, at the location 20.68 °W; 74.44 °N (see also Table 3.4).

"eastern" coast (Fig. 3.8), i.e. the coast located to the right of the outflowing surface water, in accordance with the observed distributions shown in Fig. 3.4. The depth of the mixed layer is regulated mainly by the salinity distribution, and, therefore, the temperature near the surface has a similar distribution.

Model solutions of a north-to-south transect in Young Sound from 18 June show the newly developed halocline, a mixed layer depth of about 8 m in the northern part of the section and warm water in the mixed layer (Fig. 3.9a). A time series from a location in central Young Sound shows the onset of the halocline in mid-June and the gradual heating of the water column (Fig. 3.9b). The time series also shows propagation of internal waves causing fluctuations on the pycnocline, with small-amplitude oscillations associated with the M2 tidal period of about 1 m, and larger oscillations with amplitude about 5 m and a period of about 4 days, which could be associated with an internal seiche in the fjord.

3.3.4 Sensitivity study in relation to climate change

In a warmer climate, the runoff from land would increase and this would change the circulation and influence the biological production in the fjord. The sensitivity of the fjord to changing runoff was analysed by integrating the model in the period from June to August with different scalings of the total runoff (Fig. 3.10). In the limiting case with no river discharge, the mixed layer thickness is about 9–11 m during the summer season, due to the weak pycnocline in the upper part of the water column (Table 3.4, $\lambda=0$). At a runoff corresponding to only 50 % of the runoff in 2003 ($\lambda=0.5$), the halocline is established quite quickly, and the mixed layer is about 0.7–1.6 m

Table 3.4
Monthly averaged mixed layer depth and standard deviation for model solutions with different freshwater discharge Q_f. The mixed layer depth is calculated at the position 20.68 °W, 74.44 °N, corresponding to a locality near the entrance to Tyrolerfjord. The freshwater discharge is scaled with λ in 6 different model runs, such that λ = 1 corresponds to the reference case with a total discharge based on the Zackenberg river discharge observed in 2003.

λ	*0*	*0.5*	*1.0*	*2.0*	*4.0*	*8.0*
June	10.7±5.9	8.5±6.3	4.6±2.8	4.3±2.8	4.0±2.8	3.7±2.8
July	8.7±3.8	4.7±1.9	4.0±1.6	3.5±1.4	2.8±1.2	2.2±0.7
August	11.2±3.1	6.6±2.1	5.2±1.3	4.1±1.1	3.3±1.0	2.5±1.0

deeper in July and August (than in the reference case) (λ = 1.0). In the reference case the mixed layer depth is 4.0 m and 5.2 m in July and August, respectively. At a runoff two times larger than in the reference case (λ = 2.0), the mixed layer becomes about 0.3–1.1 m shallower during the season than in the reference case, and, in an extreme case when runoff is 8 times larger (λ = 8.0), the mixed layer depth decreases to about 2.2–3.7 m during the season. The standard deviation of the monthly averaged mixed layer depth in the reference case and in case of a runoff twice as large, is 1.6 m to 1.4 m in July, and decreases to 1.3 m to 1.0 m in August, respectively.

The sensitivity study shows the importance of the runoff for controlling the depth of the mixed layer. In the case without runoff the mixed layer is controlled solely by wind-induced mixing and buoyancy fluxes at the surface. Even at a moderate runoff of only 50 % of the present level, a freshwater-controlled mixed layer is established quite early by the end of June (Fig. 3.10), and is only slightly deeper than in the reference case. In the other extreme, when runoff is large, the mixed layer depth is controlled by the strength of the surface forcing on the system, i.e. wind and air temperature. Thus, the case with no runoff puts an upper limit on the mixed layer depth of about 11 m in Young Sound during the summer season, and, correspondingly, the case when runoff is 8 times the current level puts a lower limit on the mixed layer depth of about 2 m. The reference case lies between these extremes, and, therefore, a change in runoff can influence the mixed layer depth distribution in the fjord. Doubling of the runoff will decrease the mixed layer by about 1 m or about 20 %. An increase in runoff also reduces the variability of the mixed layer because of the weaker mixing across the stronger vertical pycnocline. In a warmer climate, reduced variability could reduce new production due to further nutrient limitation above the pycnocline during the summer period. However, reduced sea ice cover in the early summer period could increase wind-induced vertical mixing which would have the opposite effect on new production.

In a future, warmer, climate scenario the runoff period might increase significantly, and this would prolong the period in which the surface conditions are controlled by freshwater discharge. However, this

Figure 3.11 (a) Bathymetry and land mask (resolution 2 and 0.5 nm, respectively) along the East Greenland coast off Young Sound (ETOPO2, 2001, Hastings et al., 1999). Hydrographical distributions of salinity and temperature (°C) (contour) along 74 °N, based on World Ocean Atlas 2001 (Conkright et al., 2002) for February **(b)** and August **(c)**.

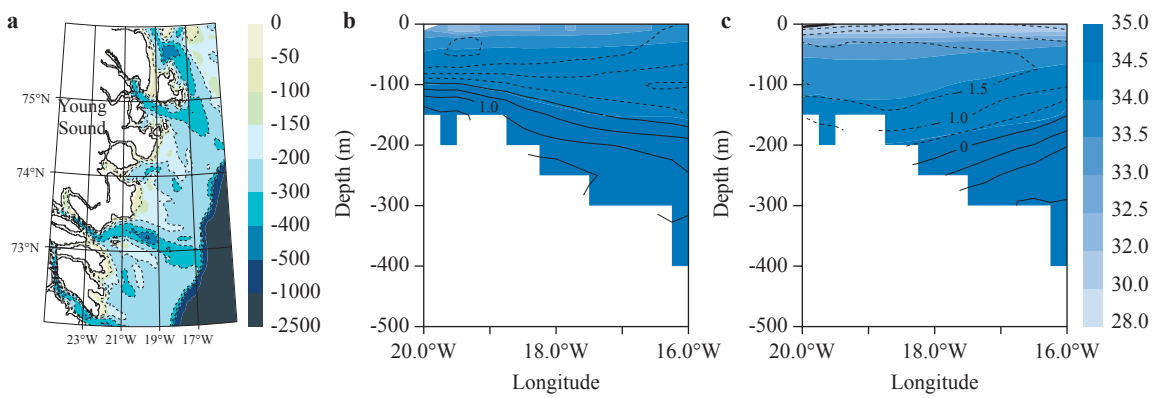

Photo: Søren Rysgaard

Research boat "Aage V. Jensen" in Young Sound at midnight, August 2004.

would not be expected to decrease the mixed layer depth below the solutions shown in Figure 3.10 significantly, as the balance between runoff and atmospheric forcing is established within a few weeks.

3.3.5 Exchanges with the East Greenland Current

During the summer season, the water masses in Young Sound have a relatively low σ_t, between 13 and 26.6 (cf. Fig. 3.3), and transports from the fjord therefore primarily influence the upper water masses of the East Greenland Current system. The East Greenland Current extends across the 100 km wide shelf outside the sill, with typical depth levels of less than 500 m (Fig. 3.11a). The water masses outside the sill in the depth range 50-300 m show large interseasonal changes. During summer, water above 200 m can be characterized as Polar Surface Water (PSW: $\sigma_t < 27.70$, $\leq 0\,^{\circ}C$) with low temperature and salinity (Rudels et al., 2005; Chapter 1). This water originates from the surface waters in the Arctic Ocean where runoff and meltwater from sea ice cause salinity and temperature to be low. Below 200 m a relatively warm ($\theta > 1\,^{\circ}C$) and saline ($S > 34.5$) water mass can be identified (Fig. 3.11c, Fig. 3.2). This water mass consists of Arctic Atlantic Water (AAW: $27.70 < \sigma_t < 27.97$, $0 < \theta \leq 2$), which also originates in the Arctic Ocean but may be modified by mixing with warmer and more saline recirculating Atlantic water from the Fram Strait. During winter, the density structure of the East Greenland Current

system changes due to a decrease in low-salinity surface water, and, consequently, the warm and denser AAW moves to depth levels between 100 and 200 m. This water mass will therefore have a larger influence on the characteristics of the deep water entering the fjord from autumn to late winter. Due to the relatively low salinity in the fjord (S < 33.2), there is probably no significant exchange of deep water from the fjord to the East Greenland Current. Even during winter when sea ice formation can increase salinity, the density of the bottom water will remain below the AAW. Density changes outside the sill on shorter time scales, i.e. days to weeks, can have a significant influence on the exchange of water across the sill, but these features can not be resolved from the current observational data set. Current-meter moorings at 74.5–75 °N across the continental shelf and slope show that the core of the East Greenland Current is located above the slope relatively far from the coast with an annual mean southward velocity of 0.16 m s^{-1} in the surface layer. The observed currents are intensified during winter due to the wind-driven gyre transport in the Greenland Sea being stronger during this period of the year (Woodgate et al., 1999).

Apart from the transport associated with the density field, tides (barotropic exchange) and runoff from land contribute significantly to the exchange. The large barotropic exchange associated with the tidal wave corresponds to about 1–2 % of the volume in the fjord twice a day, a relatively high value compared with the runoff from land, which corresponds to about 0.5 % over a 3-month period. However, the estuarine circulation caused by river runoff is amplified by about an order of magnitude due to the relatively small salinity difference between the surface and intermediate layer at the sill, and, therefore, the estuarine circulation becomes a significant part of the exchange. An estimate of the estuarine exchange through Young Sound during a 3-week period in August 2000 shows that transport in intermediate layers results in a net transport of organic carbon into Young Sound of about 15–50 t C day^{-1} (Rysgaard et al., 2003). Calculation of the transport due to the barotropic mode would require a higher spatial resolution of the organic carbon distribution than is available at present, because this transport is controlled to a large extent by the interplay between the horizontal gradients across the sill and the internal vertical mixing in the fjord.

3.4 Acknowledgements

This work was financially supported by DANCEA (the Danish Cooperation for the Environment in the Arctic) under the Danish Ministry of the Environment. This work is a contribution to the Zackenberg Basic and Nuuk Basic programs in Greenland. Aage V Jensens Charity Foundation is thanked for providing financial support for research facilities in Young Sound.

Comments from 3 reviewers as well as linguistic corrections by Anna Haxen improved the manuscript.

3.5 References

Brandt, J., Christensen, J. H., Frohn, L. M., Palmgren, F., Berkowicz, R. & Zlatev, Z. 2001. Operational air pollution forecasts from European to local scale. Atmos. Environ. 35:91-98.

Conkright, M. E., Locarnini, R. A., Garcia, H. E., O'Brien, T. D., Boyer, T. P., Stephens, C. & J. I. Antonov. 2002. World Ocean Atlas 2001: Objective analyses, data statistics, and figures, CD-ROM Documentation, National Oceanographic Data Center, Silver Spring, MD, 17 pp.

ETOPO2, U. S. Department of Commerce, National Oceanic and Atmospheric Administration, National Geophysical Data Center. 2-minute Gridded Global Relief Data, http://www.ngdc.noaa.gov/mgg/fliers/01mgg04.html, 2001.

Hastings, D. A. & Dunbar, P. K. 1999. Global land one-kilometer base elevation (GLOBE) digital elevation model, Documentation, Vol. 1.0, Key to Geophysical records documentation (KGRD) 34. National Oceanic and Atmospheric Administration, National Geophysical Data Center, 325 Broadway, Boulder, Colorado 80303, U.S.A.

Houghton, J. T., Ding, Y., Griggs, D.J., Noguer, M., van der Linden, P. J. & Xiaosu, D. 2001. IPCC Third assessment report: Climate change 2001: The scientific basis, Cambridge University Press, UK.

Luyten, P. J., Jones, J. E., Proctor, R., Tabor, A., Tett, P. & Wild-Allen, K. 1999. COHERENS – A coupled hydrodynamical-ecological model for regional and shelf seas: user documentation. MUMM report, Management Unit of the Mathematical Models of the North Sea, Belgium, 911 pp.

Pawlowicz, R., Beardsley, B. & Lentz, S. 2002. Classical tidal harmonic analysis including error estimates in MATLAB using T_TIDE. Comput. Geosci. 28: 929 – 937.

Roeckner, E., Bengtsson, L. & Feichter, J. 1999. Transient climate change simulations with a coupled atmosphere-ocean GCM including the tropospheric sulfur cycle, J. Clim. 12: 3004-3032.

Rudels, B., Fahrbach, E., Meincke, J., Budéus, G. & Eriksson, P. 2002. The East Greenland Current and its contribution to the Denmark Strait overflow. ICES J. Mar. Sci. 59: 1133-1154.

Rudels, B., Björk, G., Nilsson, J., Windsor, P., Lake, I. & Nohr, C. 2005. The interaction between waters from the Arctic Ocean and the Nordic Seas north of Fram Strait and along the East Greenland Current: results from the Arctic Ocean-02 Oden expedition. J. Mar. Sys. 55: 1–30.

Rysgaard, S., Vang, T., Stjernholm, M., Rasmussen, B., Windelin, A. & Kiilsholm, S. 2003. Physical conditions, carbon transport and climate change impacts in a NE Greenland fjord. Arct. Antarct. Alp. Res. 35: 301–312.

Rysgaard, S., Frandsen, E., Sejr, M., Dalsgaard, T., Blicher, M. E. & Christensen, P. B. 2005. Zackenberg Basic: The marine monitoring programme. In: Rasch, M. & Caning, K. (eds.). Zackenberg ecological research operations 10th annual report, 2004 – Copenhagen, Danish Polar Center, Ministry of Science, Technology and Innovation. 85 pp.

Stigebrandt, A. 2001. Fjord circulation. In: Steele, J., S. Thorpe and K. Turekian (eds.). Encyklopedia of ocean sciences: 897–902. Academic Press Inc., U.S.

Vinnikov, K. Y, Robock, A., Stouffer, R. J., Walsh, J. E., Parkinson, C. L., Cavalieri, D. J., Mitchell, J. F. B., Garret, D. & Zakharov, V. F. 1999. Global warming and northern hemisphere sea ice extent. Science. 286:1934–1937.

Woodgate, R. A., Fahrbach, E. & Rohardt, G. 1999. Structure and transports of the East Greenland Current at 75°N from moored current meters. J. Geophys. Res. 104:18059–18072.

Photo: Egon R. Frandsen

4

The sea ice in Young Sound: Implications for carbon cycling

The sea ice in Young Sound: Implications for carbon cycling

Ronnie N. Glud[1], Søren Rysgaard[2], Michael Kühl[1] and Jens W. Hansen[3]

[1]Marine Biological Laboratory, University of Copenhagen, Strandpromenaden 5, DK-3000 Helsingør, Denmark
[2] Greenland Institute of Natural Resources, Kivioq 2, Box 570, DK-3900 Nuuk, Greenland
[3] National Environmental Research Institute, Vejlsøvej 25, DK-8600 Silkeborg, Denmark

Cite as: Glud, R. N., Rysgaard, S., Kühl, M. & Hansen, J. W. 2007. The sea ice in Young Sound: Implications for carbon cycling. In: Rysgaard, S. & Glud, R. N. (Eds.), Carbon cycling in Arctic marine ecosystems: Case study Young Sound. Meddr. Grønland, Bioscience 58: 62-85.

Abstract

Most of the year, Young Sound is covered by c. 160 cm thick sea ice overlain by a 20-100 cm thick snow cover. During the last 50 years the sea-ice-free period has varied between 63 and 131 days, but during the last 10–15 years there has been a tendency towards an increase in the sea-ice-free period, and 7 of the longest sea-ice-free periods observed in 50 years were recorded after 1990. The snow and sea-ice cover regulates the activity of the light-limited marine ecosystem of Young Sound. As the snow cover melts during late May and June, the irradiance reflectance decreases, especially for red and near infrared light. Differences in snow cover thickness and patchy distribution of dry snow, wet snow and melting ponds on the sea-ice surface result in a very heterogeneous light environment at the underside of the ice. In areas with sufficient light, sea-ice algae begin to flourish on the available nutrients. The sea-ice algal community adapts efficiently to the local light environment, and in areas with natural (or man-made) holes and cracks sea-ice algae bloom. However, despite ample nutrients, the overall phototrophic biomass in Young Sound remains very low, with maximum values of c. 15–30 µg Chl a l^{-1} sea ice at the underside of the ice and with maximum area integrated values of c. 3 mg Chl a m^{-2}. We speculate that the extreme dynamics in sea-ice appearance, structure and brine percolation, which is driven primarily by large but variable freshwater inputs during snow melt and the breaking of frozen rivers, transforms the sea-ice matrix into a hostile environment for sea-ice algae. An annual estimate of sea-ice-related gross primary production for the entire outer Young Sound (Region 1 c. 76 km^2) amounted to only 2.7 t C. The primary production measurements were performed in 1999 and 2002, and we cannot exclude large inter annual variations. However, we have not experienced massive blooming of sea-ice algae in Young Sound during the last decade.

Detailed *in situ* and laboratory-based microsensor investigations documented that O_2 concentrations at the underside of the ice and within the sea-ice matrix were extremely dynamic and strongly regulated by physical processes related to freezing and thawing of sea water rather than biological activity. Enclosure experiments on sea-ice samples performed in June 2002 revealed a high heterotrophic potential causing the sea-ice environment to become anoxic within 8 days despite concurrent photosynthetic activity. The sea ice was thus net heterotrophic, at least intermittently, and the sea ice hosted a bacterial community of denitrifiers. These findings change our conceptual and quantitative understanding of sea-ice-related microbial activity - at least in settings similar to Young Sound.

4.1 Introduction

Sea-ice cover greatly affects element cycling and regulates primary production in polar environments. During ice cover, the propagation of light to the underside of the ice is strongly impeded due to strong backscattering and attenuation, primarily in the snow cover but also within the sea-ice matrix. This is reflected in a positive correlation between annual primary production and the length of the open-water period in polar and sub-polar regions (Rysgaard et al., 1999). A significant fraction of the light-limited

aquatic primary production in polar ecosystems can be associated with the sea-ice rather than with the pelagic or benthic environments (Horner & Schrader, 1982; Palmisano & Sullivan, 1983; Gosselin et al., 1997; McMinn et al., 2000). Sea-ice algae primarily flourish at the water-ice interface, but algae encrusted inside the ice matrix experience higher light levels and can contribute significantly to the total sea-ice-related primary production (Mock & Gradinger 1999).

The sea-ice algae represent a food source for metazoan grazers (Grainger & Mohammed, 1990; Gradinger & Spindler, 1999) and leakage of photosynthetic products or entrapped organic material can lead to elevated bacterial abundances within the sea ice (e.g. Gradinger & Zhang, 1997; Gradinger & Ikävalko, 1998; Giannelli et al., 2001; Meiners et al., 2003). The sea-ice biota consists of a complete food web with primary and secondary production, a microbial loop and three to four trophic levels (e.g. Horner et al., 1992; Schnack-Schiel et al., 2001). Sea-ice-related processes interact with the underlying water via ice melting/freezing, advection and grazing. In order to quantify and understand polar carbon cycling, it is therefore of prime importance to include the sea-ice-related activity.

During freezing of seawater, crystals of low-salinity water form while dissolved salts and gases freeze out, forming brine inclusions and gas bubbles within the sea-ice matrix. In contrast to freshwater ice, sea ice is thus permeated with pores and brine channels that form more or less interconnected networks in the matrix of solid ice crystals (e.g. Eicken, 2003). The total pore volume of sea ice typically ranges between 1 and 20% depending on temperature, salinity and ionic composition of the brine fluid (Weeks & Ackley, 1986). At decreasing temperatures the thermodynamic phase equilibrium drives the sea ice towards a lower pore space volume and towards increasing brine salinity. Thus, winter sea ice exposed to temperatures below -20°C contains less than 1% pore space with brine salinity levels well above 200 (Cox & Weeks 1983). The lower part of the sea ice close to the water phase is, however, kept near the freezing point of sea water (c. -1.8°C) and is thus more permeable than the upper layers of the sea ice. The individual brine inclusions vary in size from a few micrometers to several centimeters (Weissenberger et al., 1992; Golden et al., 1998), and sea-ice thus contains a variety of enclosed and semi-enclosed microniches exhibiting a variety of environmental conditions and harboring different biota and microbial activities. The degree of interconnection of the brine enclosures generally increases with temperature and the potential for percolation of brine through the sea-ice matrix therefore increases towards the polar spring (Eicken et al., 2000). The sea-ice matrix is thus highly heterogeneous, dynamic and difficult to access by standard measuring techniques, and quantification of *in situ* biogeochemical activities in sea ice represents a true challenge to any experimentalist.

A complete study on sea-ice dynamics and the associated biota requires a multidisciplinary approach involving a number of different scientific fields, and many components need careful attention. Our work on sea ice in Young Sound does not provide a complete and exhaustive investigation of the sea ice in the area, but rather a focused effort resolving light conditions, nutrient and gas dynamics, primary production and, to a lesser extent, heterotrophic activity in order to provide estimates on the quantitative importance of sea ice for the local carbon cycling. Most of the presented data were collected during two field campaigns performed from 7 June–5 July 1999 and 28 May–12 June 2002.

4.2 Methods

A number of different techniques were applied during the study. Most of these represent standard measuring routines for sea-ice studies and will not be dealt with in any detail here. For further information on these techniques please refer to the literature. However, we developed and applied *in situ* instruments that are not widely used, and these are described in some detail below.

4.2.1 Sampling and basic routine measurements

Unless anything else is specified the presented measurements were obtained in close vicinity to Station A at 74°18N, 20°15W in outer Region 1 (Chapter 3). Intact sea-ice cores (9 cm id.) were sampled by a MARK II coring system (Kovacs Enterprises, Lebanon, NH , USA). Temperature profiles were measured immediately after recovery by placing solid digital thermosensors in holes of 3 mm in diameter drilled to the center of the core. Intact sections of sea ice were completely thawed for determination of bulk salinity

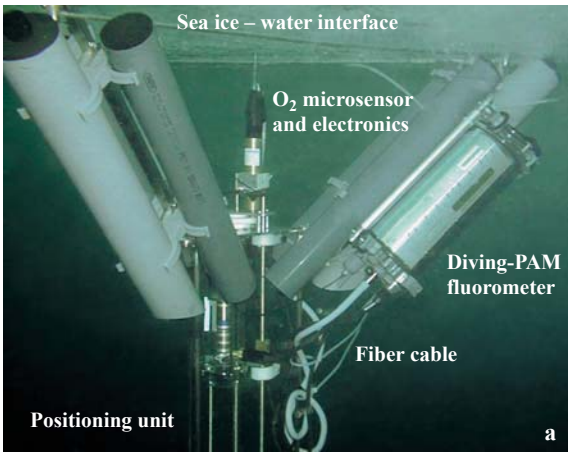

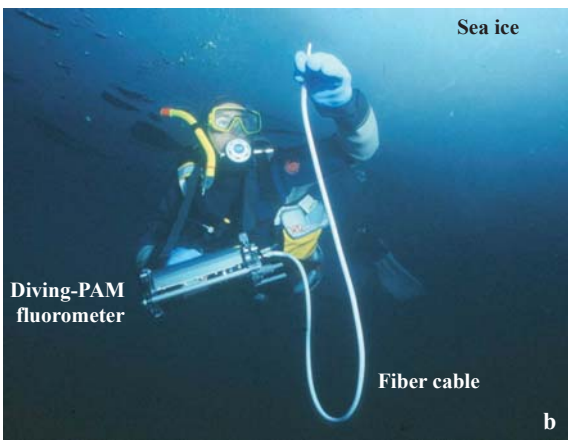

Figure 4.1 (a) The microprofiling instrument placed at the underside of the ice. The central torpedo carrying the microelectrode contains the measuring circuit and is connected to the upper sea-ice surface via a cable. The diving PAM fluorometer is mounted on one of the tripod legs. When fluorescent signals were measured via the tripod, the tip of the fiber cable was mounted on the central "torpedo". **(b)** Diver-operated PAM fluorometer used for estimating phototrophic biomass and photosynthetic activity at the underside of the ice. Photos from Rysgaard et al. (2001).

and nutrient concentrations. Brine concentrations were calculated using the equations of Cox & Weeks (1983) and Leppäranta & Manninen (1988). Samples for nutrient analysis were filtered through GF/F filters and frozen at -18°C until further analysis, while the filters were extracted for 24 h in 96% ethanol and analyzed on a fluorometer for Chl *a* (Jespersen and Christoffersen 1987). Salinity was quantified with a calibrated conductivity meter (Knick, Germany). Concentrations of NO_3^- and NO_2^- were determined as described by Braman & Hendrix (1989), and NH_4^+ concentrations were measured according to Bower & Holm-Hansen (1980). Phosphate concentrations were determined spectrophotometrically (Grasshoff et al., 1983). Dissolved organic carbon (DOC) was determined with a Shimadzu DOC-5000 Analyzer on melted sea-ice samples after filtration (combusted GF/F filters).

For determination of the gas bubble volume in the sea ice, sections of preweighed ice samples were placed in artificial seawater in 200-ml gas tight glass syringes fitted with 50-cm transparent *Tygon* tubes (id. 3mm). After thawing (at +2°C) the volume of the accumulated gas bubble was determined by pushing it into the tube and measuring the length of the bubble. The oxygen content of the thawed sea-ice sample and the gas bubble was determined by Winkler titration and GC analysis, respectively, and from these data the total O_2 concentration of sea ice samples was calculated according to Rysgaard & Glud (2004).

Sea-ice-related primary production was estimated in sections of the intact sea-ice cores or on sea-ice samples collected by divers from the underside of the ice. The samples were crushed, homogenized and mixed with GF/F-filtered seawater and subsequently incubated with ^{14}C-labeled DIC in glass bottles placed below the sea ice for approximately 2 h (Steemann-Nielsen, 1958; Rysgaard et al., 2001). The ^{14}C fixation was corrected for unspecific labeling measured in dark-incubated bottles and primary production rates were quantified as described by Rysgaard et al. (2001). Denitrification and anaerobic ammonium oxidation (*anammox*) rates in thawed sea-ice were measured by incubating samples with various combinations of $^{15}NO_3^-$, $^{15}NH_4^+$ and $^{14}NO_3^-$ (for details, see Rysgaard & Glud, 2004).

4.2.2 *In situ* microprofile measurements

The biological activity in sea ice is commonly inferred from measurements performed on thawed and homogenized samples. Consequently, the microenvironment (temperature, salinity, nutrient concentrations etc.) of the sea ice has been dramatically changed and the original activity of the sample is no longer preserved. In order to circumvent these problems we constructed a special microprofiling instrument capable of measuring *in situ* O_2 microprofiles at the ice-water interface (Fig. 4.1a). With this instrument it was our aim to obtain *in situ* information about net photosynthesis and aerobic respiration in the lowermost layer of the intact sea ice.

Clark-type oxygen microelectrodes (Revsbech, 1989) were mounted directly on a torpedo-shaped

cylinder containing a custom-made picoamperemeter (Unisense A/S, Denmark). The sensors had tip diameters of 50–150 µm, a stirring sensitivity <2% and a t_{90} response time <2 s (Glud et al., 2000). The measuring system was mounted on a motor-driven spindle fastened to a metal tripod allowing vertical positioning of the sensor tip. Signal recording and motor control was achieved via a 50 m long underwater cable connected to a controller box at the sea ice surface. Sensor calibration was performed during deployment at *in situ* temperature and salinity by exposing the sensor to anoxic and 100% air-saturated water samples. Divers carefully placed the tripod at the underside of the sea ice (avoiding local disturbance and trapping of air bubbles at the measuring site) and the positive buoyancy of air-filled tubes kept the tripod in place during measurements (Kühl et al., 2001; Rysgaard et al., 2001). The O_2 distribution across the water-ice interface was subsequently measured *in situ* under ambient flow and light conditions.

4.2.3 *In situ* Pulse Amplitude Modulated (PAM) fluorometer measurements

Proxies for microalgal biomass (F_0) and photosynthetic activity (rel. ETR) at the underside of the sea ice were measured *in situ* using a pulse amplitude modulation fluorometer (Diving-PAM, Walz GmbH, Germany). A detailed description of the measuring scheme and its application on sea ice can be found in Kühl at al. (2001) and Rysgaard et al. (2001). In short, a 1 m long (8 mm outer diameter) fiber cable guided probing light, actinic light and the variable fluorescence signals between the waterproof fluorometer and the measuring spot. A SCUBA-diver probed various sites in pre-defined grids below the sea ice (Fig. 4.1b). For longer-term measurements the fiber tip was mounted on the moving axis of the tripod described above (Fig. 4.1a).

The apparent minimal fluorescence at the measuring spots, F_0 (which is not the true F_0 value as it was impossible to completely dark adapt the spots due to midnight sun), was obtained by exposing spots with modulated non-actinic levels of probing light emitted by the integrated blue LED in the fluorometer (Schreiber et al., 1986). In order to convert the fluorescence signals into photosynthetic biomass, calibrations were performed on sea-ice-encrusted microalgal cultures with a known Chl *a* content (Rysgaard et al., 2001; Glud et al., 2002). In the applied configuration the detection limit amounted to c. 0.3 µg C l^{-1}.

The relative electron transport rate (rel. ETR) between photosystems II and I of algae inhabiting the lowermost surface of the sea ice was determined by Diving-PAM using the so-called saturation pulse method (Schreiber et al., 1995; Kühl et al., 2001). The effective quantum yield of PSII-related photosynthetic electron transport was measured at increasing levels of actinic light from a halogen lamp integrated in the Diving-PAM. The actinic light levels were determined with a Licor underwater irradiance meter. Relative electron transport rates, used here as a proxy for the relative photosynthetic rate, were calculated at each experimental irradiance as the product of effective quantum yield (ϕ_d) and the amount of actinic light. In this way, curves of rel. ETR vs. irradiance could be measured *in situ*, yielding information on photosynthetic performance and light acclimation of sea ice algae under natural conditions.

4.3 Results & discussion

4.3.1 Seasonal and interannual variation in ice cover

During the last decades, the sea-ice cover in Young Sound has typically established itself around the end of September. Initially, the sea-ice thickness increases by approximately 2 cm d^{-1}, a rate that gradually decreases to <0.5 cm d^{-1} in January to March. The maximum sea-ice thickness of 140-160 cm is usually reached in April and by then the sea ice surface is covered by a snow layer of variable thickness (20-100 cm). The snow cover strongly affects the light conditions below and within the sea ice and drifting snow introduces a marked patchiness in light distribution at the underside of the sea-ice. The sea-ice cover is hinged to the shore and mechanical stress induced by tidal variations forms cracks and patches of open water that gradually broaden and expand along the shore lines during May–June. The melting of the sea ice accelerates during June–July until the 30–120 cm thick sea-ice cover is exported to the Greenland Sea by wind or current-induced forcing on the now free-floating ice-floes. This breakup of sea ice typically occurs in mid-July (Fig. 4.2). The ice cover of Young Sound is thus characterized as fast ice (first-year sea ice) and older floes from the pack ice in the Greenland Sea are seldom trapped within the fjord.

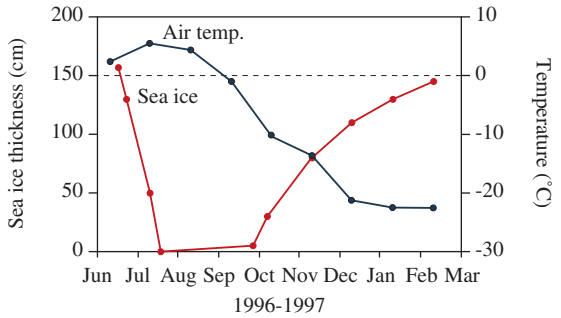

Figure 4.2 Air temperature and sea-ice thickness during 1996–1997. The data reflect the typical seasonality as experienced in Young Sound during the last decades. Data from Rysgaard et al. (1998).

The total sea-ice thickness typically remains in quasi-steady state during April to early June. During this period the sea-ice environment becomes extremely dynamic. Elevated air-temperatures lead to snow melting and the formation of a freshwater layer on top of the sea ice. During periods of colder weather, this can lead to the formation of a secondary ice layer whereby a lens of freshwater separates the thick sea ice from a thinner layer of freshwater ice below the gradually melting snow cover (Fig. 4.3). Temperature variations, tidal movements and wind-induced forcing along with macroscopic cracks and breathing holes of marine mammals can lead to periodic freshwater percolation through the sea-ice matrix. This becomes especially apparent at the bottom of

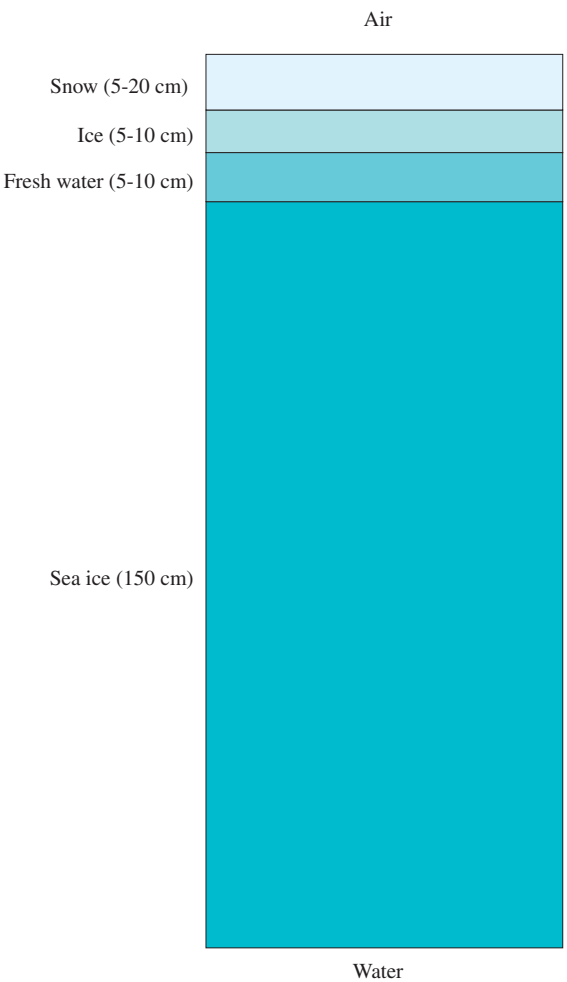

Figure 4.3 A schematic vertical profile through the snow/sea-ice cover reflecting conditions in Young Sound during the period mid-May–mid June.

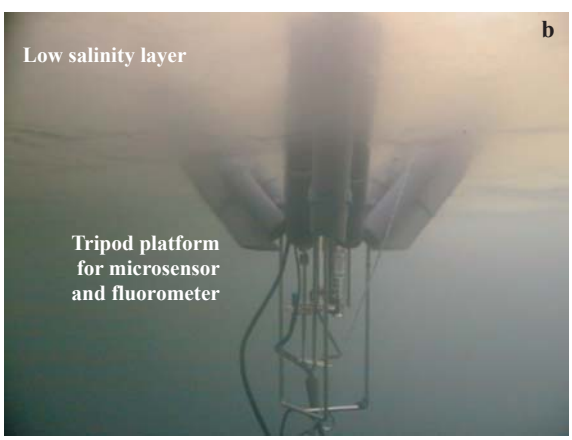

Figure 4.4 Photos of the underside of the sea ice on 14 June 1999 **(a)** and 2 July 1999 **(b)**. Together with Fig. 1a, (obtained 13 June the same year), the photos document the extreme variability in appearance of the underside of the ice during this period. Photos from Rysgaard et al. (2001).

the sea ice, where the appearance can change in a few hours from a solid homogenous surface to a spongy and highly heterogeneous structure with a topography characterized by long, spiny ice crystals, which form when meltwater from above encounters the subzero temperatures in the sea water below (Fig. 4.4a). Temperature changes in the surface water or strong tidal flows can reestablish the original hard and homogenous sea ice as the spiny structures melt or are eroded away mechanically. When a larger amount of freshwater is introduced suddenly to the bottom of the sea-ice, a large lens of low-salinity water is established. This becomes very extensive when the rivers of the area break and release millions of m^3 of freshwater into the fjord (Fig. 4.4b, see Chapter 2). The massive freshwater input has large consequences for the sea-ice environment and the associated biological activity (see below), and the dynamic behavior of the sea-ice structure during that period constantly frustrated our attempts to quantify the biogeochemical activity of the system.

During the short ice-free period, ice floes or icebergs occasionally enter Young Sound and drift around in a circular pattern in the outer fjord system until they are re-exported to the Greenland Sea (see Chapter 3). This occasional re-entry of ice into Young Sound during the "open-water" period probably has no impact on the larger-scale carbon cycling of the area. Young Sound is thus typically ice covered for 9–10 months of the year. However, the interannual variation is considerable, and during the last 50 years the ice-free period has varied between 63 and 131 days. Especially during the last few years the open-water period has been exceptionally long, and over the last decades a trend towards an extended open-water period is apparent (Fig. 4.5). The prolonged open-water period in Young Sound complies with observations of increasing temperatures and generally decreasing sea-ice cover in the Greenland Sea.

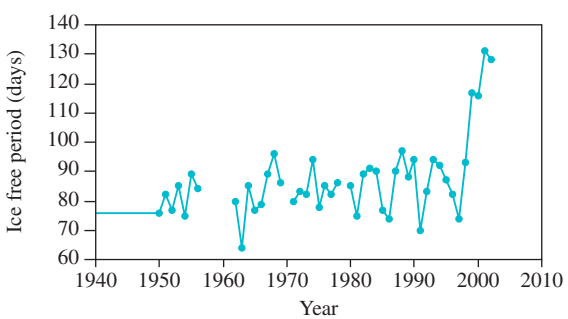

Figure 4.5 The number of ice-free days in Young Sound during the last 50 years. Most data are extracted from the logbook of the military patrol, SIRIUS, operating in the area.

4.3.2 Reflection, extinction coefficients and light spectra of the sea ice

The snow and sea-ice cover regulates the availability of light for aquatic primary production. Thus, basic information on snow and sea-ice reflectance and light attenuation is essential for a quantitative assessment of local carbon cycling. Generally, the optics of snow and sea ice is well studied (Perovich, 1996 and references therein) and several radiative transfer models have been formulated (e.g. Perovich, 2003). However, our aim with the light measurements in the present study was to obtain important background data on irradiance rather than a detailed optical characterization of the sea ice. Thus, instead of exhaustive optical measurements or the use of radiative transfer models for sea ice (Perovich, 2003), we performed a limited number of irradiance measurements with

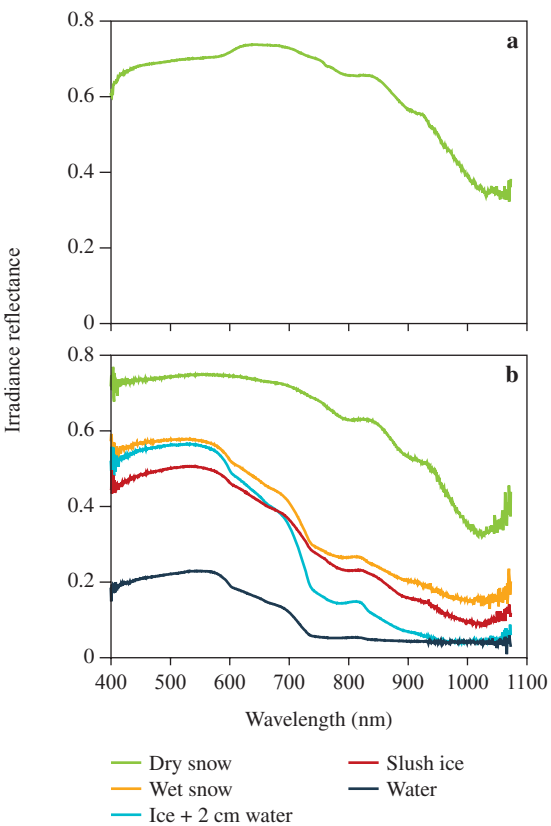

Figure 4.6 The irradiance reflectance (downwelling/upwelling irradiance) measured in different snow types around Station A on 10 and 29 June before and during melting, respectively (Figs. a and b).

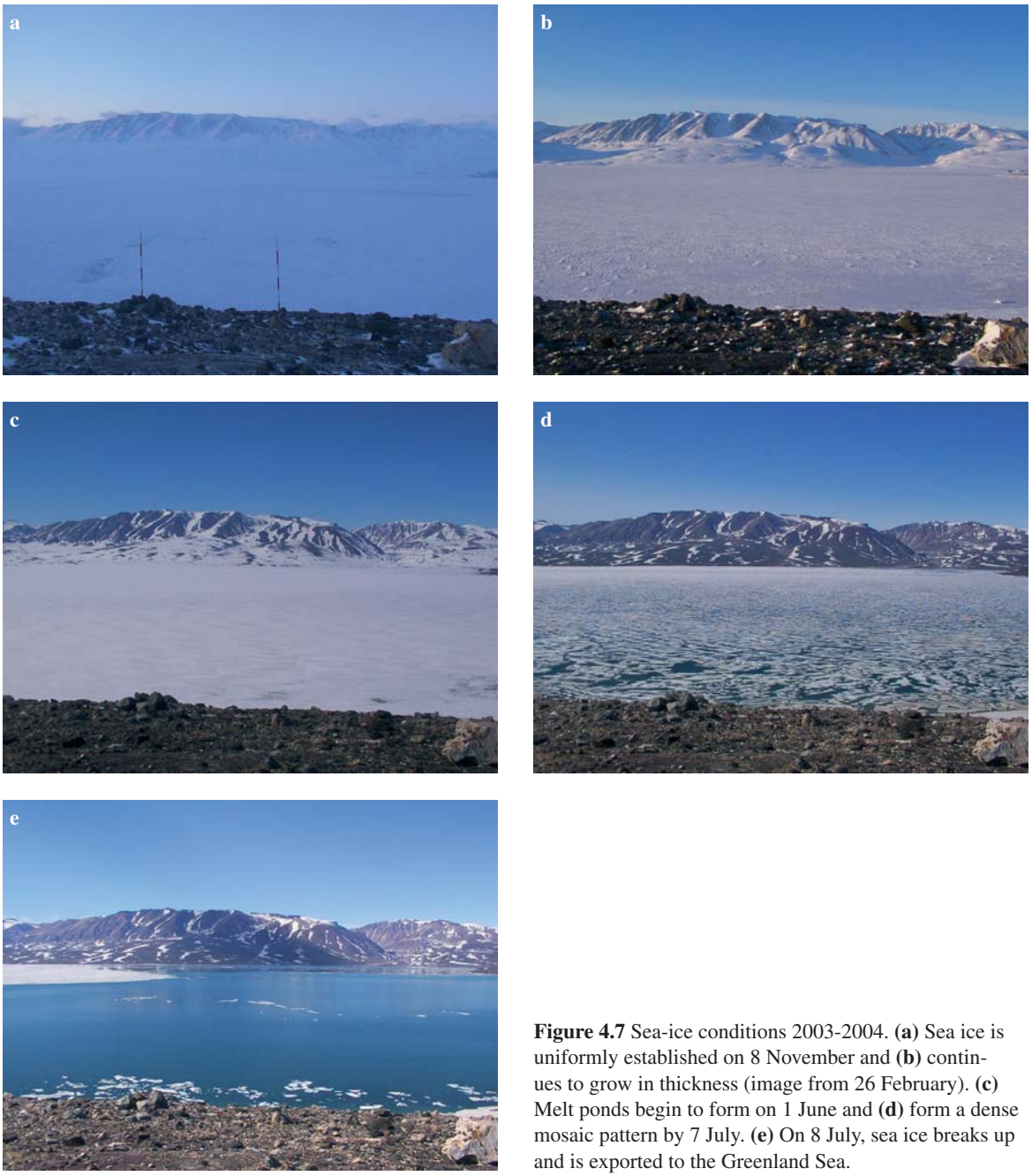

Figure 4.7 Sea-ice conditions 2003-2004. **(a)** Sea ice is uniformly established on 8 November and **(b)** continues to grow in thickness (image from 26 February). **(c)** Melt ponds begin to form on 1 June and **(d)** form a dense mosaic pattern by 7 July. **(e)** On 8 July, sea ice breaks up and is exported to the Greenland Sea.

Table 4.1 Irradiance reflectance of visible light from various types of snow and sea ice, as measured with a PAR (400–700 nm) quantum irradiance meter.

Medium	Irradiance reflectance $R_{(400–700\ nm)}$
Dry snow	0.73
Water-saturated snow	0.53
Slush ice	0.44
2 cm of water on ice	0.50
10 cm of water on ice	0.48
Sea water	0.18

a broadband PAR (400–700 nm) quantum irradiance meter (LiCor, USA) and with a spectroradiometer (FieldSpec® Analytical Spectral Devices, INC) – 380–1050 nm) during 7 June–5 July 1999. Unless otherwise indicated, all measurements were obtained under a clear sky around noon.

Early in June 1999, the sea ice was covered by a 20-100 cm thick layer of dry snow, and the irradiance reflectance, R, i.e. the ratio between the upwelling and downwelling irradiance, for the visible spectrum (PAR,

400–700 nm) amounted to 0.70–0.75 (Fig. 4.6a). Most of the incident light was thus reflected during this period. The reflectance values for NIR light (700–1050 nm) were, however, significantly lower and ranged between 0.35 and 0.50 due to the intrinsic absorption of red and NIR light in the ice-water matrix.

Later in the season the sea-ice surface turned into a mosaic of melt ponds and areas with more or less meltwater-saturated snow cover. On 29 June, we measured the irradiance reflectance in a number of spots representing different progression stages in snow-cover melt. In areas with dry snow, the situation was unchanged, while R (400–700 nm) had decreased to an average of 0.53 for wet snow, and in areas with slush ice or overlying water, the reflectance was even lower (0.48–0.40) (Fig. 4.6b). The reflectance from seawater in the emerging sea-ice holes was only 0.18. The reflectance of NIR light generally showed the same pattern, but the decrease in reflectance in dry snow versus wet snow was more pronounced in the red (<600–700nm) and NIR (>700nm) regions due to efficient absorption by water in this spectral region.

The reflectance of irradiance and the light propagation in snow is thus clearly affected by the water content. Dry snow contains a mixture of highly light-scattering snow crystals and air. The difference in refractive index between the two phases is relatively large, causing less forward scatter of the incident light. This increases the probability of incident photons being backscattered from the snow. As the water content increases, the difference in refractive index becomes less and scattering of the incident light thus becomes more forward biased (Perovich, 1996); a similar phenomenon is observed when sediments are wetted (Kühl & Jørgensen, 1994). Progressing snowmelt thus forms darker patches of more water-saturated snow on top of the sea ice (Fig. 4.7, see also Fig. 2 in Perovich, 1996 and Plate 3 in Perovich et al., 1998). The irradiance reflectance data is compiled in Table 4.1.

The high reflectance of snow causes strong light attenuation. Already below 4.5 cm of dry snow the downwelling irradiance of visible light was attenuated to <50% of the incident irradiance (Fig. 4.8). Below 24 cm of snow cover only 20–30% of the incident downwelling irradiance remained in the visible spectrum, while <5–10% of incident NIR remained. More detailed measurements of PAR transmission through snow and sea ice showed a strong exponential decrease of irradiance in the snow (Fig. 4.9) with

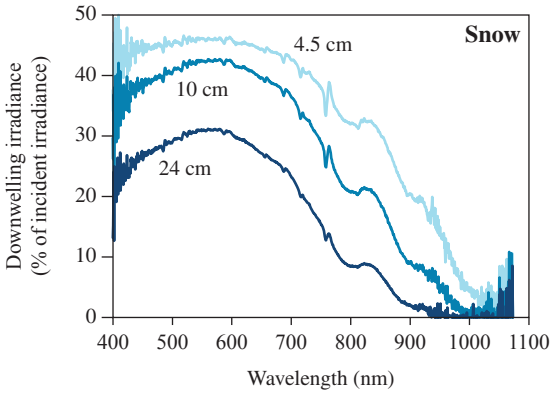

Figure 4.8 The spectral composition of the downwelling irradiance at three respective depths in dry snow.

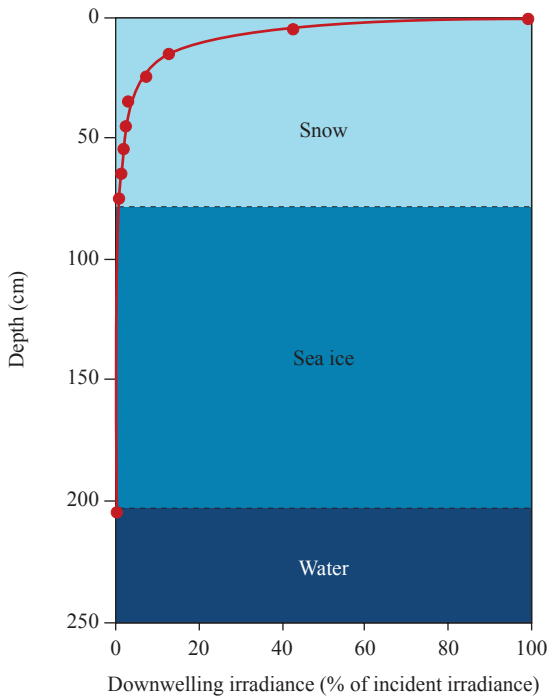

Figure 4.9 Downwelling irradiance profile (400–700 nm) through 75 cm of snow cover overlying 125 cm of sea ice.

an average attenuation coefficient of K_{snow}= 5.6 m^{-1}. However, closer inspection revealed that dry snow on top had a significantly higher light attenuation (9.5 m^{-1}), as compared to the lower layer of compressed snow at sub-zero temperature, which had an attenuation coefficient of about 1.5 m^{-1} (Fig. 4.10). The latter value was only slightly higher than in the underlying sea ice, which had an attenuation coefficient of about 0.9 m^{-1}. Attenuation coefficients in snow can vary from <4 to 40 m^{-1} and vary strongly with the water

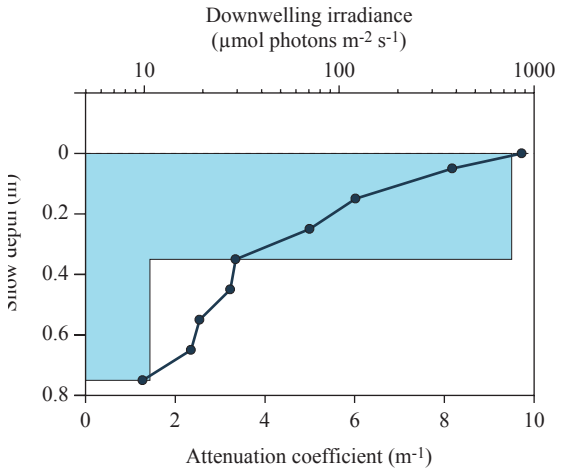

Figure 4.10 Downwelling irradiance (400–700 nm) though a 75 cm thick snow cover (from Fig. 4.6) reflecting two distinct light attenuation curves for the dry snow on top and the wet snow close to the sea ice.

content (Perovich, 1996). Perovich (1996) gives a range of 1.1–1.5 m^{-1} for attenuation coefficients in sea ice. The actual value is, however, dependent on many environmental variables such as the temperature-dependent amount of brine inclusions in the ice and the amount of air bubbles and particulate material enclosed in the ice matrix. The higher attenuation in the top layer as compared to deeper layers in the ice seems to be a general observation in sea ice (e.g. Grenfell & Maykut, 1977).

Light intensity data loggers (Onset, HOBO) were placed at the water-ice interface by divers in order to obtain a continuous record of the visible light level below the sea ice. The data loggers were intercalibrated with readings from a quantum irradiance sensor (LiCor, LI192) prior to deployments. The light levels clearly reflected a diurnal pattern with maximum values reaching 5–15 µmol photons m^{-2} s^{-1} (Fig. 4.11) around noon, corresponding to <0.1–1% of the incident downwelling irradiance, and virtually complete darkness at night due to the low sun angle during nighttime. There was a general trend of increasing light levels below the sea ice as the snow cover gradually melted (Fig. 4.11), and by the end of the melt the transmission of visible light had increased to 1–5% of the incident downwelling irradiance. The temporal variation in attenuation coefficient during the same measuring period was inferred from two simultaneous

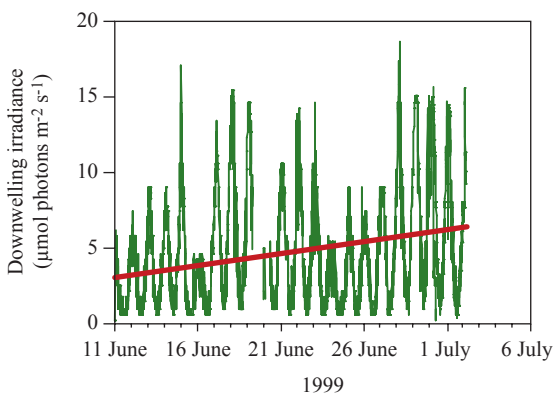

Figure 4.11 Downwelling irradiance measured below the sea ice during a 22-day period in 1999. The diurnal variation reflects the inclination of the sun as the period is characterized by midnight sun. Generally, the values showed an increasing trend towards the end of the measuring period as reflected by the linear approximation (red line), partly due to increased transparency of the ice cover and partly due to higher sun inclination. A few periods contain no data due to exchange of sensors.

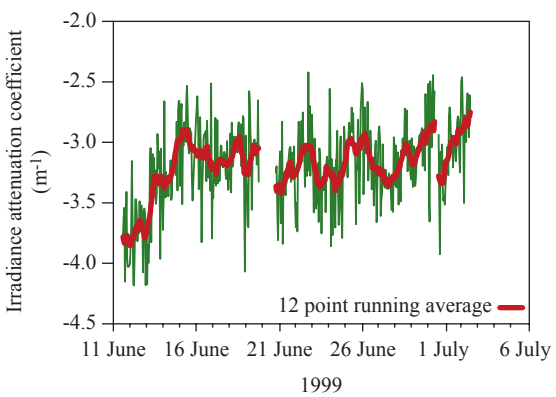

Figure 4.12 Light attenuation coefficient estimated from two continuous recordings of the light data loggers placed above and below the snow/sea-ice cover. The red line indicates a 12-point running average. The data reflects a gradual decrease in light attenuation.

recordings of light intensity loggers positioned above and below the snow/sea-ice cover, respectively (Fig. 4.12). The attenuation was highly variable but showed a decreasing trend during the first week, as the snow cover melted, and then reached a more or less stable value of c. 3.2 m^{-1} in the remaining period. The data only shows the conditions in one spot, but presumably reflects the general spring trend in Young Sound.

The spectral composition of the downwelling irradiance changed significantly during its passage through the snow and ice cover. Below the sea ice, mainly blue-green and yellow light (500–600 nm) prevailed, while blue and red light, as well as NIR light, was strongly attenuated due to the intrinsic absorption properties of water (data not shown). Very similar spectral transmission data was presented by Perovich et al. (1998) for relatively clean ice with no or very small amounts of particulate matter. The presence of particulate matter in ice will tend to decrease reflectance and increase attenuation of light. However, the ice in Young Sound generally was found to contain very low amounts of particles and only in a few cases was a distinct zone of dense material found in ice cores

Our data on reflectance and light transmission of sea ice in Young Sound is very similar to that reported in the literature on sea ice optics (e.g. Perovich, 1996). The temporal change in sea ice optical properties was studied in detail by Perovich et al. (1998) who observed similar decreases in reflectance and increasing light transmission during different stages of snow and ice melting. Our observations thus fit into the general pattern emerging from numerous studies of Arctic and Antarctic sea ice.

4.3.3 Sea-ice holes: Light effects and implications for primary production measurements.

It is generally accepted that in order to get realistic estimates of primary production it is important to incubate at *in situ* temperature and light conditions – preferably *in situ* (Clasby et al., 1973; Smith & Herman, 1991). In order to sample or access the bottom of the sea ice most studies require drilling of holes, and since sea-ice researchers often use standardized equipment, such ice holes tend to be of similar sizes, i.e. with diameters of 8–30 cm. For more elaborate sampling and SCUBA diving purposes larger holes of 80–150 cm in diameter are typical. It is also a common procedure to take advantage of the drilled hole and then place incubation flasks for O_2 exchange measurements or ^{14}C incubations within or at some distance from established holes to mimic *in situ* condition (e.g. Haecky & Andersson, 1999). Different strategies have been applied to reduce light artifacts near the hole, either by placing the bottles at different distances from the hole or covering the hole with various objects (Grossi et al., 1987; Hsiao, 1988). Furthermore, *in situ* profiling techniques adapted to work at different distances from the rim of sea-ice holes have been adapted (McMinn et al., 2000). However, no detailed studies have been published on light distribution around sea-ice holes or on the range and magnitude of light-induced artifacts.

In June 1998, a site with a homogeneous cover of c. 80 cm of dry snow was selected for studying light distribution and primary production activity around a diving hole in 150 cm thick sea ice. The amount of light passing through the snow cover was limited, and the scalar irradiance measured by a diver at the underside of the sea ice was only 0.3–1.5% of the incident downwelling irradiance (data not shown). A square hole of c. 1 m^2 was established without disturbing the snow cover on three sides of the hole. When the hole was established, the scalar irradiance was remapped. As expected, the irradiance immediately below the hole was significantly increased and at the rim (on the side with undisturbed snow cover) of the hole the underside of the ice now received c. 60% of the incident downwelling irradiance (Fig. 4.13a). As the incoming light also propagated horizontally in the snow and the sea-ice cover, a diffuse light field below the sea ice extended up to 8 m from the rim of the hole and reached a maximum water depth of 8 m at the rim. In this case, it was therefore necessary to perform any primary production incubations reflecting *in situ* conditions at least 8 m from the rim of the hole.

Water was sampled at selected depths and sea ice was collected from the bottom of the sea ice at least 8 m from the hole. ^{14}C incubations of water and sea-ice samples were performed in flasks placed at the respective depths. The light-limited primary production of sea-ice algae and phytoplankton in the upper part of the water column was significantly stimulated close to the hole (Fig. 4.13b). During two successive years with different snow cover thicknesses at the site of investigation (80 cm and 20 cm in 1998 and 1999, respectively), primary production of pelagic and sea-ice algae was investigated 4 times using parallel measurements at the center of and 8–10 m from two identical holes. Primary production in the upper 12

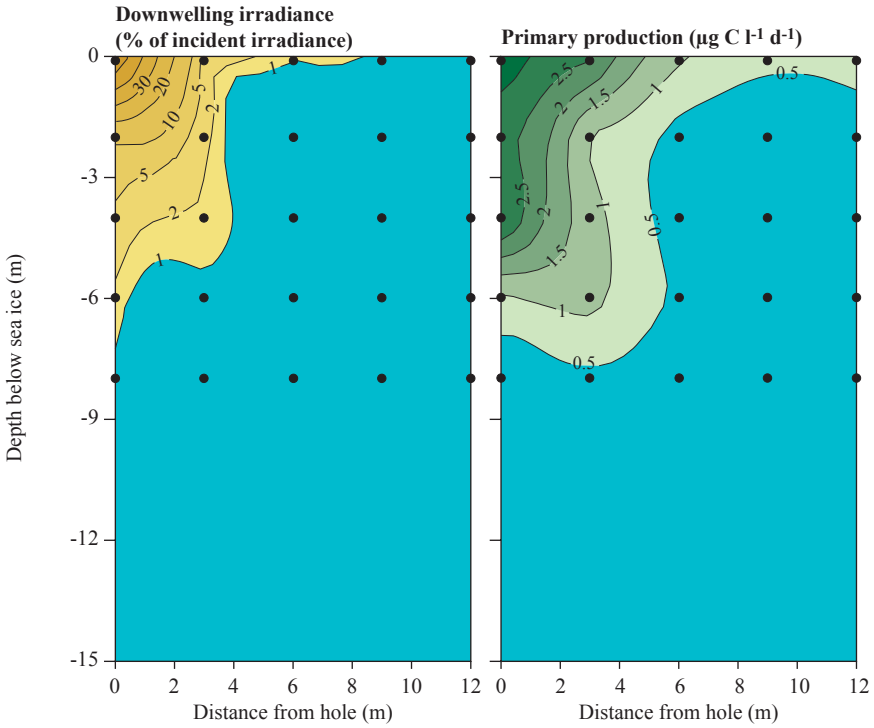

Figure 4.13 (a) Scalar irradiance relative to downwelling irradiance at the sea-ice surface as measured around the established diver hole (hole size c. 1 m^2) and **(b)** primary production measured at the same positions. Zero "0" indicates the position of the ice edge and dots the points of actual measurements.

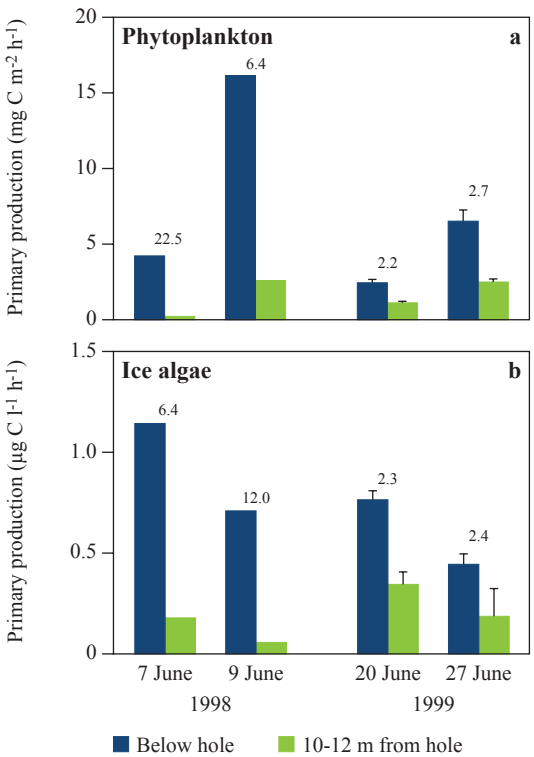

Figure 4.14 (a) Primary production measurements in water samples collected at 1 m depth and **(b)** in sea-ice samples collected at the underside of the ice as performed immediately below the hole and 10 m (or 12 m) from the edge of the sea-ice hole (hole size c. 1 m^2). The values above the columns indicate the ratio between the two respective incubations.

m of the water column and the lower 0–4 cm of sea-ice was significantly overestimated when incubations were performed in the center of the hole compared with incubations performed at a distance of 10 m from the hole (Fig. 4.14). The strongest impact was observed in 1998, when snow cover was more extensive.

Our observations underline the importance of performing primary productivity measurements in and below sea ice at the correct *in situ* irradiance and show that the light conditions below or in the vicinity of a sea-ice hole can induce significant changes in the distribution and magnitude of productivity. The horizontal displacement of measuring equipment or incubation bottles required to avoid any light-induced artifacts due to sea-ice holes is dependent on many variables, including: Snow-cover thickness, ice thickness, the diameter of the hole, the sun angle and the optical properties of snow, ice and water. Predicting the light field below a sea-ice hole under given conditions is therefore not straightforward and nor is estimating where the incubation bottles should be placed to achieve correct *in situ* incubation. For a sea-ice hole with a diameter of c. 30 cm we measured an elevated scalar irradiance (>5%) up to 3 m from the hole (data not shown), and thus recommend that incubation bottles be placed at least 3 m from sea-ice holes for any measurements or incubations in the

given settings. As the light attenuation in sea ice is relatively small (see section 4.3.2) a simple routine for eliminating irradiance-induced artifacts in sea ice is to cover the sea-ice hole with a transparent Plexiglas plate and reestablish the overlying snow cover. Using non-transparent materials may reduce the light levels below the sea-ice hole. The presented data demonstrate how natural holes and cracks in the sea-ice or e.g. the edge of ice floes can represent sites with significantly elevated primary production.

4.3.4 Temperature, salinity, nutrient and oxygen dynamics of the sea ice during spring

The sea-ice temperature at Station A was recorded in 1999 and 2002. In both years the total ice thickness was practically unchanged during the study period, and the temperature and the shape of the profiles were very similar (only data from 2002 are presented). The temperature profiles reflect the heat exchange between sea-ice, air and water, respectively, leading to minimum temperatures in the central part of the ice cores (Fig. 4.15a). The minimum zone gradually migrated downward as the air temperature increased during spring/summer.

Measurements during the first half of June 2002 showed that both the brine salinity and the bulk salinity were elevated in the central part of the sea-ice core, and that the values decreased as the ice gradually melted (e.g. Fig. 4.15b). As a result, the calculated brine volume (Cox & Weeks, 1983) gradually increased and reached maximum values of 0.2–0.4 vol/vol at the sea ice/water interface at the end of the study period (Fig. 4.15c). The period was thus characterized by an almost linear increase in the tempera-

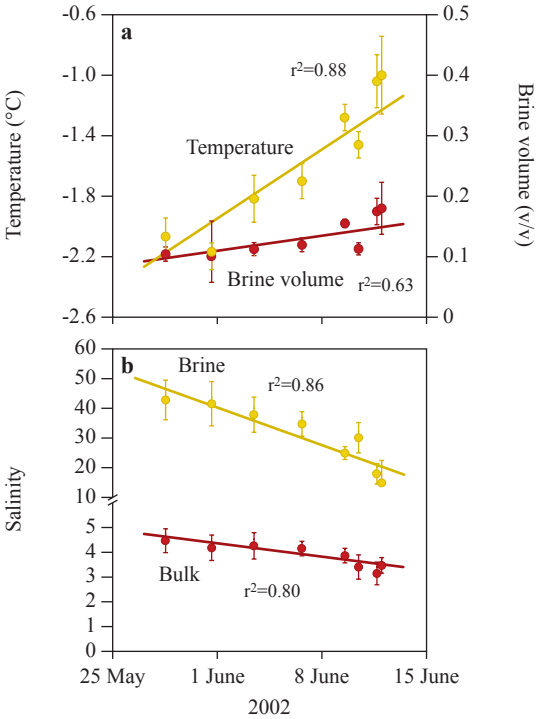

Figure 4.16 (a) Average temperature and brine volume during the study period of 2002 in the lower 0.5 m of the sea ice as derived from the values in Fig. 4.15. **(b)** The measured bulk salinity and the calculated brine salinity in the lower 0.5 m of the sea ice. Data from Rysgaard & Glud (2004).

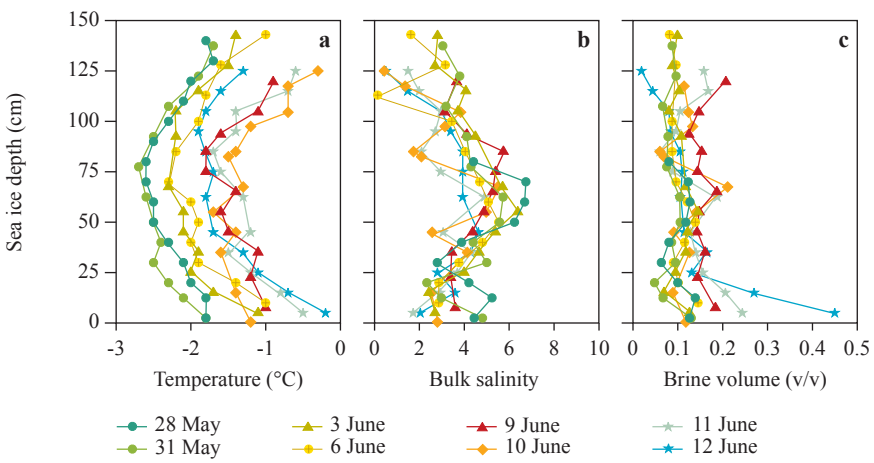

Figure 4.15. Vertical profiles of temperature **(a)** and bulk salinity **(b)** measured from 28 May to 12 June during 2002. From these data, the brine volume at the respective depths was calculated and depicted in **(c)**. "0" depth indicates the position of the sea-ice/water interface. Data from Rysgaard & Glud (2004).

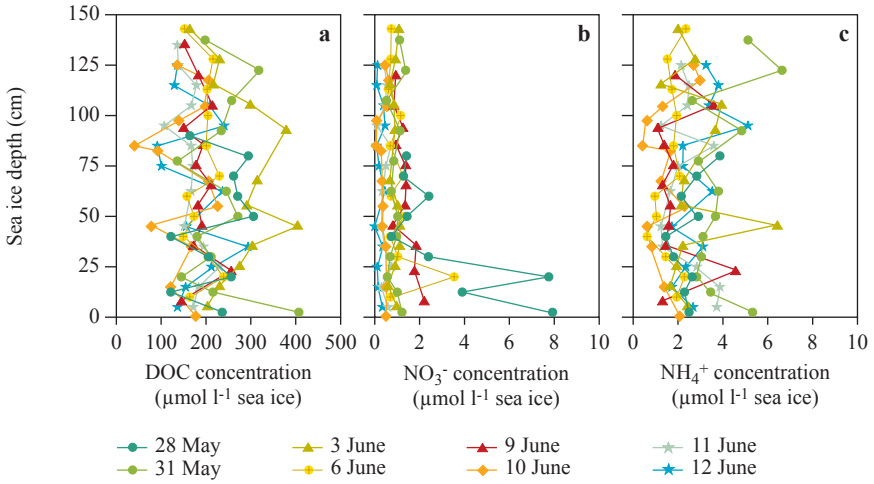

Figure 4.17 Selected vertical brine concentration profiles of DOC, NO_3^- and NH_4^+ (**a, b** and **c**) as measured during May-June 2002. Data from Rysgaard & Glud (2004).

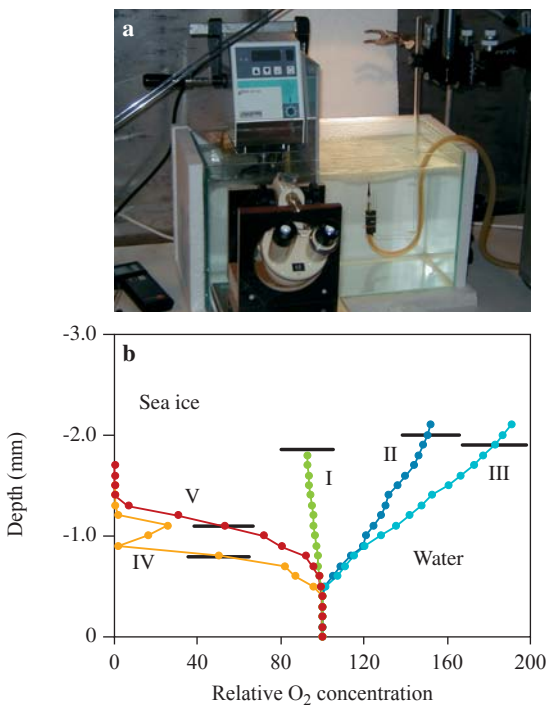

Figure 4.18 (a) A laboratory set-up, in which the temperature of air and seawater could be regulated independently. Thus, freezing of seawater and melting of sea ice could be closely regulated, while O_2 microprofile measurements were performed from below. **(b)** During sea ice formation (actively growing sea ice) O_2-enriched water was expelled from the sea-ice matrix, while meltwater leaving the receding sea-ice/water interface was O_2 depleted. The small horizontal lines indicate the position of the sea-ice/water interface for the individual O_2 microprofiles. Profiles were measured in the order I to IV as the sea ice grew in thickness (II and III) and subsequently receded (IV and V). Data from Glud et al. (2002).

ture and brine volume of the lower 0.5 m of sea ice (Fig. 4.16).

We intensively monitored the concentration of nutrients (NH_4^+, NO_3^-, PO_4^{3-}, Si) and DOC within the sea ice during the month of June in 1999 as well as in 2002. The concentrations and the shapes of the profiles were very similar during the two years (only data from 2002 are presented). The brine channels of the sea ice contained very high concentrations of DOC and relatively high concentrations of inorganic nitrogen (Fig. 4.17), while phosphorus and silicate concentrations in the brine were low (0.2–2.0 µM and 0.4–1.5 µM, respectively – data not shown). Apart from a weak tendency towards decreasing nutrient concentrations with time, there was no clear spatial or temporal pattern in the concentration profiles. All solutes were, however, present at all depths at all times. Recent studies have indicated that sea ice often contains very high concentrations of DOC (and POC) (Thomas et al., 2001; Krembs & Engel, 2001), and that a substantial fraction of this material consists of exopolymeric substances (EPS), produced by microorganisms in the brine channels under extreme conditions during the winter period (Krembs et al., 2002). EPS probably has a cryo-protective role and represents a previously overlooked source of organic carbon available for heterotrophic activity within sea ice.

While nutrient concentrations are standard parameters in many sea-ice studies, and their dynamics are well studied, the dynamics of gases in sea ice are much less investigated. Very recent studies have shown a high spatial and temporal variability in the O_2 concentration of sea-ice brine channels (Glud et

al., 2002; Mock et al., 2002). The O_2 concentration is obviously affected by photosynthesis and respiration (e.g. Gleitz et al., 1995; Günter et al., 1999) but is also highly sensitive to changes in temperature, salinity and, thus, brine volume. In sea ice without any biological activity, dissolved O_2 in principle behaves like other solutes; it accumulates in the brine as ice crystals form and only at extreme temperatures do the solutes freeze out with the developing crystals (Lappäranta & Manninen, 1988; Glud et al., 2002). The solute concentration of the brine thereby increases and becomes supersaturated with respect to O_2. As density gradients induce brine leakage from the developing sea ice, dissolved solutes and O_2 percolate out of the sea ice matrix and sink downwards (Glud et al., 2002). Conversely, when sea ice melts, O_2-depleted water is formed, and the brine now becomes undersaturated with respect to O_2 (and other gases) (Glud et al., 2002). Slight changes in air temperature around the freezing point of brine can thus lead to an oscillating leakage of supersaturated and undersaturated water from the sea-ice matrix (Fig. 4.18), potentially even on a diurnal scale. Biological activity inferred from O_2 measurements in sea ice should therefore be viewed with some reserve, especially during periods with oscillating air temperatures or during successive intervals of freezing and melting (Glud et al., 2002).

Dissolved gasses in freezing seawater can also establish bubbles. During late spring 0.5–8% of the sea ice in Young Sound consisted of gas bubbles, with a trend of increasing bubble volume towards the snow/ice interface (Fig. 4.19). This is presumably due to upward migration of bubbles in the constantly changing structure of the brine channel network. The total O_2 concentration of the sea ice exhibited a positive correlation with bubble volume, suggesting that a significant fraction of the O_2 was actually present in the gas bubbles (Fig. 4.20). However, simple mass-balance calculations revealed that both brine and gas bubbles were undersaturated with respect to O_2. Presumably, this was in part a result of ice melt, but heterotrophic microbial activity may also have contributed to the O_2 deficit (see below). The observations of a significant O_2 deficit in natural sea ice suggest potential existence of anoxic microniches and even associated anaerobic heterotrophic activity (Rysgaard & Glud, 2004).

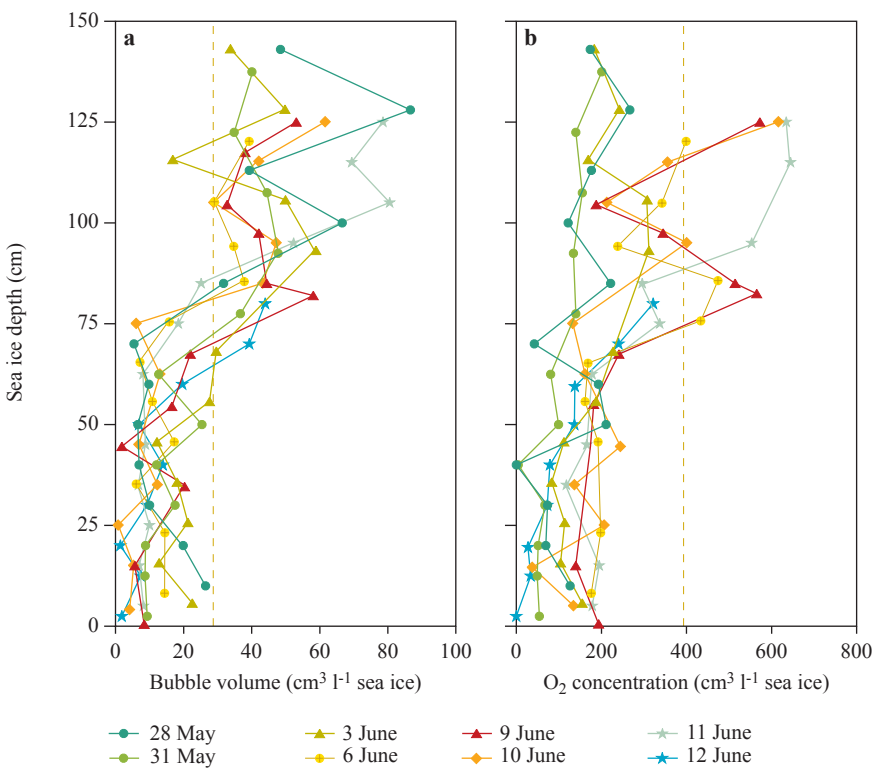

Figure 4.19 Vertical profiles of the gas bubble volume and the total O_2 concentration in sea-ice cores from Young Sound in June 2002. The vertical dotted line in **(a)** indicates the expected gas volume at -1.8°C and a bulk salinity at 4, in **(b)** the line represents the atmospheric O_2 saturation at -1.8°C and a salinity of 33 (conditions at ice formation), respectively. Data from Rysgaard & Glud (2004).

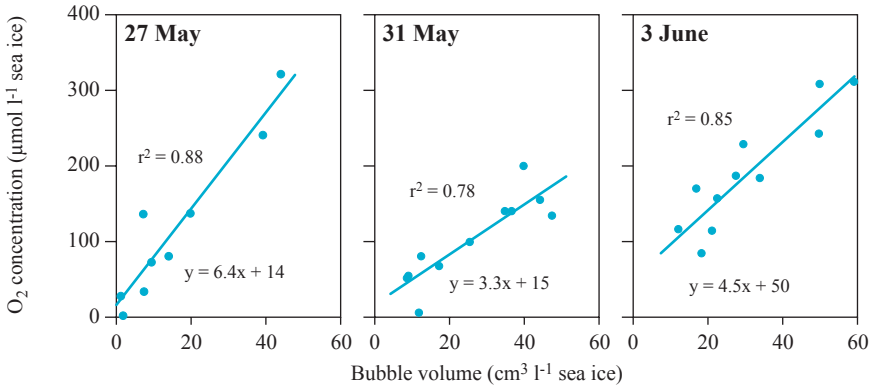

Figure 4.20 The total oxygen concentration of sea-ice sections as a function of the gas bubble volumes on three dates in 2002. Data from Rysgaard & Glud (2002).

4.3.5 Primary production of sea-ice algae in Young Sound

The importance of sea-ice algae for ecosystem carbon cycling has been addressed in various aquatic systems (Cota et al., 1991; Heckey & Andersson, 1999; Legendre et al., 1992; Arrigo, 2003). Especially in Antarctica, in the Canadian Arctic and along marginal ice zones, sea-ice-related primary production has been shown to add significantly to the ecosystem carbon production (Horner & Schrader, 1982; Palmisano & Sullivan, 1983; McMinn et al., 2000). Furthermore, it has been demonstrated that ice algae in receding ice covers may seed phytoplankton blooms and serve as an important food source for the planktonic grazers (e.g. Nelson et al., 1987; Michel et al., 1996).

In Young Sound, the dark winter (c. 3 months) and the open-water period (c. 3 months) restrict the period of potential sea-ice-related primary production to the remaining c. 6 months. Extensive snow cover on the sea ice may further narrow this period down

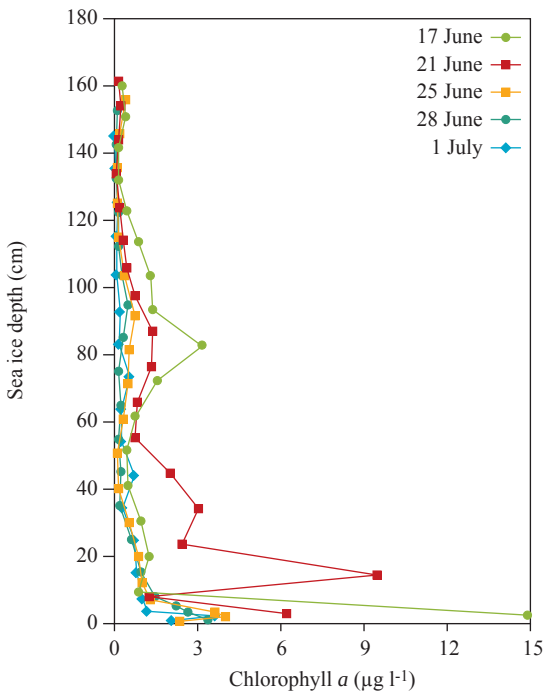

Figure 4.21 Vertical Chl *a* concentration profiles measured in sea-ice cores recovered from mid-June to early July 1999.

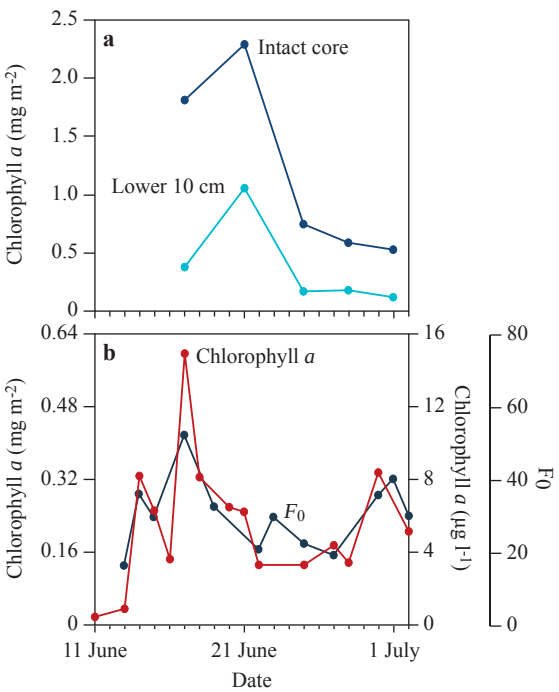

Figure 4.22 The Chl *a* concentration of intact sea-ice cores, **(a)** the lower 10 cm of the sea ice and **(b)** for the lower 4 cm of the sea ice. Panel **(b)** includes F_0 values obtained *in situ* by the diving PAM flourometer.

(see above). Sea-ice profiles of Chl *a* in Young Sound measured in June 1999 and June 2002 demonstrated that the phototrophic biomass was highest at the underside of the ice with maximum values of 9–15 µg Chl *a* l^{-1} sea ice (Fig. 4.21). However, the Chl *a* content of the lower 10 cm represented only 20–40% of the value in intact sea-ice cores. The phototrophic biomass of both the lower 10 cm and of intact sea-ice cores reached a maximum in mid-June but then quickly decreased to a lower value, which remained constant for the rest of the month (Fig. 4.22a). A similar pattern in phototrophic biomass was found in 2002 (Rysgaard & Glud, 2004). Our depth-integrated sea-ice biomass of 0.5–2.5 mg Chl *a* m^{-2} matches findings from open water in the Greenland Sea (Gradinger et al., 1999), but is significantly lower than the microalgal biomass reported from most other Arctic fast-ice areas, where values around 50–150 mg Chl *a* m^{-2} are commonly reported (Arrigo, 2003).

The biomass profiles of intact sea-ice cores were complemented with more frequently obtained Chl *a* measurements in the lower 0–4 cm of the sea ice and by *in situ* PAM fluorometric determinations of the minimum chlorophyll fluorescence yield (F_0), which can be used as a proxy for the phototrophic biomass (see section 4.2.3). These measurements revealed very low values of phototrophic biomass during early June (before the first intact sea-ice profiles were made), but then showed an increasing trend, reaching a peak value in mid-June. The phototrophic biomass subsequently decreased but reached a second peak at the beginning of July (Fig. 4.22b). The PAM-derived dynamics in biomass correlated well with fluctuations in absolute pigment concentrations observed in the lower 4 cm of sea ice (Fig. 4.22b).

On 23 June 1999, more than 600 recordings of the F_0 values were obtained within an area of approximately 12×450 m. Measurements were separated by different horizontal distances from 1 cm to 450 m, and the calibrated values (see section 4.2.3) varied between 0 and 32.5 µg Chl *a* l^{-1} in the lower cm of the sea ice (Fig. 4.23). Simple averaging yielded a phototrophic biomass of 4.2 ± 2.9 µg Chl *a* l^{-1} at the underside of the ice, very similar to values obtained from direct quantification via collected sea-ice samples (3.2–4.0 µg Chl *a* l^{-1}; Fig. 4.22). Detailed statis-

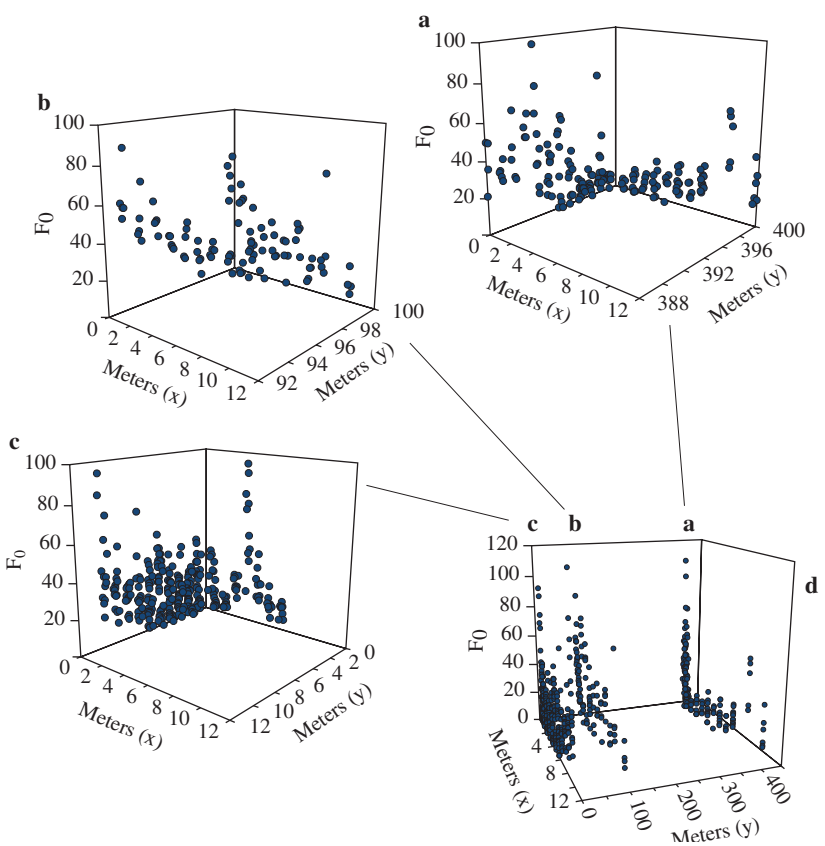

Figure 4.23 Spatial variability in the F value (a proxy for the sea-ice related phototrophic biomass) quantified from 600 individual measurements obtained on 23 June 1999. Panels **(a)**, **(b)** and **(c)** show selected areas of Panel **(d)**. Data from Rysgaard et al. (2001).

Table 4.2 Dominant diatom species at the water/sea-ice interface in Young Sound June 1999.

Chaetoceros affinis
C. socialis var. radians
Coscinodiscus cf. granii
Entomoneis alata
Fragilariopsis cylindrus
Melosira arctica
Navicula pelagica
N. vanhoeffenii
Nitzschia frigida
N. closterium
Porosira glacialis
Thalassiosira antarctica var. borealis
T. hyalina
T. nordenskioeldi

Figure 4.24 Three selected *in situ* O_2 microprofiles obtained at the sea-ice/water interface at a downwelling irradiance of 2–5 µmol photons m^{-2} s^{-1}. The profiles reflect elevated O_2 concentrations in the vicinity of the sea-ice surface. Data from Kühl et al. (2001).

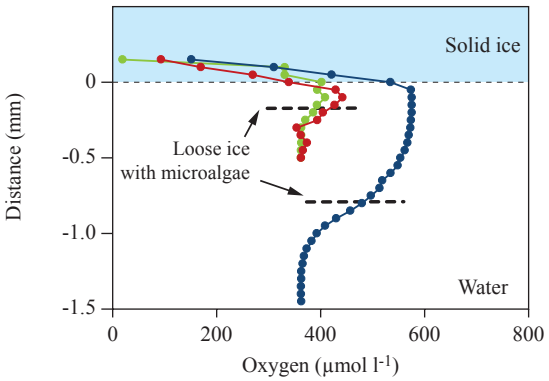

tical analysis revealed that the biomass varied on a characteristic spatial scale of 5–10 m. In other words, patches of sea-ice algae had a characteristic diameter around 5–10 m (Rysgaard et al., 2001). This size matched the typical size of the melt ponds developing on the sea-ice surface during the initial stages of snow melt, and presumably reflects how light availability at the underside of the ice controlled the spatial distribution of the phototrophic biomass in the early stages of snow melt.

We did not perform any detailed taxonomic investigations, and simple microscopic investigations performed on directly melted ice cores do not provide a trustworthy quantitative diversity analysis (Gradinger, 1999). However, microscopic inspections of melted samples in June 1999 revealed that diatoms dominated the sea-ice-algal community. Dinoflagellates (mainly thecate types) were also encountered, but represented only a minor fraction of the total algal biomass. Eleven different diatom genera were observed and the most frequently observed species are listed in Table 4.2.

In situ microprofiling from the underside of the sea ice showed that during daytime the lower mm of the sea-ice occasionally became supersaturated with O_2 (Fig. 4.24). This could be interpreted as active photosynthesis. However, replicate microprofiling revealed an extreme spatial and temporal variability at the µm-scale and often O_2 microprofiles indicated a net heterotrophic community. Due to poorly defined transport coefficients within the sea-ice matrix, ice melt at the sensor tip (due to accelerated flow) and poor control on physically induced changes in O_2 concentrations (see section 4.3.4 and Glud et al., 2002), it was impossible to quantify photosynthetic activity from such profiles (Kühl et al., 2001; Glud et al., 2002). Photosynthetic activity of sea-ice algae has previously been inferred from *in situ* O_2 microprofiles that were, however, obtained in less dynamic environments with significantly higher phototrophic biomass, where the constraints we experienced apparently were of less importance (McMinn & Ashworth, 1998; McMinn et al., 2000). In the present study, we chose to infer gross photosynthetic activity of sea-ice-algal communities from ^{14}C incubations, as it is done in most other sea-ice studies.

In 1999, primary production was determined 10 times during a period of 22 days (11 June–2 July). On each sampling date, 10 cores were collected from the underside of the ice by divers, using a steel well 4 cm deep, with an area of c. 22 cm^2. The collected samples were pooled, homogenized and incubated in three replicate bottles around noon for 2 h at *in situ* light conditions. The data was converted to daily activities (24 h) taking into account the relative fraction of incoming irradiance during the incubation period in relation to total diurnal irradiance (Steeman-Nielsen, 1958). Primary production during the first 4 sampling dates was close to zero but positive signals were obtained for the rest of the sampling period, with peak values in mid-June and early July (Fig. 4.25a). Both peaks corresponded to increases

in phototrophic biomass (Fig. 4.22a). Integrated over the entire period (22 days) the values corresponded to a primary production of 5.3 mg C m^{-2}. However, this estimate only accounts for the lower 4 cm of the sea ice. At present, it is difficult to evaluate the extent to which Chl *a* found deep inside the sea-ice core actually represented photosynthetic active algae. However, measurements performed on interior sea ice sub-sampled from an intact sea-ice cores recovered on 1 July showed that the interior sea ice did contain active primary producers with an average activity of 5.7 µg C $l^{-1}d^{-1}$ (n=3) at *in situ* light conditions. Measurements by Mock & Gradinger (1999) also demonstrated that i) sea-ice algae encrusted deep inside the sea ice can be actively photosynthesizing and ii) that the integral interior primary production of 160 cm thick sea ice was similar to or even higher than the production in the bottom 5 cm. The Chl *a*-specific photosynthetic activity within each of two environments varied markedly (by a factor of 14) and, thus, Chl *a*-specific photosynthesis in the interior and in the bottom of the ice was not significantly different (Mock & Gradinger, 1999).

In 1999, the lower 4 cm of the sea ice studied here contained roughly 15% of the Chl *a* found in the entire sea-ice core. If we assume that the remaining Chl *a* represented phototrophic biomass with a specific primary production similar to that measured in the lowermost part of the sea ice, we achieve an estimate of total sea-ice-algal primary production during the study period of 35.9 mg C m^{-2} (or an average of 1.63 mg C m^{-2} d^{-1}). This estimate must be close to that year's annual contribution as the sea ice broke up on 10 July, i.e. 8 days after the end of the measuring campaign. As this estimate is extrapolated from the entire sea-ice core, it is somewhat higher than previously published estimates for Young Sound that accounted for only the lower 4 cm of the sea ice (Rysgaard et al., 2001; Glud et al., 2002). Extrapolating the values to the area of outer Young Sound (Region 1, 76 km^2 – see Chapter 3) the gross primary production amounted to only 2.7 t C. Even if the sea-ice-related activity during the 8 remaining days had been significant, the sea-ice-related primary production amounted to only <<1% of the total ecosystem production during 1999 (see Chapters 9 and 11).

In early June 2002, primary production in the lower 30 cm of sea ice was determined 5 times during a 6-day period using similar to that incubation procedure described above (Fig. 4.25b). That year had an exceptionally long open-water period (Fig. 4.5); the snow cover diminished and large melt ponds developed already in beginning of June, leading to increased light availability within the sea ice. The measured photosynthetic rates were thus somewhat higher than the corresponding values in 1999 (Fig. 4.24), yielding an integrated activity for the 6-day period of 55.2 mg C m^{-2} (in the lowermost 30 cm of the sea ice). Roughly 60% of the phototrophic biomass was present in the lower 30 cm of the sea-ice core during that period and the estimated activity for the entire sea-ice core thus amounted to 77 mg C m^{-2} (or an average of 12.8 mg C m^{-2} d^{-1}).

Sea-ice-related primary production in early June 2002 was thus significantly higher than in 1999, reflecting the interannual variations in light conditions and snow cover. Nevertheless, in both cases our values are in the lower end of most other fast-ice studies and not all of these accounted for the interior activity (Mock & Gradinger, 1999 and references therein). We speculate that the relatively thick snow cover and the extreme dynamics in the appearance

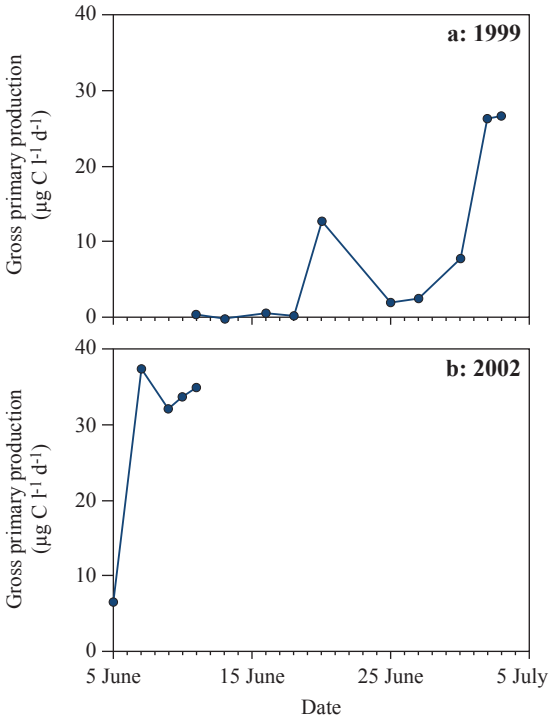

Figure 4.25 Values of sea-ice-related gross primary production measured during June **(a)** in the lower 4 cm of the sea-ice in 1999 and **(b)** in the lower 30 cm of the sea-ice in 2002.

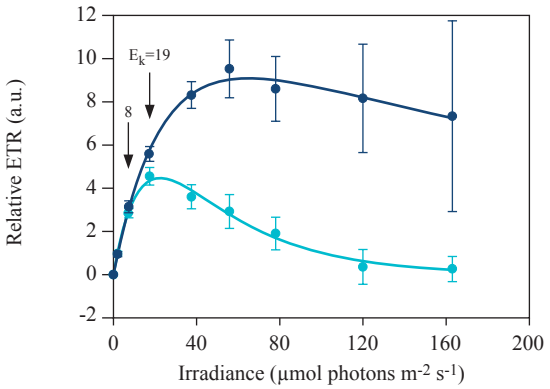

Figure 4.26 Relative ETR as a function of imposed light measured in two different sea-ice-algal communities growing at the rim of a sea-ice hole (dark blue) and 10 m from the hole (light blue). The ambient light levels during the investigation were 75 and 15 µmol photons m^{-2} s^{-1}, respectively. The light adaptation index, E_k, was calculated as $E_k = P_{max}/\alpha$, where P_{max} represents the maximum photosynthesis and α the initial slope of the light curve. Error bars indicate ± SD of 3–4 measurements. Data from Kühl et al. (2001).

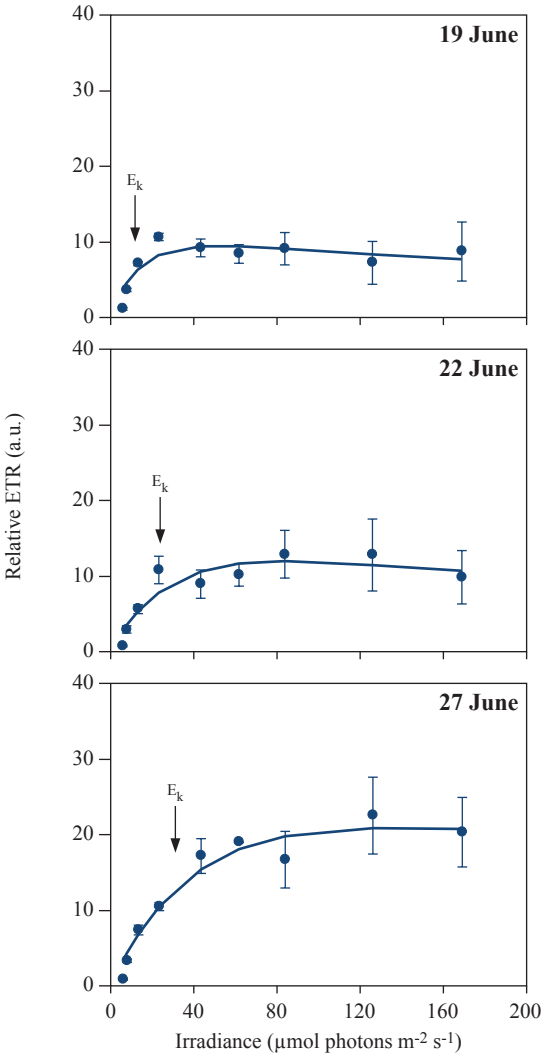

Figure 4.27 Relative ETR measured as a function of the imposed light at the same site on three different days. The E_k value of the sea-ice-algal community (calculated as $E_k = P_{max}/\alpha$) gradually increased from 12 to 35 µmol photons m^{-2} s^{-1} as the light availability below the sea ice increased. Data from Rysgaard et al. (2001).

and structure of the underside of the ice in Young Sound, which are strongly influenced by variations in freshwater input (see section 4.3.1), inhibit the establishment of larger sea-ice-algal communities in Young Sound.

The more traditional approach for estimating sea-ice-related primary production was complemented by PAM fluorometer-based measurements of sea-ice-algal activity (see section 4.2.3). Thereby, it was possible to resolve relations between light conditions and the relative photosynthetic ETR *in situ*, i.e. a proxy for the photosynthetic activity (see section 4.2.3.). The measurements showed that the sea-ice-algal community was well adapted to the ambient light levels. Communities growing in the vicinity of drilled holes and thus experiencing elevated light levels expressed a higher light adaptation index (E_k) and were only marginally photo-inhibited at 160 µmol photons m^{-2} s^{-1}, while communities growing more than 10 m from the holes were almost fully inhibited at this irradiance (Fig. 4.26). Likewise, communities underlying a developing melt pond gradually increased their light adaptation index from 12 to 35 µmol photons m^{-2} s^{-1} as the light levels below the sea ice increased (Fig. 4.27). The data clearly confirms that sea-ice-algal communities are very flexible and adapt quickly to changes in ambient light conditions (e.g. Lizotte & Sullivan, 1991).

Along with the 600 F_0 measurements recorded on 23 June 1999 we also recorded the effective quantum yield of PSII-related electron transport, ϕ_d (=ETR/ambient light) (see section 4.2.3). Statistical analysis showed that both ϕ_d and the irradiance below the sea ice expressed a characteristic spatial scale of variance of 50–100 m (Rysgaard et al., 2001). The data documented a spatial coupling between algal activity and light passing through the sea ice. Apparently the photosynthetic activity varied on a larger spatial scale than did the phototrophic biomass (see above). The lack of coupling between spatial variability of biomass and

activity could be related to differences in Chl *a*-specific activity induced by salinity variations. Another explanation could be a faster response in activity compared with biomass growth following changed light conditions as the melt pond grew in size (Rysgaard et al., 2001) or by inhomogeneous grazing patterns (Gradinger et al., 1992). Nevertheless, the data documents the close coupling between light availability and the activity of sea-ice-algal communities.

4.3.6 Heterotrophic activity of the sea ice

Sea ice contains high concentrations of POC and DOC, either i) entrapped during sea-ice formation, ii) resulting from phototrophic or heterotrophic growth within the sea ice or iii) transported into the sea ice by convective processes (Gradinger & Ikävalko, 1998; Weissenberger & Grossmann, 1998; Gradinger & Spindler, 1999). The carbon represents a potential food source for the bacterial community within the sea ice. Positive correlation has been demonstrated between the phototrophic and the heterotrophic prokaryotic biomass in some sea-ice habitats and this suggests a close metabolic coupling between the two communities (e.g. Gosink et al., 1993; Meiners et al., 2003). But other studies show no correlation between the abundances of the two communities, indicating that alternative carbon sources may also be of importance for the bacterial activity (e.g. Gradinger & Zang, 1997; Stewart & Fritsen, 2004). Recently, it was suggested that cryoprotective exopolymers of encrusted diatoms represent an important carbon source in Arctic winter sea ice (Krembs et al., 2002; Meiners et al., 2003).

Most studies on the importance of heterotrophic bacteria in sea ice have been based on simple enumeration, quantification of prokaryotic diversity or on culture work (Bowman et al., 1997; Mock et al., 1997; Huston et al., 2000; Junge et al., 2002). The lack of *in situ* data is due to the same experimental difficulties faced by scientists quantifying *in situ* photosynthetic activity (see above). The *in situ* microbial activity of sea ice has thus only been marginally explored.

During early June 2002 a number of ice cores were sampled at Station A. The lower 30 cm of each core was subsequently enclosed in water-containing gas-tight plastic bags, carefully avoiding entrapment of bubbles (Hansen et al., 2000; Rysgaard & Glud, 2004). The cores were then placed in the drilled holes and sampled at two-day intervals to determine the total O_2 concentration of the sea ice. In this way, the net aerobic activity of the enclosed sea-ice community was followed under *in situ* conditions. Surprisingly, the cores turned anoxic within 1 week due to a constant net O_2 consumption rate of 13 µM O_2 d^{-1} (Fig. 4.28). Given the concurrent photosynthetic activity measured in parallel ^{14}C incubations, corresponding to c. 2 µmol O_2 l^{-1} sea ice d^{-1} (Fig. 4.25b & Fig. 4.28), the gross heterotrophic activity thus amounted to c. 15 µmol O_2 l^{-1} d^{-1} (Rysgaard & Glud, 2004). This only accounts for the activity in the lower 30 cm of sea ice, but if we assume a similar specific rate for the rest of the sea-ice core, the O_2 consumption of the 160 cm thick sea ice of Young Sound amounted to c. 24 mmol m^{-2} d^{-1} during the investigation period (Rysgaard & Glud, 2004). This corresponds to the oxygen uptake of dark-incubated sediment from 20 m water depth (Chapter 9) and is an extremely high activity, which cannot be representative of the ice cover of Young Sound during the entire ice-covered period as that would require a continuous supply of an unidentified carbon source. We thus refrain from extrapolating these findings, but the experiment documents that heterotrophic activity of sea ice can be substantial and that it can be of potential importance for ecosystem carbon cycling. The importance of heterotrophic activity in the sea ice of Young Sound is as poorly defined as in most other polar settings.

Even though advection and percolation of the sea-ice occur *in situ*, the high heterotrophic activity of the enclosed sea ice and the melting of O_2-depleted sea-ice crystals (see section 4.3.4) strongly suggest that anoxia

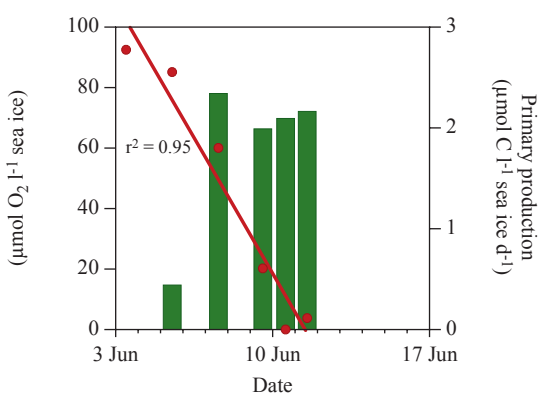

Figure 4.28 Primary production (green bars) and O_2 concentration (red line and symbols) in ice-core sections (bottom 30 cm) enclosed in a number of parallel gas-tight transparent incubation bags for a period of eight days. From Rysgaard & Glud (2004).

can develop in sea ice. This is supported by studies documenting the existence of purple anoxygenic phototrophic bacteria in Baltic sea ice (Petri & Imhoff, 2001) and the cultivation of denitrifying bacteria from sea-ice samples collected in Antarctica and in the Baltic Sea (Staley & Gosink, 1999; Kaartokallio, 2001). Sea ice collected in Young Sound did indeed host denitrifying bacteria in densities of 1.1×10^5 cells ml^{-1} sea ice, corresponding to 1.2×10^6 cells ml^{-1} brine (Rysgaard & Glud, 2004). Anoxic incubations of thawed sea-ice samples showed area-integrated denitrification rates of 10–45 µmol N m^{-2} d^{-1}, corresponding to 7–50% of the benthic denitrification activity (see Chapter 8). Thus, sea ice has a significant potential for acting as a sink in the nitrogen cycle. No sea-ice samples showed a potential for sulfate reduction, which could, however, be due to the relatively short incubation time of 24 h.

4.4 Synthesis and conclusions

Light availability is the major factor regulating the spatial distribution of biomass and activity of sea-ice algae. Before June, snow cover inhibits any significant sea-ice-related primary production in Young Sound, but as the snow becomes wet and melt ponds develop, light availability increases and the phototrophic biomass begins to flourish in the sea ice. Maximum levels of c. 15 µg Chl *a* l^{-1} were found at the underside of the ice, while the area-based ice-algal biomass reached a maximum value of c. 3 mg Chl *a* m^{-2} in mid-June. During a normal year, the melting of sea ice is accelerated during the second half of June and the interior as well as the underside of the sea ice become very dynamic habitats. Freshwater intrusions percolating through the sea-ice matrix combined with temperature fluctuations around 0°C change the sea-ice structure on a daily basis. Furthermore, the melting/freezing dynamics strongly affect salinity, nutrient and gas concentrations of the sea ice. These conditions make the sea ice in Young Sound a hostile environment, and we speculate that this is what prevents algae from colonizing the sea ice to the extent reported in other systems.

The main difference between Young Sound and most other fast-ice areas investigated is a massive snow accumulation on the ice surface during winter/early spring and a massive inflow of freshwater during the period of potential sea-ice-related primary production. Snow cover and active sea-ice melt thus limit the time window of potential sea-ice-related primary production to around 1 month or less. In 1999, the annual gross production in the underside of the ice (0–4 cm) was estimated at 5.3 mg C m^{-2} yr^{-1}, while the value for the total sea ice was c. 36 mg C m^{-2} yr^{-1}. This is equivalent to only 2.7 t C for outer Young Sound (Region 1; Chapter 3). Interannual variations in sea-ice-algal production are to be expected, and extrapolation of the study in 1999 and the few measurements in 2002 should thus be done with caution. However, during the past decade of working in Young Sound we have never experienced any massive development of sea-ice algae.

Net production may be significantly smaller than inferred from the ^{14}C incubation procedure due to associated heterotrophic activity in the sea ice. Enclosure experiments on sea-ice cores during mid-June 2002 documented that the sea ice was net heterotrophic and thus did not represent a net source of organic carbon during that period. The annual heterotrophic activity of the sea ice in Young Sound is, however, poorly defined.

Microsensor and enclosure studies strongly indicated that anoxia can develop in sea ice, and tracer experiments documented that sea ice has a denitrification potential. The fact that sea ice can be net heterotrophic and can host anaerobic bacteria changes our present understanding of the role of sea ice in element cycling both quantitatively and conceptually.

4.5 Acknowledgements

The study was supported by the Danish Natural Science Research Council, DANCEA (the Danish Cooperation for the Environment in the Arctic) under the Danish Ministry of the Environment, the University of Copenhagen, and the Carlsberg Foundation. The support is gratefully acknowledged. This work is a contribution to the Zackenberg Basic and Nuuk Basic Programs in Greenland. Furthermore, we thank Tanja Quottrup, Kitte G. Lauridsen, Marlene Skjærbæk, Egon Frandsen, Anni Glud, Jens S Laursen and Anna Haxen for excellent assistance during the study. The Danish Military Division, Sirius provided excellent support for our fieldwork in Young Sound. Anna Haxen helped with linguistic corrections and three reviewers made valuable comments that improved the manuscript.

4.6 References

Arrigo, K. 2003. Primary production of sea-ice. In: Sea Ice. Thomas, D.N. & Dieckmann, G.S., (eds.). Blackwell Science Ltd. 402 pp.

Braman, R. S. & Hendrix, S. A. 1989. Nanogram nitrite and nitrate determination inenvironmental and biological materials by Vanadium (III) reduction with chemiluminescence detection. Anal. Chem. 61: 2715-2718.

Bower, C. & Holm-Hansen, T. 1980. A salicylate-hypochlorite method for determining ammonia in seawater. Can. J. Fish. Aquat. Sci. 37: 794-798.

Bowman, J. P., Brown, M.V. & Nichols, D. S. 1997. Biodiversity and ecophysiology of bacteria associated with Antarctic sea ice. Antarct. Sci. 9: 134-142.

Clasby, R. C., Horner, R. & Alexander, V. 1973. An in situ method for measuring primary production of Arctic sea ice algae. J. Fish. Res. Board. Can. 30: 635-638.

Cota, G. F., Legendre, L., Grosselin, M. & Ingram, R. G. 1991. Ecology of bottom ice algae. I. Environmental controls and variability. J Mar Sys 2: 257-277.

Cox, G. F. N. & Weeks, W. F. 1983. Equations for determining the gas and brine volumes in sea-ice samples. J. Glaciol. 29: 306-316.

Eicken, H. 2003. From the microscopic, to the macroscopic, to the regional scale: Growth, Microstructure and Properties of sea Ice. In: Sea Ice. Thomas, D.N. & Dieckmann, G.S., (eds.). Blackwell Science Ltd. 402 pp.

Eicken, H., Bock, C., Wittig, R., Miller, H. & Poertner, H. O. 2000. Nuclear magnetic resonance imaging of sea ice pore fluids: methods and thermal evolution of pore microstructure. Cold Reg. Sci. Technol. 31: 207-225.

Giannelli, V., Thomas, D. N., Kennedy, H. A., Dieckmann, G. S., Kattner, G. & Haas, C. 2001. The behavior of dissolved organic matter during sea-ice formation, Ann. Glaciol. 33: 317-321.

Gleitz, M., Rutgers v. d. Loeff M., Thomas, D. N., Dieckmann, G. S. & Millero, F. J. 1995. Comparison of summer and winter inorganic carbon, oxygen and nutrient concentrations in Antarctic sea ice brine. Mar. Chem. 51: 81-91.

Glud, R. N., Gundersen, J. K. & Ramsing, N. B. 2000. Electrochemical and optical oxygen microsensors for *in situ* measurements. In: Buffle, J. & Horvai, G. (eds.), *In situ* analytical tecniques for water and sediment. John Wiley and Sons, Chichester: 19-75.

Glud, R. N., Rysgaard, S. & Kühl, M. 2002. A laboratory study on O_2 dynamics and photosynthesis in sea ice algal communities: Quantification by microsensors, O_2 exchange rates, ^{14}C-incubations and PAM fluorometry. Aquat. Microb. Ecol. 27: 301-311.

Golden, K. M., Ackley, S. F. & Lytle, V. I. 1998. The percolation phase transition in sea ice. Science 282: 2238-2241.

Gosink, J. J., Irgens, R. L. & Staley, J. T. 1993. Vertical distribution of bacteria in Arctic sea-ice. FEMS Microbiol. Ecol. 102: 85-90.

Gosselin, M., Levasseur, M., Wheelet P. A., Horner, R. A. & Booth, B. C. 1997. New measurements of phytoplankton and icealgae production in the Arctic Ocean. Deep-Sea Res. PII, 44: 1623-1643.

Gradinger, R. & Ikävalko, L. 1998. Organism incorporation into newly forming Arctic sea-ice in the Greenland Sea. J. Plank. Res. 20: 871-886.

Gradinger, R., Friedrich, C. & Spindler, C. F. M. 1999. Abundance, biomass and composition of sea-ice biota of the Greenland sea pack ice. Deep-sea Res. PII, 46: 1457-1472.

Gradinger, R. 1999. Vertical fine structure of the biomass and composition of algal communities in Arctic pack ice. Mar. Biol. 133: 745-754.

Gradinger, J.J. & Zhang, Q. 1997. Vertical distribution of bacteria in Arctic sea ice from Barents and Laptev Seas. Polar Biol 17: 448-454

Gradinger, R., Spindler, M. & Weissenberger, J. 1992. On the structure and development of Arctic pack ice communities in Fram Strait – a multivariate approach. Polar Biol. 12: 727-733

Grainger, E. H. & Mohammed, A. A. 1990. High salinity tolerance in sea-ice copepods. Ophelia 31: 177-185.

Grasshoff, K., Erhardt, M. & Kremling, K. 1983. Methods of seawater analysis. 2nd revised and extended version. Weinheim, Verlage Chemie, 419 pp.

Grossi, S. McG., Kottmeier, S. T., Moe, R. L., Taylor, G. T. & Sullivan, C.W. 1987. Sea ice microbial communities. VI. Growth and primary production in bottom ice under graded snow cover. Mar. Ecol. Prog. Ser. 35: 153-164.

Günter, S., Gleitz, M. & Dieckmann, G. S. 1999. Biogeochemistry of Antarctic sea ice: a case study on platelet ice layers at Drescher inlet, Weddell Sea. Mar. Ecol. Prog. Ser. 177: 1-13.

Haecky, P. & Andersson, A. 1999. Primary and bacterial production in sea ice in the northern Baltic Sea. Mar. Ecol. Prog. Ser. 20: 107-118.

Hansen, J. W., Thamdrup, B. & Jørgensen, B. B. 2000. Anoxic incubation of sediment in gas-tight plastic bags: A method for biogeochemical process studies. Mar. Ecol. Prog. Ser. 208: 273-282.

Hsiao, S. I. C. 1988. Spatial and seasonal variations in primary production of sea ice microalgae and phytoplankton in Frobisher Bay, Arctic Canada. Mar. Ecol. Prog. Ser. 44: 275-285.

Horner, R. A. & Schrader, G. C. 1982. Relative contribution of ice algae, phytoplankton, and benthic microalgae to primary production in nearshore regions of the Beaufort Sea. Arctic 35: 485-503.

Horner, R. A., Ackley, S. F., Dieckmann, G., Gulliksen, B., Hoshiai, T., Legendre, L., Melnikov, I. A., Reeburgh, W. S., Spindler, M. & Sullivan, C. W. 1992 . Ecology of sea-ice biota. 1. Habitat, terminology, and methodology. Polar Biol. 12: 417-427.

Huston, A. L., Krieger-Brockett, B. B. & Deming, J. W. 2000. Remarkably low temperature optima for extracellular enzyme activity from Arctic bacteria and sea-ice. Environ. Microbiol. 2: 383-388.

Jespersen, A. M. & Christoffersen, K. 1987. Measurements of Chlorophyll *a* from phytoplankton, using ethanol as extraction solvent. Arch. Hydrobiol. 109: 445-454.

Junge, K., Imhoff, F., Staley, T. & Deming, J. W. 2002. Phylogenetic diversity of numerically important Arctic sea-ice bacteria cultured at subzero temperature. Microb. Ecol. 43: 315-328.

Kaartokallio, H. 2001. Evidence for active microbial nitrogen transformation in sea ice (Gulf of Bothnia, Baltic Sea) in midwinter. Polar Biol. 24: 21-28.

Krembs, C. & Engel, A. 2001. Abundance and variability of microorganisms and transparent exopolymer particles across the ice-water interface of melting first-year sea ice in the Laptev Sea (Arctic). Mar. Biol. 138: 173-185.

Krembs, C., Eicken, H., Junge K. & Deming. 2002. High concentrations of exopolymeric substances in Arctic winter sea-ice: Implications of the polar ocean carbon cycle and cryoprotection of diatoms. Deep-Sea Res. PI, 49: 2163-2181.

Kühl, M. & Jørgensen, B. B. 1994. The light field of micro-benthic communities: radiance distribution and microscale optics of sandy coastal sediments. Limnol. Oceanogr. 39: 1368-1398.

Kühl, M., Glud, R. N., Borum, J., Roberts, R. & Rysgaard, S. 2001. Photosynthetic performance of surface associated algae below sea ice as measured with a pulse amplitude modulated (PAM) fluorometer and O_2 microsensors. Mar. Ecol. Prog. Ser. 223: 1-14.

Lappäranta, M. & Manninen, T. 1988. The brine and gas content of sea ice with attention to low salinities and high temperatures. Finnish Inst. Mar. Res. Internal Rep. 88-2.

Legendre, L., Ackley, S. F., Dieckmann, G. S., Gulliksen, B. & others. 1992. Ecology of sea-ice biota. 2. Global significance. Polar Biol. 12: 429-444.

Lizotte, M. P. & Sullivan, C. W. 1991. Rates of photoadaption in sea ice diatoms from McMurdo Sound, Antartica. J. Phycol. 27: 429-444.

McMinn, A. & Ashworth, C. 1998. The use of microelectrodes to determine the net production by Antarctic sea ice algae community. Antarct. Sci. 10: 39-44.

McMinn, A., Ashworth, C. & Ryan, K.-G. 2000. *In situ* net primary productivity of an Antarctic fast ice bottom algal community. Aquat. Microb. Ecol. 21: 177-185.

Meiners, K., Gradinger, R., Fehling, J., Civitarese, G. & Spindler, M. 2003. Vertical distribution of exopolymer particles in sea-ice of the Fram strait (Arctic) during autumn. Mar. Ecol. Prog. Ser. 248: 1-13.

Michel, C., Legendre, L., Ingram R. G., Gosselin, M. & Levasseur, M. 1996. Carbon budget of sea-ice algae in spring: evidence of a significant transfer to zooplankton grazers. J. Geophys. Res-Oceans. 101(C8): 18345-18360.

Mock, T., Meiners, K. M. & Giesenhagen, H. C. 1997. Bacteria in sea ice and underlying brackish water at 54 degrees 26'50''N (Baltic Sea, Kiel Bight). Mar. Ecol. Prog. Ser. 158: 23-40.

Mock, T. & Gradinger, R. 1999. Determination of Arctic ice algal production with a new *in situ* incubation technique. Mar. Ecol. Prog. Ser. 177: 15-26.

Mock, T., Dieckmann, G. S., Haas, C., Krell, A., Tison, J. L., Belem, A. L., Papadimitriou, S. & Thomas, D. N. 2002. Micro-optodes in sea ice: a new approach to investigate oxygen dynamics during sea-ice formation. Aquat. Microb. Ecol. 29: 297-306.

Nelson, D. M., Smith, W. O, Gordon, L. I. & Huber, B. A. 1987. Spring distribution of density nutrients and phytoplankton biomass in the ice edge zone of the Weddell-Scotia Sea. J. Geophys. Res. 92: 7181-7190.

Palmisano, A. C. & Sullivan, C. W. 1983. Sea ice microbial communities (SIMCO), 1. Distribution, abundance and primary production of microalgae in Mc. Murdo Sound, Antarctica in 1980. Polar Biol. 2: 171-177.

Perovich, D. K. 2003. Complex yet translucent: the optical properties of sea ice. Physica B 338: 107-114.

Perovich, D. K. 1996. The optical properties of sea ice, CRREL Monograph, 96-1, 25 pp.

Perovich, D. K., Roesler, C.S. & Pegau, W.S. 1998. Variability in sea ice optical properties, J. Geophys. Res. 103: 1193-1209.

Petri, R. & Imhoff, J. F. 2001. Genetic analysis of sea-ice bacterial communities in the Western Baltic Sea using an improved double gradient method. Polar Biol. 24: 252-257.

Revsbech, N. P. 1989. An oxygen microelectrode with a guard cathode. Limnol. Oceanogr. 34: 474-478.

Rysgaard, S., Nielsen, T. G. & Hansen, B. W. 1999. Seasonal variation in nutrients, pelagic primary production and grazing in a high-Arctic coastal marine ecosystem, Young Sound, Northeast Greenland. Mar. Ecol. Prog. Ser. 179: 13-25.

Rysgaard, S., Kühl, M., Glud, R. N., & Hansen, J. W. 2001. Biomass, production and horizontal patchiness of sea ice algae in a high-Arctic fjord (Young Sound, NE Greenland). Mar. Ecol. Prog. Ser. 223: 15-26.

Rysgaard, S. & Glud, R. N. 2004. Anaerobic N_2 production in Arctic sea-ice. Limnol. Oceanogr. 49: 86-94.

Schreiber, U., Hormann, H., Neubauer, C. & Klughammer, C. 1995. Assesment of photosystem II photochemical quantum yield by chlorophyll fluorescence quenching analysis. Aust. J. Plant. Physiol. 22: 209-220.

Schreiber, U., Schliwa, U. & Bilger, W. 1986. Continuous recording of photochemical and non-photochemical chlorophyll fluorescence quenching with a new type of modulation fluorometer. Photosynth. Res. 10: 51-62.

Smith, R. E. H. & Herman, A.W. 1991. Productivity of sea ice algae: *In situ* vs. incubator methods. J. Mar. Syst. 2: 97-110.

Staley, J. T. & Gosink, J. J. 1999. Poles apart: Biodiversity and biogeography of sea ice bacteria. Ann. Rev. Microbiol. 53: 189-215.

Steenmann-Nielsen, E. 1958. A survey of recent Danish measurements of the organic productivity in the sea. Rapp. PV Réun. Cons. Perm. Int. Explor. Mer. 144: 92-95.

Stewart, F. J. & Fritsen, C.H. 2004. Bacteria-algae relationships in Antarctic sea ice. Antar Science 16: 143-156

Thomas, D. N., Kennedy, H., Kattner, G., Gerdes, D., Gough, C. & Dieckmann, G. S. 2001. Biogeochemistry of platelet ice: Its influence on particle flux under fast ice in the Weddell Sea, Antarctica. Polar Biol. 24: 486-496.

Weeks, W. F. & Ackley, S. F. 1986. The growth, structure and properties of sea-ice. In: Untersteiner, N. (ed), The geophysics of sea ice. Martinus Nijhoff Publishers Dordrecht (NATO ASI B146): 9-164.

Weissenberger, J., Dieckmann, G. S., Gradinger, R. & Spindler, M. 1992. Sea ice: A cast technique to examine and analyze brine pockets and channel structure. Limnol. Oceanogr. 37: 179-183.

Weissenberger, J. & Grossmann, S. 1998. Experimental formation of sea ice: Importance of water circulation and wave action for incorporation of phytoplankton and bacteria. Polar Biol. 20: 178-188.

Photo: Søren Rysgaard

5

Structure and function of the pelagic ecosystem in Young Sound, NE Greenland

Structure and function of the pelagic ecosystem in Young Sound, NE Greenland

Torkel G. Nielsen[1], Lars D. Ottosen[2] & Benni W. Hansen[3]*

[1]Department of Marine Ecology, National Environmental Research Institute, PO Box 358, DK-4000 Roskilde, Denmark
[2]Unisense A/S, Brendstrupgaardsvej 21F, DK-8200 Aarhus N, Denmark
[3]Department of Life Sciences and Chemistry, Roskilde University, PO Box 260, DK-4000 Roskilde, Denmark
[*]Present address: Skejby Sygehus, Aarhus University Hospital, Fertility Clinic, Brendstrupgaardsvej 100, DK-8200 Aarhus N, Denmark

Cite as: Nielsen, T. G., Ottosen, L. D. & Hansen, B. W. 2007. Structure and function of the pelagic ecosystem in Young Sound, NE Greenland. In: Rysgaard, S. & Glud, R. N. (Eds.), Carbon cycling in Arctic marine ecosystems: Case study Young Sound. Meddr. Grønland, Bioscience 58: 88-107.

Abstract

An annual carbon budget of the pelagic food web is constructed for a 36 m deep station in Young Sound. Data were collected during a 2-week mid-summer sea-ice covered period in 1999, during the open-water period of 1996, 2003, 2004, 2005 and during winters of 1997 and 2003. The measurements revealed that during sea-ice cover the water column of outer Young Sound was strongly heterotrophic and sustained by organic material advected into the fjord from the open sea. The pelagic community thus originated from the marginal ice zone at the entrance to the fjord. No succession was observed in the plankton community during this period, and the grazing pressure of the dominating zooplankton groups (ciliates, heterotrophic dinoflagellates, meroplankton and copepods) was 10 times higher than primary production, while the bacterial carbon demand was three times higher than primary production.

During the open-water period, the grazing community was completely dominated by copepods, which were capable of grazing down the entire primary production. This contrasts with several other investigated Arctic marine pelagic ecosystems further south, where the protozooplankton community is quantitatively more important than copepods. In Young Sound, both zooplankton groups are present simultaneously, and copepods thus act both as competitors for food and as predators in relation to the protozooplankton. On an annual basis, the carbon budget was unbalanced; the total carbon need of the grazers equaled primary production, leaving no room for the estimated bacterial carbon demand, which was of the same size as the carbon demand of the grazers. Thus, Young Sound is a net heterotrophic system relying on import of organic material from the open sea or possibly from land.

5.1 Introduction

Deep fjords are characteristic elements of the Greenland coastline (Chapter 3). They constitute a key element in the land-ocean interface and, consequently, in the nutrient and carbon dynamics of the coastal zone. In the Young Sound the freshwater input is very pulsed and the main impact is associated with the flushing of the Zackenberg River around midsummer (Chapter 2). This freshwater input creates a stratification of the upper part of the water column through establishment of a strong halocline, which is further strengthened by solar heating of the surface water. Consequently, the freshwater input has major implications for the stratification of the fjord and thus the vertical distribution and production of plankton in fjord systems (Rysgaard et al., 1999; Chapter 3).

In the past, most pelagic food-web investigations off Greenland have been associated with fisheries research and exploitation of the marine resources,

and the main focus has been on primary production (Smidt, 1979) and the distribution of mesozooplankton, i.e. the direct link to the fish stocks (Jespersen, 1934; Ussing, 1938; Smidt, 1979; Digby, 1953). These investigations have demonstrated the prominent role of the large copepod genus *Calanus* in the plankton around Greenland. But information about the pelagic ecology and the potential role of the other potential components of the food web is limited.

Knowledge about plankton dynamics in ice-covered Arctic fjords is scarce. Because of the thick ice cover the pelagic primary production is insignificant and the primary production is predominantly associated with the ice-water interface. This continues until sea-ice break-up, when ice algae, if any, are released to the water column and the pelagic primary producers start to flourish. Young Sound is normally ice-covered until mid-summer and is only open for a few months (Chapter 4).

During the last decades, methodological and technical advancements and process-oriented scientific approaches have demonstrated a more diverse picture of the Arctic pelagic ecosystem, in which the microbial food web has a key role (Levinsen & Nielsen, 2002). In an earlier study in Young Sound, the seasonal cycle of the pelagic food web (Rysgaard et al., 1999) suggested that the large *Calanus* copepods dominated pelagic grazing, and that all activity was restricted to the short open-water period. This contrasts with investigations in the Disko Bay, W. Greenland (Levinsen & Nielsen, 2002) where the protozooplankton community is highly important in the re-cycling of primary production. This difference is caused by strong predation on protozooplankton by copepods, as these co-occur in the short production window associated with the open-water period of Young Sound (Levinsen et al., 2000b).

The present investigation primarily presents a measuring campaign prior to sea-ice break with high radiation and unlimited nutrients, and the major purposes were to 1) describe the most important pelagic processes during this period, 2) resolve the pelagic dynamics under the ice cover, 3) evaluate the pelagic carbon flow pathways through establishment of a budget for the pelagic during June 1999 and compare this with previous investigations during the open-water period (Rysgaard et al., 1999), and, finally, 4) establish an annual pelagic carbon budget for Station A in Young Sound.

5.2 Methods

The present chapter combines the annual study conducted in 1996 (Rysgaard et al., 1999) with an ice-cover campaign carried out from 11 to 27 June 1999 in Young Sound prior to sea-ice break-up. Furthermore, data are included from the MarineBasic monitoring program during the ice-free period of 2002, 2004, 2005 as well as from research programs during the winters of 1997 and 2003. The applied methods and measured parameters were the same in all studies except that bacteria and nanoflagellates were considered only in 1999. All samples were taken around noon at a 36 m deep station (Station A; Fig. 5.1) through a hole in the ice, using a hand-driven winch and a tripod. Depth profiles of temperature, salinity and fluorescence were recorded throughout the water column using a CTD (DataSonde4 Hydrolab, Austin, USA) with a calibrated Dr. Hardt fluorometer. The salinity probe was calibrated against water samples collected at 5 to 7 depths per sampling day and measured in the laboratory using a Guildline Salinometer. Based on the water column structure and the depth distribution of fluorescence profiles, 7 depths (1, 2, 5, 10, 15, 25 and 35 m) were selected for further chemical and biological measurements. Water samples were collected using a 5-l Niskin bottle. Samples for the determination of nutrient concentrations (NO_2^-, NO_3^-, PO_4^{3-}, SiO_4^{3-}) were frozen immediately and measured at the National Environmental Research Institute (NERI) according to Nielsen & Hansen (1995).

Subsamples, some of them size fractionated, of 100–200 ml for chlorophyll a (Chl *a*) and phaeopigment (Phaeo.) were collected within 4 hours of sampling and processed according to Jespersen & Christoffersen (1987) and Strickland & Parsons (1972). To convert to carbon, 600 ml of seawater was filtered in duplicate onto pre-muffled GF/F filters and stored at -20°C until analysis. Filters were dried in a desiccator and analyzed for carbon on a CHN analyzer (EA 1110 CHNS, CE Instruments).

Primary production was measured *in situ* using the ^{14}C method (Steemann-Nielsen, 1952). Water samples from each of the selected depths were incubated for 2 h around noon (2 light and 1 dark Jena bottles; 100 ml) containing 4 µCi $H^{14}CO_3^-$ (International Agency for ^{14}C Determination) according to Nielsen & Hansen (1995). Daily primary production per m^2 was calculated by extrapolating to diurnal irradiance at the respective water depths by trapezoidal depth integration down to 36 m.

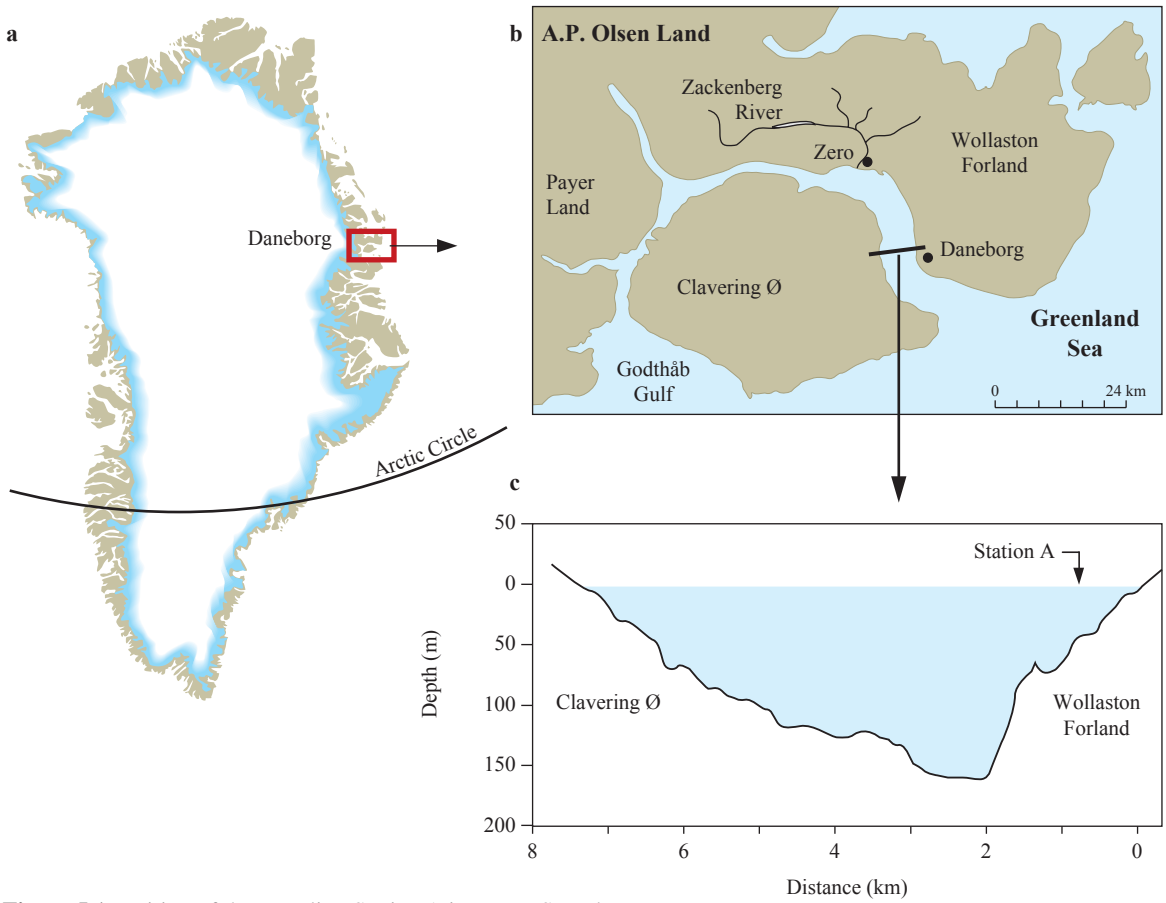

Figure 5.1 Position of the sampling Station A in Young Sound.

Bacterial abundance was quantified on a FACS Calibur flow cytometer (Becton Dickinson) after staining of the fixed cells with the nucleic acid stain SYBR Green 1 (Molecular Probes) according to Marie et al. (1997). Bacterial volume was determined on slides stained with acridine orange (0.1%) and at least 50 cells per slide were analyzed using digital image analysis. Biovolumes were converted to biomass using a carbon-to-volume factor of 0.22 pg C μm^{-3} (Bratbak & Dundas, 1984).

Bacterial production was measured by incorporation of ^{3}H-thymidine (Fuhrman & Azam, 1980) using the assumptions of Riemann et al. (1987). The carbon requirement of the bacterioplankton was estimated assuming a growth efficiency of 33% as for the other heterotrophic components of the pelagic food web (Hansen et al., 1997).

The abundance of heterotrophic nanoflagellates and diatoms < 20 µm was determined by epifluorescense microscopy of filters stained with proflavine (Haas, 1982) and processed according to Nielsen & Hansen (1995). A 500-ml water sample for enumeration of heterotrophic/mixotrophic protozoa was fixed in 1% Lugol's solution (final concentration), and a subsample of 50 or 100 ml was counted after 24 hours of sedimentation using an inverted microscope. Biovolumes of cells were estimated from measurements of linear dimensions assuming simple geometrical shapes and converted to biomass according to Edler (1979). To investigate the population dynamics of the microprotozooplankton, a microcosm experiment was conducted. On 12 June, three 25-l Nalgene polycarbonate carboys were filled with 20 l of water from just below the ice. The growth potentials of ciliates and dinoflagellates were followed in a mesozooplankton-free incubation, i.e. surface water < 45 µm. A carboy spiked with 300 ml *Rhodomonas salina* culture (6×10^5 cells ml^{-1}) and a carboy with sieved surface water served as controls. A diver placed the carboys under the ice about 10 m from the hole to

Table 5.1 Young Sound June 1999. Length vs. weight regressions used to provide biomass estimates for the individual mesozooplankton groups. Individual biomass (mg C) = $a \times L_{(\mu m)}^{b}$. Carbon = 0.45 × Dry weight.

Taxa	a	b	Reference
Calanus finmarchicus	$4.45x10^{-3}$	3.3838	Hirche and Mumm (1992)
Calanus glacialis	$4.45x10^{-3}$	3.3838	Hirche and Mumm (1992)
Calanus hyperboreus	$1.40x10^{-3}$	3.3899	Hirche and Mumm (1992)
Metridia longa	$6.05x10^{-3}$	3.0167	Hirche and Mumm (1992)
Acartia spp.	$1.11x10^{-11}$	2.92	Berggreen et al. (1988)
Pseudocalanus spp.	$0.45x(1.22x10^{-10})$	2.7302	Klein Breteler et al. (1982)
Microcalanus spp.	$9.47x10^{-10}$	2.16	Sabatini and Kiørboe (1995) as *Oithona* sp.
Oithona spp.	$9.47x10^{-10}$	2.16	Sabatini and Kiørboe (1995)
Oncaea spp.	$9.47x10^{-10}$	2.16	Sabatini and Kiørboe (1995) as *Oithona* sp.
Microsetella spp.	$8.5x10^{-5}$	1.0275	Satapoomin (2000)
Nauplii spp.	$4.17x10^{-9}$	2.03	Hygum et al. (2000)
Bivalvia	$3.06x10^{-11}$	2.88	Fotel et al. (1999)
Thecosomata			$2.27x10^{-2}$ ind^{-1} Beers (1996)
Gastropoda	$2.31x10^{-8}$	2.05	Hansen and Ockelmann (1991)
Polychaeta	$1.58x10^{-7}$	1.38	Hansen (1999) as *Polydora* spp.
Hyperiidae	$1.40x10^{-3}$	3.3899	Hirche and Mumm (1992) as *Calanus hyperboreus*
Decapoda			$2.50x10^{-1}$ ind^{-1} Uye (1982)
Echinodermata	$3.06x10^{-11}$	2.88	Fotel et al. (1998) as Bivalvia
Appendicularia	$7.33x10^{-11}$	2.627	King et al. (1980)
Others	$3.06x10^{-11}$	2.88	Fotel et al. (1999) as Bivalvia

avoid the altered light regime in the vicinity of the hole (Chapter 4).

Mesozooplankton were sampled from the bottom to the surface by triplicate vertical hauls using a modified WP-2 net (45-µm mesh) equipped with a flowmeter (Digital Model 438 110, Hydro Bios) and a large flow-meter non-filtering cod-end. The samples were preserved in buffered formalin (2% final concentration) and at least 300 individuals were analyzed. To distinguish between copepodites of *Calanus* spp., the cephalothorax length criteria of Madsen et al. (2001) were used. Copepod nauplii were not distinguished to species, but according to size the majority was *Calanus* spp. Biomass of meroplanktonic organisms and planktotrophic holoplankton other than copepods was calculated from length measurements. Individual biomass of all mesozooplankton was calculated according to length regressions taken from the literature (Table 5.1).

To determine egg production by free-spawning species of copepods, a sample of gently collected zooplankton was diluted with surface water and brought to the laboratory. Production of eggs by *Calanus glacialis* and *C. finmarchicus* and the fraction of reproductively active females were measured by incubating individual females in 600-ml polycarbonate bottles filled with 50-µm sieved *in situ* water (at least 12 replicates) for approximately 24 h. The bottles were incubated in the dark in a thermo box covered with snow to mimic *in situ* temperature. At the end of the experiments, the spawned eggs were counted and egg size was measured on a batch of eggs. Weight-specific egg production (SEP) was calculated from individual female carbon content according to Hirche & Mumm (1992) assuming a body carbon:dry weight ratio of 0.6 (Eilertsen et al., 1989), and an egg carbon content of 0.14 pg C μm^{-3} (Kiørboe et al., 1985). The egg production and SEP of egg-carrying *Oithona* spp. was calculated according to the equations in Nielsen et al. (2002). Egg numbers in sacs from at least 25 individuals per net

haul were counted. Secondary production by all the copepods was calculated from the weight-specific egg production of *C. glacialis* for the calanoids and *Oithona* for the non-calanoid copepods, assuming juvenile somatic growth rates resembling SEP (Berggreen et al., 1988). Copepod community grazing was assumed to be 3 times SEP as in Hansen et al. (1997). Meroplankton (all considered as planktotrophic) and planktotrophic holoplankton other that copepods were assumed to have a specific growth rate of 0.05 d^{-1} (Hansen et al., 1999) and be grazed by the same efficiency as for the copepods (Hansen et al., 1997).

To establish a pelagic carbon budget for the sea-ice campaign in 1999, mean ± SE of depth-integrated values of biomass, carbon demand and production of all components in the pelagic are presented in a flow chart as mg C m^{-2} d^{-1}. In the case of heterotrophic nanoflagellates, ciliates and heterotrophic dinoflagellates, of which rates were not measured, daily clearance (F) was calculated according to Hansen et al. (1997) and grazing (I) as $I = F \times C$, where C is the integrated prey biomass. Production was calculated by assuming a growth efficiency of 33% (Hansen et al., 1997). Secondary production of all copepods was calculated by multiplying the specific egg production (SEP) by total copepod biomass. Ingestion was calculated by assuming a growth efficiency of 33% (Hansen et al., 1997).

The annual carbon budget for the pelagic community in Young Sound was approximated by combining the present data set from June with the data from 1996 (Rysgaard et al., 1999). In the case of bacteria, which were not included in the 1996 study, the annual production was calculated assuming that the midwinter value obtained in 2005 by Rysgaard et al. (*in press*) of 3.1 mg C m^{-2} d^{-1} represents 271 d, the present investigation covering 14 days during the ice cover, and the bacterial production during the open-water period (80 d) is calculated as 20% of the primary production according to Rysgaard et al. (1999).

5.3 Results

5.3.1 Hydrography, nutrients and chlorophyll

The locality sampled was covered with 1.8 m of sea ice and was strongly influenced by advection, so no clear succession pattern of the water column characteristics could be identified during the 1999 campaign. Consequently, the depth distributions of physical and chemical parameters are presented as averages (Fig. 5.2 and Table 5.2). In particular, the water-column salinity was highly variable. Just below the ice the salinity was 30.6, decreasing to a minimum of 28.3 1 m below the ice, from where it increased to 32.0 at 10 m and gradually to 32.6

Figure 5.2 Young Sound June 1999. Vertical distribution of **(a)** Salinity, **(b)** Temperature (°C), **(c)** Nutrients (dark blue) phosphorus, (light blue) nitrate , (red) silicate and **(d)** Chlorophyll *a* concentration (µg Chl *a* l^{-1}).

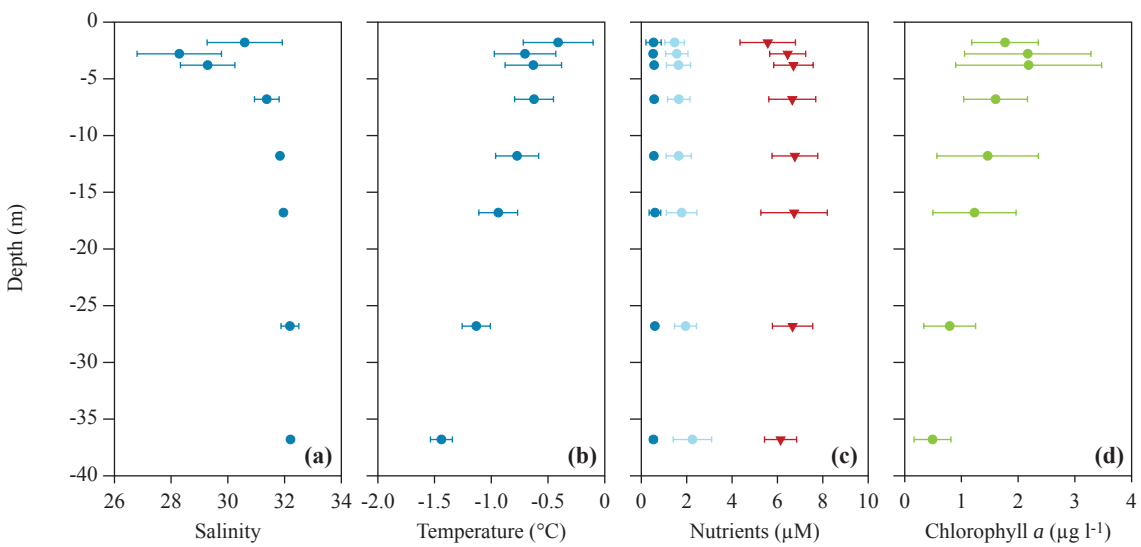

Table 5.2 Young Sound June 1999. Water column characteristics at the sampling depths, mean ±SD, range (min-max) and % CV (= SD/mean × 100) of parameters considered.

Depth (m)	Salinity	Temp. (°C)	PO_4 (µM)	NO_3 (µM)	SiO (µM)	Chl a (µg l^{-1})
	30.59±1.32	-0,41±0,31	0.54±0.34	1.47±0.43	5.58±1.22	1,77±0.59
0	27.09-31.74	-1.03-0.03	0.29-1.35	0.95-2.13	3.34-7.40	0.50-2.27
	4.33	75	62	29	22	33
	28.29± 0.49	-0,70±0,27	0.52±0.14	1.57±0.50	6.45±0.79	2,17±1.11
1	26.13-30.27	-1.00-0.15	0.26-0.69	0.85-2.33	5.11-7.24	1.19-4.81
	5.26	39	27	32	12	51
	29.29±0.96	-0,63±0,25	0.57±0.13	1.64±0.53	6.71±0.87	2,19±1.29
2	27.91-30.76	1.01-0.15	0.36-1.73	1.08-2.45	5.15-7.58	1.10-5.26
	3.27	40	23	33	13	59
	31.37±0.43	-0,62±0,17	0.57±0.15	1.65±0.50	6.66±1.03	1,60±0.56
5	30.54-31.84	-0.93-0.42	0.34-0.75	0.89-2.42	4.86-7.63	0.74-2.22
	1.38	27	26	30	16	35
	31.84±0.11	-0,77±0,19	0.56±0.11	1.65±0.55	6.77±1.01	1,46±0.90
10	31.63-32.01	-1.03-0.47	0.40-0.78	0.68-2.34	5.06-8.04	0.52-2.80
	0.34	25	20	34	15	61
	31.96±0.08	-0,94±0,17	0.60±0.26	1.78±0.67	6.74±1.46	1,23±0.73
15	31.84-32.10	-1.15-0.66	0.19-0.95	0.80-2.58	4.27-8.07	0.38-2.25
	0.25	18	43	38	22	60
	32.19±0.31	-1,13±0,12	0.60±0.13	1.95±0.48	6.67±0.89	0,79±0.46
25	31.98-32.99	-1.32-0.83	0.37-0.79	1.26-2.87	5.17-8.13	0.23-1.47
	0.97	11	22	25	13	58
	32.21±0.09	-1,44±0,10	0.54±0.15	2.25±0.85	6.14±0.71	0,49±0.33
35	32.06-32.32	-1.53-1.27	0.37-0.85	1.44-4.05	5.16-7.30	0.18-1.01
	0.27	7	28	38	12	66

close to the sea floor. The same overall pattern was observed for temperature, i.e. a quite high variability at the surface, decreasing toward more stable conditions above the bottom (Table 5.2). Because of the thick sea ice cover and the unstable water column, the pelagic primary production was low. Consequently, all nutrients were present in the surface water at quite high concentrations throughout the investigation. The major nutrients, phosphorus, nitrate, and silicate, were all present in excess, and no vertical difference was observed in concentrations. In general, the highest Chl *a* concentration was observed in connection with the low salinity few meters below the sea ice (Fig. 5.2). A carbon:Chl *a* ratio of 58 was calculated by linear regression between POC and Chl *a*.

Following the break-up of sea ice, the immediate increase in light penetration to the water column triggered a steep increase in pelagic primary production and Chl *a* values (Fig. 5.3). Diatoms dominate the phytoplankton community and constitute 62–74% of the total phytoplankton assemblage during the ice-free period (Rysgaard et al., 2004; Rysgaard et al., 2005). When the sea ice breaks up, the spring bloom quickly depletes the nutrients in the surface layer, causing the highest concentration of Chl *a* to be located at a water

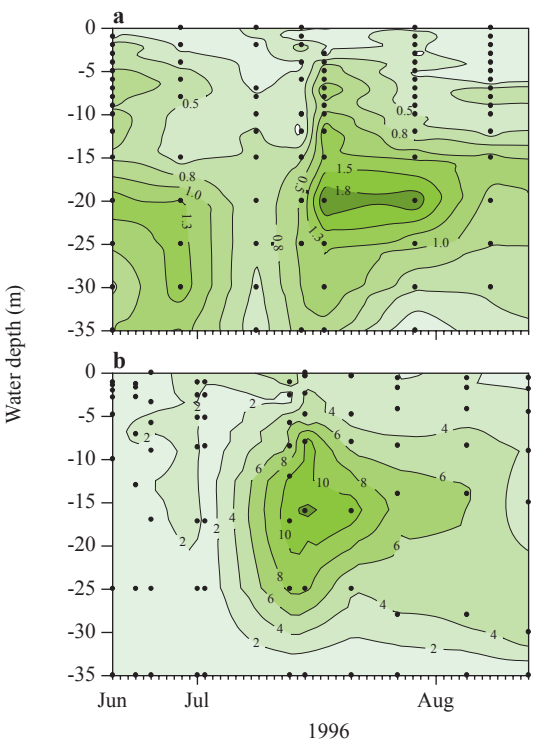

Figure 5.3 Young Sound June-August 1996. Vertical distribution of **(a)** Chl *a* (µg l^{-1}), and **(b)** primary production (µg C l^{-1} d^{-1}). Dots indicate the resolution of measurements. Data from Rysgaard et al. (1999).

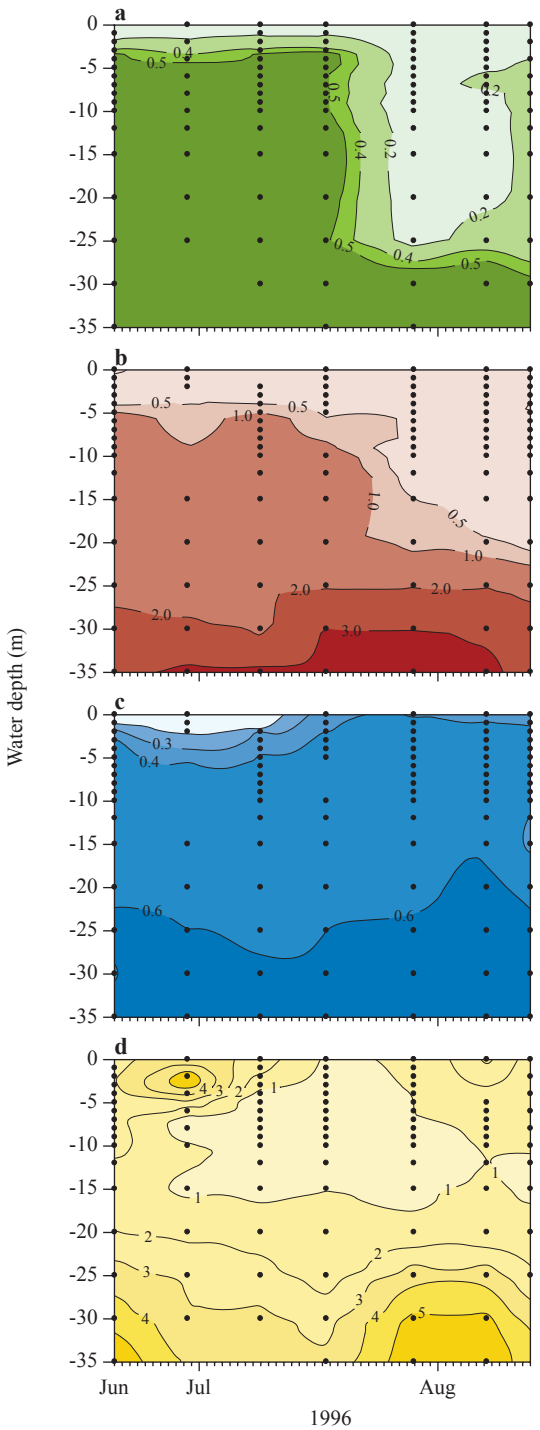

Figure 5.4 Young Sound June-August 1996. Vertical distribution of **(a)** ammonium, **(b)** nitrate, **(c)** phosphorus and **(d)** silicate. All measurements are in µM values, and dots indicate the resolution of measurements. Data from Rysgaard et al. (1999).

depth of 15–20 m. The stability of the water column during the summer season effectively seals the nutrients in the deeper water layers. Thus, the subsurface bloom usually lasts until August when primary production starts to descend to greater water depths (Fig. 5.4) due to initial limitation by SiO_4, followed by NO_3^- and NH_4^+, whereas PO_4^{3-} does not seem to limit production (Fig. 5.4; Rysgaard et al., 1999).

5.3.2 Primary producers

There was a pronounced decrease in depth-integrated phytoplankton biomass from about 4 g C m^{-2} to 2 g C m^{-2} at the end of the sea ice covered campaign (Fig. 5.5a). The reduction in the standing stock of phytoplankton was related to a shift in composition of the phytoplankton community. This change is illustrated by a shift in size fractions of the phytoplankton, from dominance of the Chl *a* fraction >11 µm at the beginning of the study to dominance of the smaller size fractions by the end of June (Fig. 5.5b). The change in size fractions is corroborated by the microscopic phytoplankton counts, according to which the diatoms (dominated by *Chaetoceros* spp.) present during the first days were succeeded by a community of autotrophic flagellates, primarily *Pyramimonas amylifers*, *P. grossi/orientalis*, *Dinobryon* spp. and *Apedinella/Pseudopedinella* (Fig. 5.5c). The overall mean biomass of primary producers during the sea-ice-covered period studied here was 2634 ± 405 mg C m^{-2}.

Because of the thick sea ice cover and poor light conditions, pelagic primary production was very low. The integrated primary production followed the development in the phytoplankton standing stock and showed a pronounced decrease from 122.5 to 28 mg C m^{-2} d^{-1} during the investigation (Fig. 5.5a, right axis) with a mean ± SE of 44.3 ± 11.8 mg C m^{-2} d^{-1}. After the ice breaks up, the spring bloom quickly develops and the pelagic primary production increases (Fig. 5.3b). The annual pelagic primary production, based on 11 direct measurements during the productive summer season and 1 during the unproductive winter is 10.5 g C m^{-2} yr^{-1} (Rysgaard et al., 1999)

5.3.3 Bacterioplankton and HNF

The depth-integrated bacterial biomass was quite stable throughout the ice-covered campaign 691 ± 45 mg C m^{-2} (Fig. 5.6a). In contrast, the bacterial production was more variable, but reached an average value of 52 ± 9 mg C m^{-2} d^{-1}, which corresponds to an average

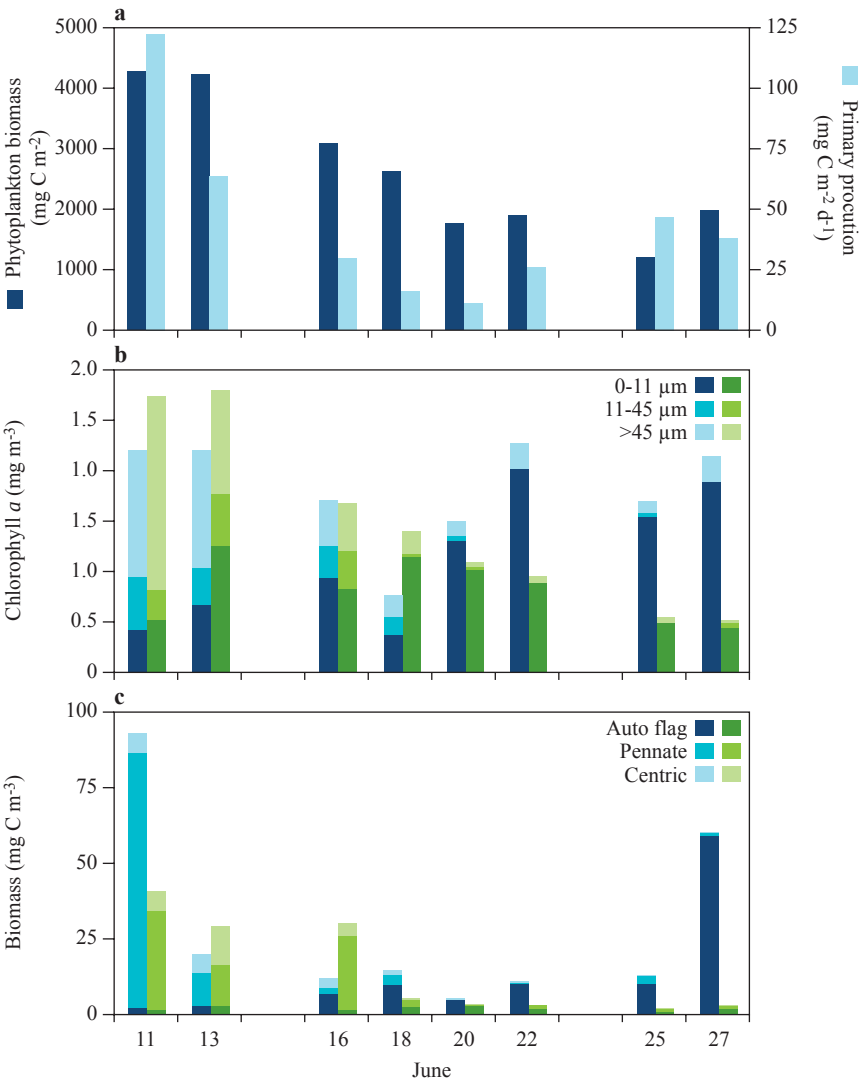

Figure 5.5 Young Sound June 1999. **(a)** Integrated phytoplankton biomass (0-36 m) calculated from the vertical profiles of chlorophyll *a* fluorescence (light blue bars; left axis) and integrated primary production (dark blue bars; right axis), **(b)** Size fractions of the phytoplankton community just below the ice (blue bars) and in 10 m (green bars), and **(c)** Main taxonomic phytoplankton groups just below the ice (blue bars) and in 10 m (green bars).

turnover of the bacterial standing stock of 8 ± 3% d^{-1} (Fig. 5.6b). Small heterotrophic nanoflagellates with an average cell volume of 60 ± 25 μm^3, n = 21 dominated the community of protist bacterial grazers, but the depth-integrated biomass remained low at 48 ± 7 mg C m^{-2} (Fig. 5.5c). The estimated clearance potential of the heterotrophic nanoflagellates was 0.5% of the water column per day giving rise to a grazing potential of 3.7 ± 0.4 mg C m^{-2}, which corresponds to < 10% of the daily bacterial production.

5.3.4 Microprotozooplankton

Naked oligotrich ciliates dominated the microprotozooplankton. In association with the change in phytoplankton community composition the ciliate biomass increased (Fig. 5.7a). At the two first sampling dates, where larger phytoplankton species dominated, the heterotrophic dinoflagellates constituted 40% of the microprotozooplankton biomass (Fig 5.7b) and the biomass of the heterotrophic dinoflagellates was quite constant throughout the investigation (40 ± 3 mg C m^{-2}), giving a grazing potential of 6 ± 1 mg C m^{-2} d^{-1}. However, because of the increase in the ciliate biomass the relative contribution of heterotrophic dinoflagellates decreased to 25% at the end of the investigation. The ciliate biomass was 98 ± 14 mg C m^{-2} with an estimated grazing of 73 ± 10 mg C m^{-2} d^{-1}. The average cell volume of ciliates and heterotrophic dinoflagellates was 5614 and 7060 μm^3, respectively, and the estimated mean grazing of ciliates was a factor of 10 higher than that of heterotrophic dinoflagellates. The initial biomass levels

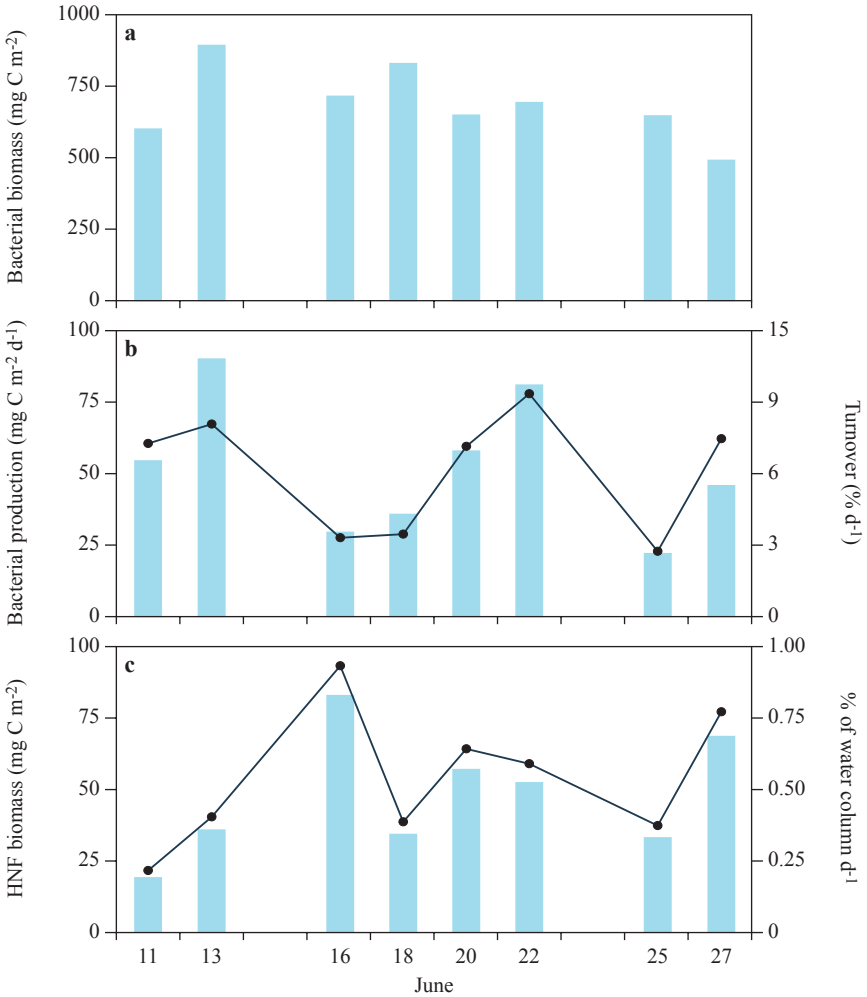

Figure 5.6 Young Sound June 1999. **(a)** Integrated bacterial biomass, **(b)** bacterial production (bars) and turnover rate, and **(c)** integrated biomass of heterotrophic nanoflagellates (bars) and their clearance capacity in % of the water column d^{-1}.

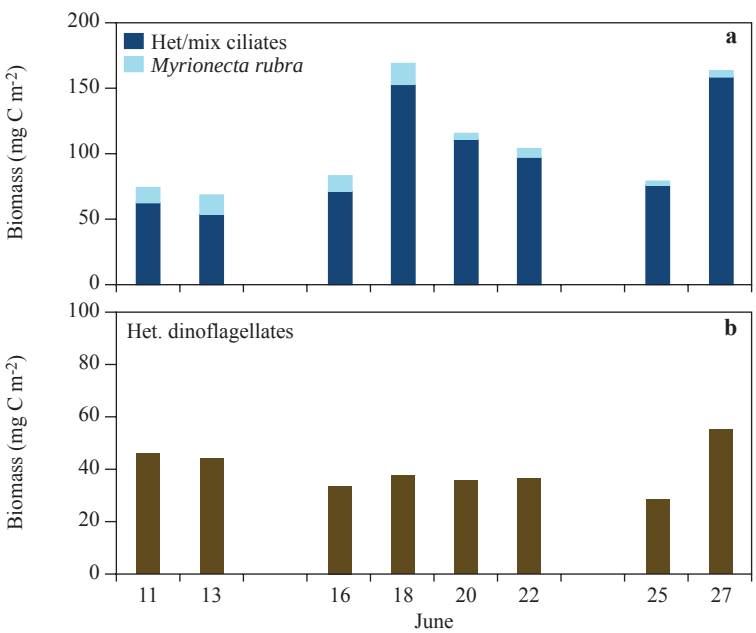

Figure 5.7 Young Sound June 1999. **(a)** Integrated biomass of ciliates, and **(b)** integrated biomass of heterotrophic dinoflagellates.

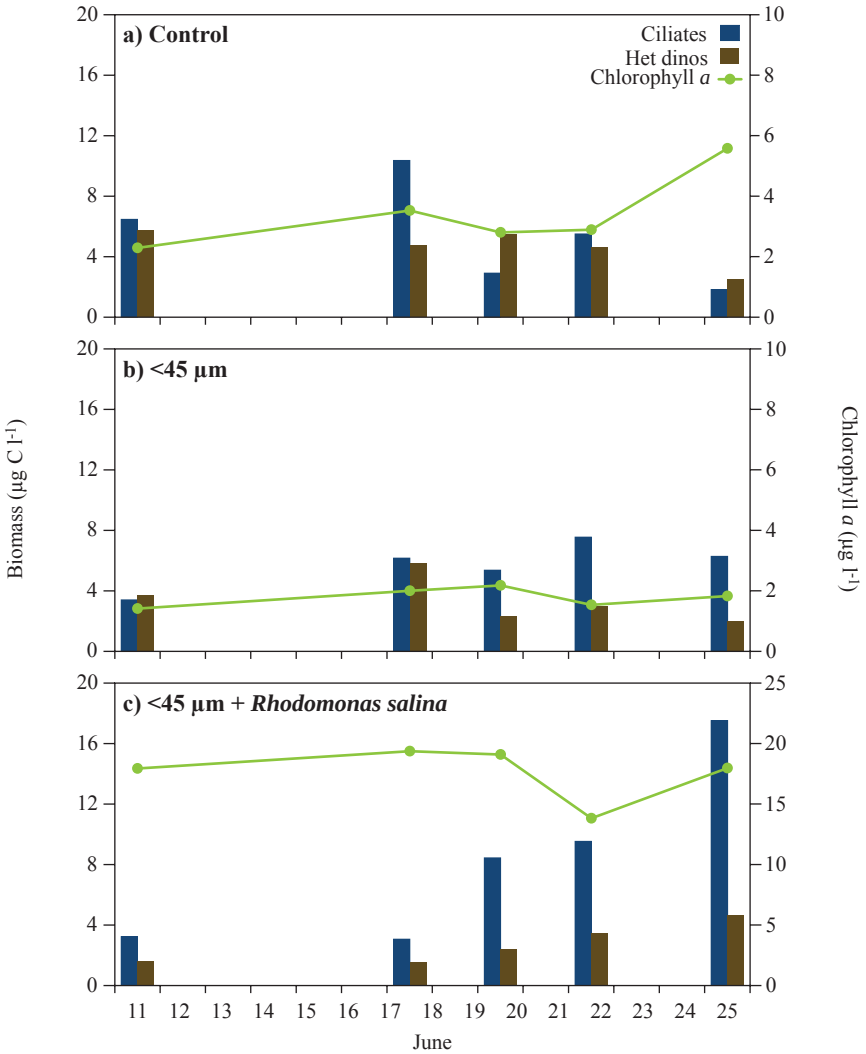

Figure 5.8 Young Sound June 1999. Microcosm experiments **(a)** control, **(b)** 45-µm fractionated surface water, and **(c)** 45-µm fractionated surface water spiked with the flagellate *Rhodomonas salina*.

of ciliates and heterotrophic dinoflagellates in the microcosm experiment were significantly higher in the control compared with the biomass in the phytoplankton size-fractionated carboys (Fig 5.8). This was primarily due to the removal of the largest ciliates (*Strombidium*, *Legardiella*) and the heterotrophic dinoflagellates (*Gyrodinium spirale*). In the control, the biomass of the ciliates increased initially followed by a gradual decrease, and the biomass of dinoflagellates was quite stable until the final days (Fig. 5.8a). In the 45-µm fractionated carboy the ciliate community increased-slightly, while the heterotrophic dinoflagellates decreased after the second sampling (Fig. 5.8b). In the *Rhodomonas*-spiked carboy, however, both protozooplankton groups increased during the incubation, indicating that the microprotozooplankton community in the fjord was food limited during this period (Fig. 5.8c).

The two main components of the microzooplankton, the ciliates and the heterotrophic dinoflagellates, contribute equally to the protozooplankton biomass in Young Sound, and the vertical and seasonal distributions of protozooplankton generally follow those of the phytoplankton (Rysgaard et al., 1999). The species composition and relative contribution of the two groups of protozoa are comparable with observations from the Disko Bay on the west coast of Greenland (Nielsen & Hansen, 1995; Levinsen et al., 1999). However, the absolute biomasses of ciliates and heterotrophic dinoflagellates in Young Sound are lower compared with the more productive Disko Bay (Levinsen & Nielsen, 2002).

5.3.5 Mesozooplankton

Young Sound mesozooplankton was numerically dominated by holoplankton, mainly copepods (Fig. 5.9 and Fig. 5.10). The copepods were present at mean abundances of 500–1200 ind m^{-3} and dominated by the cyclopoid species *Oithona* spp. and *Oncaea* spp. However, *Calanus* spp. and in particular *C. glacialis* and *C. hyperboreus* were nearly as abundant. The development of either total or species-specific abundance did not show any trend during the study. *Calanus finmarchicus* was represented by all copepodite stages except males, but the main components were CIV and V copepodites. The same stage composition was observed for *C. glacialis*, except that a few males were recorded. In contrast, *C. hyperboreus* was represented predominantly by CI-II copepodites, with fewer later copepodites, although some females were present. All the small calanoid and cyclopoid copepod species were present in all six copepodite stages, with only a few males. The harpacticoid *Microsetella* spp. was represented by CIV adults (Table 5.3). In terms of copepod biomass, the community was totally dominated by *Calanus* spp., particularly *C. glacialis* (Fig. 5.9b). No temporal trend was observed, and the total mean biomass was 40.7 ± 4.4 mg C m^{-3}, equal to 1465 ± 158 mg C m^{-2} (Fig. 5.9b).

The meroplankton was assumed to be planktotrophic, and holoplankton other than copepods were represented by 10 taxa. The gastropods, the polychaetes and the bivalves were the most important meroplankton groups, and the hyperiidae and the thecosomata dominated the holoplankton (Fig. 5.10). The development of both total abundance and relative species abundance showed a clear pattern during the study. The total abundance decreased from >600 ind. m^{-3} on the first three sampling dates to <100 ind. m^{-3} during the rest of the period. The thecosomata accounted for the main part of the biomass, followed by the hyperiidae and the gastropods. The total biomass was 2.7–3.8 mg C m^{-3} in the first three samplings, decreasing to 1 mg C m^{-3} in the rest of the period (Fig. 5.10b & Table 5.5), and the mean area biomass was 65 ± 49 mg C m^{-2}.

Seasonal studies covering the open-water period in Young Sound (Rysgaard et al., 1999; Rysgaard et al., 2004; Rysgaard et al., 2005) have shown that the mesozooplankton community is composed of *Calanus* spp., *Pseudocalanus* spp., *Microcalanus* spp., *Oithona* sp., *Oncaea* spp. and harpacticoid copepods. In addition, a few pelagic larvae of bivalvia, gastropoda and polychaeta have been identified, and the appendicularians are represented by *Fritillaria* sp.

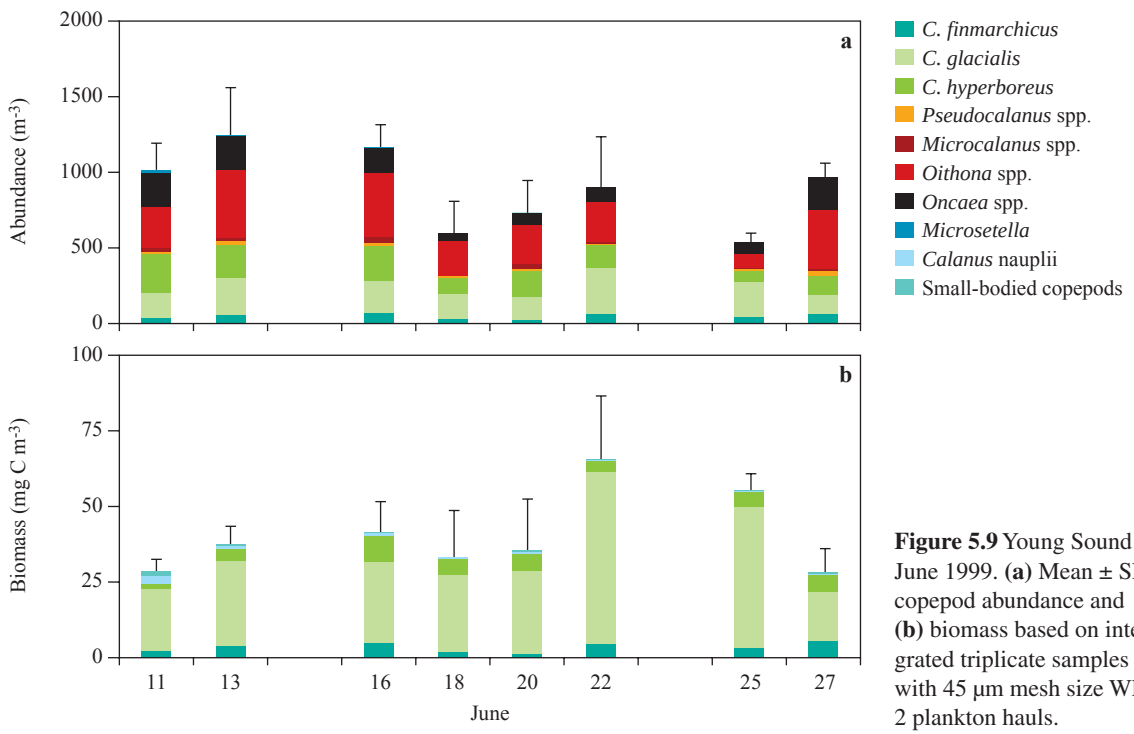

Figure 5.9 Young Sound June 1999. **(a)** Mean ± SE copepod abundance and **(b)** biomass based on integrated triplicate samples with 45 µm mesh size WP-2 plankton hauls.

and *Oikopleura* sp. In general, the mesozooplankton community is dominated numerically by copepods. In terms of biomass, the three *Calanus* species *C. glacialis*, *C. hyperboreus* and *C. finmarchicus* dominate the standing stock, constituting 70–90% of the total copepod biomass (Rysgaard et al., 1999).

Only few ripe *Calanus finmarchicus* females were present during the 1999 campaign and those incubated did not produce any eggs (data not shown). The initial egg production by *C. glacialis* was, however, high, 68.3 eggs female^{-1} d^{-1}, corresponding to a SEP of 0.10 d^{-1} (Fig. 5.11a & Table 5.4). However, the production consequently decreased with time, reaching zero at the end of June. This development was supported by the observation that the fraction of reproductively active females decreased (Fig. 5.11a), as did the abundance of free-floating copepod eggs and copepod nauplii (Fig. 5.11b & Fig. 5.11c). In contrast, the egg production of the egg-carrying cyclopoid *Oithona* spp. was less variable throughout the investigation. When the egg production by *C. glacialis* approached zero, the *Oithona* egg production remained high (Fig 5.11c & Table 5.4). The SEP of *Oithona* spp. was, however, several orders of magnitude lower than that of *C. glacialis* (Fig. 5.11a & Table 5.4).

The secondary production by the copepod community was calculated by multiplying SEP by the total biomass. This yielded a secondary production within the range 2.9–0.1 mg C m^{-3} d^{-1}, with a mean of 1.3 ± 0.4 mg C m^{-3} d^{-1} (Table 5.4). Calculating the copepod community grazing from the secondary production gave a mean of 3.9 ± 1.1 mg C m^{-3} d^{-1}, which is considered an underestimation, since a copepod biomass was present despite no SEP on the last two dates. Assuming that the entire copepod biomass was actively grazing throughout the study period at a specific rate corresponding to cover the SEP as recorded initially, 0.10 d^{-1} for *C. glacialis* (Nielsen & Hansen, 1995), the community grazing ends up at 441 ± 42 mg C m^{-2} d^{-1}, which is assumed to be more valid, and is therefore the one incorporated into the pelagic carbon budgets (see below). The mean secondary production by the meroplankton and holoplankters other than copepods was calculated at 0.09 ± 0.02 mg C m^{-3} d^{-1}, equal to 3.2 mg C m^{-2} d^{-1}, giving rise to a community grazing an order of magnitude lower than that of the copepod community (Table 5.5).

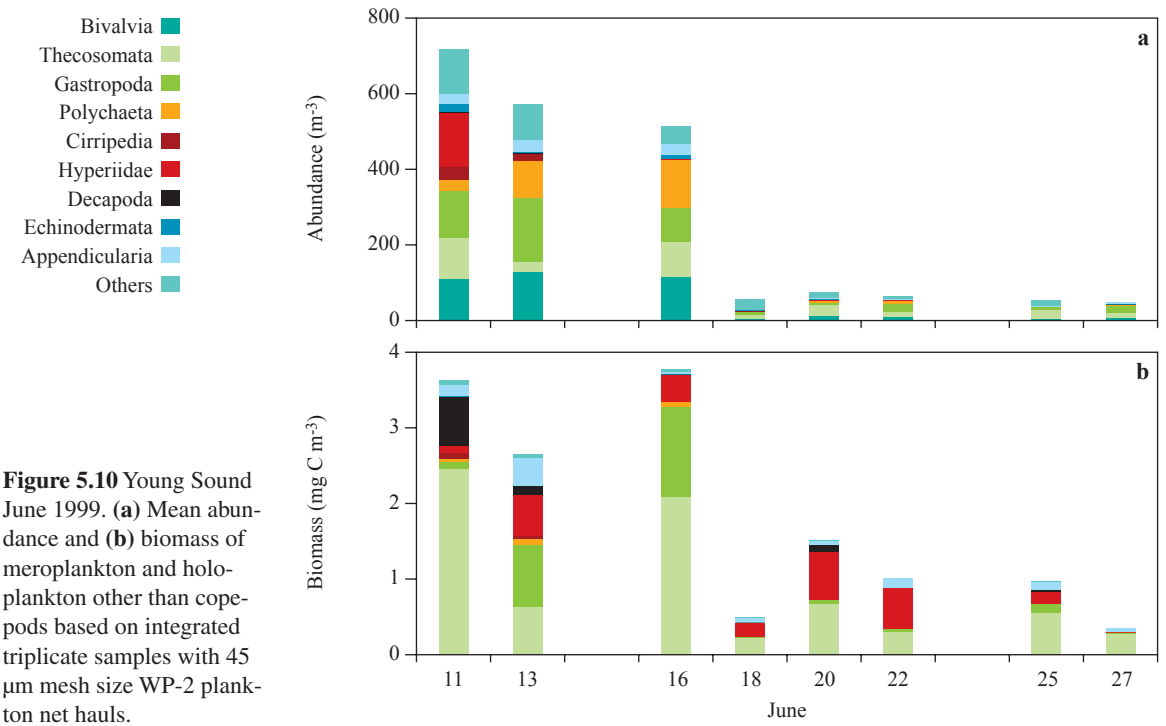

Figure 5.10 Young Sound June 1999. **(a)** Mean abundance and **(b)** biomass of meroplankton and holoplankton other than copepods based on integrated triplicate samples with 45 µm mesh size WP-2 plankton net hauls.

Table 5.3 Young Sound June 1999. Copepod species and mean ± SD. stagewise abundance (numbers m^{-3}) based on 8 sampling dates with 3 replicates per date = 24 samples.

Taxa	CI	CII	CIII	CIV	CV	Male	Female
Calanus finmarchicus	3.1±4.7	1.5±2.2	2.6±2.5	21.1±25.5	15.5±13.1	0	3.8±3.5
Calanus glacialis	15.5±22.8	6.8±8.0	11.7±12.1	98.7±53.2	56.2±43.9	0.1±0.2	11.2±8.5
Calanus hyperboreus	94.6±61.9	45.8±24.2	4.9±4.1	11.7±10.0	9.2±9.2	0	0.9±1.2
Metridia longa	0.2±0.6	0	0	0	0	0	0.5±1.8
Pseudocalanus spp.	4.7±5.6	3.5±3.9	2.0±2.5	1.4±2.3	1.2±1.9	0.3±0.7	2.8±1.9
Microcalanus spp.	6.2±5.8	4.0±4.6	3.4±4.3	4.1±4.6	1.2±2.4	0.1±0.3	0.6±1.1
Oithona spp.	68.9±54.7	56.0±66.3	14.4±12.5	18.8±17.1	58.0±40.8	5.1±3.7	43.7±30.1
Oncaea spp.	2.6±9.7	13.5±26.6	31.9±32.0	65.6±62.5	22.7±24.2	3.1±3.1	0.9±1.5
Microsetella spp.	0	0	0	0.3±1.1	1.6±5.2	0.2±0.6	1.8±5.3

Table 5.4 Young Sound June 1999. Egg production and specific egg production (SEP) of *Calanus glacialis* (mean ± SE. max. min. number of observations) and egg production and specific egg production of *Oithona* spp.

	June 11	June 13	June 16	June 18	June 20	June 22	June 25	June 27
C. glacialis Eggs fem.$^{-1}$d^{-1}	68.3±10.3 122.6; 4.1 15	52.2±10.2 142.6; 4.9 12	22.2±11.1 121.0; 0.0 13	26.5±10.9 109.6; 0.0 16	21.3±5.3 55.7;0.0 13	2.4±1.5 21.6; 0.0 15	No females	No females
SEP d^{-1}	0.10±0.017 0.20; 0.05	0.08±0.01 0.18; 0.01	0.04±0.023 0.29; 0.0	0.04±0.02 0.14; 0.0	0.03±0.01 0.08; 0.0	0.004±0.003 0.04; 0.0		
Oithona Eggs fem.$^{-1}$ d^{-1}	0.16	0.09	0.11	0.10	0.10	0.12	0.12	0.15
SEP d^{-1}	0.0024	0.0014	0.0018	0.0016	0.0015	0.0018	0.0018	0.0023

Table 5.5 Young Sound June 1999. Planktotrophic meroplankton and holoplankton other than copepods. Mean biomass ±SE (mg C m^{-3} and m^{-2} of triplicate plankton hauls); community secondary production (G = mean biomass × 0.05 d^{-1}; Hansen et al., 1999); and community grazing (I = G × 3; Hansen et al., 1997).

	June 11	June 13	June 16	June 18	June 20	June 22	June 25	June 27	Mean±SE m^{-3}	Mean±SE m^{-2}
Biomass mg C m^{-3}	3.61±3.73	2.65±1.00	3.79±1.28	0.52±0.48	1.52±0.98	1.02±1.39	0.96±0.11	0.37±0.40	1.81±4.46	65±49
Secondary production mg C m^{-3} d^{-1}	0.18	0.13	0.19	0.026	0.076	0.051	0.048	0.019	0.090±0.022	3.2±0.8
Community grazing mg C m^{-3} d^{-1}	0.54	0.39	0.57	0.078	0.23	0.153	0.144	0.138	0.280±0.01	10.1±2.3

Table 5.6 Young Sound. Annual pelagic carbon budget on the 36 m deep Station A based on the investigations in 1996 and 1999 (Rysgaard et al., 1999 and the present chapter).

	Carbon need (g C m^{-2} yr^{-1})	Production (g C m^{-2} yr^{-1})	Origin
Phytoplankton		10.4	Rysgaard et al. 1999
Bacteria	10.8	3.6	Present paper*
Ciliates	0. 8	0.3	Rysgaard et al. 1999
Dinoflagellates	0.6	0.2	Rysgaard et al. 1999
Copepods	9.7	3.2	Rysgaard et al. 1999
Total	**21.9**		

* Assuming that the mid winter data from Rysgaard et al. (*in press*) of 3.1 mg C m^{-2} d^{-1} represents 271 d, the present investigation covering 14 d during the ice cover, and bacterial production during the open-water period (80 d) is considered as 20% of the primary production according to Rysgaard et al. (1999).

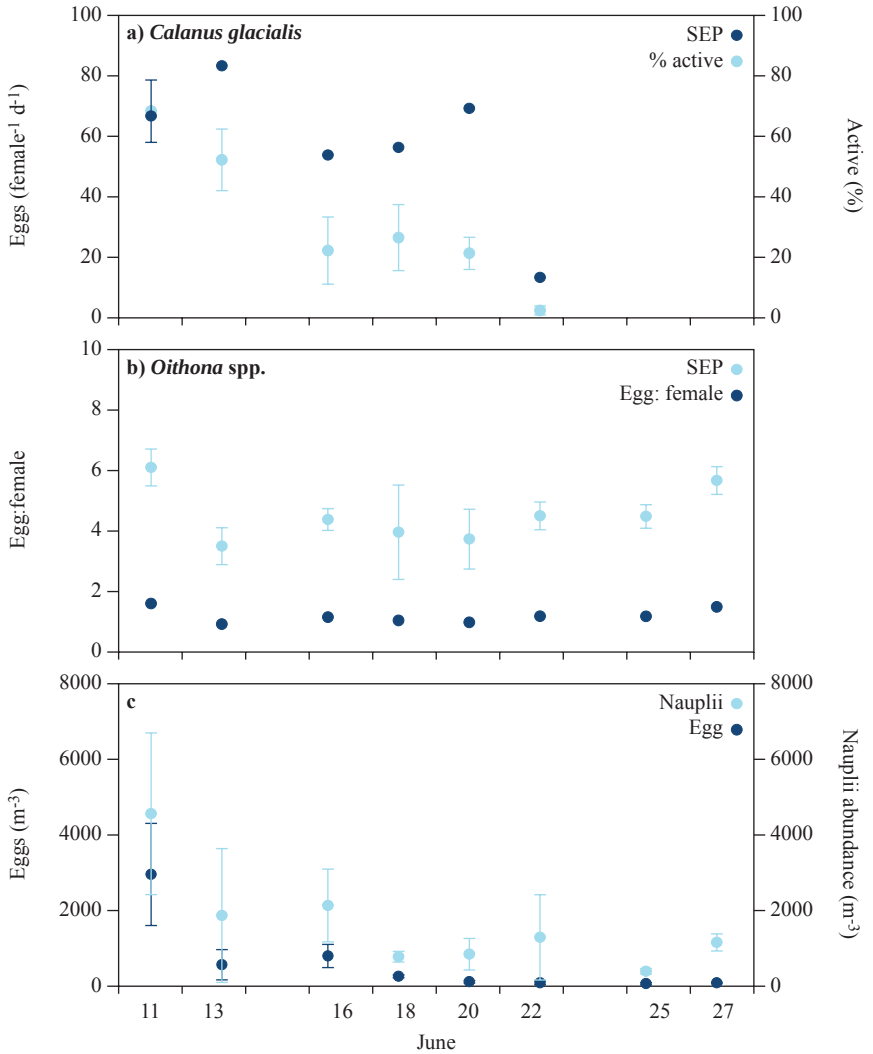

Figure 5.11 Young Sound June 1999. **(a)** *Calanus glacialis* egg production mean ± SE (left axis) and fraction of incubated females reproductively active (right axis), **(b)** *Oithona* spp. egg production (left axis) and egg: female ratio (right axis) and **(c)** mean ± SE abundance of free-floating copepod eggs (left axis) and copepod nauplii abundance (right axis).

5.3.6 Pelagic carbon budget for the ice-covered period

The total loss due to pelagic grazing was higher than the primary production during the 1999 field campaign, the carbon need of the grazers (copepods, meroplankters, ciliates and heterotrophic dinoflagellates) being 20% of the standing stock of phytoplankton (Fig. 5.12). This was presumably the reason for the observed decrease in phytoplankton biomass during the study period (Fig. 5.5a). In general, the copepod grazing was much more important that the rest of the pelagic grazing.

Photo: Peter B. Christensen

Incubation flasks for primary production incubated *in situ* below sea ice. Flasks are mounted in the sea ice with an ice-auger (front). Microprofiling instrument is seen in back (see Chapter 4).

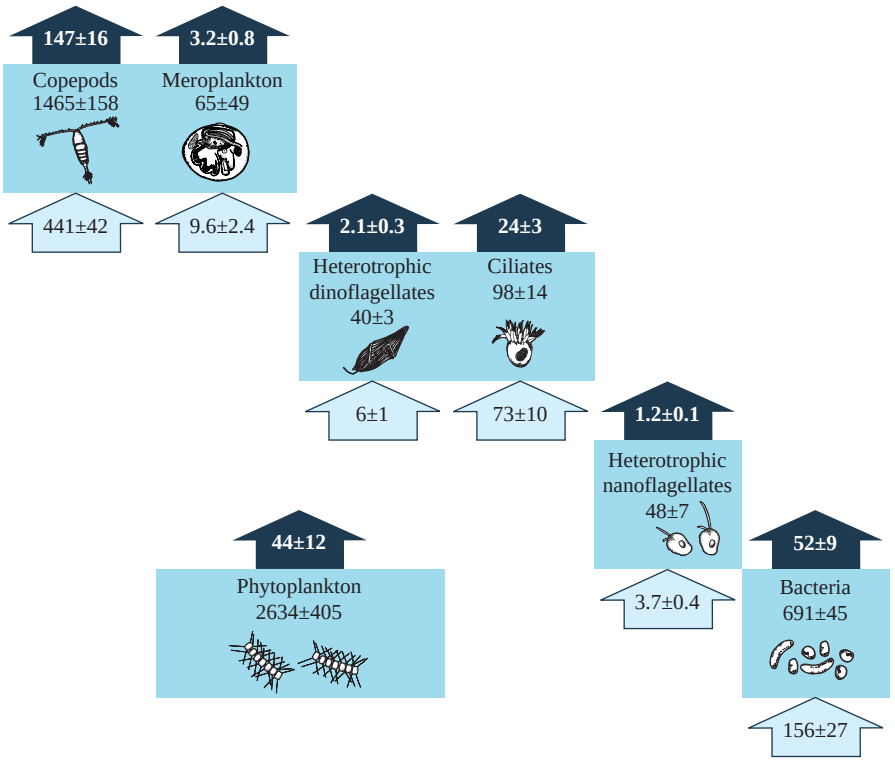

Figure 5.12 Young Sound June 1999. Carbon budget constructed as integrated mean ±SE (0-36 m) values of 8 sampling dates. Biomass in boxes (mg C m^{-2}), grazing in arrows going into the boxes, and production in arrows leaving the boxes (mg C m^{-2} d^{-1}).

5.3.7 The annual pelagic carbon budget

The annual pelagic carbon budget for Young Sound (Table 5.6) illustrates that the primary production at Station A (10.4 g C m^{-2} y^{-1}) cannot, on its own, cover the carbon need of the heterotrophic components of the pelagic food web (21.9 g C m^{-2} y^{-1}).

Calanus hyperboreus from Young Sound.

Photo: Torkel G. Nielsen.

5.4 Discussion

Combining the study performed at Station A during sea-ice cover with the open-water study conducted in 1996 at the same station (Rysgaard et al., 1999), documented that most of the annual pelagic productivity took place during the short open-water period (Fig. 5.13). The integrated annual carbon budget (Table 5.6) revealed that the estimated carbon need of the heterotrophs was more than twice the annual pelagic primary production at Station A, underlining the fact that Young Sound is a net heterotrophic system relying on import of organic material from the open sea or possibly from land.

Although a high phytoplankton biomass was present under the sea-ice cover during mid-summer, the low irradiance prevented nutrients from limiting primary production. However, nutrient limitation does occur when the sea ice breaks up and the pelagic community is exposed to full mid-summer irradiance in the middle of July, causing primary production to accelerate (Fig. 5.3; Rysgaard et al., 1999). During sea-ice cover, the relatively high phytoplankton biomass, 2634 mg C m^{-2}, expresses only a low productivity of, on average, 44 mg C m^{-2} d^{-1}. Bacterial production was higher than primary pro-

duction, 52 mg C m^{-2} d^{-1}, illustrating the importance of the microbial food web in this light-limited Arctic environment. Phytoplankton was grazed by copepods at a rate of 441 mg C m^{-2} d^{-1} and by ciliates, heterotrophic dinoflagellates and meroplankton at rates of 73, 6 and 10 mg C m^{-2} d^{-1}, respectively. Thus, total zooplankton ingestion corresponds to c. 20% of the total phytoplankton biomass and grazing therefore exceeds daily primary production by a factor of ten. Despite the high carbon demand of the heterotrophic compartments of the pelagic food web, the phytoplankton biomass did not change accordingly during June 1999, illustrating that the pelagic community must be renewed from elsewhere. The most plausible source is the open areas at the entrance to the fjord. As soon as the sea ice broke up, and meltwater from sea ice and from terrestrial runoff stabilized the water column, the developing spring bloom changed the entire pelagic system from heterotrophic to autotrophic dominance until the sea ice reformed and once again reduced pelagic photosynthesis.

In recent monitoring reports on the Young Sound pelagic seasonal cycle, Rysgaard et al. (2004; 2005) observed that *Pseudocalanus* spp., *Oithona* spp. and *C. hyperboreus* dominate during August. Furthermore, Rysgaard et al. (1999) showed that *Calanus* spp. dominated the pelagic grazing during the short open-water period. Hence, the food web structure of the pelagic community was comparable with observations reported during spring in other Arctic ecosystems with longer open-water periods, i.e. with significant contributions from *Calanus* (Nielsen and Hansen, 1995; Hansen et al. 1996; Hirche & Kwasniewski, 1997; Levinsen & Nielsen 2002; Ringuette et al., 2002; Møller et al., 2006). However, the total dominance of the *Calanus* genus contrasted with reports from the Disko Bay, W. Greenland (69°N), where the protozooplankton succeeded as the main grazers after mid-summer when *Calanus* left the euphotic zone to descend to hibernation depths (Levinsen & Nielsen, 2002). Thus, the protozooplankton community in the Young Sound is of less importance in the re-cycling of primary production. This pronounced difference is probably caused by significant predation on the protozooplankton by the copepods (Levinsen et al., 2000b) due to the temporal co-occurrence of protozooplankton and copepods in the short production window associated with the open-water period.

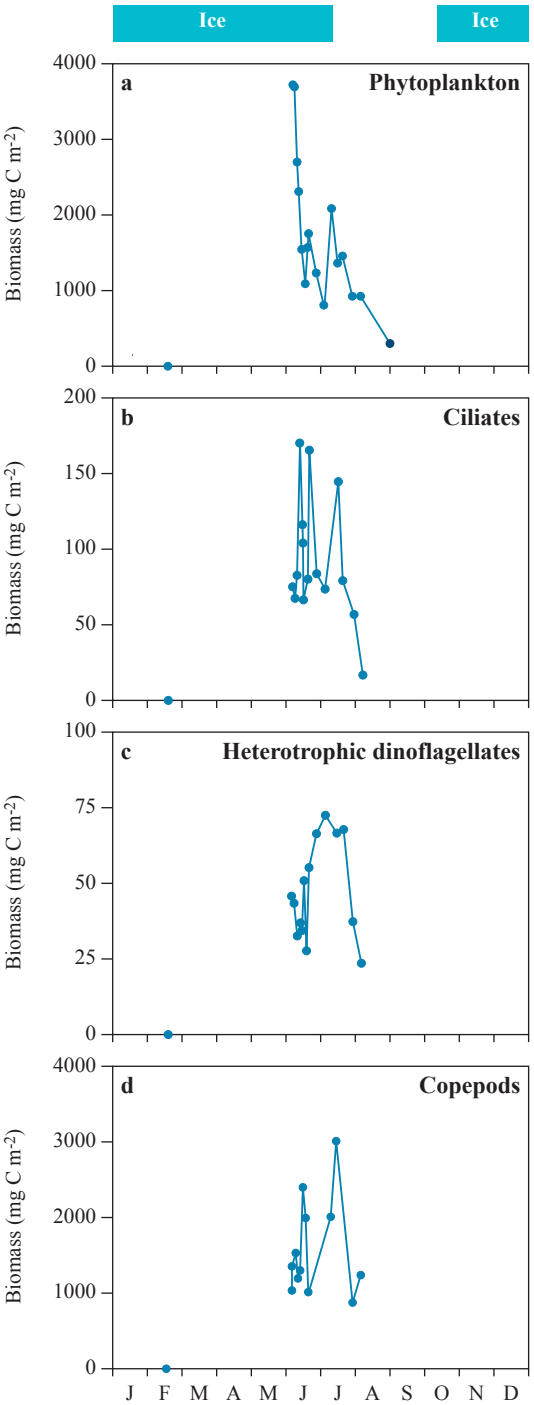

Figure 5.13 Young Sound. Annual cycle of integrated biomasses (mg C m^{-2}) of **(a)** phytoplankton, **(b)** ciliates, **(c)** dinoflagellates, and **(d)** copepods based on a combination of the investigations performed by Rysgaard et al. (1999) during 1996 and the present study in 1999.

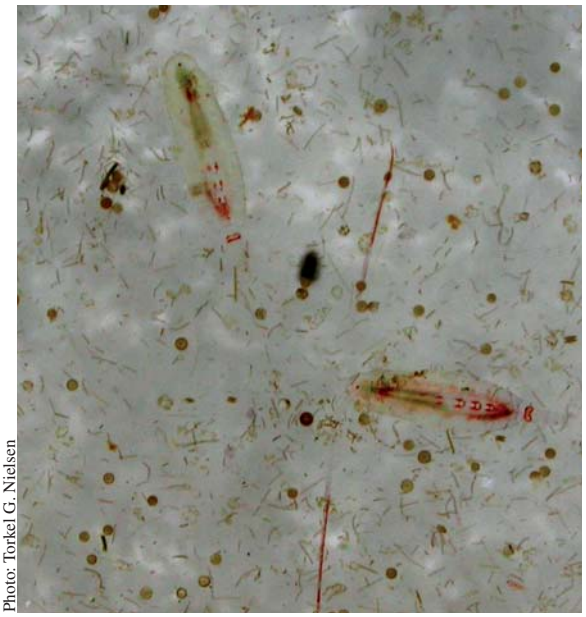

Photo: Torkel G. Nielsen

Copepods swimming in algal soup. Sample from Young Sound.

The main contributor to the copepod biomass was *Calanus* spp. Rysgaard et al. (2004; 2005) and Sejr et al. (2006) likewise reported dominance by this genus. During the ice-covered campaign the vast majority of copepods consisted of *C. glacialis* copepodite stages IV and V and females. This indicates that the population had reached maturity and that juvenile copepodites had grown up. *Calanus glacialis* was, however, not present in August 2003 and was assumed to have migrated to deeper waters, i.e. outside Young Sound or in the deeper parts of the fjord. The decrease in egg production rate, in the fraction of spawning females in the population, and in abundance of free-floating eggs and nauplii suggests that *C. glacialis* had its peak spawning in late May to early June. In Disko Bay, a high egg production rate was observed throughout June and July until descent of *C. glacialis* (Madsen et al., 2001). The *C. finmarchicus* population probably initiated spawning after *C. glacialis* as observed in the Disko Bay population (Madsen et al., 2001), and was indeed increasingly present during August 2003, 2004, and 2005 (Rysgaard et al., 2004; Rysgaard et al., 2005; Sejr et al., 2006). The *C. hyperboreus* was not present as advanced copepodites but primarily as CI copepodites, indicating pre-bloom reproduction as described elsewhere (e.g. Hirche & Niehoff, 1996; Madsen et al., 2001; Niehoff et al., 2002). In contrast, *C. hyperboreus* was numerous during August 2004 (Sejr et al., 2006).

In general, the relatively low water depth in the outer parts of Young Sound, far below reported diapause depth requirements for all three *Calanus* spp. (e.g. Hirche, 1998), indicates that no self-sustaining populations of any of the *Calanus* species exist here. Hence, all reproduction must be based on advected adult specimens originating from the Greenland Sea or from further inside the fjords where deeper waters are found (Chapter 3). Based on several years of monitoring during the program MarineBasic (Chapter 12) a decreased ratio between *C. hyperboreus* and *C. finmarchicus* is proposed to be indicative of an increased influence of Atlantic Water, as *C. finmarchicus* is considered an Atlantic Water species and *C. hyperboreus* a typical Arctic species. In contrast to the large copepods, all small-bodied calanoids were present in all copepodite stages, confirming the presence of several generations per year in Young Sound. The dominant cyclopoid *Oithona* spp., also reported by Rysgaard et al. (2004) and Rysgaard et al. (2005), apparently continued its reproduction after the large free-spawning species had terminated theirs. This pattern resembles those reported from West Greenland and the Greenland Sea (Møller et al., 2006).

The relative importance of the microbial food web qualitatively confirms the observations from the Greenland Sea (Møller et al., 2006), the Barents Sea (Hansen et al., 1996) and the Disko Bay, West Greenland, (Nielsen & Hansen, 1995; Møller & Nielsen, 2000; Levinsen & Nielsen, 2002). However, in contrast to the Barents Sea and Disko Bay the classical food chain seems to dominate the grazing pattern in Young Sound. Grazing, biomass as well as secondary production by copepods appears to be the major pathways for converting phytoplankton to higher trophic levels. Hence, the major structural difference between Young Sound and Disko Bay plankton communities is apparently that the observed succession, i.e. large *Calanus* spp. followed by protozoans and eventually by small copepods (Levinsen et al., 2000a; Madsen et al., 2001), does not take place in Young Sound. This difference is most likely due to the much deeper Disko Bay offering hibernation habitats for *Calanus* spp. and also the limited open-water period in Young Sound forcing all the major trophic groups to be temporarily present in concert.

To fully resolve the pelagic dynamics and model the succession of the pelagic food web in the Young Sound, more knowledge about the exchange processes between Young Sound and the Greenland Sea is essential. Additionally, better knowledge of the horizontal resolution of all the interacting compartments would enable us to obtain a comprehensive overview of the biological oceanography of Young Sound. Knowledge of the structure, succession and productivity of the pelagic community at the entrance to the Sound is especially crucial, since we hypothesize that this is what periodically fuels the ice-covered Young Sound with organic material.

5.5 Acknowledgements

This work was supported by the Danish Natural Science Research Council, by DANCEA (the Danish Cooperation for Environment in the Arctic) under the Danish Ministry of the Environment, by the Carlsberg Foundation and by the Commission of Scientific Research in Greenland. This work is a contribution to the Zackenberg Basic and Nuuk Basic Programs in Greenland. We thank E. R. Frandsen and J. W. Hansen for logistic support, and A. Haxen and the Editors as well as 3 anonymous reviewers for scientific and linguistic correction of earlier versions of this contribution.

5.6 References

Beers, J. R. 1996. Studies of the chemical composition of the major zooplankton groups in the Sargasso Sea off Bermuda. Limnol. Oceanogr. 11: 520-528.

Berggreen, U, Hansen, B. & Kiørboe, T. 1988. Food size spectra, ingestion and growth of the copepod *Acartia tonsa* during development: implications for determination of copepod production. Mar. Biol. 99: 341-352.

Bratbak, D. & Dundas, J. 1984. Bacterial dry matter content and biomass estimations. Appl. Environ. Microbiol. 48: 755-757.

Digby, P. S. B. 1953. Plankton production in Scoresby Sound, East Greenland. J. Anim. Ecol. 22: 289-322.

Edler, L. 1979. Recommendations for marine biological studies in the Baltic sea. – Baltic Mar. Biol. Publ. 5: 1-38.

Eilertsen, H. C., Tande, K. S. & Taasen, J. P. 1989. Vertical distribution of primary production, and grazing by *Calanus glacialis* Jaschnov and *C. hyperboreus* Krøyer in Arctic waters (Barents Sea). Polar Biol. 9: 253-260.

Fotel, F. L., Jensen, N. J., Wittrup, L. & Hansen, B. W. 1999. *In situ* laboratory growth by a population of blue mussel larvae (*Mytilus edulis* L.) from a Danish embayment, Knebel Vig. J. Exp. Mar. Biol. Ecol. 233: 213-230.

Fuhrman, J. A. & Azam, F. 1980. Bacterioplankton secondary production estimates for coastal waters of British Columbia, Antarctica and California. Appl. Environ. Microbiol. 39: 1085-1095.

Haas, L. W. 1982. Improved epifluorescence microscopy for observing planktonic microorganisms. Annls. Inst. Océanogr. 58: 261-266.

Hansen, B. W. 1999. Cohort growth of planktotrophic polychaete larvae – are they food limited? Mar. Ecol. Prog. Ser. 178: 109-119.

Hansen, B., Christiansen, S. & Pedersen, G. 1996. Plankton dynamics in the marginal ice zone of the central Barents Sea during spring: carbon flow and structure of the grazer food chain. Polar Biol. 16: 115-128.

Hansen B. & Ockelmann, K. W. 1991. Feeding behaviour in larvae of the opistobranch *Philine aperta*. I. Growth and functional response at different developmental stages. Mar. Biol. 111: 225-261.

Hansen, B. W., Nielsen, T. G. & Levinsen, H. 1999. Plankton community structure and carbon cycling on the western coast of Greenland during the stratified situation. III. Mesozooplankton. Aquat. Microb. Ecol. 16:233-249.

Hansen, P. J., Bjørnsen, P. K. & Hansen, B. 1997. Zooplankton grazing and growth: scaling within the 2-2,000 µm body size range. Limnol. Ocenogr. 42: 687-704.

Hirche, H. J. 1998. Dormancy in three *Calanus* species (*C. finmarchicus*, *C. glacialis* and *C. hyperboreus*) from the North Atlantic. Arch. Hydrobiol. Spec. Issues 52:359-369.

Hirche, H. J. & Mumm, N. 1992. Distribution of dominant copepods in the Nansen Basin, Arctic Ocean, in summer. Deep Sea Res. 39:485-505.

Hirche, H. J. & Niehoff, B. 1996. reproduction of the Arctic copepod *Calanus hyperboreus* in the Greenland Sea – field and laboratory observations. Polar Biol. 16:209-219.

Hirche, H. J. & Kwasniewski, S. 1997. Distribution, reproduction and development of *Calanus* species in the Northeast water in relation to environmental conditions. J. Mar. Sys. 10:299-317.

Hygum, B. H., Rey, C. & Hansen, B. W. 2000. Growth and developmental rates of *Calanus finmarchicus* (Gunnerus) nauplii during a diatom spring bloom. Mar. Biol. 136: 1075-1085.

Jespersen, P. 1934. Copepoda. The Godthaab Expedition 1928. Medd. Grønland. 79(10), 166 pp.

Jespersen, A. M. & Christoffersen, K. 1987. Measurements of chlorophyll-a from phytoplankton using ethanol as extraction solvent. Arch. Hydrobiol. 109: 445-454.

King, K. R., Hollibaugh, J. T. & Azam, F. 1980. Predator-prey interactions between the larvacean *Oikopleura dioica* and bacterioplankton in enclosed water columns. Mar. Biol. 56: 49-57.

Kiørboe, T., Møhlenberg, F. & Hamburger, K. 1985. Bioenergetics of the planktonic copepod *Acartia tonsa*: relation between feeding, egg production and respiration, and compopsition of specific dynamic action. Mar. Ecol. Prog. Ser. 26: 85-97.

Levinsen, H. & Nielsen, T. G. 2002. The trophic role of marine pelagic ciliates and heterotrophic dinoflagellates in arctic and temperate coastal ecosystems: A cross latitude comparison. Limnol. Oceanogr. 47: 427-439.

Levinsen, H., Nielsen, T. G. & Hansen, B. W. 2000a. Annual succession of marine pelagic protozoans in Disko Bay, West Greenland, with emphasis on winter dynamics. Mar. Ecol. Prog. Ser. 206: 119-134.

Levinsen, H., Turner, J. T., Nielsen, T. G. & Hansen, B. W. 2000b. On the trophic coupling between protists and copepods in Arctic marine Ecosystems. Mar. Ecol. Prog. Ser. 204: 65-77.

Madsen, S. D., Nielsen, T. G. & Hansen, B. W. 2001. Annual population development and production by *Calanus finmarchicus*, *C. glacialis* and *C. hyperboreus* in Disko Bay, western Greenland. Mar. Biol. 139: 75-93.

Marie D, Partensky F, Jacquet S & Vaulot D. 1997. Enumeration and cell cycle analysis of natural populations of marine picoplankton by Flow Cytometry using the nucleic acid stain SYBR Green I. Appl. Environ. Microbiol. 63: 186-193.

Møller, E. F., Nielsen, T. G. & Richardson, K. 2006. The zooplankton community in the Greenland Sea; composition and role in carbon turnover. Deep Sea Res. I. 53: 76-93.

Niehoff, B., Madsen, S. D., Hansen, B. W. & Nielsen, T. G. 2002. Reproductive cycles of three dominant *Calanus* species in the Disko Bay, West-Greenland. Mar. Biol. 140: 567-576.

Nielsen, T. G. & Hansen, B. W. 1995. Plankton community structure and carbon cycling on the western coast of Greenland during and after the sedimentation of a diatom bloom. Mar. Ecol. Prog. Ser. 125: 239-257.

Nielsen, T. G., Møller, E. F., Satapoomin, S., Ringuette, M. & Hopcroft, R. R. 2002. Egg hatching rate of the cyclopoid copepod *Oithona similis* in arctic and temperate waters. Mar. Ecol. Prog. Ser. 236: 301-306.

Riemann, B., Bjørnsen, P. K., Newell, S. & Fallon, R. 1987. Calculation of cell production of coastal marine bacteria based on measured incorporation of 3H-thymidine. Limnol. Oceanogr. 32: 471-476.

Ringuette, M., Fortier, L., Fortier, M., Runge, J. A., Bélanger, S., Larouche, P., Weslawski, J.-M. & Kwasniewski, S. 2002. Advanced recruitment and accelerated population development in Arctic calanoid copepods of the North Water. Deep-Sea Res. PII, 49: 5081-5099.

Rysgaard, S., Glud, R. N., Sejr, M. K., Bentsen, J. & Christensen, P. B. (*in press*) Inorganic carbon transport during sea ice growth and decay: A carbon pump in polar seas. J. Geophys. Res. Ocean 2006jc003572

Rysgaard, S., Nielsen, T. G., & Hansen, B. W. 1999. Seasonal variation in nutrients, pelagic primary production and grazing in a High-Arctic coastal marine ecosystem, Young Sound; North Eastern Greenland. Mar. Ecol. Prog. Ser. 179: 13-25.

Rysgaard, S., Frandsen, E., Sejr & Christensen, P. B. (2004) Zackenberg Basic: The MarineBasic Programme. In: Zackenberg Ecological Research Operations, 9th annual report 2003. Rasch, M & Caning, K. (eds.). Danish Polar Center, Ministry of Science, Technology and Innovation. Copenhagen, 91 pp.

Rysgaard, S., Frandsen, E., Sejr, M. K., Dalsgaard, T., Blicker, M. E. & Christensen, P. B. (2005) Zackenberg Basic: The MarineBasic Programme. In Zackenberg Ecological Research Operations, 10th annual report 2004. Rasch, M & Caning, K. (eds.). Danish Polar Center, Ministry of Science, Technology and Innovation. Copenhagen, 85 pp.

Sabatini, M. & Kiørboe, T. 1995. Egg production, growth and development of the cyclopoid copepod *Oithona similis*. J. Plankton Res. 16: 1329-1351.

Satapoomin, S. 2000. Carbon content of some tropical Andaman Sea copepods. J. Plankton Res. 21: 2117-2123.

Sejr, M. K., Dalsgaard, T., Rysgaard, S., Frandsen, E. & Christensen, P. B. (2006) Zackenberg Basic: The Marine-Basic Programme. In Zackenberg Ecological Research Operations, 11th annual report 2005. Klitgaard, A. B. & Caning, K. (eds.). Danish Polar Center, Ministry of Science, Technology and Innovation. Copenhagen, 111 pp.

Smidt, E. L. B. 1979. Annual cycles of primary production and of zooplankton at Southwest Greenland. Medd. Grønland, Biosci. 1: 52 pp.

Steemann Nielsen, E. 1952. The use of radio-active carbon (C^{14}) for measuring organic production in the sea. J. Cons. Int. Explor. Mer. 18: 117-140.

Strickland, J. D. & Parsons, T. R. (1972) A practical handbook of seawater analysis. Bull. Fish. Res. Bd. Can. 167: 1-310.

Ussing, H. H. 1938. The biology of some important plankton animals in the fjord of East Greenland. Medd. Grønland. 100: 1-108.

Uye, S.-I. 1982. Length-weight relationships of important zooplankton from the Inland Sea of Japan. J. Oceanogr. Soc. Japan. 38: 149-158.

Photo: Søren Rysgaard

6

Vertical flux of particulate organic matter in a High Arctic fjord: Relative importance of terrestrial and marine sources

Vertical flux of particulate organic matter in a High Arctic fjord: Relative importance of terrestrial and marine sources

Søren Rysgaard[1] and Mikael K. Sejr[2]

[1]Greenland Institute of Natural Resources, Kivioq 2, Box 570, DK-3900 Nuuk, Greenland
[2]National Environmental Research Institute, Department of Marine Ecology, Vejlsøvej 25, DK-8600 Silkeborg, Denmark

Cite as: Rysgaard, S. & Sejr, M. K. 2007. Vertical flux of particulate organic matter in a High Arctic fjord: Relative importance of terrestrial and marine sources. In: Rysgaard, S. & Glud, R. N. (Eds.), Carbon cycling in Arctic marine ecosystems: Case study Young Sound. Meddr. Grønland, Bioscience 58: 110-119.

Abstract

Vertical flux of particulate matter was recorded using a moored sediment trap during 2002-03 in the outer region of the 90 km long NE Greenland fjord Young Sound (74°18'N, 20°18'W). Sea ice covered the fjord for c. 9 months during the deployment. At 65 m depth total flux of material was 1420 g dry weight m^{-2} and annual fluxes of carbonate (g m^{-2}), chlorophyll (mg m^{-2}), particulate organic carbon (POC, g C m^{-2}) and nitrogen (PON, g N m^{-2}), were, 9, 53, 17 and 1.2 respectively. A steep increase in fluxes was observed during the summer thaw when sea ice broke up and water discharge from land began. Within the two months (July and August), >90% of the total annual vertical flux occurred. Isotopic ($\delta^{13}C$ & $\delta^{15}N$) analysis of particulate organic material (POM) in the sediment trap, in phytoplankton and in the river material indicated that a maximum of c. 50% of the POM material originated from land. This is supported by the high C:N ratio (by atoms) of up to 22 found in the trapped organic material during the summer thaw as compared with 7–9 during winter and spring, when no discharge from land occurred. Seasonal measurements of the POC discharge from rivers to the outer region of the fjord corresponded to c. 40% of the vertical POC flux measured in the sediment trap, which further indicates a significant terrestrial contribution to the settling material in the outer fjord area.

Besides POC, dissolved organic carbon (DOC) is discharged in an equal amount to the fjord from rivers, resulting in a total organic carbon (TOC) input from land to the outer region of Young Sound of 13 g C m^{-2} yr^{-1}. This corresponds to c. 40% of the net TOC input from the Greenland Sea and to the outer part of the fjord during the ice-free productive period underlining the significant terrestrial contribution to sedimentation in the outer part of the fjord.

Mean permanent accumulation rates based on the depth distributions of ^{210}Pb, ^{137}Cs and TOC in sediments at 60 m water depth in the outer fjord area revealed a burial of carbon within the sediment of 7.9 g C m^{-2} yr^{-1}. In agreement with the sediment trap measurements, $\delta^{13}C$ values within the sediment suggest that a substantial amount (c. 40%) of the POC in the sediment was of terrestrial origin. At the same sites, previous studies have reported an annual release of dissolved inorganic carbon (DIC) due to mineralization from the sediment of 12.6 g C m^{-2} yr^{-1}. The sum of the annual DIC release and the burial within the sediment represents an expected total input to the sediment of 20.5 g C m^{-2} yr^{-1} and compares well with the vertical flux measurement from the sediment trap of 17.0 g C m^{-2} yr^{-1} during the present study.

6.1 Introduction

The vertical flux of organic matter from the pelagic environment determines the input of food to benthic animals, rates of benthic mineralization as well as the burial of material in sediments below the photic zone. In the Arctic marine environment, the amount of particulate organic matter originating from primary production is strongly influenced by the presence or absence of sea ice, which is the main factor control-

ling the availability of light for primary producers. Thus, a strong seasonal variation in the vertical export of particulate organic matter has been observed in Arctic waters with low export rates during sea-ice cover and elevated export rates during the open-water period (Atkinson & Wacasey, 1987; Bauerfeind et al., 1997). A peak in sedimentation is often associated with sea-ice break-up due to the release of ice-algal material from the sea-ice matrix (Fortier et al., 2002). Ice algae live in and on the underside of sea ice and are present primarily during April through June until sea-ice break-up (Horner & Schrader, 1982; Chapter 4). Prior to, or in association with, the break-up of sea ice and the development of the spring phytoplankton bloom, copepods ascend from wintering depths to surface waters to graze on the bloom (Madsen et al., 2001). Grazing by copepods leads to production of fecal pellets that sink rapidly in the water column and thus enhance the vertical export to the sea floor (Sampei et al., 2002). Due to release of dissolved organic matter from copepod fecal pellets (Urban-Rich, 1999) and degradation of sinking aggregates (Ploug & Grossart, 2000) the amount of particulate organic matter reaching the sediment is expected to decrease with depth.

In addition to the marine sources of organic matter, Arctic rivers discharge 30×10^6 tons of total organic carbon (TOC) into the Arctic Ocean on an annual basis (Rachold et al., 2004). River discharge is particularly important in the Arctic Ocean, as it receives 11% of global runoff while containing only 1% of the world ocean water (Shiklomanov, 1998). The content of POC relative to POC + DOC in river water varies greatly between the Arctic rivers from 4% in the Yenisei river to 62% in the Mackenzie River (Rachold et al., 2004).

The environmental changes in the Arctic observed over the last two decades have increased the interest in discharge of freshwater and organic matter from land to ocean (Benner et al., 2004). Although the Greenland Ice Sheet represents a huge freshwater source that potentially may have a profound influence on river discharge, erosion and organic matter transport to Greenland fjords and offshore areas, very little is known of this transport. In 1995, a research and monitoring station ZERO (Zackenberg Ecological Research Operations) was established in NE Greenland to increase knowledge about climate-ecosystem interactions. As part of an extensive monitoring program, the discharge of water and organic matter from the Zackenberg River has been monitored since 1995 (Rasch et al., 2000; Hasholt & Hagedorn, 2000; Chapter 2). The total freshwater discharge takes place over a 3-month period during June–August, when air temperatures exceed 0°C, and 65% of the discharge often occurs within a few weeks. The very pulsed freshwater discharge greatly affects the physical circulation in the fjord. The outer parts of the fjord are minimally influenced by discharge from glaciers, but pulsed terrestrial runoff occurs during the short summer thaw generating an estuarine circulation in which lighter low-salinity water is moved seaward above denser incoming water from the Greenland Sea (Rysgaard et al., 2003; Chapter 3). Previous studies have shown that the net TOC input to the outer fjord area during the productive ice-free period is 15–50 t d^{-1} (Rysgaard et al., 2003).

In order to determine the annual vertical flux of particulate organic matter and to evaluate the relative importance of marine and terrestrial sources in a NE Greenland fjord, a mooring equipped with a time-series sediment trap was deployed in the outer region of Young Sound. Sedimenting particles were collected at c. 65 m water depth during 2002-03 at 20 individually programmed time intervals. The material was analyzed for its content of total dry weight, carbonate, chlorophyll, POC, PON and isotopic signal ($\delta^{13}C$ & $\delta^{15}N$). In parallel, water samples of the Zackenberg River were collected frequently during May–September 2003 to determine the flux of POC and DOC as well as the isotopic signal from the catchment area. Finally, we compare the vertical flux from the sediment trap with the sediment mineralization processes and discuss the relative importance of terrestrial and marine sources of carbon for permanent burial in the sediment.

6.2 Methods

6.2.1 Study area

The study was carried out in 2002-03 in Young Sound, a NE Greenland fjord (74°18'N, 20°18'W) situated in the Northeast Greenland National Park. The fjord is c. 90 km long and 2–7 km wide with a 40-50-m deep sill at the entrance (Fig. 6.1). Mean air temperature is below freezing 9 months of the year, and only the months of June through August have positive mean air temperatures of up to 4°C (Cappelen et al.,

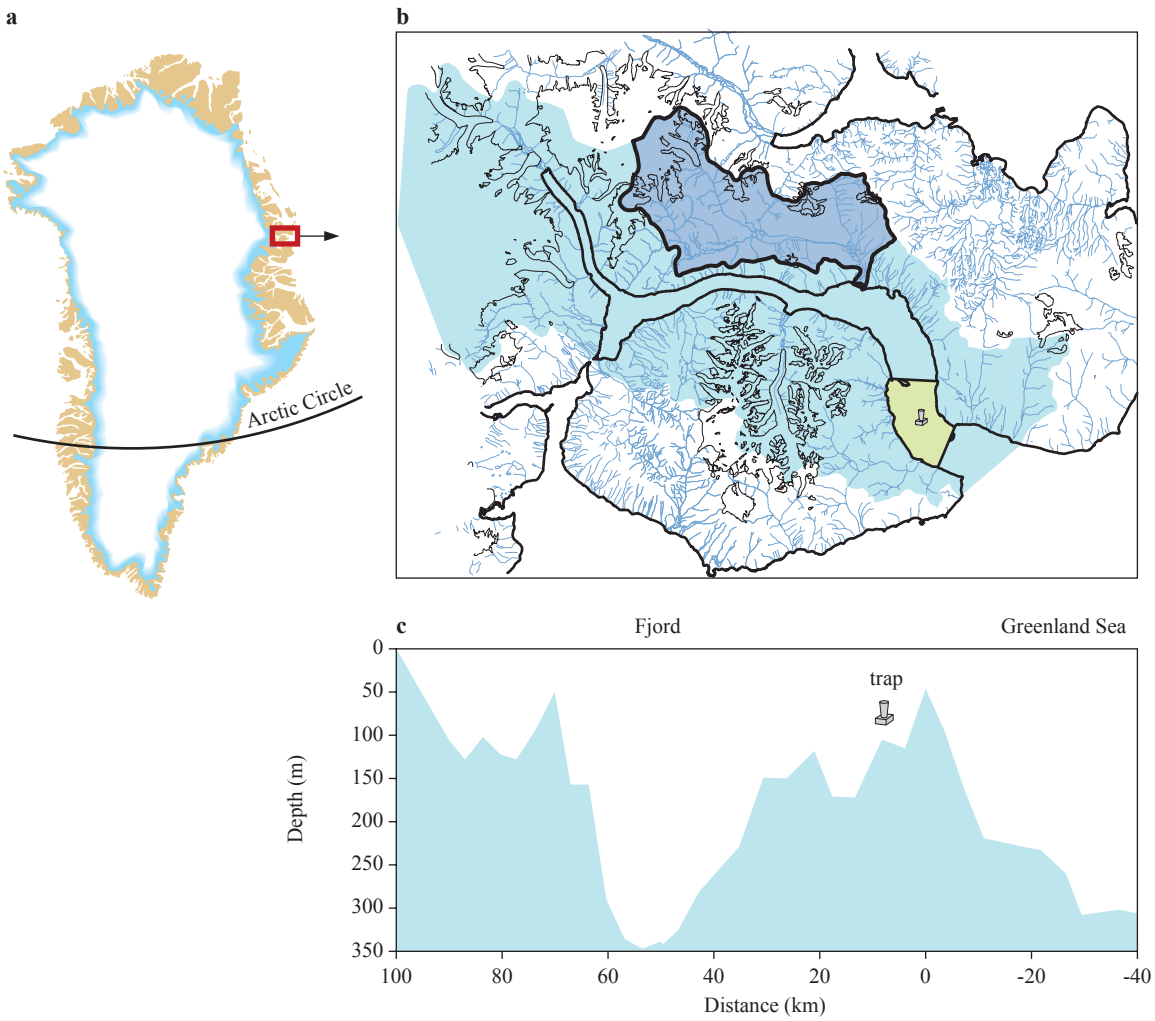

Figure 6.1 (a) The study site is located 1000 kilometers north of the Arctic Circle. **(b)** Catchment area of the Young Sound/Tyrolerfjord system (shaded area) showing the drainage basin of the Zackenberg River (blue area) and the study area "Region 1" (light green area) with the position of the sediment trap. **(c)** Length section of the fjord showing the site of the moored sediment trap.

2001). Sea ice covers the fjord for 9–10 months of the year. During summer, a surface layer (0–10 m) of low salinity (<30) and with a temperature of 2–4°C is present due to melting sea ice and freshwater input from land. Below this layer, salinity increases to >33 with sub-zero temperatures forming a stable halocline at 15–20 m (Rysgaard et al., 1999, 2003; Chapter 3). The thick sea-ice and snow cover regulates activity in the light-limited Young Sound ecosystem. Primary production of sea ice algae in Young Sound is low due to the poor light conditions below the snow cover and because river discharge removes and/or inhibits algae at the sea ice/water interface through physical disturbance and exposure to freshwater (Rysgaard et al., 2001; Chapter 4). After the break-up of sea ice, however, phytoplankton bloom in the surface water and rapidly deplete nutrients above the well-established halocline, causing maximum photosynthesis to occur in a subsurface layer at 15–20 m depth (Rysgaard et al., 1999). Phytoplankton primary production is tightly coupled to the grazer community in Young Sound and it has been estimated earlier that copepods account for >80% of the grazing pressure upon phytoplankton during the short productive ice-free period (Rysgaard et al., 1999; Chapter 5). When sea ice breaks up, benthic mineralization is immediately stimulated (Rysgaard et al., 1998; Berg et al., 2003; Chapter 8), presumably due to a peak in vertical export from the water column.

6.2.2 Sediment trap measurements

In September 2002, a mooring equipped with a time-series Kiel sediment trap (opening 0.5 m^2, K/MT 320, K.U.M, Kiel GmbH, Germany) was deployed in the outer region of Young Sound (74°18.93'N, 20°16.70'W) (Fig. 6.1). The trap was positioned at c. 65 m water depth to collect material vertically exported from the productive photic zone of the upper c. 40 m. To prevent icebergs from removing or destroying the trap the upper buoyancy was positioned at c. 40 m water depth. A sill 45 m deep at the entrance to the fjord prevents larger icebergs from entering the fjord and no icebergs are released from the inner parts of Young Sound. Water depth at the position was c. 100 m. Sedimenting particles were collected from 15 September 2002 to 20 September 2003 at 20 individually programmed time intervals.

Prior to launching, the collector cups of the sediment trap were filled with GF/F-filtered bottom water and poisoned with $HgCl_2$ (1 ml saturated solution per 100 ml water). NaCl was also added to the cup solution to increase salinity to c. 40. The mooring was acoustically released from its position after 1 year of sampling. After recovery, another 0.5 ml of the $HgCl_2$ solution was added to each 100-ml cup and samples were stored at 4°C. In the laboratory, zooplankton "swimmers" were removed from all samples prior to further treatment. Samples were then freeze-dried and weighed to determine total fluxes (dry weight, dw), and homogenized sub-samples of known weight were taken for analyses of particulate organic carbon (POC), particulate organic nitrogen (PON), chlorophyll (Chl) and calcium carbonate ($CaCO_3$). Total carbon contents (TC) were determined on an elemental analyzer (Europa Scientific RoboPrep). The POC and PON contents were obtained by analyses of decalcified samples. Decalcification was achieved by H_2SO_3 treatment and heating to 80°C. The $CaCO_3$ content was calculated as TC - POC. Stable isotopic composition of the decalcified samples was analyzed on an elemental analyzer in line with a mass spectrometer (Triple Collector Europa Scientific 20-20 IRMS). Isotope measurements are presented using the conventional $\delta^{13}C$ notation relative to PDB, and the $\delta^{15}N$ notation relative to air. The chlorophyll content (total pigments) of the cup material was analyzed by spectrophotometry on acetone extractions of freeze-dried samples (Dalsgaard et al., 2000).

Launching sediment trap mooring in Young Sound.

Photo: Søren Rysgaard

6.2.3 Sediment analysis

The upper 0–5 cm of sediment cores collected at 60 m water depth was freeze-dried, treated with H_2SO_3 and heated to 80°C to remove $CaCO_3$, homogenized and weighed into sample boats. The total carbon content and the stable isotopic signal of $\delta^{13}C$ were analyzed as described above. Data on carbon burial in the sediment was taken from earlier measurements reported in Chapter 8.

6.2.4 Sea ice measurements

The Danish Military Patrol Sirius collected data on sea ice thickness during 2002–03, using an ice-drill and a measuring stick at a position (74°18.59'N, 20°15.04 W) close to the sediment trap. These data are part of the long-term monitoring program at Zackenberg (Rysgaard et al., 2005; Chapter 4).

6.2.5 River discharge measurements

The drainage basin for the largest river in the area, Zackenberg River, covers an area of 514 km^2 (Fig. 6.1; Chapter 2). A hydrometric station at the outer part of the river recorded the water level every 15 minutes via sonic range and pressure sensors. The measured water level was converted to meters above sea level, which in turn was converted to discharge,

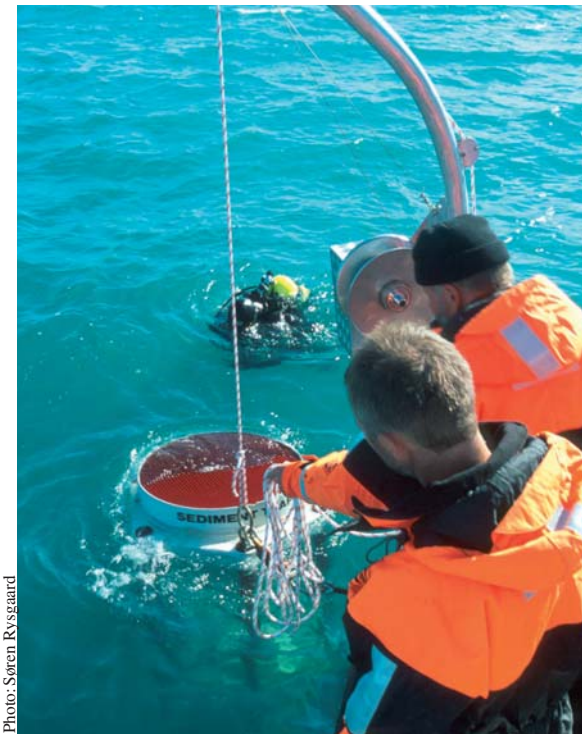

Photo: Søren Rysgaard

Retrieving sediment trap mooring 1 year after launching.

using an established relationship between water level and discharge. Water samples were collected daily from the river during May–September 2003 using a depth-integrated sampler. The collected water (0.8 l) was filtered (combusted GF/C) and filters frozen and decalcified before analyzing for POC and PON as described above. The DOC concentration in the filtered water samples was analyzed with a Shimadzu TOC-5000A Analyzer. These data are part of the long-term monitoring program Zackenberg Basic (www.Zackenberg.dk).

6.2.6 Horizontal carbon transport

During 2000–2001, a net carbon budget for the outer fjord area (Region 1) was established based on total organic carbon (TOC) measurements in the water column and a volume-mass model (Rysgaard et al., 2003). In short, the carbon export towards the sea was estimated along two separate transects enclosing Region 1 (76 km^2) during the ice-free period. During the investigation period, the TOC concentration in the water column ranged from 60 to 110 µM. Elevated concentrations were found in the upper 10–25 m in association with the pycnocline in the period 2–12 August. A total net retention of 28 t C d^{-1} (range 15–50 t C d^{-1}) in Region 1 during the ice-free period was reported.

6.3 Results & discussion

6.3.1 Seasonal variation in sea ice cover and river discharge

Normally, sea ice forms in late September or early October and stays until the following summer thaw (Rysgaard et al., 2005; Chapter 4). However, in 2002, sea ice suddenly broke on 25 December and was exported to the Greenland Sea due to high wind speeds from the north and lack of sea ice outside the fjord. New ice reached a maximum thickness of 120 cm with a 40-cm snow cover on top in April–May 2003. Sea ice broke on 3 July 2003 in outer Young Sound, 3 weeks earlier than normal (Fig. 6.2a).

Break-up of the Zackenberg River occurred on 30 May 2003, resulting in a steep increase in freshwater discharge to 78 m^3 s^{-1} at the end of June, after which it gradually decreased and ceased in September (Fig. 6.2a). This is in agreement with earlier observations that the annual runoff generally peaks in the beginning of June to July, mainly due to melting snow from the catchment area (Chapter 2).

6.3.2 Flux of particulate matter

A steep increase in the vertical flux of material was observed in association with the break-up of sea ice and peak in freshwater discharge from the River Zackenberg (Fig. 6.2). Within two months (July and August), more than 90% of the total annual vertical flux occurred. Our data support previous reports of a strong seasonal variation in the vertical flux of particulate material in Arctic waters, with low flux rates under sea ice cover and elevated export rates during sea-ice break-up and during open-water conditions. In the Northeast Water Polynya and in Baffin Bay, 40–70% of the annual vertical particle flux was observed from June–October (Bauerfeind et al., 1997; Hargrave et al., 2002), and in Frobisher Bay, Arctic Canada, 45% of the annual POC flux occurred during July–August (Atkinson & Wacasey, 1987). During spring, a pronounced signal in the vertical flux has sometime been observed in seasonally ice-covered seas due to ice-edge production (Hebbeln & Wefer, 1991; Wassmann et al., 1991) or ice-algal material released from sea ice (Fortier et al., 2002; Bauerfeind et al., 2005). In Young Sound, however, sea-ice-algal primary production and biomass were very low due to thick snow cover (40 cm) in 2002–03 (Chapter 4; Rysgaard et al., 2005). Furthermore, previous stud-

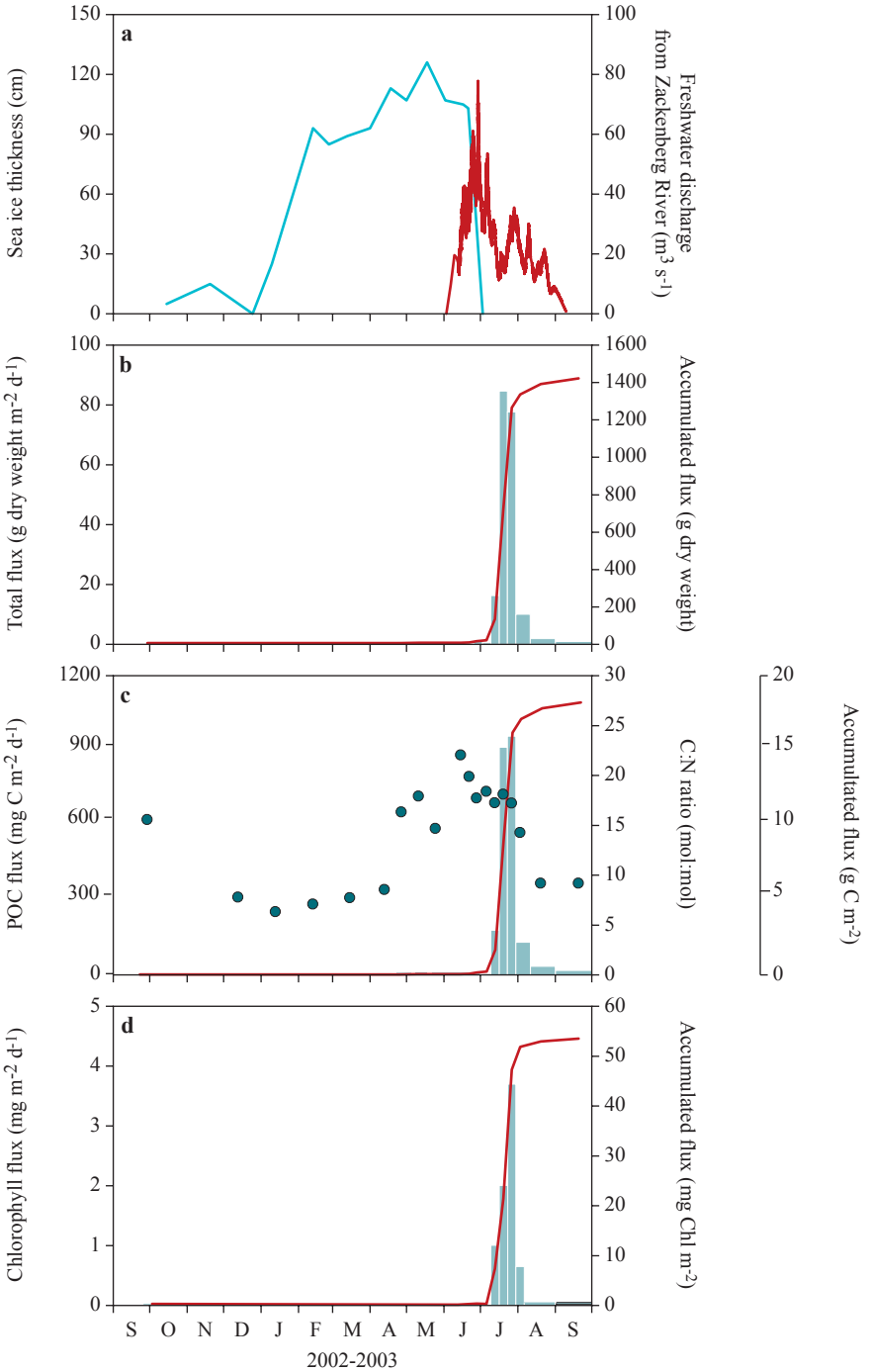

Figure 6.2 **(a)** Sea ice thickness (blue line) and freshwater discharge (red line) at the investigation site. **(b)** Vertical flux rate of particulate matter (bars) and accumulated flux (red line). **(c)** Vertical flux of particulate organic carbon (bars), accumulated flux (red line) and C:N ratio in organic matter (dots). **(d)** Vertical flux of chlorophyll (bars) and accumulated flux (red line).

ies have suggested that sea-ice-algal biomass is very low in the fjord due to extreme dynamics in sea-ice appearance, structure and brine percolation, which is driven primarily by the large but variable freshwater input during snow melt and breaking of frozen rivers, transforming the sea ice matrix into a hostile environment for sea ice algae, despite good light and nutrient availability (Rysgaard et al., 2001; Chapter 4). Thus, the very large vertical POC flux following sea ice break-up made the winter and spring vertical POC fluxes insignificant, although detectable (0.07–0.2 mg C m^{-2} d^{-1}) (Fig. 6.2).

In Young Sound, the annual vertical flux rate at 65 m water depth was 1420 g dry weight material m^{-2} and 17 g POC m^{-2} (Fig. 6.2bc). This is lower than rates from Frobisher Bay (33 m) but higher than rates

further offshore from East Greenland (245 m), from the Northeast Water Polynya (150–350 m), Baffin Bay (>200 m) and several offshore localities (>500 m) in the Greenland Sea, the Fram Strait, the Barents Sea and the Norwegian Sea (Honjo et al., 1988; Hebbeln & Wefer 1991; Hebbeln, 2000; Wassmann et al., 1991; Bauerfeind et al., 1997; Hargrave et al., 2002; Bauerfeind et al., 2005). On an annual basis, the vertical flux of POC in the sediment trap material, in Young Sound corresponded to 1.2% of the total dry weight flux. This agrees well with the measured organic carbon content in the sediments at 36–163 m water depth in the same area, which ranged from 1.1 to 1.4% (Glud et al., 2000). Furthermore, the vertical flux of calcium carbonate accounted for less than 1% of the flux of dry weight material, which supports earlier measurements of low calcium carbonate contents in the sediment of the outer part of the fjord (Chapter 8). However, it differs strongly from observations further offshore from East Greenland that c. 30% of the annual particle flux could be ascribed to calcium carbonate (Bauerfeind et al., 2005).

The C:N ratio in the organic sediment trap material ranged from 7 during winter, when sea ice cover was present and very low vertical flux rates occurred, to 15–22 during May–July (Fig. 6.2c). C:N ratios in organic material close to the Redfield ratio of 7 (by atoms) is normally interpreted as sedimentation of marine phytoplankton. The vertical flux of chlorophyll peaked when sea ice broke up and was highly correlated (r^2 = 0.9, P<<0.001) with the vertical flux of POC (Fig. 6.2cd). Pennate diatoms (Naviculales, Achnanthales, Lyrellales and Bacillariales) dominated the phytoplankton in the sediment trap material but dinoflagellates (*Protoperidinium* spp., *Ceratium* spp., *Prorocentrum* spp. and *Dinophysis* spp.) were also present. Both diatoms and dinoflagellates were present in the trap material throughout the year, although low cell numbers were encountered during winter (data not shown).

6.3.3. Marine and terrestrial sources

The high C:N ratio in the sediment trap organic material of up to 22 during the summer thaw, as compared with 7–9 during winter and spring, when no discharge from land occurred, suggests that carbon sources other than marine phytoplankton are important in the outer fjord area (Fig. 6.2c). As POC:Chl ratios <100 are characteristic of seston enriched with phytoplankton, the ratio of 320 observed in the present study (calculation based on annual dataset) further indicates that carbon sources other than phytoplankton cells contribute to the vertical export in the fjord. Seasonal measurements of the POC and DOC discharge from the Zackenberg River show that large quantities of terrestrial carbon are being transported into the fjord (Fig. 6.3). Within the 3 months of June–August, 416 tons of POC and 421 tons of DOC enter the fjord from the Zackenberg River. Thus, the content of POC relative to POC+DOC in the Zackenberg River is quite high (50%) and compares with conditions in the Mackenzie River (Rachold et al., 2004). The C:N ratio in river-borne POC ranged from 10–40 with a mean value of 18 throughout the study period. The C:N ratio of DOM was not determined, but ratios of 50–60 found in other Arctic rivers (e.g. Köhler et al., 2003) suggest that the C:N ratio of river-borne total organic material (TOM) was higher than that of POM. The extent to which DOM precipitation contributed to sedimentation is not known.

Figure 6.3 (a) Particulate organic carbon (blue dotted) and dissolved organic carbon (red dotted) discharge from the Zackenberg River. Accumulated transport of POC (blue line) and of DOC (red line). **(b)** C:N ratio in river-borne particulate organic matter.

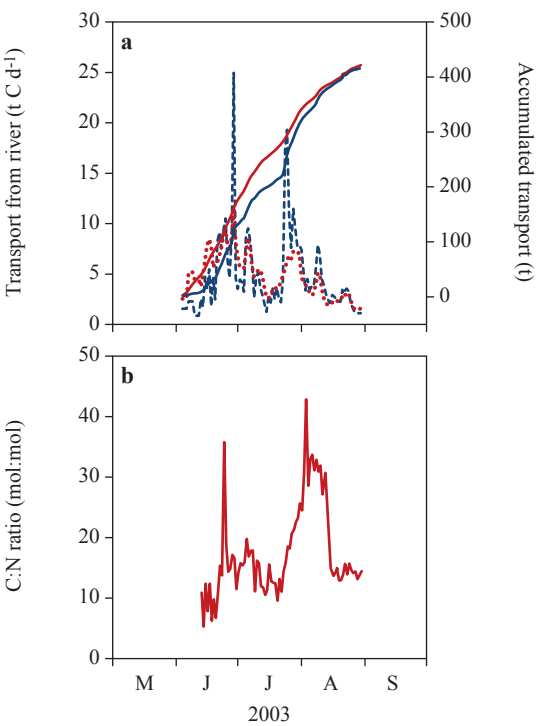

Table 6.1. Isotopic signals in organic matter from primary producers, sediment trap material, sediment and the Zackenberg River.

Sample	$\delta^{13}C$ (‰)	$\delta^{15}N$ (‰)	n
[a]Pelagic primary producers	-21.6 ± 0.8	5.4 ± 0.8	5
[b]POM from sediment trap (summer mean)	-23.6 ± 0.1	4.7 ± 0.2	7
[c]POM in the sediment at 60 m water depth	-23.1 ± 0.4	nd	20
[d]POM in the Zackenberg River	-25.6 ± 0.1	4.3 ± 0.3	23

[a]POM. (Hobson & Welch, 1992)
[b]Mean value of samples collected in trap through June–September.
[c]Mean value of upper 5 cm of the sediment at 60 m water depth.
[d]Mean value in suspended particulate matter of the Zackenberg River.

The high C:N ratios observed during May are presumably due to air-borne terrestrial material being incorporated into the sea ice and liberated to the water column as air temperatures increase during spring. Isotopic ($\delta^{13}C$ & $\delta^{15}N$) analysis of particulate organic matter (POM) showed that the composition of the sediment trap material was close to the average of the composition of phytoplankton and river material (Table 6.1). This indicates that c. 50% of the depositing POM originates from land (Table 6.1) and hence supports the high C:N ratios observed in the trap material during June–July 2003.

Previous mass and volume budgets of TOC covering the outer part of the fjord have revealed a net input of TOC of 28 t C d^{-1} to Region 1 (Fig. 6.1) from the adjacent Greenland Sea and surrounding land during the ice-free productive period (Rysgaard et al., 2003). During that study it was not possible to distinguish between marine and terrestrial carbon sources, but it appeared that the freshwater discharge from land was the primary factor determining the net TOC input through its influence on the estuarine circulation in the fjord. Thus, the net TOC input to Region 1 during the productive period is 2436 t C yr^{-1} (Table 6.2), given an annual freshwater discharge during the present investigation very similar to that in 2001 (Chapter 2; Rysgaard et al., 2003) and assuming that water-column TOC concentrations were similar in the two years. This corresponds to a net input of 32 g C m^{-2} yr^{-1} to Region 1 in the outer part of the fjord (Fig. 6.1; Table 6.2).

Assuming that the Zackenberg catchment area (512 km^2) is representative of the entire catchment area of 3109 km^2 of the Young Sound/Tyrolerfjord system, and that the discharge from the Zackenberg River can be linearly scaled to the entire catchment area, 2526 t POC yr^{-1} should enter the fjord from the terrestrial compartment (Table 6.2). Scaling this input to the outer Region 1 of the fjord, it corresponds to 6.5 g POC m^{-2} yr^{-1}, which is very similar to the carbon burial observed in the sediment in this region (see below). Besides POC, dissolved organic carbon is discharged in an equal amount to the fjord from rivers and results in a total organic carbon (TOC) input from land to the outer region of Young Sound of 20.5 g C m^{-2} yr^{-1}. This amount corresponds to c. 40% of the net TOC input from the Greenland Sea and land (Table 6.2), further supporting the conclusion that the terrestrial input to the outer part of Young Sound is significant.


Photo: Magnus Elander

Preserving samples from the sediment trap system.

6.3.4 Vertical flux, mineralization and burial

Depth distributions of ^{210}Pb, ^{137}Cs and TOC in sediments at 60 m water depth close to the sediment trap reveal that 7.9 g C m^{-2} yr^{-1} is buried within the sediment (Table 6.3; Chapter 8). This rate is in the same range as the estimated terrestrial POC transport to the outer fjord. Furthermore, the $\delta^{13}C$ values within the sediment suggest that a substantial amount (c. 40%) of the POC in the sediment is of terrestrial origin (Table 6.1).

Previous studies have reported an annual release of dissolved inorganic carbon (DIC) due to miner-

Table 6.2 The annual net input of carbon to the outer region of the fjord and the annual carbon flux from land.

Sources	C flux (t C yr^{-1})	[d]C input from entire catchment area (t C yr^{-1})	[e]C input to Region 1 (g C m^{-2} yr^{-1})
[a]Net TOC input to Region 1	2436 (1300 – 4400)		32 (17 – 58)
[b]POC from the Zackenberg River	416	2526	6.5
[b]DOC from the Zackenberg River	421	2556	6.6
[c]TOC from the Zackenberg River	837	5082	13

[a]Net input to Region 1 (76 km^2) from land and the Greenland Sea.
[b]POC input from the Zackenberg River to Young Sound (the Zackenberg River catchment area is 512 km^2).
[c]POC + DOC in the Zackenberg River.
[d]Carbon input from the Zackenberg River catchment area scaled to entire catchment area (3109 km^2) of Young Sound (389 km^2) (Fig. 6.1).
[e]Carbon input scaled to Region 1 during 2002–2003.
The numbers in brackets represent the maximum range of uncertainty.

alization in the sediment of 12.6 g C m^{-2} yr^{-1} at 60 m water depth in the outer region of the fjord (Glud et al., 2000; Chapter 8). The sum of the annual DIC release and the sediment burial represent an expected total input to the sediment of 20.5 g C m^{-2} yr^{-1}, which compares reasonably well with the vertical flux measurement from the sediment trap of 17 g C m^{-2} yr^{-1} obtained in present study.

Table 6.3 Annual carbon fluxes in the water column and sediment.

	g C m^{-2} yr^{-1}
[a]Vertical POC flux	17.0
[b]DIC release from sediment (60 m)	12.6
[b]Carbon burial in sediment (60 m)	7.9
[c]Total (60 m)	20.5

[a)] This study
[b)] Glud et al. (2002) and Chapter 8).
[c)] Sum of sediment DIC release and burial

6.4 Acknowledgements

This work was financially supported by DANCEA (the Danish Cooperation for the Environment in the Arctic) under the Danish Ministry of the Environment. This work is a contribution to the Zackenberg Basic and Nuuk Basic programs in Greenland. Aage V Jensen Charity Foundation is thanked for providing financial support for research facilities in Young Sound.

Anna Haxen helped with linguistic corrections and three reviewers made valuable comments that improved the manuscript.

6.5 References

Atkinson, E. R. & Wacasey, J. W. 1987. Sedimentation in Arctic Canada: particulateorganic carbon flux to a shallow marine benthic community in Frobisher Bay. Polar Biol. 8: 3-7.

Bauerfeind, E., Garrity, C., Krumbholz, M., Ramseir, R. O. & Voss, M. 1997. Seasonal variability of sediment trap collections in the Northeast Water Polynya. Part 2. Biochemical and microscopic composition of sedimenting matter. J. Mar. Sys. 10: 371-389.

Bauerfeind, E., Leipe, T. & Ramseier, R. O. 2005. Sedimentation at permanently ice-covered Greenland continental shelf (74°57.7´/12°58.7´W): significance of biogenic and lithogenic particles in particulate matter flux. J. Mar. Sys. 56: 151-166.

Benner, R., Benitez-Nelson, B., Kaiser, K. & Aman, R. M. W. 2004. Export of young terrigenous dissolved organic carbon from rivers to the Arctic Ocean. Geophys. Res. Lett. 31: Art. No. L05305 Mar 10 2004.

Berg, P., Rysgaard, S. & Thamdrup, B. 2003. General dynamic modeling of early diagenesis and nutrient cycling; Applied to an Arctic marine sediment. J. Am. Science 303: 905-955.

Cappelen, J., Jørgensen, B. V., Laursen, E. V., Stannius, L. S., & Thomsen, R. S. 2001. The Observed Climate of Greenland, 1958–99 – with Climatological Standard Normals, 1961–90. Danish Meterological Institute, Copenhagen, Technical Report 00–18.

Dalsgaard T., Nielsen L. P., Brotas V., Viaroli P., Underwood G., Nedwell D., Sundbäck K., Rysgaard S., Miles A., Bartoli M., Dong L., Thornton D. O. C., Ottosen L. D. M. , Castaldelli G. & Risgaard-Petersen N. 2000. Protocol handbook for NICE –Nitrogen cycling in estuaries: a project under the EU research programme: Marine Science and Technology (MAST III). National Environmental Research Institute, Denmark, 62 pp.

Fortier, M., Fortier, L., Michel, C. & Legendre, L. 2002. Climatic and biological forcing of the vertical flux of biogenic particles under seasonal Arctic sea ice. Mar. Ecol. Prog. Ser. 225: 1-16.

Glud, R. N., Risgaard-Petersen, N., Thamdrup, B., Fossing, H. & Rysgaard, S. 2000. Benthic carbon mineralization in a high-Arctic sound (Young Sound, NE Greenland). Mar. Ecol. Prog. Ser. 206: 59-71.

Hargrave, B. T., Walsh, I. D. & Murray, D. W. 2002. Seasonal and spatial patterns in mass and organic matter sedimentation in the North Water. Deep-Sea Res. PII: 5227-5244.

Hasholt, B. & Hagedorn, B. 2000. Hydrology and geochemistry of river-borne material in a high Arctic drainage system, Zackenberg, Northeast Greenland. Arct. Antarct. Alp. Res. 32: 84-94.

Hebbeln, D. 2000. Flux of ice-rafter detritus from sea ice in the Fram Strait. Deep-Sea Res. PII, 47: 1773-1790.

Hebbeln, D. & Wefer, G. 1991. Effects of ice coverage and ice-rafteed material on sedimentation in the Fram Strait. Nature 350: 409-411.

Hobson, K. A. & Welch, H. E. 1992. Determination of trophic relationships within a high Arctic marine food web using $\delta^{13}C$ and $\delta^{15}N$ analysis. Mar. Ecol. Prog. Ser. 84: 9-18.

Honjo, S., Manganini, S. J. & Wefer, G. 1988. Annual particle flux and winter outburst of sedimentation in the northern Norwegian Sea. Deep-Sea Res. PII, 35: 1223-1234.

Horner, R. & Schrader, G. C. 1982. Relativ contributions of ice algae, phytoplankton, and benthic microalgae to primary production in nearshore regions of the Beaufort Sea. Arctic 35: 485-503.

Köhler, H., Meon, B., Gordeev, V. V., Spitzy, A. & Amon, R.M.W. 2003. Dissolved organic matter (DOM) in the estuaries of Ob and Yenisei and the adjacent Kara-Sea, Russia. – In: R. Stein, Fahl, K., Fütterer, D.K., Galimov, E.M., & Stepanets, O.V. (eds.). Siberian river run-off in the Kara Sea. Proc. Mar. Sci. 6**:** 281–308.

Madsen, S. D., Nielsen, T. G. & Hansen, B. W. 2001. Annual population development and production by *Calanus finmarchicus*, *C. glacialis* and *C. hyperboreus* in Disko Bay, western Greenland. Mar. Biol. 139: 75-93.

Ploug, H. & Grossart, H.-P. 2000. Bacterial growth and grazing on diatom aggregates: Respiratory carbon turnover as a function of aggregate size and sinking velocity. Limnol. Oceanogr. 45: 1467-1475.

Rachold, V., Eicken, H., Gordeev, V. V., Grigoriev, M. N., Hubberten, H.–W., Lisitzin, A. P., Shevchenko, V. P. & Schirrmeister, L. 2004. Modern terrigenous organic carbon input to the Arctic Ocean. – In: Stein, R. & Macdonnald, R. W. (eds.). The organic carbon cycle in the Arctic Ocean. Springer-Verlag Berlin Heidelberg, 33-55 pp.

Rasch, M., Elberling, B., Jakobsen, B. H. & Hasholt, B. 2000. High-resolution measurements of water discharge, sediment, and solute transport in the river Zackenbergelven, Northeast Greenland. Arct. Antarct. & Alp. Res. 32: 336-345.

Rysgaard S., Thamdrup B., Risgaard-Petersen N., Berg P., Fossing H., Christensen P. B. & Dalsgaard T. 1998. Seasonal carbon and nitrogen mineralization in the sediment of Young Sound, Northeast Greenland. Mar. Ecol. Prog. Ser. 175: 261-276.

Rysgaard, S., Frandsen, E., Sejr, M. K., Dalsgaard, T., Blicker, M. E. & Christensen, P. B. 2005. Zackenberg Basic: The marine monitoring programme. In: Rasch, M. & Caning, K (eds.). Zackenberg ecological research operations 10th annual report, 2004. Danish Polar Center, Ministry of Science, Technology and Innovation, Copenhagen, 85 pp.

Rysgaard, S., Kühl, M., Glud, R. N. & Hansen, J. W. 2001. Biomass, production, and horizontal patchiness of sea ice algae in a high-Arctic fjord (Young Sound, NE-Greenland). Mar. Ecol. Prog. Ser. 223: 15-26.

Rysgaard, S., Nielsen, T. G. & Hansen, B. 1999. Seasonal variation in nutrients, pelagic primary production and grazing in a high-Arctic coastal marine ecosystem, Young Sound, Northeast Greenland. Mar. Ecol. Prog. Ser. 179: 13-25.

Rysgaard, S., Vang, T., Stjernholm, M., Rasmussen, B., Windelin, A. & Kiilsholm, S. 2003. Physical conditions, carbon transport and climate change impacts in a NE Greenland fjord. Arct. Antarct. Alp. Res. 35: 301-312.

Sampei, M., Sasaki, H., Hattori, H., Kudoh, S., Kashino, Y. & Fukuchi, M. 2002. Seasonal and spatial variability in the flux of biogenic particles in the North Water, 1997-1998. Deep-Sea Res. PII 49: 5245-5257.

Shiklomanov, I. A. 1998. Comprehensive assessment of the freshwater resources of the World: Assessment of eater resources and water availability in the World. WMO,UNDP, UNED, FAO et al., WMO, Geneva, 88 pp.

Urban-Rich, J. 1999. Release of dissolved organic carbon from copepod fecal pellets in the Greenland Sea. J. Exp. Mar. Biol. 232: 107-124.

Wassmann, P., Peinert, R. & Smetacek, V. 1991. Patterns of production and sedimentation in the boreal and polar Northeast Atlantic. Polar Res. 10: 209-228.

Photo: Göran Ehlmé

7

Growth, production and carbon demand of macrofauna in Young Sound, with special emphasis on the bivalves *Hiatella arctica* and *Mya truncata*

Growth, production and carbon demand of macrofauna in Young Sound, with special emphasis on the bivalves *Hiatella arctica* and *Mya truncata*

Mikael K. Sejr[1] and Peter B. Christensen[1]

[1]National Environmental Research Institute, Dept. of Marine Ecology, Vejlsøvej 25, DK-8600 Silkeborg, Denmark

Cite as: Sejr, M. K. & Christensen, P. B. 2007: Growth, production and carbon demand of macrofauna in Young Sound, with special emphasis on the bivalves *Hiatella arctica* and *Mya truncata*. In: Rysgaard, S. & Glud, R. N. (Eds.), Carbon cycling in Arctic marine ecosystems: Case study Young Sound. Meddr. Grønland, Bioscience 58: 122-135.

Abstract

Composition, abundance and biomass of macrobenthos in the outer part of a NE Greenland fjord, Young Sound (74°18'N, 20°18'W) were examined by grab sampling and photography along six transects, each with a depth range of 10 to 60 m. We found a species-rich fauna, dominated by brittle stars and bivalves. Annual growth and production of two bivalve species, *Mya truncata* and *Hiatella arctica*, were estimated by analysis of shell increments. Both species exhibited growth patterns typical of the Arctic, i.e. long life span and low annual growth. To investigate the exceptionally slow growth of *H. arctica*, laboratory experiments were conducted. Food availability was identified as the primary constraint on annual growth, whereas low temperature caused lower energy requirements and hence prolonged the growth season for bivalves. The strong influence of food limitation was also demonstrated in a study of the year-to-year variation in growth of *M. truncata*. A relative growth index was constructed for the period 1962–2000 based on measurements of individual increments. The index demonstrated a significant influence of ice cover on growth of bivalves, suggesting that the length of the ice-free season, which determines phytoplankton production, affects the growth pattern. Carbon demands of dominant species were estimated by three empirical models available in the literature and used to evaluate the role of the benthos in carbon cycling. Modelled carbon demands for *M. truncata* and *H. arctica* were well above those derived from actual production estimates from Young Sound. A conservative approach was adopted based on minimum estimates yielding an average of 15 mg C m^{-2} d^{-1} for the macrobenthos. Taking into account the different approaches used, the carbon demand of macrobenthos in Young Sound is among the highest reported from the Arctic.

7.1 Introduction

Benthic macrofauna species are an important component of coastal ecosystems. They consume a significant fraction of the available production and are in turn an important source of food for fish, seabirds and mammals. This is also the case in the Arctic, were approximately 20% of the world's shelf areas are located (Menard & Smith, 1966) and where a high standing stock of benthic macrofauna is found in spite of a low and highly seasonal input of food. This is possible because large areas of the Arctic consist of relatively shallow shelf areas with a tight benthic-pelagic coupling. Also, the low temperature reduces the energy requirements of the benthos, allowing a relatively large biomass to be supported by a low

primary production. Finally, in areas with a stable physical environment, the long life span of benthic species will allow a large biomass to accumulate over decades in spite of low annual production. Brittle stars have been found to be the most characteristic group of the Arctic shelf. Abundances of 100–200 individuals m^{-2} have been reported from the Barents Sea, the Laptev Sea, the Greenland Sea (Piepenburg, 2000) and the Chuckchi Sea (Ambrose et al., 2001) with single observations of up to 500 ind. m^{-2}. The biomass of brittle stars is typically in the range 400–600 mg C m^{-2} (Piepenburg, 2000). Food availability is one of the major driving forces influencing the biomass and composition of benthic assemblages in the Arctic. Hence, maximum biomass is found in the highly productive Chuckchi Sea with biomass values of up to 60 g C m^{-2} (Grebmeier et al., 1988). In East Greenland fjords, Thorson (1933, 1934) reported benthic biomass in the range 200–500 g wet weight m^{-2} (approximately 15–40 g C m^{-2} converted).

Compared with plankton, which show high spatial and temporal variability in biomass, the macrobenthos are a predictable food source for higher trophic levels such as grey whale (Highsmith & Coyle, 1990), walrus (Born et al., 2003), bearded seal (Hobson et al., 2002) and eider (Richman & Lovvorn, 2003). Despite their obvious importance for the marine food web, very little is known about the life history traits of benthic populations; growth rates, mortality, reproductive strategies etc. Such information is critical since estimates of consumption and production of populations are significant for the description of the trophic flow through an ecosystem (Brey, 1999). Studies of populations are also important when it comes to quantifying biological consequences of the predicted changes in the Arctic climate in the near future.

Extensive fjord systems are a characteristic feature of the East Greenland coast, but compared with the East Greenland shelf these areas have received relatively little attention. In this chapter we try to evaluate the role of the macrobenthos in the carbon flow in Young Sound. We do this based on information on the composition and abundance of the benthic community combined with data on growth and production of two dominant bivalves (*Hiatella arctica* and *Mya truncata*). In addition, we estimate production and carbon demand of dominant species by applying empirical models available in the literature.

7.2 Methods

7.2.1 Study area

This study was conducted in the outer part of Young Sound, NE Greenland (74°18'N, 20°18'W) between 1999 and 2003. The fjord is approximately 90 km long and 2–7 km wide. The maximum depth is c. 340 m and near the entrance is a sill at a depth of 40 to 50 m. The fjord is ice-covered 9 to 10 months of the year. The phytoplankton production is primarily confined to the ice-free period, when bloom conditions rapidly deplete nutrients above the halocline, causing production to sink to subsurface levels at about 20 m. (Rysgaard et al., 1999; Chapter 5). Above the halocline, the temperature can reach 5°C during summer, while it stays below -1°C below the halocline (Rysgaard et al., 2005). Details on sediment composition and carbon content can by found in Sejr et al. (2000) and in Chapter 8.

7.2.2 Composition, abundance and biomass of fauna

Identification and quantification of the entire macrobenthic fauna was performed at Transect 2 (Fig. 7.1). Ten van Veen grabs (0.04 m^2) were collected at each of the following depths: 20, 35, 60 and 85 m and sieved through a 0.5-mm screen (Sejr et al., 2000). Collected specimens were identified to species level if possible and counted. At the remaining transects photography was used to study the abundance of large dominant groups only, such as brittle stars, bivalves and sea urchins. Transects 1–6 were studied in August 1999 using a digital video camera covering 0.7 m^2. In 2003, Transects 1, 3 and 5 were studied again using a high-resolution digital still camera covering approximately 0.3 m^2 (Fig. 7.2). The image quality allowed positive identification of brittle stars with a disc diameter down to 2 mm. Abundances of dominant groups identified from photos were transformed into biomass by multiplying abundance values with mean individual biomass. Specimens used for assessing size distribution and individual biomass were collected from dredge hauls (brittle stars, sea urchins) or by suction sampling (*Mya truncata*) at 20 to 30 m along Transect 2. In addition to photography, the abundance and biomass (shell-free dry weight) of *Hiatella arctica* was estimated by van Veen grab sampling (0.04 m^2) at Transects 1–6 (Sejr et al., 2002a).

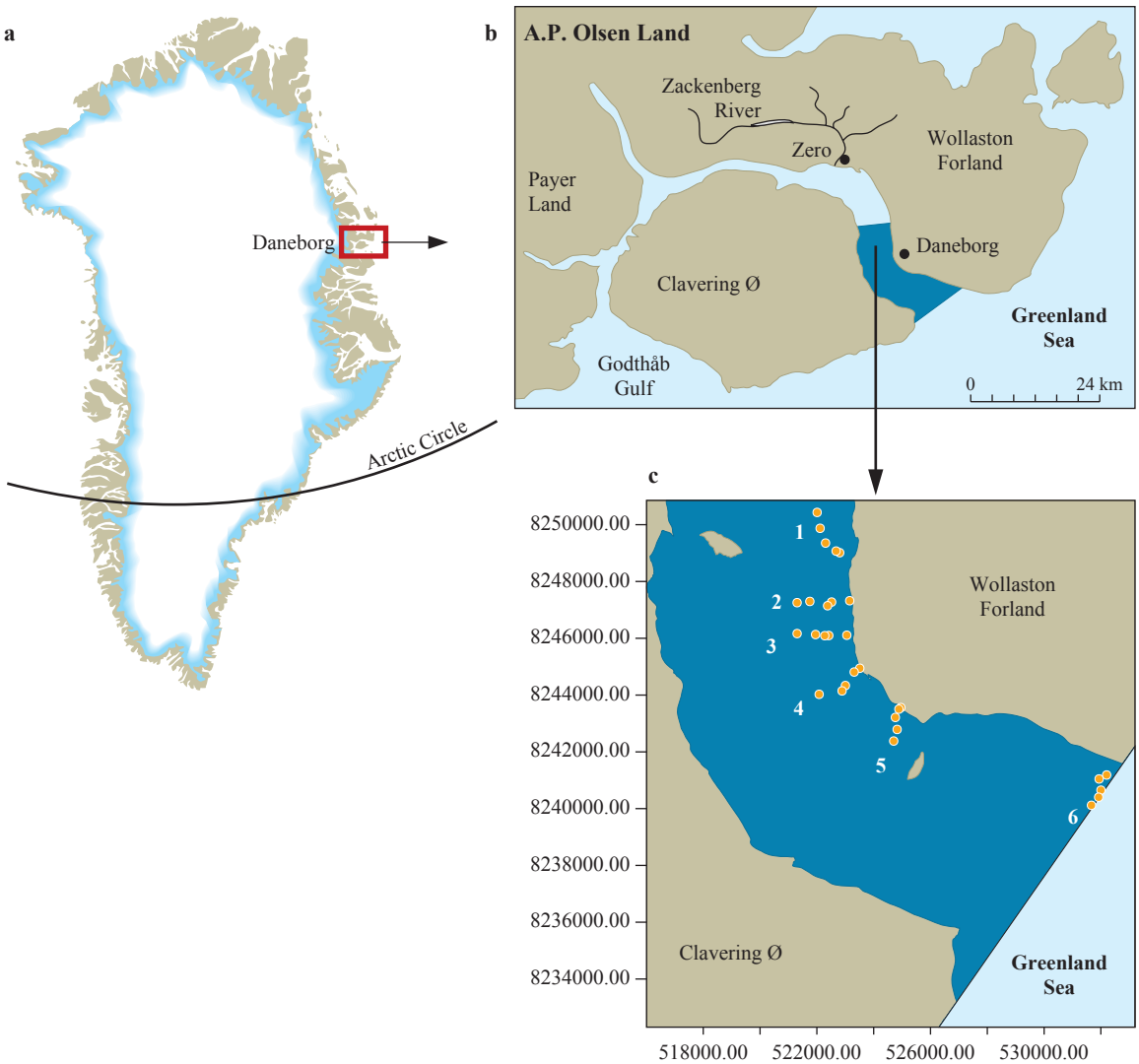

Fig. 7.1 Map of the area studied in Young Sound showing transects were benthos where sampled.

Fig. 7.2 Photo from Transect 2, 40 m from Young Sound, showing abundance of bivalves and brittle stars.

Photo: Peter B. Christensen & Mikael K. Sejr

7.2.3 Population dynamics of bivalves

Annual growth of *Hiatella arctica* and *Mya truncata* was studied by using growth increments in the shell (Fig. 7.3) to estimate individual age (see Sejr et al. (2002a) for details and references on the method). A mark-recapture study showed growth increments to be produced annually for *Hiatella arctica* (Sejr et al., 2002b) and this was assumed to be the case for *Mya truncata*. The number of increments could thus be used as a proxy for individual age. Annual increments have previously been shown for *Mya arenaria* (MacDonald & Thomas, 1980) and other polar bivalves (Brey & Meckensen, 1997) and seem to

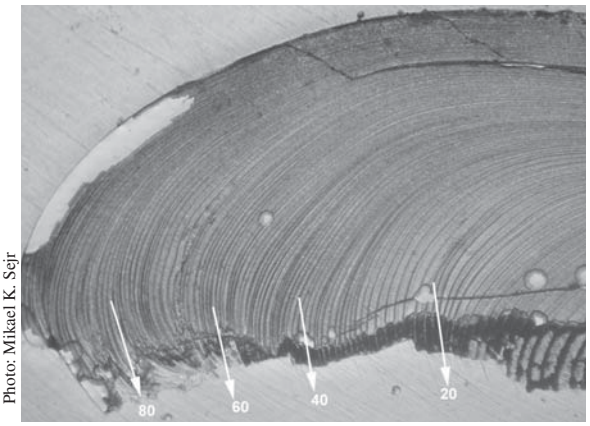

Photo: Mikael K. Sejr

Fig. 7.3 Cross-section of the umbo region of *Mya truncata* showing growth increments at c. 40 magnification.

be a general feature in polar areas with pronounced seasonality. The specialised Von Bertalanffy growth function was fitted to length-at-age data for both species. Individual production was then calculated using the weight-specific method (Brey, 2001). Mortality of each bivalve population was estimated from the size-converted catch curve using a single negative exponential model (Brey, 2001).

To study long-term changes in bivalve growth, the width of individual growth bands was measured in 28 *M. truncata* individuals. Actual growth (in µm) was log*e* transformed before the ontogenetic trend in growth was removed by applying a common smoothing spline. The residuals from the spline were then used as an estimate of relative growth for each individual.

7.2.4 Physiology of bivalves

To study the physiological effects of low temperature on bivalve filtration rate the response to changes in temperature was determined (Petersen et al., 2003). Filtration rate was determined using the clearance method (Riisgård, 2001) from the exponential reduction of added *Rhodomonas* sp. cells. Measurements were conducted on specimens of *Hiatella arctica* and *Mya truncata* from Young Sound and compared with values for *Hiatella* sp. collected in Sweden.

To further study the physiological basis for the observed growth pattern, rates of filtration, assimilation, respiration and ammonia excretion were measured in individuals of *H. arctica* from Young Sound kept at -1.5 C° and fed different concentrations of the algae *Rhodomonas* sp. (Sejr et al., 2004). From these measurements the amount of assimilated energy at different food levels could be calculated and converted into tissue growth by applying estimated growth efficiencies.

7.2.5 Carbon demand of benthos

Estimates of carbon demand of dominant groups were obtained by three different empirical models: 1. The model of Brey (1999), which predicts the production-to-biomass ratio (P/B) of benthic populations based on inputs of water depth, temperature, individual size, biomass and taxonomic and functional group. 2. The model of Tombiolo & Downing (1994), which estimates annual production based on inputs of temperature, maximum individual biomass, population biomass per m^2 and depth. 3. Individual respiration rates of brittle stars were estimated using the formula developed by Mahaut et al. (1995) and used to estimate respiration rate and carbon demand in Arctic brittle stars (Piepenburg, 2000). For models 1 and 2 estimates of production were converted into total carbon demand assuming an assimilation efficiency of 80% and a growth efficiency of 30% (Piepenburg, 2000). In addition, the carbon demands of *M. truncata* and *H. arctica* were estimated from production estimates in Young Sound, and the production of the sea urchin *Strongylocentrotus* sp. was calculated using the growth model for *Strongylocentrotus pallidus* from the northern Barents Sea (Bluhm et al., 1998).

7.3 Results & discussion

7.3.1 Benthic composition, abundance and biomass

In spite of the long seasonal ice cover and limited production, a relatively high macrobenthic biomass dominated by bivalves has built up in outer Young Sound. High sediment heterogeneity and little disturbance from ice and particles from land have allowed populations of slow-growing infaunal and epifaunal species to develop, resulting in a diverse community. On average, 47 (range 43–52) different species are found per 201 specimens in Young Sound (Table 7.1) compared with an average of 38 (range 33–43) from Svalbard and 33 and 35–44 from the Java Sea and the North Sea, respectively (Kendall, 1996). Polychaetes dominated the infauna, constituting up to 80% of the total abundance. The ten most abundant species in 56 grab samples (0.04 m^2) collected at 20 to

Table 7.1 Total infaunal abundance (individuals per m^2) in grab samples (0.04 m^2) at Transect 2 in outer Young Sound. Diversity is given by Shannons diversity index (H´). Number of species is per grab sample. ES_{201} gives the number of species per 201 individuals using Hurlberts rarefaction term. Median and 95% confidence limits (CL) are given for all except ES_{201}. Redrawn from Sejr et al. (2000).

Depth (m)	20	35	60	85
Abundance (ind. m^{-2})				
Median	2675	1125	1075	863
CL	1575–3625	650–1575	675–1850	775–1125
Diversity (H´)				
Median	2.8	2.6	2.8	2.6
CL	2.6–3.0	2.2–2.8	2.6–2.9	2.4–2.7
Number of species				
Median	26	17	19	17
CL	23–32	13–20	18–28	14–20
ES_{201}	47	48	49	43

Table 7.2 List of most abundant infaunal species found in 56 grab samples (0.04 m^2) at Transect 2. Total abundance in all samples and relative contribution are given. Redrawn from Sejr et al. (2000).

	Total (individuals)	Proportion (%)	Cumulative (%)
Cirratulus cirratus	398	13.5	13.5
Lumbriclymene minor	228	7.7	21.2
Maldane sarsi	161	5.5	26.7
Terebellides stroemi	145	4.9	31.6
Lumbrineris fragilis	145	4.9	36.5
Hamothoe spp.	126	4.8	41.3
Aricidae suecica	121	4.3	45.6
Polydora quadrilobata	118	4.0	49.6
Hiatella arctica	81	2.7	52.3
Astarte spp.	45	1.5	53.8

85 m depth at transect 2 are presented in Table 7.2. Some of the most abundant infaunal species include the polychaetes *Cirratulus cirratus*, *Maldane sarsi* and *Terebellides stroemi* and the bivalve *Astarte* spp. Deposit feeders constituted about 75% of all specimens in grab samples. Infaunal abundance decreased from a median of 2675 ind. m^{-2} at 20 m to 863 ind. m^{-2} at 85 m (Table 7.1) combined with a clear shift in faunal composition (Sejr et al., 2000), most likely due to depth-related changes in food supply and sediment characteristics. Both in terms of total abundance and dominant species, the fauna in Young Sound is very similar to that of other fjords in East Greenland (Thorson, 1933; Thorson, 1934), Svalbard (Holte & Gulliksen, 1998) and eastern Canada (Thomson et al., 1982). On the East Greenland shelf, mean abun-

Table 7.3 Depth-specific abundance (mean ± 95% CI) of selected benthos in Young Sound across 6 transects.

Depth (m)	*Mya truncata* (ind. m^{-2})	*Hiatella arctica* (ind. m^{-2})	*Strongylocentrotus* sp. (ind. m^{-2})	*Ophiuroidea* spp. (ind. m^{-2})	*Cucumaria* sp. (ind. m^{-2})
10	2.4 ± 1.5	2.7 ± 0.8	0.02 ± 0.05	4.9 ± 1.3	0
20	18.3 ± 3.3	33.7 ± 6.3	0.9 ± 0.5	36.2 ± 8.0	0
30	18.0 ± 3.3	59.3 ± 12.3	2.3 ± 0.8	120 ± 12.2	0.1 ± 0.2
40	15.5 ± 7.5	17.0 ± 6.1	0.6 ± 0.3	125 ± 19.5	0.9 ± 0.4
50	1.0 ± 0.8	8.1 ± 3.6	0.2 ± 0.2	144 ± 20.1	0.9 ± 0.5
60	0.1 ± 0.2	1.3 ± 0.8	0.1 ± 0.1	216 ± 17.6	1.2 ± 0.7

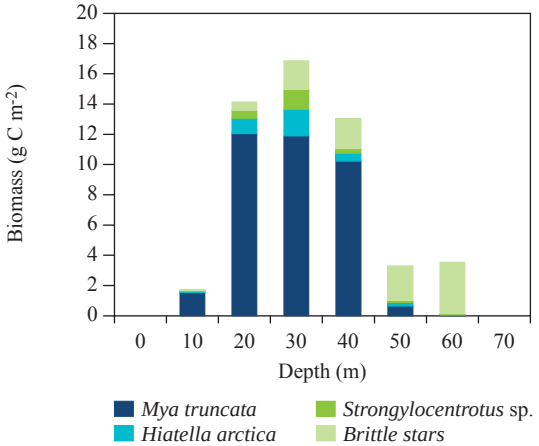

Fig. 7.4 Mean depth-specific biomass (g C m^{-2}) of abundant species of macrofauna in Young Sound.

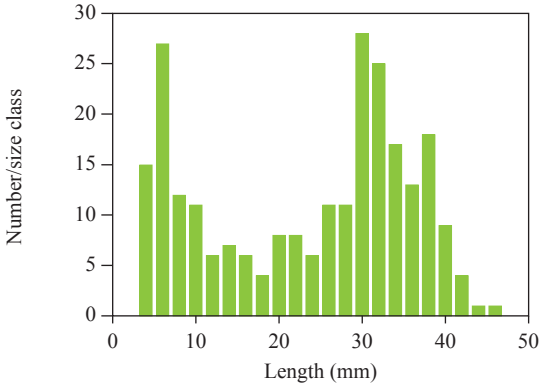

Fig. 7.5 Size distribution (shell length; mm) of the bivalve *Hiatella arctica* in Young Sound. N=244.

dances of 5000–9500 ind. m^{-2} have been reported in ice-free waters of the Northeast Water Polynya, whereas the abundance in nearby ice-covered areas dropped to 1200–3500 ind. m^{-2} (Ambrose & Renaud, 1995), which is comparable with the abundance in Young Sound. The high biomass of bivalves in outer Young Sound seems to be a characteristic feature of the fjords compared with the deeper shelf along the East Greenland coast.

The epifauna was dominated by brittle stars, with a maximum abundance of 216 ind. m^{-2} at 60 m (Table 7.3). The different species of brittle stars could not be distinguished with certainty in photos but three species were found in dredge samples from 50 m; *Ophiacantha bidentata*, *Ophiura robusta* and *Ophiocten sericeum*. Of the three species, *O. sericeum* was the most numerous, constituting 53% of the total abundance in dredges. Brittle stars are the most characteristic epibenthic animals of the Arctic seabed, and the species *O. sericeum* is abundant in shallow parts of the Greenland, Barents and Laptev Seas (Piepenburg, 2000). The mean abundance of 216 ind. m^{-2} with a biomass of 3.42 g C m^{-2} is among the highest reported in the Arctic. As in Young Sound, brittle stars typically exhibit a depth-related zonation in abundance, the maximum being found typically between 50 and 100 m (Piepenburg, 2000). Unfortunately, we were unable to estimate brittle star abundance at depths below 60 m in Young Sound, but a considerable biomass is most probably present in deeper parts of the fjord. In addition to brittle stars, echinoderms such as the sea urchin *Strongylocentrotus* sp., the feather star *Heliometra glacialis* and the sea cucumber *Cucumaria* sp. were abundant (Table 7.3).

In terms of biomass, bivalves are clearly dominant (Fig. 7.4). Abundant species in the Young Sound study area include *Mya truncata*, *Hiatella arctica*, *Astarte* spp. and *Macoma calcarea*, all of which are characteristic of shallow (<50 m) areas of fjords in East Greenland, Svalbard and NE Canada. The high biomass is attained through a combination of longevity and low mortality as shown for *Hiatella arctica*. Clear bimodal size distribution indicates dominance of small (<10 mm) and large (>30 mm) individuals (Fig. 7.5). The relatively narrow peak in bivalve abundance at 20 to 40 m observed in Young Sound is most likely a result of a combination of depth-related differences in mortality and food supply. The slow growth of *H. arctica* and *M. truncata* (see below) makes them vulnerable to disturbance from ice, which limits their biomass in the upper 0–10 m. At depths down to c. 35 m a combination of benthic diatoms and subsurface phytoplankton blooms ensures access to high-quality food, whereas at greater depths specimens have to rely on sedimenting carbon of lower quality. Decreasing food availability was also identified by Ockelmann (1958) as the primary reason for the decline in bivalve biomass with distance from the sea in several East Greenland fjords. That food availability should influence patterns of bivalve biomass within East Greenland fjords is in good agreement with observations of large-scale variations of total benthic biomass reflecting productivity of overlying water masses (Grebmeier et al., 1988).

7.3.2 Growth and production of the bivalves *Hiatella arctica* and *Mya truncata*

Age estimated from growth increments showed bivalves to be very long-lived (Fig. 7.6). The oldest specimen of *H. arctica* was 126 years old, whereas *M. truncata* reached ages of up to 50 years. Although specimens of *Arctica islandica* can live even longer (Ropes, 1985) it is a good example of the longevity often observed in polar benthos. From the size-converted catch curve the mortality can be estimated for the small and large size groups of *Hiatella arctica* (Fig. 7.7). Small individuals are subject to an annual mortality of Z = 0.58 which drops to Z = 0.15 for large individuals. Due to the extreme longevity of this species, the number of individuals surviving the first critical phase will accumulate over almost a century, causing high biomass and dominance of old individuals. The growth model fitted to age-at-length data shows a distinct difference between the two species; *M. truncata* continues to increase in shell length throughout its entire life span whereas *H. Arctica* stops increasing shell length after 40–45 years. Also, because of the difference in size, the individual annual production of *H. arctica* is much smaller than that of *M. truncata*; 0.03 g dw yr^{-1} for *H. arctica* compared with 0.28 g dw yr^{-1} for *M. truncata* (Fig. 7.8).

The extremely slow growth of *H. arctica* was studied in two sets of laboratory experiments. First, the influence of temperature on clearance rates was compared in two populations of *Hiatella*, one from Young Sound and one from Tjärnö, Sweden (Petersen et al., 2003). The Arctic population showed adaptation to low temperatures by being fully active even at a temperature of –1°C. The size-specific clearance rates were much lower than those of the Swedish population at 12°C. In a second study (Sejr et al., 2004), specimens of *H. arctica* from Young Sound were kept at –1.2°C and exposed to different food concentrations. By combining measurements of clearance rates with measurements of assimilation efficiency the amount of assimilated energy could be estimated at a maximum of 3 J h^{-1} or 12–25% of that of other species of similar size at higher temperature (Sejr et al., 2004). The low temperature in Young Sound thus clearly limits the growth potential of *H. arctica* by reducing clearance rates and, hence, the amount of energy available for growth. However, the low

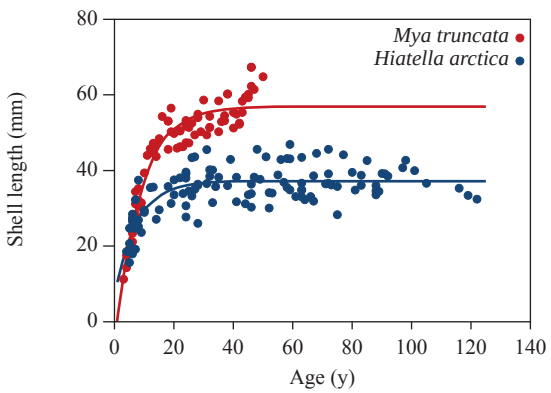

Fig. 7.6 Von Bertalanffy growth function fitted to length-at-age data for *Mya truncata* and *Hiatella arctica* from Young Sound. *H. arctica*: L_∞ = 37.2 mm, K = 0.14 yr^{-1}, t_0 = -1.4 yr, n = 117, r^2 = 0.56. *M. truncata*: L_∞ = 56.8 mm, K = 0.12 yr^{-1}, t_0 = 1.1 yr, n = 77, r^2 = 0.83.

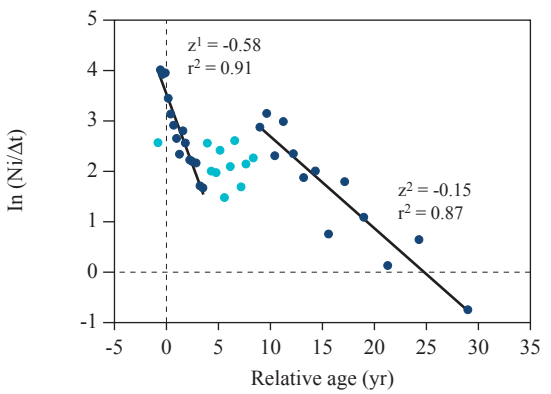

Fig. 7.7 Size-specific mortality of the bivalve *Hiatella arctica* in Young Sound obtained using a single negative exponential mortality model on size distribution. The model was fitted on part of the data (dark blue dots) while intermediate age stages were excluded (light blue dots).

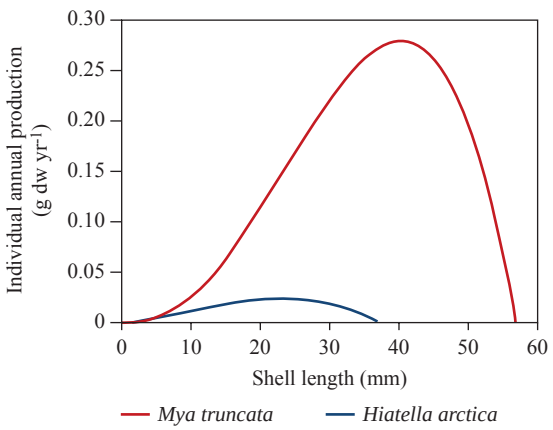

Fig. 7.8 Relationship between size (shell length; mm) and annual individual production (g dw yr^{-1}) of the bivalves *Hiatella arctica* and *Mya truncata* in Young Sound.

Photo: Søren Rysgaard

Marking bivalves (*Hiatella arctica*) for a recapture study on annual growth bands in Young Sound.

temperature also reduces metabolism and, thereby, energy requirements. From the laboratory studies it was estimated that individual *H. arctica* require algae concentrations of only 0.34 µg Chl *a* l^{-1} at –1.3°C to maintain a positive energy budget (Sejr et al., 2004), whereas individuals of *Mytilus edulis* of similar size require 1.03 µg Chl *a* l^{-1} at 15°C (Clausen & Riisgård, 1996). Low food levels are therefore sufficient to cover basic metabolic expenses – a great advantage in an environment where food supply is limited most of the year. Estimated laboratory growth of *H. arctic* from Young Sound fed on a monoalgal diet was further compared with the annual growth of the natural population of *H. arctica* in Young Sound (Sejr et al., 2004). Specimens kept in the laboratory at optimal food conditions and at a temperature similar to that prevailing in Young Sound were able to achieve a growth equivalent to the *in situ* annual production in just 23 days. This shows that despite the limiting effect of temperature on the growth potential of *H. arctica* in Young Sound, the growth potential is not fully realized because food is limiting through long periods of the year in Young Sound. Phytoplankton production in Young Sound is usually concentrated within a two-month period in July and August (see Chapter 5) and the energy budgets of bivalves in Young Sound are most likely positive only during the three to four months of open water. During the rest of the year, bivalves rely on resuspended material and stored energy. A good example of the seasonal energy budget of a polar bivalve was given by Brockington (2001) in a study on the Antarctic bivalve *Laternula elliptica*. Here, individuals stopped feeding for four months during winter and reduced metabolism to a minimum of just 33% of their summer metabolism. During the non-feeding season, energy requirements were covered by catabolism of stored energy.

In addition to studying individual growth at a seasonal level, it is of interest to look at year-to-year variation in growth in the population. Analogously to the growth rings in trees, increments in the shells of bivalves can be used to reconstruct past variations in growth. Analysis of year-to-year variation in each individual revealed a significant autoregressive component, indicating that conditions in one year affect the growth in the following year. Most likely this is because of the strong dependence on stored energy, which allows individuals to carry the effects of a good year into the next in the form of extra stored energy. For *M. truncata* the standardised growth index shows clear variation in time (Fig. 7.9), a significant part of which could be explained by variations in the duration of the open-water period during summer (Schmidt et al., *submitted*). Primary producers in Young Sound are clearly limited by light during spring when ice cover reduces incoming sunlight (Rysgaard et al., 1999; Borum et al., 2002; Glud et al., 2002; Chapters 4, 5 & 9). In years when sea ice disappears early, increased

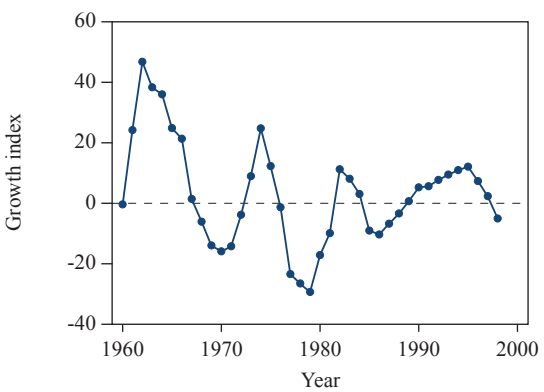

Fig. 7.9 Three-year moving average of growth index for the bivalve *Mya truncata* showing the long-term variation in annual growth in Young Sound. Index is based on measurements of growth increments in the shell.

production of phytoplankton can thus be expected. As bivalves apparently are food-limited, their growth will reflect food conditions, and changes in ice conditions will cascade down and influence growth of bivalves. A similar relationship has been observed in the North Sea. Here, long-term growth patterns of the bivalve *Arctica islandica* are influenced by the climatic effect on copepods (Witbaard et al., 2003). During years with high NAO index values in winter, water-column stratification develops later, depressing the copepod population and, hence, resulting in higher vertical flux of phytoplankton. This produces better food conditions and increased growth rates for *A. islandica*. The copepods in Young Sound also play an important part in the vertical flux of carbon (Chapter 5). However, subsurface blooms in Young Sound make primary production directly available to benthic populations at depths of 20–30 m. Since the individuals of *M. truncata* studied here were collected at 20 m depth, they have access to phytoplankton, resulting in a direct link between climate, sea-ice cover, primary production and bivalve growth.

7.3.3 Carbon demand of benthos

Carbon demand calculated from benthic biomass combined with conversion factors and empirical models from the literature only yield a rough estimate of the role of macrobenthos. However, it is often the only possible way, as measurements of species-specific rates are very sparse for Arctic macrobenthos. Hence, this approach has been used by several authors (Klages et al., 2003; Piepenburg, 2000). In our study, we can evaluate the output from the models by comparing their results with the actual production estimates for *H. arctica* and *M. truncata* in Young Sound (Table 7.2). The predicted carbon demand based on the model of Tombiolo & Downing is a factor of 5 to 6 higher than that predicted by Brey's model, which in turn is twice the value of the carbon demand estimated from actual production estimates for *M. truncata* and *H. arctica*. This discrepancy is due to the uncertainties associated with the model output and also the fact that Young Sound is a low-productive area and, therefore, bound to show production values below the "average" predicted by such models. An alternative method was employed by Piepenburg et al. (1995) who used shipboard measurements to estimate respiration rates of benthic groups. Rates from that study were used to estimate the carbon demand of polychaetes in Young Sound (Glud et al., 2000). In the case of molluscs, Piepenburg et al. (1995) used a mean mass-specific respiration rate of 0.05 µmol O_2 g^{-1} h^{-1} for individuals with mass >1 g wet weight (ww) and 0.15 µmol O_2 g^{-1} h^{-1} for individuals with mass <1 g ww. When transformed into daily carbon demands, these rates are equivalent to 0.077 and 0.57 mg C ind^{-1} d^{-1} for average-sized *H. arctica* and *M. truncata*, respectively. For equal-sized individuals, carbon demands based on actual production estimates are 0.045 and 0.74 mg C ind^{-1} d^{-1} for *H. arc-*

Photo: Göran Ehlmé

Sea anemones (Class Anthozoa) at 36 m depth in outer Young Sound.

Table 7.4 Estimated carbon demand (mg C m^{-2} d^{-1}) for dominant species of benthos in Young Sound at 10–60 m depth.

Method	*Mya truncata* (mg C m^{-2} d^{-1})	*Hiatella arctica* (mg C m^{-2} d^{-1})	*Ophiuroidea* spp. (mg C m^{-2} d^{-1})	*Strongylocentrotus* sp. (mg C m^{-2} d^{-1})
Ind. production				
Mean	6.81	0.92		0.16
Max	13.50	2.69		0.54
Min	0.08	0.05		0.01
Brey et al. 1999				
Mean	12.70	1.92	3.21	0.68
Max	25.27	5.59	6.42	2.27
Min	0.14	0.12	0.12	0.02
Tombiolo et al. 1994				
Mean	32.22	6.29	8.09	3.01
Max	66.06	17.76	15.10	10.96
Min	0.41	0.40	0.52	0.16
Mahaut et al. 1995				
Mean			6.04	
Max			12.09	
Min			0.27	

Table 7.5 Carbon demand (mg C m^{-2} d^{-1}) of Arctic benthos.

Study	Location	Depth (m)	Organisms	Carbon demand (mg C m^{-2} d^{-1})
This study	Young Sound	10–60	Mega and macrobenthos	Mean 15
Klages et al. (2003)	Kara Sea	10–68	Macrobenthos	3.5–43.2
Piepenburg et al. (1995)	NW Barents Sea	80–240	Mega and macrobenthos	16.5
Klages et al. (2004)	Central Arctic ocean	150–4500	Macrobenthos	Median 0.7
Ambrose et al. (2001)	NE Chuckchi Sea	36–50	Brittle stars	Median 3.4
Piepenburg (2000)	NE Greenland shelf banks	40–150	Brittle stars	Median 5.3
Piepenburg (2000)	Barents Sea shelf banks	80–100	Brittle stars	Median 3.6
Piepenburg (2000)	Laptev Sea	30–45	Brittle stars	Median 6.2

tica and *M. truncata*, respectively. This comparison illustrates the uncertainties associated with estimating carbon demand using different methods. Here we use a conservative approach and base our estimate on minimum values, i.e. actual production estimates or predicted production values (for brittle stars). It is important to keep in mind that carbon demand estimates based on somatic production neglect the energy expended during reproduction, which for old individuals often exceeds the amount invested in growth. In an extreme example, a population of the Antarctic sea urchin *Sterechinus neumayeri* invested 95% of its total production in reproduction (Brey et al., 1995).

Macrobenthic carbon demand in Young Sound is dominated by bivalves and brittle stars (Table 7.4). The carbon demand of *M. truncata* and *H. arctica* reaches 16 mg C m^{-2} d^{-1} at 30 m whereas the demand of brittle stars peaks at 60 m with an estimated consumption of 6 mg C m^{-2} d^{-1}. The importance of brittle stars for the remineralisation of carbon in the Arctic has been noted in several studies (Piepenburg, 2000; Ambrose et al., 2001). Our study highlights the fact that in shallow coastal areas the carbon demand of bivalves can exceed that of brittle stars, at least at shallow depths, but also that bivalves can contribute significantly when values are integrated across the entire area. It is important to remember that several other species of bivalves are present in Young Sound. Specifically species such as *Astarte* spp., *Macoma calcarea* and *Portlandia* spp. may, combined, reach biomass values equivalent to those of *M. truncata* and *H. arctica* (Thorson, 1933, 1934). Their contribution is not included in our estimate of carbon

Photo: Magnus Elander

Bivalve *Hiatella arctica* from outer Young Sound.

demand. Additionally, based on the importance as prey for walruses (Chapter 10) the species *Serripes groenlandicus* could also be expected to contribute significantly to total carbon demand of bivalves.

To our knowledge, only one other study has attempted to estimate the carbon demand of Arctic bivalves. In a study from the Lancaster Sound region, Welch et al. (1992) estimated the carbon demand of *Mya truncata* based on annual production from 0–100 m depth at 634 kJ m^{-2} yr^{-1} equivalent to 38 mg C m^{-2} d^{-1}. The higher carbon demand of *M. truncata* in Lancaster Sound compared with Young Sound was predominantly due to higher abundance of clams. Since bivalves have been found to be numerous and attain high standing stocks in several other coastal areas, we believe that the relative importance of bivalves in our study should be representative of other regions.

The average carbon demand of brittle stars (10–60 m) based on predicted annual production was 3.2 mg C m^{-2} d^{-1}. Typically, median values for shallow shelf areas range between 3 and 6 mg C m^{-2} d^{-1} (Table 7.5). The latter values are obtained using respiration rates for deep-sea organisms, which results in higher carbon demands than when predicted production is used based on Brey's model. The carbon demand of brittle stars in Young Sound is therefore among the highest reported for Arctic areas. Unfortunately, estimates of brittle star abundance are not available from depths below 60 m and a considerable biomass is likely to be present in deeper parts of the area. The overall contribution of brittle stars to the remineralisation of carbon in Young Sound is thus even higher and their relative contribution compared with bivalves more important, which underlines the importance of brittle stars not only in shelf areas but also in the vast fjord systems of East Greenland.

The grand mean carbon demand (across depths and taxa), including that of polychaetes (Glud et al., 2000), is 15 mg C m^{-2} d^{-1}, ranging from 2 mg C m^{-2} d^{-1} at 10 m to 23 mg C m^{-2} d^{-1} at 30 m. This is comparable with estimates for both the Kara and Barents Seas (Table 7.5), where, however, carbon demand was calculated based on biomass measurements comprising the entire zoobenthic fauna. Despite the conservative estimate, the fauna in Young Sound was found to account for 20% of the total mineralisation at 60 m depth, while the estimate at 40 m was 30%. This shows that the fauna directly influences carbon cycling by ingesting a significant fraction of the available carbon. Shallow depth and low levels of physical disturbance are probably important factors causing the high carbon demand of benthos in the present study. At depths of 10 to 30 m macrofaunal organisms have direct access to subsurface blooms of phytoplankton as well as a considerable production of benthic diatoms (Glud et al., 2002). At 30 to 60 m depth a considerable vertical export of carbon (Chapter 6) allows a high biomass of especially bivalves to build up despite low annual production.

Although both bivalves and brittle stars ingest an important proportion of the produced carbon, they probably have different roles in the trophic net. Both *H. arctica* and *M. truncata* are filter feeders and at their preferred depths (20–30 m) they can effectively exploit the subsurface peak of phytoplankton biomass. Walruses in Young Sound feed almost exclusively on bivalves during summer to build up their energy stores (Chapter 10). Hence, bivalves are a direct trophic link between microscopic algae and large mammals, creat-

ing a short and energetically efficient food chain that allows a population of large mammals to persist in a low-productive environment. Bivalves are also the favored prey of seals, eiders and scavenging amphipods. Therefore, they are important structuring components of the marine food web. On the other hand, brittle stars are thought to be generalists (Piepenburg, 2000). Few if any predators prey on brittle stars, which therefore become a trophic dead end.

In the calculation of macrobenthic carbon demand in Young Sound an assimilation efficiency of 80% was applied (Piepenburg, 2000; Klages et al., 2003), which is in good agreement with actual measurements of *Hiatella arctica* feeding on *Rhodomonas* sp. (Sejr et al., 2004). This implies that c. 20% of the carbon ingested by zoobenthos is not assimilated and that the benthos therefore exert an indirect influence on the carbon flow in the system. Large infaunal filter feeders such as *H. arctica* and *M. truncata* increase sedimentation by filtering phytoplankton from the water column, and, in addition, 20% of the filtered material passes through the gut and is excreted 5 to 20 cm into the sediment, where it is further decomposed by bacteria. Faunal activity thereby changes the relative importance of different oxidation pathways and indirectly increases the importance of the anaerobic bacteria.

7.4 Acknowledgements

Egon Frandsen is thanked for valuable assistance in the field. This study was made possible by the financial support of the Danish Natural Science Research Council, the Carlsberg Foundation, KVUG and by DANCEA (the Danish Cooperation for the Environment in the Arctic) under the Danish Ministry of the Environment. This work is, furthermore, a contribution to the Zackenberg Basic and Nuuk Basic programs in Greenland. Anna Haxen helped with linguistic corrections and three anonymous reviewers made valuable comments that improved the manuscript.

7.5 References

Ambrose, W., Clough L., Tilney, P. R. & Beer, L. 2001. Role of echinoderms in benthic remineralization in the Chuckchi Sea. Mar. Biol. 139: 937-949.

Ambrose, W. & Renaud, P. 1995. Benthic response to water column productivity patterns: Evidence for benthic-pelagic coupling in the Northeast Water Polynea. J. Geophys. Res. 100(c3): 4411-4421.

Bluhm, B., Piepenburg, D. & Juterzenka, K. 1998. Distribution, standing stock, growth, mortality and production of *Strongylocentrotus pallidus* (Echinodermata: Echinoidea) in the northern Barents Sea. Polar Biol. 20: 325-334.

Born, E. W., Rysgaard, S., Ehlmé, G., Sejr, M. K., Acquarone, M. & Levemann, N. 2003. Underwater observations of foraging free-living Atlantic walruses (*Odobenus rosmarus rosmarus*) and estimates of their food consumption. Polar Biol. 26: 348-357.

Borum, J., Pedersen, M. F., Krause-Jensen, D., Christensen, P. B. & Nielsen, K. 2002. Biomass, photosynthesis and growth of *Laminaria saccharina* in a high-Arctic fjord, NE Greenland. Mar. Biol. 141: 11-19.

Brey, T., Pearse, J., Basch, L., McClintock, J. & Slattery, M. 1995. Growth and production of *Sterechinus neumayeri* (Echinoidea: Echinodermata) in McMurdo Sound, Antarctica. Mar. Biol. 124: 279-292.

Brey, T. & Meckensen, A. 1997. Stable isotopes prove shell growth bands in the Antarctic bivalve *Laternula elliptica* to be formed annually. Polar Biol. 17(5): 465-468.

Brey, T. 1999. A collection of empirical relations for use in ecological modelling. NAGA The ICLARM Quarterly 22(3): 24-28.

Brey, T. 2001. Population dynamics in benthic invertebrates. A virtual handbook. Version 01.2.
http://www.awi-bremerhaven.de/Benthic/Ecosystem/FoodWeb/Handbook/main.html
Alfred Wegener Institute for Polar and Marine Research, Germany.

Brockington, S. 2001. The seasonal energetics of the Antarctic bivalve *Laternula elliptica* (King and Broderip) at Rothera Point, Adelaide Island. Polar Biol. 24: 523-530.

Clausen, I. & Riisgård, H. U. 1996. Growth, filtration and respiration in the mussel *Mytilus edulis*: no evidence for physiological regulation of the filter-pump to nutritional needs. Mar. Ecol. Prog. Ser. 141: 37-45.

Glud, R. N., Risgaard-Petersen, N., Thamdrup, B., Fossing, H. & Rysgaard, S. 2000. Benthic carbon mineralization in a High-Arctic sound (Young Sound, NE Greenland). Mar. Ecol. Prog. Ser. 206: 59-71.

Glud, R. N., Kühl, M., Wenzhöfer, F. & Rysgaard, S. 2002. Benthic diatoms of a high Arctic fjord (Young Sound, NE Greenland): importance for ecosystem primary production. Mar. Ecol. Prog. Ser. 238: 15-29.

Grebmeier, J. M., McRoy, C. P., & Feder, H. M. 1988. Pelagic-benthic coupling on the shelf of the northern Bering and Chuckchi Seas. I. Food supply source and benthic biomass. Mar. Ecol. Prog. Ser. 48: 57-67.

Highsmith, R. & Coyle, K. 1990. High productivity of northern Bering Sea benthic amphipods. Nature 344: 862-864.

Hobson, K. A., Fisk, A., Karnovsky, N., Holst, M., Gagnon, J.-M. & Fortier, M. 2002. A stable isotope ($\delta^{13}C$, $\delta^{15}N$) model for the North Water food web: implications for evaluating trophodynamics and the flow of energy and contaminants. Deep-Sea Res. 49: 5131-5150.

Holte, B. & Gulliksen, B. 1998. Common macrofaunal dominant species in the sediments of some north Norwegian and Svalbard glacial fjords. Polar Biol. 19: 375-382.

Kendall, M. 1996. Are Arctic soft-sediment macrobenthic communities impoverished? Polar Biol. 16: 393-399.

Klages, M., Boetius, A., Christensen, J. P., Deubel, H., Piepenburg, D., Schewe, I. & Soltwedel, T. 2003. The benthos of the Arctic Seas and its role for the organic carbon cycle at the seafloor. In: Stein, R. & MacDonald, R. (eds.). The organic carbon cycle in the Arctic Ocean, Springer. Berlin: 139-168.

MacDonald, B. A. & Thomas, M. H. L. 1980. Age determination of the soft-shell clam *Mya arenaria* using shell internal growth lines. Mar. Biol 58: 105-109.

Mahaut, M.-L., Sibuet, M. & Shirayama, Y. 1995. Weight-dependent respiration rates in deep-sea organisms. Deep-Sea Res. 42(9): 1575-1582.

Menard, H. W. & Smith, S. M. 1966. Hypsometry of the ocean basin provinces. J. Geophys. Res. 71: 4305-4325.

Ockelmann, W. 1958. The zoology of East Greenland: marine Lamellibranchiata. Meddr. Grønland 122(4).

Petersen, J. K., Sejr, M. K. & Larsen, J. E. N. 2003. Clearance rates in the Arctic bivalves *Hiatella arctica* and *Mya* sp. Polar Biol. 26: 334-341.

Piepenburg, D. 2000. Arctic brittle stars (Echinodermata: Ophiuroidea). Oceanogr. Mar. Biol. Ann. Rev. 38: 189-256.

Piepenburg, D., Blackburn, T. H., von Dorrien, C. F., Gutt, J., Hall, P. O. J., Hulth, S., Kendall, M. A., Opalinski, K. W., Rachor, E. & Schmid, M. K. 1995. Partitioning of the benthic community respiration in the Arctic (Northwestern Barents Sea). Mar. Ecol. Prog. Ser. 118: 199-213.

Richman, S. E. & Lovvorn, S. R. 2003. Effects of clam species dominance on nutrients and energy acquisition by spectacled eiders in the Bering Sea. Mar. Ecol. Prog. Ser. 261: 283-297.

Ropes, J. W. 1985. Procedures for preparing acetate peels and evidence validating annual periodicity of growth lines formed in the shells of *Arctica islandica*. Mar. Fish. Rev. 46: 27-35.

Riisgård, H. U. 2001. On measurements of filtration rates in bivalves -the stony road to reliable data: review and interpretation. Mar. Ecol. Prog. Ser. 211: 275-291.

Rysgaard, S., Nielsen, T. & Hansen, B. W. 1999. Seasonal variation in nutrients, pelagic primary production and grazing in a high-Arctic coastal marine ecosystem, Young Sound, Northeast Greenland. Mar. Ecol. Prog. Ser. 179: 13-25.

Rysgaard, S., Frandsen, E., Sejr, M. K., Dalsgaard, T., Blicher, M. E., Christensen, P. B. 2005. Zackenberg Basic: The marine monitoring programme. In: Rasch, M. & Caning, K. (eds.). Zackenberg ecological research operations 10th annual report, 2004. Danish Polar Center, Ministry of Science, Technology and Innovation. Copenhagen, 85 pp.

Schmidt, N. M., Sejr, M. K., Høye, T. T., Rysgaard, S. & Forchhammer, M. C. Sea ice cover influence annual growth of terrestrial and marine organisms from a coastal region in the Arctic. *Submitted.*

Sejr, M. K., Jensen, K. T. & Rysgaard, S. 2000. Macrozoobenthic community structure in a high-Arctic East Greenland fjord. Polar Biol. 23: 792-801.

Sejr, M. K., Sand, M. K., Jensen, K. T., Petersen, J. K., Christensen, P. B. & Rysgaard, S. 2002a. Growth and production of *Hiatella arctic*a (Bivalvia) in a high-Arctic fjord (Young Sound, Northeast Greenland). Mar. Ecol. Prog. Ser. 244: 163-169.

Sejr, M. K., Jensen, K. T. & Rysgaard, S. 2002b. Annual growth bands in the bivalve *Hiatella arctica* validated by a mark-recapture study in NE Greenland. Polar Biol. 25: 794-796.

Sejr, M. K., Petersen, J. K., Jensen, K. T. & Rysgaard, S. 2004. Effects of food concentration on clearance rate and energy budget of the Arctic bivalve *Hiatella arctica* (L) at subzero temperature. J. Exp. Mar. Ecol. Biol. 311: 171-183.

Thomson, D. 1982. Marine benthos in the Eastern Canadian high Arctic: Multivariate analyses of standing crop and community structure. Arctic. 35: 61-74.

Thorson, G. 1933. Investigations on shallow water animal communities in the Franz Joseph Fjord (East Greenland) and adjacent waters. Meddr. Grønland 100(2): 1-68.

Thorson, G. 1934. Contributions to the animal ecology of the Scoresby Sound Fjord complex (East Greenland). Meddr. Grønland 100(3): 1-67.

Tombiolo, M. L. & Downing, J. A. 1994. An empirical model for the prediction of secondary production in marine benthic invertebrate populations. Mar. Ecol. Prog. Ser. 114: 165-174.

Welch, H. E., Bergmann, M. A., Siferd, T. D., Martin, K. A., Curtis, M. F., Crawford, R. E., Conover, R. J. & Hop, H. 1992. Energy flow through the marine ecosystem of the Lancaster Sound region, Arctic Canada. Arctic 45(4): 343-357.

Witbaard, A., Jansma, E. & Saas Klaassen, U. 2003. Copepods link quahog growth to climate. J. Sea Res. 50: 77-83.

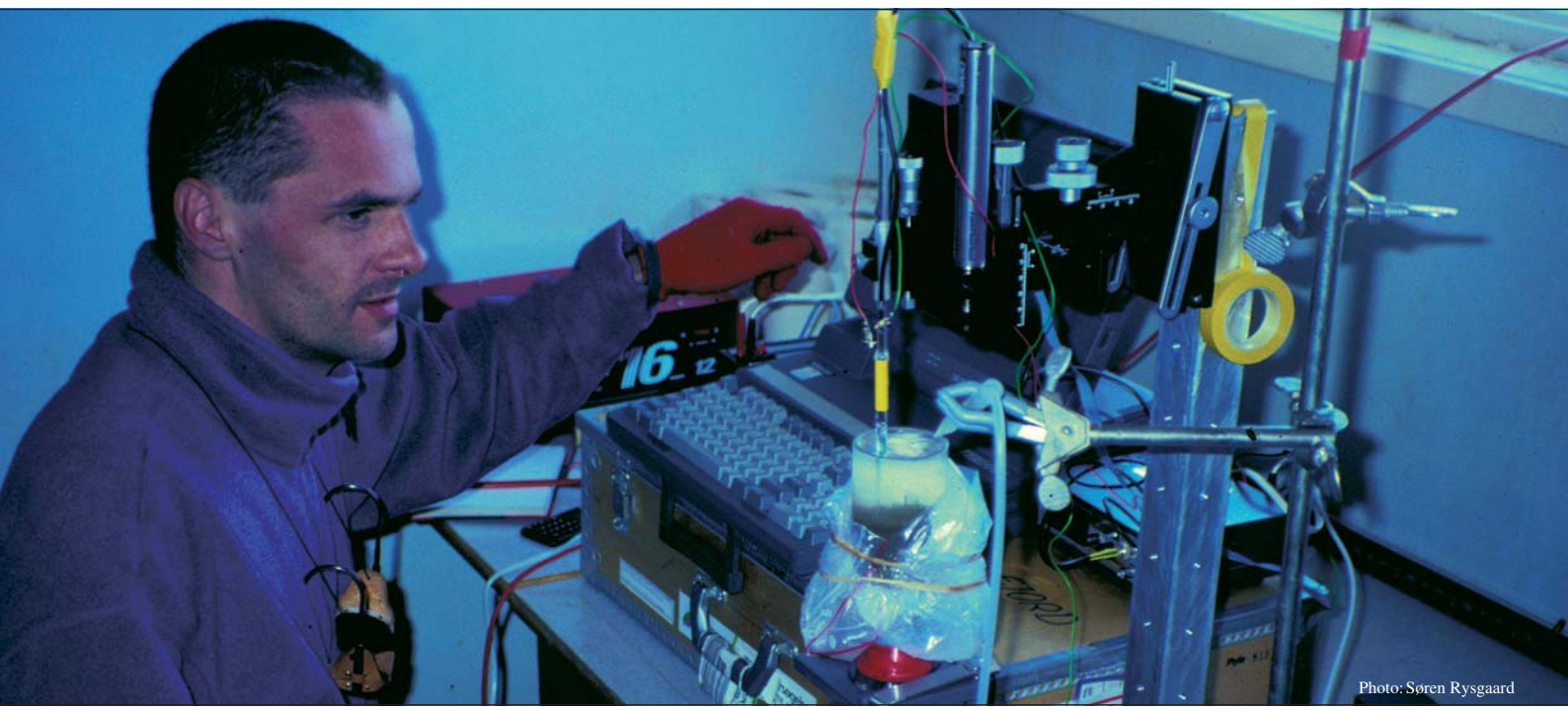

Photo: Søren Rysgaard

8

Benthic carbon cycling in Young Sound, Northeast Greenland

Benthic carbon cycling in Young Sound, Northeast Greenland

Bo Thamdrup[1], Ronnie N. Glud[2] and Jens W. Hansen[3]

[1]Institute of Biology, University of Southern Denmark, Campusvej 55, DK-5230 Odense M, Denmark
[2]Marine Biological Laboratory, Institute of Zoology, University of Copenhagen, Strandpromenaden 25 DK-3000 Helsingør, Denmark
[3]National Environmental Research Institute, Vejlsøvej 25, DK-8600 Silkeborg, Denmark

Cite as: Thamdrup, B., Glud, R. N. & Hansen, J. W. 2007. Benthic carbon cycling in Young Sound, Northeast Greenland. – In: Rysgaard, S. & Glud, R. N. (Eds.), Carbon cycling in Arctic marine ecosystems: Case study Young Sound. Meddr. Grønland, Bioscience 58: 138-157.

Abstract

We present a synthesis of studies on benthic carbon cycling and related biogeochemical aspects performed in High Arctic Young Sound. Benthic carbon oxidation rates measured as the exchange of oxygen and DIC across the sediment/water interface increased rapidly from c. 5 to 10 mmol m^{-2} d^{-1} following the summer thaw in response to the settling of planktonic debris. Within few weeks, the exchange rates at 36 m depth returned to c. 5 mmol m^{-2} d^{-1}. This background level was maintained throughout the rest of the annual cycle and found repeatedly over several years. The background activity was also maintained for 400 days in sediment cores incubated without external carbon sources, demonstrating that benthic carbon cycling was fuelled mainly by a large pool of relatively inert organic matter with a half-life >>1 yr. Carbon oxidation rates decreased exponentially with water depth, the difference between 20 m and 163 m being approximately a factor of 6, while oxygen penetration increased from 7 to 16 mm over this range. Except for the shallowest sites, sulfate reduction was the most important carbon oxidation process, contributing 40–50%, while denitrification accounted for less than 5%. The remaining mineralization was shared equally between microbial iron reduction and aerobic respiration. Integrated over the entire outer Young Sound area, 1.3 Gg organic C was oxidized and 0.57 Gg organic C was buried. Thus, c. 30% of the organic carbon flux to the seafloor was preserved in the sedimentary record. Half of the carbon oxidation occurred at water depths shallower than 30 m, while burial was focused at the depths of around 80–100 m dominating the basin hypsometry. Sediment incubation experiments showed Q_{10} values of 2–3 for carbon oxidation rates, which agrees well with data from temperate sediments. Thus, patterns of carbon mineralization are qualitatively similar in Arctic and temperate sediments, but the low water temperature during settlement of spring and summer blooms leads to a less pronounced benthic-pelagic coupling in Arctic than in temperate coastal waters.

8.1 Introduction

Sediments represent an important part of coastal marine ecosystems as sites for remineralization of organic matter and associated nutrient regeneration. The flux of organic material to the seafloor in bays and fjords may correspond to as much as 50% of the primary production in the overlying water column (Wollast, 1991; Canfield, 1993). Typically, most of this matter is degraded to soluble inorganic building blocks, most of which are released back to the water column, while a minor fraction of the organic matter is buried in the sediment and thereby permanently lost from the ecosystem. Although the major constit-

Photo: Søren Rysgaard

Sampling sediment cores from a hole in the sea ice during June 1999.

uents of the organic matter are recycled to the water column, the sediment serves as a short-term sink of the carbon and nutrients bound in a settling phytoplankton bloom. Thus, the timing of remineralization relative to sedimentation is a key factor for the benthic-pelagic coupling.

Most of the remineralization in marine sediments occurs through microbial processes (e.g. Glud et al., 2003). A great diversity of different types of metabolism combined through a web of interactions leads to the oxidation of organic carbon to CO_2 and the release of organically bound phosphorus and nitrogen as phosphate and ammonium, nitrate, or N_2 (Fenchel & Blackburn, 1979). The bulk rates of remineralization resulting from these interactions are to a first approximation a function of the composition and quantity of the organic matter, with a tendency towards more rapid degradation of the more nutrient-rich constituents and relatively slow degradation of e.g. structural carbohydrates. Thus, the kinetics of carbon mineralization in sediments are often quite well described by division of the total organic carbon content into a few pools, each decaying with different half-lives (Westrich & Berner, 1984).

In addition to oxygen, nitrate, oxides of manganese and iron, and sulfate may serve as electron acceptors in microbial respiration. Together, these anaerobic respiratory pathways are frequently more important than aerobic respiration during carbon oxidation in coastal sediments (Jørgensen, 1982; Thamdrup, 2000). The relative importance of the different respiratory classes in any given sediment strongly influences the benthic environment and benthic-pelagic coupling. For example, many organic compounds are more rapidly degraded under oxic conditions than under anoxic conditions (e.g., Kristensen et al., 1995; Sun et al., 2002), and the higher growth yield of aerobes may allow a more rapid numerical response to substrate enrichment, leading to overall more efficient remineralization compared with anaerobic organisms (e.g., Harvey et al., 1995; Hulthe et al., 1998; Bastviken et al., 2004). Bacterial sulfate reduction produces hydrogen sulfide, which is toxic to higher organisms, and dominance of this type of respiration may thus lead to defaunation of the sediment and, in extreme cases, to the release of hydrogen sulfide to the water column.

While only a minor fraction of benthic respiration is due to fauna, bottom-dwelling animals influence sediment processes through their activities (Chapter 7). Unspecific effects include the mixing of sediment particles through burrowing, and the advective porewater transport by irrigation. Such bioturbation is essential, e.g. for the maintenance of a ferric iron pool capable of serving as electron acceptor for iron-reducing bacteria and acting as a buffer for hydrogen sulfide release (Canfield et al., 1993b; Thamdrup et al., 1994a).

Our understanding of benthic biogeochemistry rests mainly on studies of temperate sediments at temperatures >5°C. As temperature decreases, e.g. during experimental manipulations, microbial processes in natural communities slow down, typical Q_{10} values being 2–4 (Q_{10} is the relative change in rate at a temperature *increase* of 10 degrees) (e.g. Vosjan, 1974; Kaplan et al., 1988; Westrich & Berner, 1988; Thamdrup & Fleischer, 1998). It is not clear, however, how results from short-term experiments translate to natural environments of permanently low temperatures, where changes in cell physiology and in community size and composition may also affect the rates.

Apart from Young Sound, the relatively small database describing sediments of temperatures permanently around 0°C includes mainly open shelf and slope sites (Pfannkuche & Thiel, 1987; Grebmeier & McRoy, 1989; Hulth et al., 1994; Rowe et al., 1997; Boetius et al., 1998; Glud et al., 1998; Grant et al., 2002). Here, integrated rates of benthic carbon mineralization fall within the range observed for warmer

locations at the same depth, indicating that, overall, the efficiency of remineralization does not depend strongly on temperature. One detailed study of carbon oxidation pathways also suggested that regulation of the relative importance of these pathways in very cold and in warmer sediments is similar (Kostka et al., 1999). Due to large regional variability, however, such comparisons, based on snapshot investigations of different locations, are not likely to reveal the finer effects of temperature. Such differences may be more evident from detailed investigations of the dynamics of carbon mineralization, either over a natural annual cycle or during experimental manipulations.

In this chapter, we provide a synthesis of biogeochemical investigations of the sediments of Young Sound carried out since 1994 as part of a wider effort to describe the carbon and nutrient dynamics of a High Arctic marine ecosystem (Chapter 11, Chapter 12). When this study was initiated, very little information was available on benthic metabolism in permanently cold sediments (see references above). It was therefore the aim to quantify rates and pathways of benthic respiration and to characterize their regulation. Central questions included:

- What are the seasonal dynamics of benthic respiration when organic inputs presumably are restricted to a brief summer bloom?
- How do permanent subzero temperatures affect the rates and pathways of carbon mineralization?
- What is the integrated benthic contribution to carbon cycling in the fjord?

Parts of the results presented here were published previously (Rysgaard et al., 1996, 1998, 2003; Glud et al., 2000; Sejr et al., 2000; Berg et al., 2001, 2003b), whereas other results are new and were obtained in collaboration with Henrik Fossing, Lars Mørk Ottosen, and Søren Rysgaard, whom we thank for their contributions and for permitting us to cite the results here.

8.2 Methods

The techniques used for the sediment studies are only briefly mentioned here, as they were described in detail in previous publications (Rysgaard et al., 1998; Glud et al., 2000).

Table 8.1 Location and bottom-water characteristics[1)] of sediment sampling sites along a transect at 74° 18' 58'N from the "Kystens Perle" field station[2)].

Station	Position	Depth (m)	Temperature (°C)	Salinity
A0	20° 14' 48" W	20	–0.9	31.8
A	20° 15' 04" W	36	–1.3	32.2
B	20° 15' 74" W	60	–1.3	33.0
C	20° 16' 92" W	85	–1.3	33.0
D	20° 18' 00" W	163	–1.3	33.0

[1)] Measured in July 1996.
[2)] From Glud et al. (2000)

Sediment was sampled along a North-South transect perpendicular to the coast at the field laboratory "Kystens Perle" in Daneborg towards the deepest part of Young Sound. Stations A0, A, B, C, and D from 20 to 163 m water depth were all sampled during July 1996 (Table 8.1). Station A, at 36 m, was sampled repeatedly from May to August 1996 to follow the dynamics of the summer season, and this station was sampled again on several occasions during the following years to fill in gaps in the seasonal pattern, and for kinetics

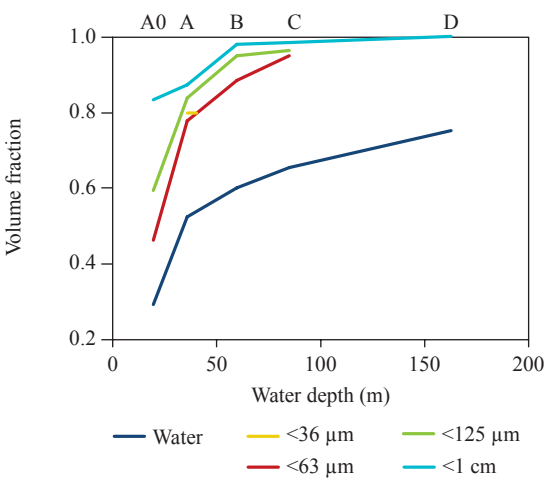

Figure 8.1 Cumulative plot of sediment porosity and texture of the upper 5 cm of the sediment as a function of water depth in outer Young Sound. Volume fractions of solids are calculated assuming the same density for all solid fractions <1 cm. The 36-µm sieve was used at St. A, only, and only stones were sieved at St. D. Data from Glud et al. (2000), Sejr et al. (2000), Berg et al. (2001).

experiments. Sediment for a smaller analytical program was obtained from a site at 40 m depth c. 1 km south of Station C (Rysgaard et al., 1996).

The sediment was retrieved in Plexiglas core tubes (id. 5.2 cm) using a hand-deployed Kajak sampler either through holes in the ice or from an inflatable boat. Cores were kept on ice until return to the laboratory where they were maintained at –1 ± 0.5°C. Oxygen microprofiles were measured using Clark type microelectrodes as described in Rasmussen and Jørgensen (1992). Benthic fluxes were determined from the change in solute concentrations of the overlying water during intact core incubations, throughout which the water was stirred by a small rotating magnet positioned above the sediment surface (Rasmussen & Jørgensen, 1992). On one occasion, fluxes were also measured *in situ* using a benthic lander (Glud et al., 1995). Rates of denitrification and bacterial sulfate reduction were quantified by the ^{15}N isotope pairing technique (Nielsen, 1992) and the $^{35}SO_4^{2-}$ tracer technique (Jørgensen, 1978). The depth distributions of carbon mineralization and of the different respiratory pathways within the sediment were determined through anoxic incubations of sediment from discrete depth intervals (Thamdrup & Canfield, 1996).

8.3 Results & discussion

8.3.1 Physical and chemical sediment characteristics

Porosity and texture: Sediments along the transect were predominantly silts or clays with an increasing content of dropstones towards shallower depths (Fig. 8.1). At the intensely studied Station A at 36 m depth, the dropstone content was 13%. The stones were estimated to cover 2–4% of the sediment surface as inferred from video recordings. Most stones were covered with crustose coralline red algae (Roberts et al., 2002). At 20 m, the sediment was sandy with many stones paving the surface, and nearest to the shore, the bottom consisted entirely of coarse gravel and stones. These conditions hampered sediment sampling for process studies at the shallow sites and only few intact cores were recovered.

Accumulation rates: At Stations A and D, respectively, sediment accumulation rates of 0.14 and 0.23 cm yr^{-1} were determined from depth distributions of unsupported ^{210}Pb and ^{137}Cs (Rysgaard et al., 1998; Glud et al., 2000; Fig. 8.2). The accumulation rate at 40 m depth south of the main transect was 0.12 cm yr^{-1} (Rysgaard et al., 1996). While accumula-

Figure 8.2 Depth distributions of tracers of sediment accumulation and mixing. **(Left):** Unsupported ^{210}Pb at stations A, B, and D. **(Center):** ^{137}Cs at Stations A, B, and D. **(Right):** Chlorophyll *a* at St. A. Measurements from June 1999 (± SD, n = 3) are compared with theoretical distributions based on Equation 1 (see text) assuming reported values of D_B [2.3×10^{-7} cm^2 s^{-1}; Berg et al. (2001)] and k [0.014 d^{-1} for aerobic degradation, 0.3 d^{-1} for anaerobic degradation; Sun et al. (1991, 1993)], as well as a D_B of half the value determined by Berg et al. (2001). Chlorophyll *a* was determined by fluorometry after extraction of c. 0.5 g of previously frozen sediment in 10 ml 96 % ethanol. Theoretical distributions were calculated as least-squares fits to the data with C_0 and $C\infty$ as free parameters using Solver in MS Excel 2001. Radionuclide data from Rysgaard et al. (1996), Glud et al. (2000), and S. Rysgaard (unpubl. res.).

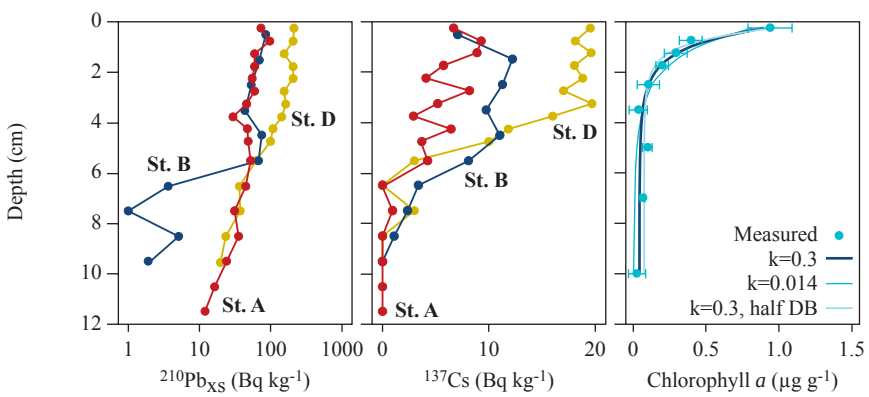

tion at the 40-m site was derived assuming that the upper 4 cm of the sediment was affected by bioturbation, effects of bioturbation had not previously been considered with regard to Stations A and D. Later experiments indicated that ^{210}Pb distributions at Station A and the 40-m station were indeed affected by bioturbation to 6–8 cm depth, and that, consequently, only the deeper part of the profiles should be used for estimating accumulation rates (Berg et al., 2001; see also below). Similarly, the convex shape of the ^{210}Pb profile indicated bioturbation to at least 3–4 cm depth at Station D, and recent measurements at Station B indicate intense mixing to 6 cm (Fig. 8.2). Accumulation rates inferred from ^{210}Pb and ^{137}Cs thus need to be re-evaluated.

In order to revise the sediment accumulation rates, we need to identify sediment layers that are currently not subject to significant mixing, and where a decrease in ^{210}Pb with depth is attributed solely to radioactive decay. The low levels of ^{137}Cs (originating mainly from atmospheric bomb tests, which peaked in 1963) below 8 cm, 4.5 cm, and 6 cm at stations A, D and the 40-m site, respectively, indicate that these depths fit those criteria (Fig. 8.2). Hence, using only the deepest parts of the ^{210}Pb profiles, we obtain revised sediment accumulation rates of 0.089, 0.090, and 0.059 cm yr^{-1} (equivalent to 0.079, 0.082, and 0.054 g cm^{-2} yr^{-1}) for these three sites. At Station B, the irregular distribution of ^{210}Pb and the deep penetration of ^{137}Cs preclude such calculations. Assuming that ^{137}Cs deposition peaked in 1963, 40 years before the core was sampled, the broad peak of ^{137}Cs between 1.5 and 4.5 cm at that site limits the accumulation rate to 0.04–0.11 cm yr^{-1}, which is roughly similar to those found at the other sites. The ^{210}Pb-based rates from the other sites are also in agreement with the ^{137}Cs distributions there. Given the narrow range of the revised accumulation rates, we used the average of the three ^{210}Pb-based values (0.080 cm yr^{-1}, or 0.072 g cm^{-2} yr^{-1}) as an estimate for water depths deeper than 10 m in our budget calculations. Sediment burial at shallower depths dominated by stones and gravel was estimated to be negligible. Overall, the revised accumulation rate estimates are significantly lower than previously anticipated (Rysgaard et al., 1998; Glud et al., 2000).

Bioturbation: Like many continental sediments underlying well-oxygenated waters, Young Sound sediments are reworked by an active and diverse infauna (Chapter 7). Mixing of sediment particles is evident from the even distribution of the radio-tracers in the upper centimeters of the sediment (Fig. 8.2). Particle mixing was investigated at Station A by addition of glass beads to the surface of sediment cores, which were subsequently incubated for up to 10 days (Berg et al., 2001). This experiment indicated a biodiffusivity for solids (Berner, 1980) of $(2.7 \pm 1.5) \times 10^{-7}$ cm^2 s^{-1} in the upper 0–1 cm. Analysis of the upper part of the ^{210}Pb profiles supported this result and indicated that a similar biodiffusivity ($2.2–2.4 \times 10^{-7}$ cm^2 s^{-1}) applied down to 6–8 cm depth, which is well within the range of solid biodiffusivities reported for sediments with similar accumulation rates (Boudreau, 1994).

The estimates of biodiffusivity can be further supported by analysis of the distribution of chlorophyll *a* in the sediments. Chlorophyll can be used as a natural tracer of particle mixing and displays a typical half-life of a few weeks in sediments (Sun et al., 1991). At typical mixing rates, chlorophyll *a* is a much more sensitive indicator of mixing than ^{210}Pb, the half-life of which is 21 years. Assuming approximate steady state, concentrations of chlorophyll *a* as a function of depth, *C(x)*, can be fitted by the equation (Sun et al., 1991):

$$C(x) = (C_0 - C_\infty) \cdot e^{(-x\sqrt{k_d / D_B})} + C_\infty \qquad (1)$$

where C_0 is the concentration at the sediment surface, C_∞ is the asymptotic concentration at depth, k_d is the degradation rate constant, and D_B is the biodiffusivity. In Long Island Sound sediments, Sun and co-workers (1991, 1993) determined a $k_{d\ anaerobic}$ of 0.03 ± 0.01 d^{-1} for anaerobic degradation with little temperature dependence from 4 to 25°C, and a similar value for aerobic degradation at 10°C with an activation energy of 51 kJ mol^{-1} over the same temperature interval. The activation energy corresponds to $Q_{10\ (0\text{-}10°C)} = 2.2$, which is similar to values derived for bulk organic carbon mineralization rates in Young Sound (see below). Using this value to extrapolate the rate constant determined by Sun and coworkers to 0°C, yields $k_{d\ aerobic} = 0.014$ d^{-1}. At an oxygen penetration depth of c. 1 cm, both aerobic and anaerobic processes should contribute to chlorophyll degradation in Young Sound. The measured concentrations of chlorophyll *a* at Station A are closely bracketed by those predicted by Equation 1 at $D_B = 2.3 \times 10^{-7}$ cm^2 s^{-1}, as determined from the^{210}Pb distributions, and $k_d = 0.03$ d^{-1} or $k_d = 0.014$ d^{-1} (Fig. 8.2). Thus, assuming

that degradation kinetics for chlorophyll *a* in Young Sound are similar to those in Long Island Sound, chlorophyll *a* distributions are consistent with the D_B estimates obtained by other methods.

During sediment reworking, the infauna moves water to a much greater extent than solids. Macrofauna mainly transport water through irrigation of burrows, while protozoan and meiofauna activity increase dispersion, resulting in enhanced diffusion coefficients, assuming homogeneous distribution (Glud & Fenchel, 1999). Bromide-tracer experiments and comparison of oxygen micro-distributions and oxygen fluxes in sediments from Station A showed c. 50% enhancement of diffusional transport relative to molecular diffusion, the effect being detectable to 8 cm depth (Berg et al., 2001). Irrigation, described as non-local mixing of pore water with bottom water (Boudreau, 1997), was quantified as part of fitting a comprehensive diagenetic model to the data from Station A (Berg et al., 2003). Best fits were obtained at an exchange coefficient decreasing linearly from 48 yr^{-1} at the sediment surface to zero at 16 cm depth. The surface value is near the mean of exchange coefficients determined in coastal sediments, which typically fall within the range 5–300 yr^{-1} (Wang & Van Cappellen, 1996; Boudreau, 1997).

Biodiffusion and irrigation are likely to vary seasonally in response to the availability of fresh organic matter, but such variation cannot be discerned from the available data. Likewise, a decrease in intensity of the transport processes is expected with the decrease in biomass towards deeper waters (Chapter 7). This effect is, however, difficult to evaluate quantitatively from the given dataset.

Carbon pools: Organic material reaching the sediment surface originates either from pelagic (or sea-ice-related) production, benthic production, surrounding terrestrial sources, or may represent input from the Greenland Sea (Chapter 6, Chapter 9). The organic carbon content of the sediment at Stations A to D was 1.1–1.4% wt. (average 1.2%) and displayed no obvious trend with water depth, while the content at Station A0 was only 0.6% (Glud et al., 2000). Inorganic carbon contents, excluding macroscopic shell debris, were ≤0.1% wt (S. Rysgaard, unpublished results). Carbon-to-nitrogen ratios were similar at all sites, 10–12 mol:mol (Glud et al., 2000), in line with other fine-grained coastal sediments (e.g. Rysgaard et al., 2001). The combination of carbon contents and sediment accumulation rates yields an annual burial of 4.7×10^7 mol, or 0.57 Gg, of organic carbon in outer Young Sound (Table 8.2).

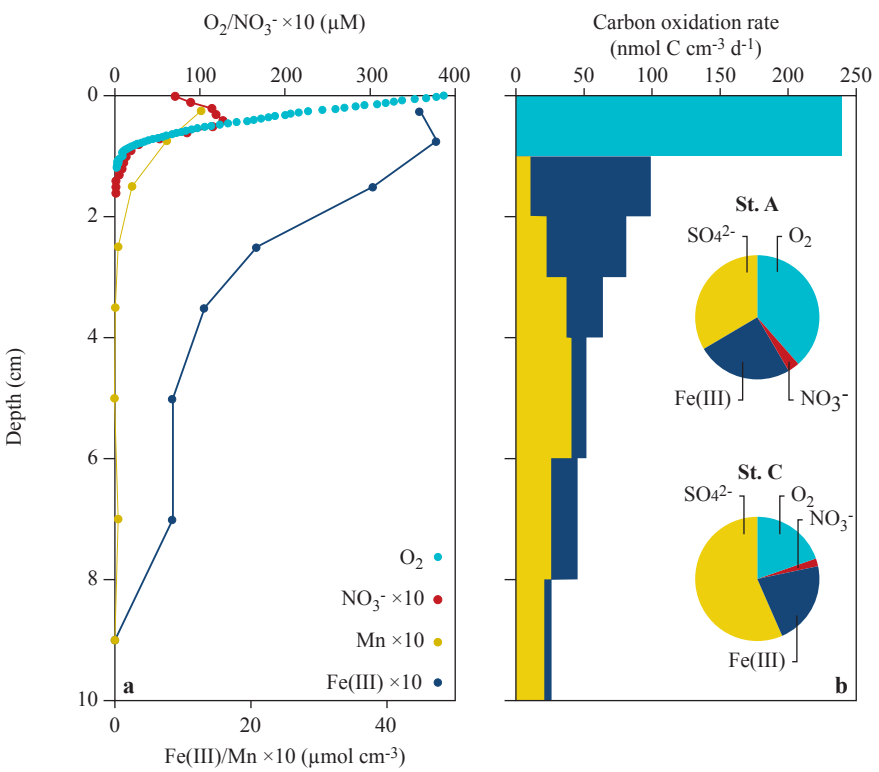

Figure 8.3 (a) Depth distributions at Station A of electron acceptors for carbon mineralization and **(b)** of carbon oxidation rates partitioned into terminal electron-accepting processes (Inferior contribution from denitrification not shown). Pie inserts show the relative contributions of electron acceptors to carbon oxidation at Stations A and C. In the left graph, note separate axes for solutes (in µmol per liter of pore water) and particulates (in µmol per cm^3 of wet sediment) and that concentrations of nitrate and manganese were multiplied by 10. Data from Rysgaard et al. (1998) and Glud et al. (2000).

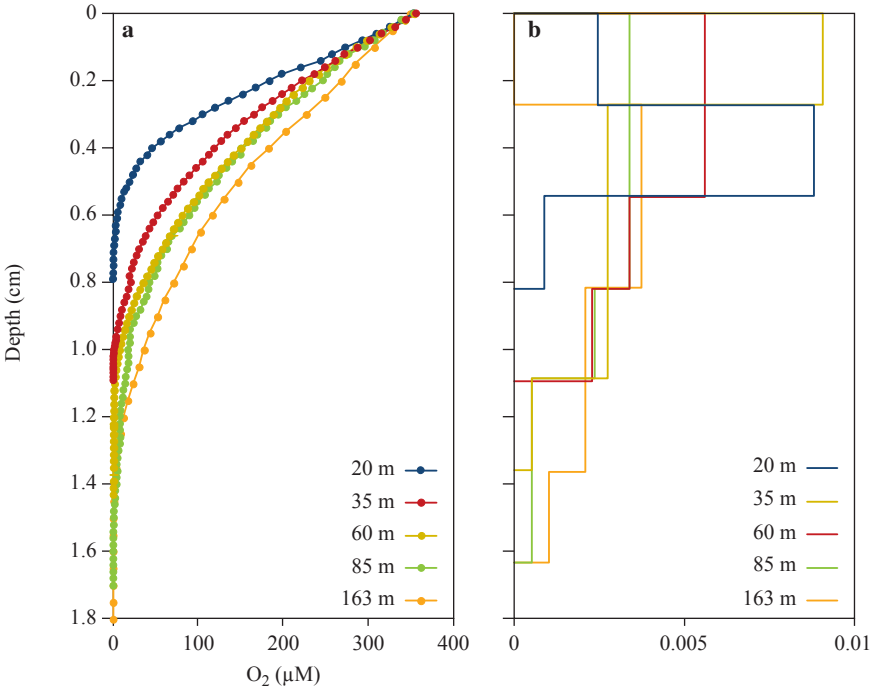

Figure 8.4 (a) Microscale oxygen distributions and **(b)** oxygen consumption rates at five stations along a transect across Young Sound. Profiles were measured during the summer activity peak. Oxygen consumption rates were determined by automated parabolic curve fitting to concentration profiles using the program PROFILE (Berg et al., 1998). Data from Glud et al. (2000).

8.3.2 Zonation of diagenetic processes

Electron acceptors: The typical sequential depletion of the major electron acceptors, oxygen, nitrate, manganese oxide, iron oxide, and sulfate with increasing depth in the sediment (e.g. Froelich et al., 1979) was well resolved in Young Sound (Fig. 8.3). At Station A, oxygen penetrated c. 10 mm into the sediment, and nitrate reached only a few mm deeper. The manganese oxide content was relatively low for fine-grained coastal sediments (e.g. Aller, 1994; Thamdrup et al., 1994a) and reactive manganese oxide was depleted within 2 cm of the surface. The sediment was rich in iron oxides, the poorly crystalline fraction reaching 8 cm depth, while more crystalline oxides were present throughout the investigated sediment column (Rysgaard et al., 1998). Sulfate concentrations decreased slightly through the upper sediment layers.

Only a slight seasonal variation was seen in benthic oxygen penetration, but the settling of the summer bloom markedly shifted the depth distribution of oxygen consumption rates within the oxic zone (Rysgaard et al., 1998). Thus, before the bloom in June, oxygen consumption peaked near the bottom of the oxic zone, likely coupled to the reoxidation of inorganic metabolites from below. In late July, the activity was concentrated in the upper 2 mm, coupled to the degradation of the newly settled bloom (Fig. 8.4).

Oxygen penetration increased with water depth from 7 mm at Station A0 to 16 mm at Station D (Fig. 8.4). Distributions of the remaining electron acceptors along the transect were not investigated, but the accumulation rates of soluble reduced manganese and iron at Station C, and the distribution of sulfate reduction rates along the transect indicate a stretching of the entire redox zonation with increasing water depth (see below).

Pathways of organic carbon oxidation: At Stations A and C, rates of organic carbon oxidation, determined as the production of dissolved inorganic carbon, decreased with sediment depth, reaching low rates at 10 cm depth (Fig. 8.3). In accordance with the chemical zonation, oxygen, iron oxide and sulfate were the most important electron acceptors for carbon oxidation, aerobic respiration being dominant at Station A, while bacterial sulfate reduction dominated at Station C (Fig. 8.3). Denitrification contributed only 2–3% to carbon oxidation, while dissimilatory manganese reduction was undetectable. The detection limit for this process, based on the applied bag-incubation technique, is estimated at 5–10% of the DIC production rate (Thamdrup, 2000). The partitioning of carbon oxidation between the electron acceptors was similar to results from temperate fine-grained sediments with moderate organic loading and well-oxygenated bottom water (Thamdrup, 2000; Rysgaard et al., 2001), and comparable with permanently

cold sediments from the fjords of Svalbard (Kostka et al., 1999). Also, the partitioning of anaerobic carbon oxidation into dissimilatory iron reduction and sulfate reduction showed the same dependency on the concentration of poorly crystalline iron oxide as that found at other locations, a gradual transition being seen between the two pathways in parallel to the decreasing iron oxide concentration (Fig. 8.3; Thamdrup, 2000; Jensen et al., 2003).

At Stations B and D, the relative contribution of bacterial sulfate reduction to carbon mineralization was 46%, which lies between the values for Stations A and C, while the contribution was only 16% at the sandy Station A0 (Fig. 8.5). Although quantified only at Stations A and C, denitrification was likely of minor importance for carbon oxidation throughout the transect, as is the case for other shelf transects covering the same range of oxygen penetration depths and bottom-water nitrate concentrations (e.g., Thamdrup, 2000; Rysgaard et al., 2001). The importance of dissimilatory iron reduction is mainly

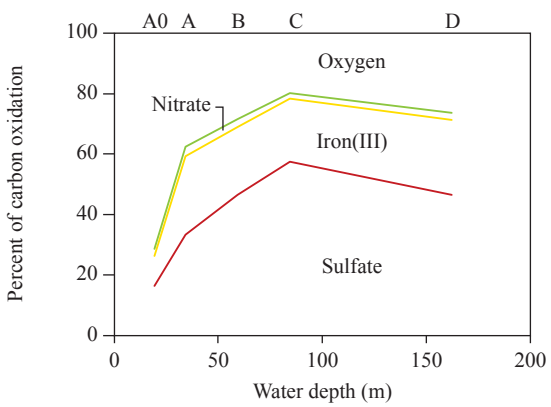

Figure 8.5 Relative partitioning of carbon oxidation pathways along a section of outer Young Sound based on data from Glud et al. (2000). Complete partitioning of carbon oxidation pathways was only available for Stations A and C, while oxygen consumption and sulfate reduction were determined at all stations. At Stations A0, B and D, the contribution from denitrification was estimated at 2.5% as the average of the results from stations A and C (3 and 2%). Likewise, the contribution from iron reduction at Stations B and D was set at 24% as the average of Stations A and C (26 and 21%). The 10% contribution from iron reduction at Station A0 is a maximum estimate based on other studies of coarse-grained sediments. See text for further details on calculation and discussion of the rationale behind estimates.

regulated through reactive iron contents and bioturbation intensities (Canfield et al., 1993a; Jensen et al., 2003). Thus, although extrapolation to the entire transect is difficult, the contributions at Station B and D are expected to be of a magnitude similar to that found at Station A and C (Fig. 8.5). This approximation is justified by our observation that sulfate reduction rates at all sites were suppressed in the upper centimeters of the anoxic sediment to 4 cm depth or deeper, which indicates active dissimilatory iron reduction (Sørensen & Jørgensen, 1987; Hines et al., 1991; Thamdrup, 2000). The fact that the combined contributions from iron and sulfate reduction at the four outer sites are relatively alike indicates that the fractions of the organic carbon reaching anoxic layers are similar. By contrast, Station A0 exhibited a lower contribution from sulfate reduction, indicating less anaerobic mineralization in general. Furthermore, iron reduction is generally of limited importance in sandy sediments, likely due to low iron contents (Slomp et al., 1997; Jensen et al., 2003). We therefore expect that iron reduction is of little importance at this site, and that oxygen respiration dominates the cumulated anaerobic pathways.

Reoxidation reactions: Hydrogen sulfide, the soluble product of bacterial sulfate reduction, was not detected in the pore waters, due to rapid precipitation of elemental sulfur and iron sulfides, mainly pyrite (FeS_2; Rysgaard et al., 1998; Berg et al., 2003). Soluble Fe^{2+} accumulated in the pore water, but as in most other coastal sediments, most of the ferrous iron formed through bacterial iron reduction or abiotic reduction by hydrogen sulfide accumulated in the solid phase (e.g. Thamdrup et al., 1994a). At the sediment accumulation rate of 0.09 cm yr^{-1} at Station A, the burial of reduced iron and sulfur compounds amounted to 0.37 mol electron equivalents m^{-2} yr^{-1} ([82 µmol Fe(II) cm^{-3} × 1 eq. + 2 µmol FeS × 9 eq. + 21 µmol FeS_2 × 15 eq.] × 0.09 cm yr^{-1}; concentrations from Rysgaard et al. (1998)), equivalent to <1‰ of the annual carbon oxidation. Benthic release rates of soluble reduced manganese, iron, and hydrogen sulfide from sediments underlying well-oxygenated bottom water are typically insignificant relative to the metabolic rates of the sediment (e.g. Thamdrup et al., 1994b; Berelson et al., 2003). Thus, in Young Sound, as in most other marine sediments, almost all of the reduced inorganic metabolites formed during anaerobic carbon mineralization were reoxidized within the

sediments, and oxygen was the ultimate acceptor of almost all electron equivalents released during carbon oxidation.

In addition to oxygen consumption coupled directly or indirectly to carbon oxidation, oxygen was used for nitrification of ammonium released during mineralization, and nitrate formed in this way was the main source for denitrification (Rysgaard et al., 1998). Annual fluxes of ammonium and nitrate from the sediment at Station A were similar (33 and 30 mmol m^{-2}, respectively), while the flux of N_2 was 71 mmol N m^{-2}. Thus, oxygen consumption coupled to nitrification (with or without subsequent denitrification) was 202 mmol m^{-2} ([30 mmol m^{-2} + 71 mmol m^{-2}] × 2; two mol O_2 consumed per mol NH_4^+ oxidized to NO_3^-), corresponding to 9% of the benthic oxygen consumption (Rysgaard et al., 1998).

An estimate of oxygen consumption by macrofauna has previously been deduced from preliminary estimates of biomass of the dominant macrofauna and mass-specific metabolic rates from the literature (Glud et al., 2000). The relative contribution to total benthic oxygen consumption, and the equivalent carbon mineralization, was only between 4 and 9% at Stations A0 to C, corresponding to contributions to organotrophic oxygen respiration of 24% and 35% at Stations A and C, respectively, and likely to similar or smaller contributions at the other sites (Fig. 8.5). This value does not take into account megafauna like larger brittlestars and mussels and may thus represent an underestimate of the total benthic fauna contribution (See Chapter 7). Macrofauna may greatly stimulate mineralization processes indirectly through particle and solute transport. However, their direct contribution to total (aerobic and anaerobic) carbon oxidation is generally of minor importance compared with microbial activity.

8.3.3 Benthic respiration rates

Benthic respiration rates were determined from the fluxes of oxygen and dissolved inorganic carbon (DIC) across the sediment/water interface during incubations of sediment cores. One flux determination was achieved *in situ* at Station A using a benthic flux chamber (Glud et al., 2000). The *in situ* rates, 11.7 and 13.1 mmol m^{-2} d^{-1} for O_2 and DIC, respectively, were not significantly different from the rates of 9.9 ± 2.7 mmol O_2 m^{-2} d^{-1} and 9.7 ± 2.4 mmol DIC m^{-2} d^{-1} measured in laboratory incubations of cores retrieved at the same time. Although this result still needs to be verified by replication, it indicates that the available laboratory-based fluxes are reasonable estimates of *in situ* values, and, hence, that the underestimation of benthic fluxes frequently observed for core incubations (e.g. Archer & Devol, 1992; Glud et al., 1998; Glud et al., 2003) was not critical in Young Sound.

The annual oxygen respiration and carbon oxidation rates at Station A during the period 1996–97 were 2350 and 2295 mmol m^{-2} (Rysgaard et al., 1998). After subtraction of oxygen consumed by nitrification and of carbon oxidation coupled to denitrification (because resulting N_2 escapes from the sediment and unlike the other products of anaerobic respiration is not reoxidized with oxygen; see data above) we obtain a respiratory quotient of [2350 – 202]/[2295 – (71 × 1.25)] = 0.97. This corresponds to an average oxidation state of zero for the oxidized organic carbon. A similar balance of oxygen and DIC fluxes was found at the other stations (Glud et al., 2000).

Seasonal and depth variation: The benthic respiration rate at Station A was c. 6 mmol C m^{-2} d^{-1} through most of the 1996–97 study, and similar rates have been measured repeatedly since then (Fig. 8.6). Within the first two weeks of July, however, the rates almost doubled, after which the activity declined, reaching the baseline level in early August. The peak in microbial activity coincided with the settling of the

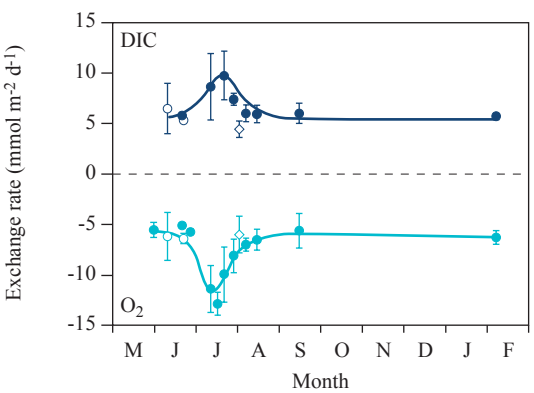

Figure 8.6 Seasonal variation of benthic exchange rates of dissolved inorganic carbon (dark blue) and oxygen (light blue) at Station A. Negative fluxes denote benthic uptake. Filled circles: June 1996–February 1997 (Rysgaard et al., 1998), open circles: June 1999 (B. Thamdrup & H. Fossing, unpubl. res.), open diamond: August 2000 (J.W. Hansen, unpubl. res.).

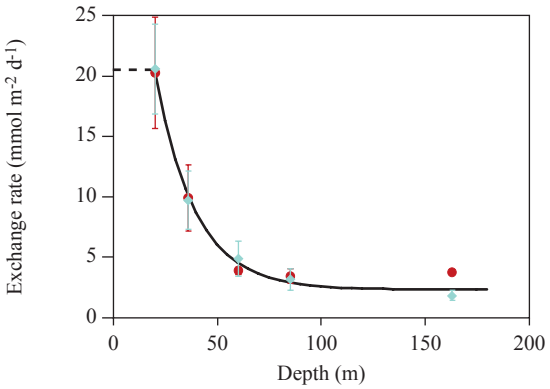

Figure 8.7 Absolute benthic exchange rates of oxygen (blue) and dissolved inorganic carbon (red) as a function of water depth in Young Sound. An exponential function fitted to the DIC data is shown in black for 20–180 m. The dotted line inside 20 m indicates the constant DIC flux assumed for calculation of a basin-wide rate (see text for details). Data from Glud et al. (2000).

summer bloom (Chapter 5), and represents the degradation of the most reactive fraction of the detritus resulting from this bloom. The lower baseline respiration was fuelled by organic material of lower reactivity, which had accumulated over several years (see also below).

Benthic respiration rates decreased asymptotically with increasing water depth from 20 mmol C m^{-2} d^{-1} at Station A0 to 2–3 mmol m^{-2} d^{-1} at Stations C and D (Fig. 8.7). For DIC production, the following exponential function was fitted to the data, where *Z* is depth in meters (Glud et al., 2000 – note that the pre-exponential function was previously incorrectly typed):

$$DIC_{release} = 2.26 + 18.2\ e^{1.05-(0.0525 \times Z)} \quad (2)$$

The transect was analyzed in the second half of July, when the rate at Station A was almost twice the baseline level. Seasonality is expected to attenuate with depth due to longer transport times, but as rapidly sinking fecal pellets account for most of the organic matter deposition (Chapter 6), this attenuation may be small. An effect of the summer bloom at the deeper stations was also indicated by the enhanced oxygen consumption in the upper part of the oxic zone, consistent with the observation at Station A of a shift in the highest oxygen consumption rates from the deeper part of the oxic zone during winter to the upper part during summer (Fig. 8.4). Although seasonal variations at the deeper sites need further quantification, we assume, based on the available evidence, that the respiration rates in Fig. 8.7 represent elevated summer rates. At all depths, these rates scale to the annual mean rates by the same factor as that determined for fluxes at Station A at the same time (Fig. 8.6). At Station A, the maximum DIC flux, measured at the time when the transect study took place, was 10.0/6.3 = 1.6 times higher than the mean. Thus, the best estimate of the annual mean benthic carbon oxidation rate as a function of water depth is obtained by division of Equation 2 by 1.6.

Equation 2 predicts that carbon oxidation rates continue to increase shoreward from Station A0 at 20 m, which was the shallowest station used to derive the equation. However, a recent study of benthic primary production demonstrated relatively constant fluxes of DIC and oxygen in dark incubations of cores from this region sampled in August (DIC flux 12.8 and 10.7 mmol m^{-2} d^{-1} at 5 and 10 m, respectively (Glud et al., 2002); see also Chapter 9). These fluxes were also similar to the annual average flux of 12.9 mmol m^{-2} d^{-1} calculated for 20 m when correcting Equation 2 for seasonality. Thus, for all depths shallower than 20 m, we assume the same carbon oxidation rate for the carbon budget as that calculated for 20 m. We note, however, that determination of benthic fluxes in coarse-grained sediments like those found in this zone, is often complicated by the high sediment permeability, which allows pore-water advection driven by bottom-water currents (Huettel & Gust, 1992; Reimers et al., 2004). Furthermore, the presence of benthic microalgae often complicates the determination of mineralization rates at such locations (Glud et al., 2002).

Combining the depth-dependent carbon oxidation rates with the hypsometry of outer Young Sound yields a total benthic carbon oxidation rate of 1.1 × 10^8 mol or 1.3 Gg yr^{-1} (Table 8.2). The estimated contribution from 0–20 m depth is 38% of the total (Table 8.2), which, considering our reservations regarding the rate estimates from this region, emphasizes the need for further studies of benthic respiration in this zone. A novel, non-intrusive approach for flux determinations (Berg et al., 2003a) may be particularly useful in this type of environment.

Flux of dissolved organic carbon (DOC) from the sediment to the water column is another potentially

Table 8.2 Organic carbon budget for outer Young Sound[1)].

Zone[2)]	Depth	Area		Accumulation	C_{org}	Burial		Oxidation rate[3)]		
	(m)	(km^2)	(%)	(g cm^2 yr^{-1})	(mmol g^{-1})	(mol yr^{-1})	(%)	(mmol m^{-2} d^{-1})	(mol yr^{-1})	(%)
0–10 m	0–10	5.2	7	0	n.a.	0.0E+0	0	13.7	2.6E+7	24
10 m–A0	10–20	3.1	4	0.072	0.50	1.1E+6	2	13.7	1.6E+7	14
A0	20–30	3.4	4	0.072	0.83	2.0E+6	8	10.3	1.3E+7	12
A	30–50	7.5	10	0.072	1.17	6.3E+6	13	5.6	1.5E+7	14
B	50–70	10.2	13	0.072	0.92	6.7E+6	14	2.9	1.1E+7	10
C	70–120	39.7	52	0.072	0.92	2.6E+7	55	1.7	2.5E+7	23
D	120–180	6.8	9	0.072	1.00	4.9E+6	10	1.4	3.6E+6	3
Total:		76.1				4.7E+7			1.1E+8	
Total carbon input (burial + oxidation):									1.6E+8 mol yr^{-1}	
Fraction oxidized:									70%	

[1)] Hypsometry of Region 1 (Balsaltø to Sandøen) of Rysgaard et al. (2003), remaining data from Glud et al. (2000) with modifications as discussed in the text, except sediment accumulation rates from this study. See text for details.
[2)] Depth intervals separated approximately midway between the main stations A0–D
[3)] Estimated annual mean (see text), averaged over depth interval by integration of Equation 2 in text.

significant loss term for the benthic carbon budget. The benthic DOC flux was measured in sediment cores collected 2 August 2000 for the long-term whole-core incubation described below. During the first ten days of incubation, the DOC flux was 0.34 ± 0.66 mmol m^{-2} d^{-1}, calculated as the mean ± SE of four consecutive flux determinations on each of five cores. This mean value corresponds to 6% of the DIC flux of 5.4 ± 0.5 mmol m^{-2} d^{-1} measured in the same cores, suggesting that DOC loss has a minor role as a sink for sediment carbon. Comparable small contributions have been reported from other marine sediments exhibiting mineralization rates in the range observed in Young Sound (Alperin et al., 1999; Burdige et al., 1999). Thus, with the further support supplied by these studies, we assume that DOC fluxes are unimportant for the benthic carbon budget in Young Sound.

From the rates of mineralization and burial of organic carbon in the sedimentary record we obtain a total loss of carbon from the surface sediment of 1.5 × 10^8 mol yr^{-1}. Assuming that the sediments are close to steady state with respect to carbon fluxes, this value is also an estimate of the total carbon flux to the sediment. Remineralization accounts for 69% of deposition, which is close to the center of the range for sediments with similar sediment accumulation rates (Canfield, 1993).

8.3.4 Kinetics of mineralization.

A central question in the investigations of benthic respiration in Young Sound has been whether or not the rates and pathways of organic carbon oxidation are substantially different from those in warmer locations. As discussed above, the array of microbial processes active in Young Sound, as well as their relative importance, is the same as in continental shelf sediments at lower latitudes. Benthic respiration rates are a function of substrate availability, and since only a lesser fraction of the deposited organic matter is permanently buried in the sediment of Young Sound (Table 8.2), like in other regions, the depth-integrated rates are ultimately set by the flux of organic matter to the sediment. Thus, any effects of the low temperature on metabolism should be sought in the kinetics of the processes rather than in their integrated rates.

Diagenetic modeling: The kinetics of carbon oxidation was explored both by modeling and experiments. By an inverse modeling approach, a comprehensive diagenetic reaction-transport model (Berg et al. 2003b) was fitted to the biogeochemical data obtained in 1996-97 (Rysgaard et al., 1998). The result documented that both the temporal and the spatial variations of carbon oxidation rates at Station A could be fully described by assuming that the organic matter consisted of two degradable pools, and an undegradable residue (Berg et al., 2003b). The rapidly and slowly degradable fractions decayed accord-

ing to first-order kinetics, with rate constants of 76 and 0.095 yr^{-1}, respectively, and the two fractions deposited at an average annual ratio of 1:3. The two rate constants represent one pool of organic carbon that decays within a few days, and one is degraded only in the order of a decade. This slowly degradable fraction sustained the almost constant carbon oxidation rates during the long period of ice cover (Fig. 8.6).

As discussed by Berg and coworkers (2003b), the rate constants are similar to those determined in sediments or in organic matter decay experiments at higher temperatures, indicating that low temperature has no marked effect on the kinetics of carbon oxidation. However, order-of-magnitude variations in rate constants from other comparable environments prohibit any attempt to quantify temperature effects such as the doubling of the rate with a temperature increase of 10 degrees (Q_{10} = 2) typically observed for individual microbial processes (see below).

To explore in greater detail the dynamics of carbon oxidation and the influence of temperature, incubation experiments with addition of organic matter were carried out, including 1) anoxic incubations of homogenized sediment at different temperatures with addition of organic detritus, and 2) year-long whole-core incubations at *in situ* temperature exploring the decay of the native organic pool. These experiments are discussed below.

Anoxic sediment incubations: To explore the dynamics of organic matter mineralization as a function of temperature and carbon concentration, sediment from Station A was amended with different amounts of complex organic matter in the form of freeze-dried, finely ground cyanobacteria of the genus *Arthrospira* (commercial name *Spirulina*, Aldrich). The sediment was incubated anoxically in gas-tight plastic bags (Hansen et al., 2000) for two weeks at 0, 9 and 20°C, and the mineralization of organic matter was quantified from the production of DIC and ammonium, and from sulfate reduction rates during this period (Thamdrup & Canfield, 2000); only DIC results will be discussed here.

Both organic additions and increases in temperature stimulated the rate of DIC production with little or no lag phase, and DIC concentrations increased quasi-linearly in all incubations, indicating an immediate and stable response of carbon mineralization processes to the environmental changes (data not shown). Rates increased in an exponential-like manner as a function of temperature (Fig. 8.8), and non-linear fits of the Arrhenius equation to the data yielded an activation energy of 42.5 ± 2.5 kJ mol^{-1} in the non-amended sediment, and a similar mean value of 43.5 ± 5.6 kJ mol^{-1} in the organic-amended incubations. The mean activation energy for all incubations corresponded to a Q_{10} for the 0–10°C interval of 2.0. This value is similar to the Q_{10} of 1.8 for oxygen respiration and in the lower end of the range of 1.9–3.2 for bacterial sulfate reduction found in Arctic sediments from Svalbard (Sagemann et al., 1998; Thamdrup & Fleischer, 1998). The low Q_{10} value indicates that the benthic microbial community of Young Sound is only moderately affected by the very low *in situ* temperature, a response characteristic of psychrophilic or psychrotolerant organisms.

The experiment demonstrated the ability of the microbial community to respond rapidly to an input

Measuring the microdistribution of oxygen in the upper sediment layer using an *in situ* profiling instrument.

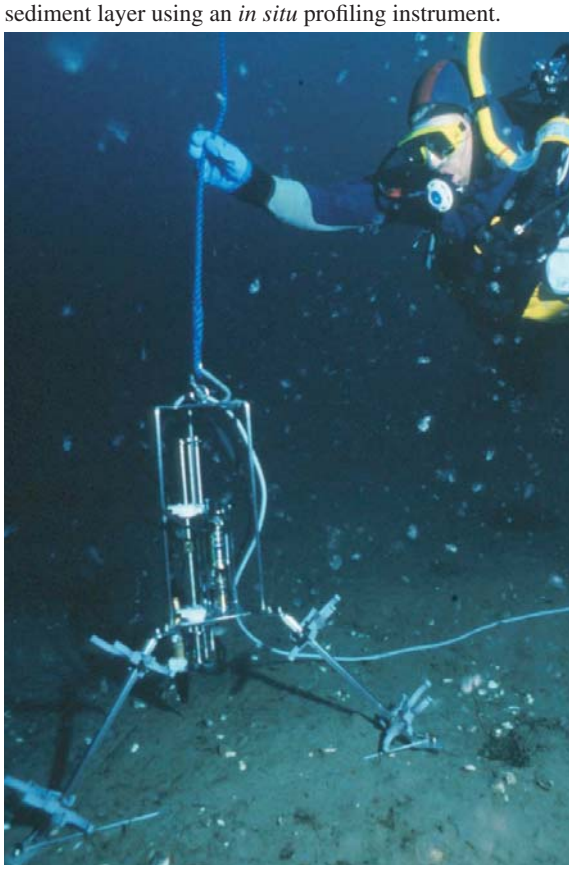

Photo: Jens S. Laursen

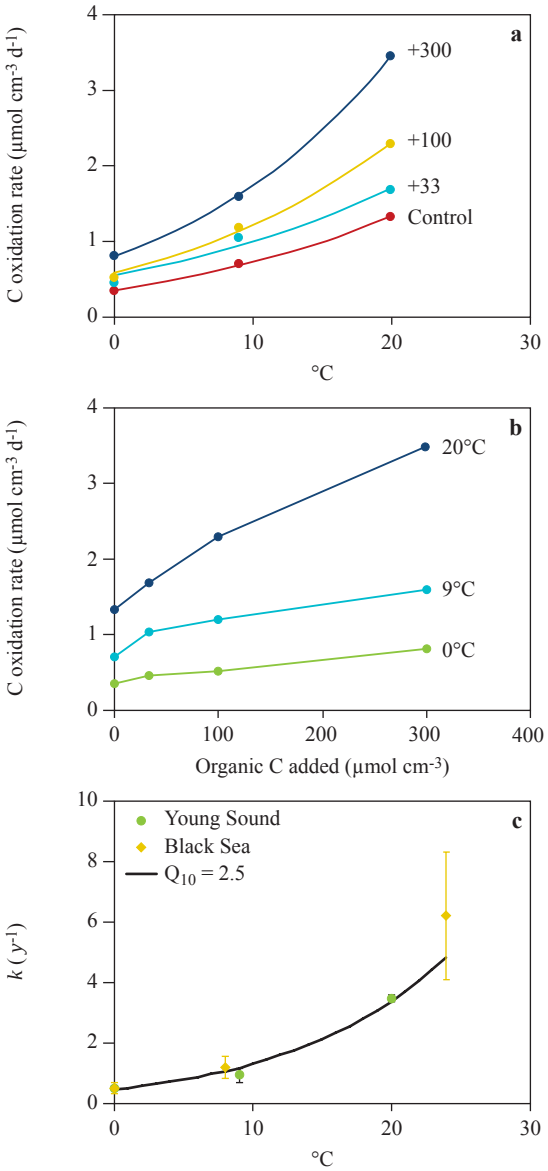

Figure 8.8 Anaerobic carbon mineralization rates in sediment from Station A sampled in July 1996 and amended with cyanobacterial biomass. **(a)** Temperature dependence. Datasets represent the addition of (bottom to top) 0, 33, 100, and 300 µmol added organic C per cm^3. Curves are least-squares non-linear fits of the Arrhenius equation. **(b)** Dependence on organic carbon addition. Datasets represent incubations at (bottom to top) 0, 9 and 20 °C. **(c)**: Temperature dependence of bulk 1st-order rate constants of added organic carbon oxidation in Young Sound sediment compared with a temperate location in the Black Sea (data from Rosselló-Mora et al. (1999)). Black curve represents Q_{10} = 2.75.

of complex organic matter even at subzero temperatures, consistent with the rapid increase in fluxes observed during summer (Fig. 8.6). The largest addition increased the carbon mineralization rate by a factor of 2.3 (Fig. 8.8). There was no change in total bacterial counts during the incubations (data not shown). Although growth rates of bacteria in this sediment are not known, the rapid response suggests that the change reflects increased metabolic rates in individual cells, rather than growth. In a similar experiment, in which Black Sea sediment was amended with organic matter (Rosselló-Móra et al., 1999), activation of cells already present in the sediment was likewise seen to dominate over growth.

At 0 and 9°C, carbon mineralization rates increased approximately linearly as a function of the amount of organic carbon added, while some saturation was indicated at the largest addition at 20°C (Fig. 8.8). The observed linearity is consistent with first-order reaction kinetics of organic carbon at the rate constant given by the slope of the line (see also Westrich & Berner, 1984). Rate constants obtained by linear regression increased from 0.54 ± 0.05 yr^{-1} at 0°C to 3,5 ± 0.11 yr^{-1} at 20°C (Fig. 8.8; largest amendment at 20°C excluded from regression). These rate constants represent the added organic carbon in bulk and therefore underestimate the more reactive fraction of the organic carbon pool that dominates carbon mineralization during the initial stages (e.g. Westrich & Berner, 1984). Assuming that carbon mineralization is fuelled by a rapidly decaying pool accounting for 17% of the total organic carbon added, as is typical of fresh phytodetritus and as found in the Young Sound sediment (Westrich & Berner, 1984; Berg et al., 2003b), we obtain a rate constant for this fraction of 0.54/0.17 = 3.2 ± 0.3 yr^{-1} at 0°C. Rate constants obtained by similar approaches at 20–22°C range from 3–33 yr^{-1} for aerobic mineralization and 7.2–8.8 yr^{-1} for mineralization coupled to sulfate reduction (Westrich & Berner, 1984). Assuming Q_{10} = 2.0 as determined above, this range corresponds to 0.75–8.3 yr^{-1} at 0°C. The rate constant estimated in the present experiment falls near the center of this range. Thus, the results indicate that the kinetics of carbon mineralization in Young Sound sediments does indeed scale with that observed at higher temperatures by a factor reflecting this relatively weak temperature dependence, and that the microbial population is not disproportionately inhibited by low temperature, as

previously hypothesized for other cold environments (Pomeroy & Deibel, 1986). For further discussion see Nedwell (1999) and Pomeroy & Wiebe (2001).

The above conclusion is further strengthened by a direct comparison of the results with those of an analogous experiment, in which non-euxinic Black Sea sediment, with a stable temperature of 11°C *in situ*, was incubated at different temperatures after additions of varying amounts of *Arthrospira* biomass, in a procedure similar to that used in the present study (Rosselló-Mora et al., 1999). Rate constants in the Black Sea sediment were very similar to those from Young Sound (Fig. 8.8). In addition to supporting the conclusion of a "normal" temperature effect of near-freezing temperatures on carbon oxidation rates, the similarity of the results from the two experiments involving sediments exhibiting a difference in *in situ* temperature of 12°C, suggests that the overall temperature characteristics of the microbial populations at the two sites are similar, rather than being the result of specialized adaptations to a narrow temperature range around the *in situ* temperatures.

Long-term whole-core incubations: The model-derived carbon mineralization kinetics was further tested experimentally in sediment incubations stretching over a year with no input of organic matter. Sediment cores for this experiment were collected at Station A on 2 August 2000. Twenty cores without visible macrofauna were brought back to the laboratory, where the total exchange rates of nutrients, O_2 and DIC (only oxygen data are presented here) were measured at *in situ* temperature (-1.0 °C) at regular time intervals. Before the first flux measurement, the sediment surfaces of some cores were supplied, in groups of five, with organic debris in the form of A) freshly collected fecal pellets from the bivalve *Hiatella arctica* (93 mmol C_{org} m^{-2}), B) a freeze-killed fresh culture of the diatom *Ditylum brightwellii* (97 mmol C_{org} m^{-2}), or C) a freeze-killed fresh culture of the cryptomonad *Rhodomonas salina* (157 mmol C_{org} m^{-2}), while five cores remained non-amended. Two weeks later, one core from each of the four treatments was transferred to Denmark in an insulated box to be placed at *in situ* temperature in a temperature-regulated room in order to follow the solute exchange rates over a year (measurements were performed approximately once every month). The ambient water of the submerged cores was replaced with sand-filtered seawater at regular time intervals to avoid excessive build-up of solutes released from the sediment. While the cores amended with algal debris initially showed elevated oxygen fluxes (data not shown), there was no significant difference in average oxygen uptake between the four different treatments after 19 days following the transport home (fluxes in mmol m^{-2} d^{-1}: 4.8 ± 0.5, 4.6 ± 0.6, 5.4 ± 0.6, 5.6 ± 0.6 in treatments A, B, C and control, respectively; n = 13). Thus, fluxes after day 19 are presented as the average of all four cores, while earlier fluxes are averages of the five control cores.

Except for the first flux measurement (Fig. 8.9), the initial oxygen uptake rates corresponded to typical summer peak rates (Fig. 8.6), presumably due to summer enrichment with reactive organic matter. The total oxygen uptake gradually declined during the first c. 50 days as the sediment was deprived of any external organic carbon source. After this period, the rate reached a constant level of c. 4.5 mmol m^{-2} d^{-1}, which persisted until the experiment ended at c. 400 days. This pattern was similar to that observed in the seasonal study of 1996, although the return to the winter level was somewhat protracted (Fig. 8.10).

The data confirmed that the degradation of organic carbon is described well by two pools of material that degrade at widely different paces, as also concluded by Berg and coworkers (Berg et al., 2003b). The results also demonstrated that the sediment of Young Sound sustained a relatively high mineralization rate during extended periods without external inputs of organic material, fuelled by relatively refractory

Photo taken by diver from below sea ice of scientists collecting intact sediment samples with a sea floor sampler (Kajak).

Photo: Søren Rysgaard

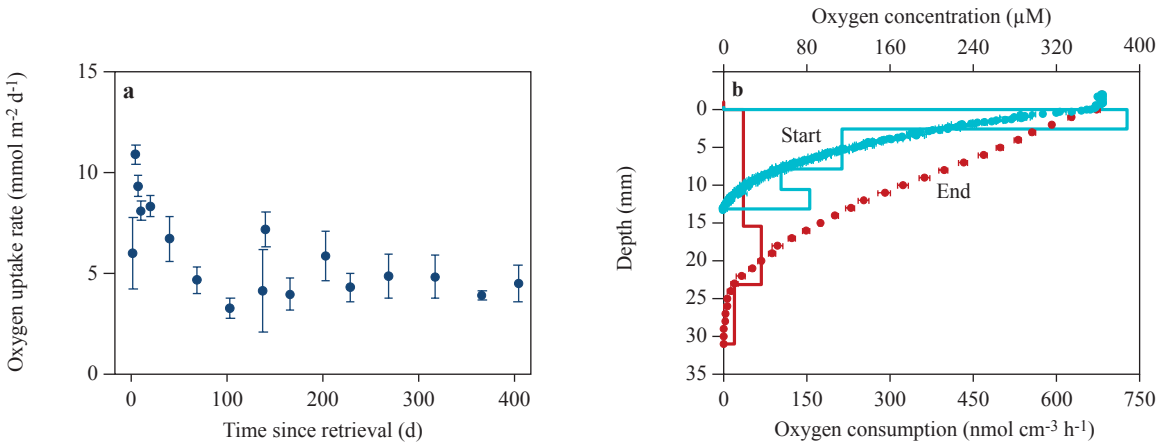

Figure 8.9 Changes in oxygen uptake and oxygen penetration in sediment cores incubated at *in situ* temperature for 400 days with no carbon input. **(a)** Benthic oxygen uptake as function of time. Mean ± SE, n = 4 except first four samplings: n = 5. **(b)** Oxygen distribution in sediment from the start (blue) and end (red) of the experiment. Step functions are oxygen consumption rates (lower axis) derived from the concentration profiles using the fitting program PROFILE (Berg et al., 1998).

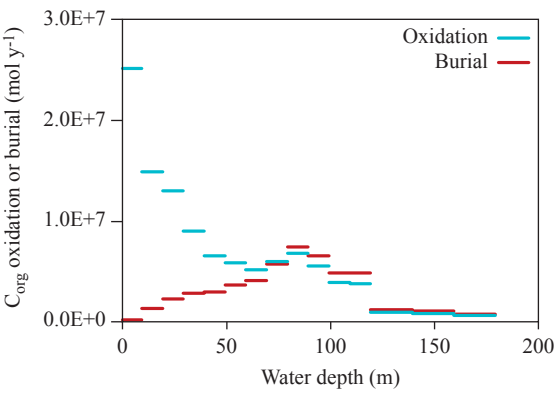

Figure 8.10 Annual organic carbon oxidation and organic carbon burial in outer Young Sound integrated over 10-m depth intervals.

material with a first-order rate constant of >>1 yr^{-1}. Integrated over the entire c. 400-day period the activity corresponded to the degradation of 1.7 mol C m^{-2} (assuming a respiratory quotient of 1.0). This is still a minor fraction of the total pool of organic material available in the sediment (0.8% of 206 mol m^{-2} to 20 cm depth). The measurements also suggest that interannual variability in organic carbon production is not expressed proportionally in the benthic mineralization activity, as a significant fraction of the degraded material at any given time is many years old. Year-to-year variations in the winter activity may therefore be relatively invariable, despite large variations in the summer production.

Oxygen microprofiles measured immediately after core sampling and again at the end of the experiment further supported the conclusions from the oxygen uptake measurements (Fig. 8.9). Initially, the sediment exhibited shallow O_2 penetration, maximum volume-specific activity being found at the organic-carbon-enriched sediment surface and gradually declining with sediment depth. After 400 days, the O_2 penetration depth had increased by a factor of 2, and the volume-specific activity was almost depth-independent, indicating a more evenly distributed source of reductants.

8.3.5 Synthesis and conclusions

The integrated carbon budget for outer Young Sound sediments showed that c. 70% of the organic carbon arriving at the seafloor is oxidized (Table 8.2). The c. 30% retention of organic matter in these sediments is substantial, but well within the wide range of values estimated for other depositional coastal areas of similar water depths (e.g. 9–50% for Danish waters (Jørgensen et al., 1990; Jørgensen, 1996; see also Canfield, 1993). Comparison of oxidation and burial as a function of water depth, however, demonstrated large variations in the relative importance of these two sinks for organic carbon in surface sediments (Fig. 8.10). Thus, while carbon oxidation occurred mainly

in relatively shallow waters – 49% of the basin's oxidation occuring inside 30 m depth – organic carbon burial followed the hypsometry of the basin, the largest fraction accumulating around 80–90 m depth. The different distributions of oxidation and burial resulted in low relative carbon preservation in shallow waters (including depths where net deposition was assumed to occur), while preservation slightly exceeded oxidation from 80 m depth to the bottom of the basin. This high fraction of preservation could be related to the input of more refractory organics from land and from the Greenland Sea (Chapter 6).

Figure 10 emphasizes that further studies towards a more accurate benthic carbon budget should focus mainly on mineralization processes in the shallower sediments, and on carbon burial at intermediate depths in the fjord. In addition to extension of the sampling grid, further investigations could include a ground-truthing of lab-based exchange rates by *in situ* measurements using benthic chambers or non-invasive techniques (Berg et al., 2003a; Glud et al., 2003). At other locations, exchange rates measured in cores in the laboratory have shown a downward bias relative to *in situ* measurements (e.g. Glud et al., 2003). Conversely, ^{210}Pb-based sediment accumulation rates tend to overestimate burial when the effect of bioturbation is ignored, as demonstrated in this study. Thus, effects of bioturbation deep in the sediment are an important issue for future investigations of carbon and nutrient burial.

No effect of low temperature on the balance between carbon oxidation and burial was discerna-

Sea floor at 60 m water depth. Note the numerous brittle stars on the sea floor at these depths.

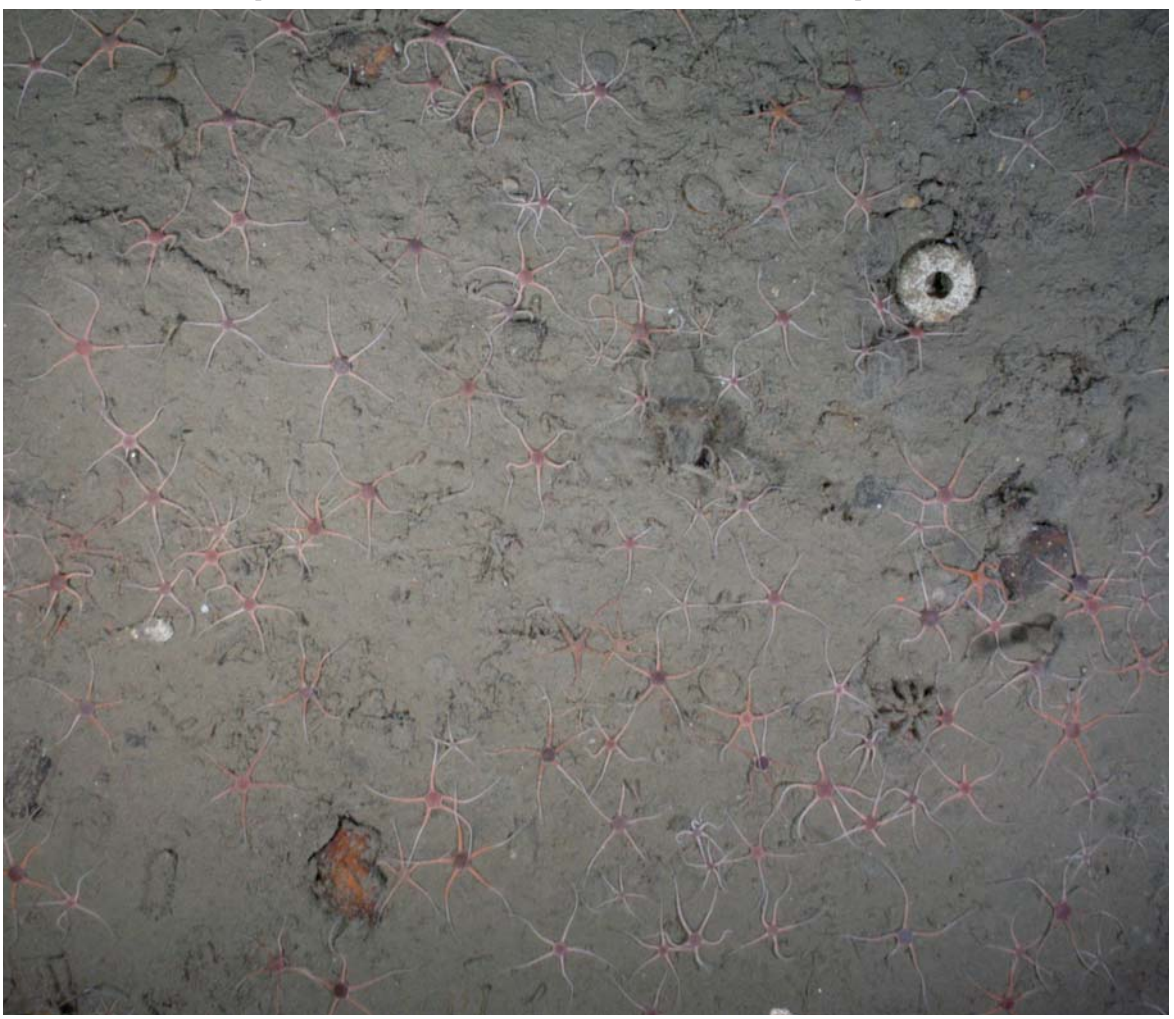

Photo: Peter B. Christensen & Mikael K. Sejr

ble, and the partitioning of carbon oxidation between different electron acceptors and the slight dominance of anaerobic processes resembled conditions in warmer sediments with moderate carbon inputs and oxic bottom water. Temperature mainly affected the dynamics of carbon oxidation, rate constants being a factor of 2–3 lower at the in situ temperature of –1°C than at 10°C. If mineralization of carbon and nutrients follows the same kinetics, consistent with diagenetic modeling (Berg et al., 2003a), the effect of temperature implies that benthic-pelagic coupling is less pronounced in Arctic than in temperate waters. Thus, release of nutrients from the sediment after settling of the summer bloom is slower, which may lead to less post-bloom primary productivity.

8.4 Acknowledgements

This work was financially supported by the Danish Natural Science Research Council, by DANCEA (the Danish Cooperation for the Environment in the Arctic) under the Danish Ministry of the Environment and by the Carlsberg Foundation. Furthermore, this work is a contribution to the Zackenberg Basic and Nuuk Basic programs in Greenland. Three reviewers are acknowledged for their comments that improved the manuscript.

8.5 References

Aller, R. C. 1994. The sedimentary Mn cycle in Long Island Sound: its role as intermediate oxidant and the influence of bioturbation, O_2 and C_{org} flux on diagenetic reaction balance. J. Mar. Res. 52: 259-295.

Alperin, M.J., Martens, C. S., Albert, D. B., Suyah, I. B., Benninger, L. K., Blair, N. E. & Janke, R. A. 1999. Benthic fluxes and porewater concentration profiles of dissolved organic carbon in sediments from the North Carolina continental slope. Geochim. Cosmochim. Acta 63: 427-448.

Archer, D., & A. Devol. 1992. Benthic oxygen fluxes on the Washington shelf and slope - a comparison of in situ microelectrode and chamber flux measurements. Limnol. Oceanogr. 37: 614-629.

Bastviken, D., L., Persson, G., Odham, & Tranvik, L. 2004. Degradation of dissolved organic matter in oxic and anoxic lake water. Limnol. Oceanogr. 49: 109-116.

Berelson, W. & others 2003. A time series of benthic flux measurements from Monterey Bay, CA. Cont. Shelf Res. 23: 457-481.

Berg, P., Risgaard-Petersen, N & Rysgaard, S. 1998. Interpretation of measured concentration profiles in sediment pore water. Limnol. Oceanogr. 43: 1500-1510.

Berg, P., Roy, H., Janssen, F., Meyer, V., Jørgensen, B. B., Huettel, M. & de Beer, D. 2003a. Oxygen uptake by aquatic sediments measured with a novel non-invasive eddy-correlation technique. Mar. Ecol. Prog. Ser. 261: 75-83.

Berg, P., Rysgaard, S., Funch, P. & Sejr, M. K. 2001. Effects of bioturbation on solutes and solids in marine sediments. Aquat. Microb. Ecol. 26: 81-94.

Berg, P., Rysgaard, S. & Thamdrup, B. 2003b. Dynamic modeling of early diagenesis and nutrient cycling. A case study in an Arctic marine sediment. Am. J. Sci. 303: 905-955.

Berner, R. A. 1980. Early Diagenesis. Princeton University Press, Princeton, N.J.

Boetius, A. & Damm, E. 1998. Benthic oxygen uptake, hydrolytic potentials and microbial biomass at the Arctic continental slope. Deep-Sea Res. PI, 45: 239-275.

Boudreau, B. P. 1994. Is burial velocity a master parameter for bioturbation. Geochim. Cosmochim. Acta 58: 1243-1249.

Boudreau, B. P. 1997. Diagenetic models and their implementation. Springer, Berlin.

Burdige, D. J., Berelson, W. M., Coale, K. H., McManus, J. & Johnson, K. S. 1999. Fluxes of dissolved organic carbon from California continental margin sediments. Geochim. Cosmochim. Acta 63: 1507-1515.

Canfield, D. E. 1993. Organic matter oxidation in marine sediments. In Wollast, R., Mackenzie, F. T. & Chou, L. (eds.). Interactions of C, N, P, and S biogeochemical cycles and global change. NATO ASI Series. Springer, Berlin: p. 333-363.

Canfield, D. E. & others 1993a. Pathways of organic carbon oxidation in three continental margin sediments. Mar. Geol. 113: 27-40.

Canfield, D. E., Thamdrup, B. & Hansen, J. W. 1993b. The anaerobic degradation of organic matter in Danish coastal sediments: Fe reduction, Mn reduction and sulfate reduction. Geochim. Cosmochim. Acta 57: 2563-2570.

Fenchel, T. & Blackburn, T. H. 1979. Bacteria and mineral cycling. Academic Press, London.

Froelich, P. N. & others 1979. Early oxidation of organic matter in pelagic sediments of the eastern equatorial Atlantic: suboxic diagenesis. Geochim. Cosmochim. Acta 43: 1075-1090.

Glud, R. N., & Fenchel, T. 1999. The importance of ciliates for interstitial solute transport in benthic communities. Mar. Ecol. Prog. Ser. 186: 87-93.

Glud, R. N., Gundersen, J. K., Roy, H. & Jørgensen, B. B. 2003. Seasonal dynamics of benthic O_2 uptake in a semienclosed bay: Importance of diffusion and faunal activity. Limnol. Oceanogr. 48: 1265-1276.

Glud, R. N., Holby, O., Hoffmann, F. & Canfield, D. E. 1998. Benthic mineralization and exchange in Arctic sediments (Svalbard, Norway). Mar. Ecol. Prog. Ser. 173: 237-251.

Glud, R. N., Kuhl, M., Wenzhofer, F. & Rysgaard, S. 2002. Benthic diatoms of a high Arctic fjord (Young Sound, NE Greenland): importance for ecosystem primary production. Mar. Ecol. Prog. Ser. 238: 15-29.

Glud, R. N., Risgaard-Petersen, N., Thamdrup, B., Fossing, H. & Rysgaard, S. 2000. Benthic carbon mineralization in a high-Arctic sound (Young Sound, NE Greenland). Mar. Ecol. Prog. Ser. 206: 59-71.

Grant, J., Hargrave, B. & MacPherson, P. 2002. Sediment properties and benthic-pelagic coupling in the North Water. Deep-Sea Res. PII, 49: 5259-5275.

Grebmeier, J. M., McRoy, C. P. & Feder, H. M. 1989. Pelagic-benthic coupling on the shelf of the northern Bering and Chuckchi Seas. I. benthic community structure. Mar. Ecol. Progr. Ser. 48: 57-67.

Hansen, J. W., Thamdrup, B. & Jørgensen, B. B. 2000. Anoxic incubation of sediment in gas-tight plastic bags: a method for biogeochemical process studies. Mar. Ecol. Progr. Ser. 208: 273-280.

Harvey, H. R., Tuttle, J. H. & Bell, J. T. 1995. Kinetics of phytoplankton decay during simulated sedimentation – changes in biochemical-composition and microbial activity under oxic and anoxic conditions. Geochim. Cosmochim. Acta 59: 3367-3377.

Hines, M. E., Bazylinski, D. A., Tugel, J. B. & Lyons, W. B. 1991. Anaerobic microbial biogeochemistry in sediments from two basins in the Gulf of Maine: evidence for iron and manganese. Estuar. Coast. Shelf Sci. 32: 313-324.

Huettel, M., & Gust, G. 1992. Solute release mechanisms from confined sediment cores in stirred benthic chambers and flume flows. Mar. Ecol. Prog. Ser. 82: 187-197.

Hult, S., Blackburn, T. H. & Hall, P. O. J. 1994. Arctic sediments (Svalbard): consumption and microdistribution of oxygen. Mar. Chem. 46: 293-316.

Hulthe, G., Hulth, S. & Hall, P. O. J. 1998. Effect of oxygen on degradation rate of refractory and labile organic matter in continental margin sediments. Geochim. Cosmochim. Acta 62: 1319-1328.

Jensen, M. M., Thamdrup, B., Rysgaard, S., Holmer, M. & Fossing, H. 2003. Rates and regulation of microbial iron reduction in sediments of the Baltic-North Sea transition. Biogeochemistry 65: 295-317.

Jørgensen, B. B. 1982. Mineralization of organic matter in the sea bed - role of sulphate reduction. Nature 296: 643-645.

Jørgensen, B. B. 1996. Case study – Aarhus Bay. In Richardson, K. & Jørgensen, B. B. (eds.). Eutrophication in coastal marine ecosystems. Coastal and estuarine studies. American Geophysical Union, Washington: p. 137-154.

Jørgensen, B. B., Bang, M. & Blackburn, T. H. 1990. Anaerobic mineralization in marine sediments from the Baltic Sea-North Sea transition. Mar. Ecol. Prog. Ser. 59: 39-54.

Kaplan, W. A., Teal, J. M. & Valiela, I. 1977. Denitrification in salt marsh sediments: evidence for seasonal temperature selection among populations of denitrifiers. Microb. Ecol. 3: 193-204.

Kostka, J. E., Canfield, D. E. & Thamdrup, B. 1999. Rates and pathways of carbon oxidation in permanently cold Arctic sediments. Mar. Ecol. Prog. Ser. 180: 7-21.

Kristensen, E., Ahmed, S. I. & Devol, A. H. 1995. Aerobic and anaerobic decomposition of organic matter in marine sediment: which is fastest? Limnol. Oceanogr. 40: 1430-1437.

Nedwell, D. B. 1999. Effect of low temperature on microbial growth: lowered affinity for substrates limits growth at low temperature. FEMS Microbiol. Ecol. 30: 101-111.

Nielsen, L. P. 1992. Denitrification in sediment determined from nitrogen isotope pairing. FEMS Microbiol. Ecol. 86: 357-362.

Pfannenkuche, O. & Thiel, H. 1987. Meiobenthic stocks and benthic activity on the NE-Svalbard shelf and in the Nansen Basin. Polar Biol. 7: 253-266.

Pomeroy, L. E. & Deibel, D. 1986. Temperature regulation of bacterial activity during the spring bloom in Newfoundland coastal waters. Science 233: 359-361.

Pomeroy, L. R. & Wiebe, W. J. 2001. Temperature and substrates as interactive limiting factors for marine heterotrophic bacteria. Aquat. Microb. Ecol. 23: 187-204.

Rasmussen, H. & Jørgensen, B. B. 1992. Microelectrode studies of seasonal oxygen uptake in a coastal sediment: role of molecular diffusion. Mar. Ecol. Prog. Ser. 81: 289-303.

Reimers, C. E., Stecher, H. A. Taghon, G. L. Fuller, C. M. Huettel, M. Rusch, A. Ryckelynck, N. & Wild, C. 2004. In situ measurements of advective solute transport in permeable shelf sands. Cont. Shelf Res. 24: 183-201.

Roberts, R. D., Kuhl, M., Glud, R. N. & Rysgaard, S. 2002. Primary production of crustose coralline red algae in a high Arctic fjord. J. Phycol. 38: 273-283.

Rosselló-Móra, R., Thamdrup, B., Schäfer, H., Weller, R. & Amann, R. 1999. The response of the microbial community of marine sediments to organic carbon input under anaerobic conditions. Syst. Appl. Microbiol. 22: 237-248.

Rowe, G. T. & others. 1997. Sediment community biomass and respiration in the Northeast Water Polynya, Greenland: A numerical simulation of benthic lander and spade core data. J. Marine Syst. 10: 497-515.

Rysgaard, S., Finster, K. & Dahlgaard, H. 1996. Primary production, nutrient dynamics and mineralisation in a northeastern Greenland fjord during the summer thaw. Polar Biol. 16: 497-506.

Rysgaard, S., Fossing, H. & Jensen, M. M. 2001. Organic matter degradation through oxygen respiration, denitrification, and manganese, iron, and sulfate reduction in marine sediments (the Kattegat and the Skagerrak). Ophelia 55: 77-91.

Rysgaard, S., Thamdrup, B. Risgaard-Petersen, N., Fossing, H., Berg, P., Christensen, P. B. & Dalsgaard, T. 1998. Seasonal carbon and nutrient mineralization in a high-Arctic coastal marine sediment, Young Sound, Northeast Greenland. Mar. Ecol. Prog. Ser. 175: 261-276.

Rysgaard, S., Vang, T. Stjernholm, M. Rasmussen, B. Windelin, A. & Kiilsholm, S. 2003. Physical conditions, carbon transport, and climate change impacts in a northeast Greenland fjord. Arct. Antarct. Alp. Res. 35: 301-312.

Sagemann, J., B. B. Jorgensen, and O. Greeff. 1998. Temperature dependence and rates of sulfate reduction in cold sediments of Svalbard, Arctic Ocean. Geomicrobiol. J. 15: 85-100.

Sejr, M. K., Jensen, K. T. & Rysgaard, S. 2000. Macrozoobenthic community structure in a High-Arctic East Greenland fjord. Polar Biol. 23: 792-801.

Slomp, C. P., Malschaert, J. F. P., Lohse, L. & Van Raaphorst, W. 1997. Iron and manganese cycling in different sedimentary environments on the North Sea continental margin. Cont. Shelf Res. 17: 1083-1117.

Sun, M. Y., Aller, R. C. & Lee, C. 1991. Early diagenesis of chlorophyll-*a* in Long-Island Sound sediments - a measure of carbon flux and particle reworking. J. Mar. Res. 49: 379-401.

Sun, M. Y., Aller, R. C., Lee, C. & Wakeham, S. G. 2002. Effects of oxygen and redox oscillation on degradation of cell-associated lipids in surficial marine sediments. Geochim. Cosmochim. Acta 66: 2003-2012.

Sun, M. Y., Lee, C. & Aller, R. C. 1993. Laboratory studies of oxic and anoxic degradation of Chlorophyll-a in Long-Island Sound sediments. Geochim. Cosmochim. Acta 57: 147-157.

Sørensen, J. & Jørgensen, B. B. 1987. Early diagenesis in sediments from Danish coastal waters: microbial activity and Mn-Fe-S geochemistry. Geochim. Cosmochim. Acta 51: 1583-1590.

Thamdrup, B. 2000. Microbial manganese and iron reduction in aquatic sediments. Adv. Microb. Ecol. 16: 41-84.

Thamdrup, B., & Canfield, D. E. 1996. Pathways of carbon oxidation in continental margin sediments off central Chile. Limnol. Oceanogr. 41: 1629-1650.

Thamdrup, B. 2000. Benthic respiration in aquatic sediments. In O. Sala, Mooney, H., Jackson, R. & Howarth, R. (eds.). Methods in Ecosystem Science. Springer, New York: p. 86-103

Thamdrup, B. & Fleischer, S. 1998. Temperature dependence of oxygen respiration, nitrogen mineralization, and nitrification in Arctic sediments. Aquat. Microb. Ecol. 15: 191-199.

Thamdrup, B., Fossing, H. & Jørgensen, B. B. 1994a. Manganese, iron, and sulfur cycling in a coastal marine sediment, Aarhus Bay, Denmark. Geochim. Cosmochim. Acta 58: 5115-5129.

Thamdrup, B., Glud, R. N. & Hansen, J. W. 1994b. Manganese oxidation and in situ fluxes from a coastal sediment. Geochim. Cosmochim. Acta 58: 2563-2570.

Vosjan, J. H. 1974. Sulphate in water and sediment of the Dutch Wadden Sea. Neth. J. Sea Res. 8: 208-213.

Wang, Y. F. & Van Cappellen, P. 1996. A multicomponent reactive transport model of early diagenesis - application to redox cycling in coastal marine sediments. Geochim. Cosmochim. Acta 60: 2993-3014.

Westrich, J. T. & Berner, R. A. 1984. The role of sedimentary organic matter in bacterial sulfate reduction - the G model tested. Limnol. Oceanogr. 29: 236-249.

Westrich, J. T. 1988. The effect of temperature on rates of sulfate reduction in marine sediments. Geomicrobiol. J. 6: 99-117.

Wollast, R. 1991. The coastal organic carbon cycle: fluxes, sources, and sinks. In: Mantoura, R. F. C., Martin, J.-M. & Wollast, R. (eds.). Ocean Marine Processes in Global Change. John Wiley & Sons, New York: p. 365-381.

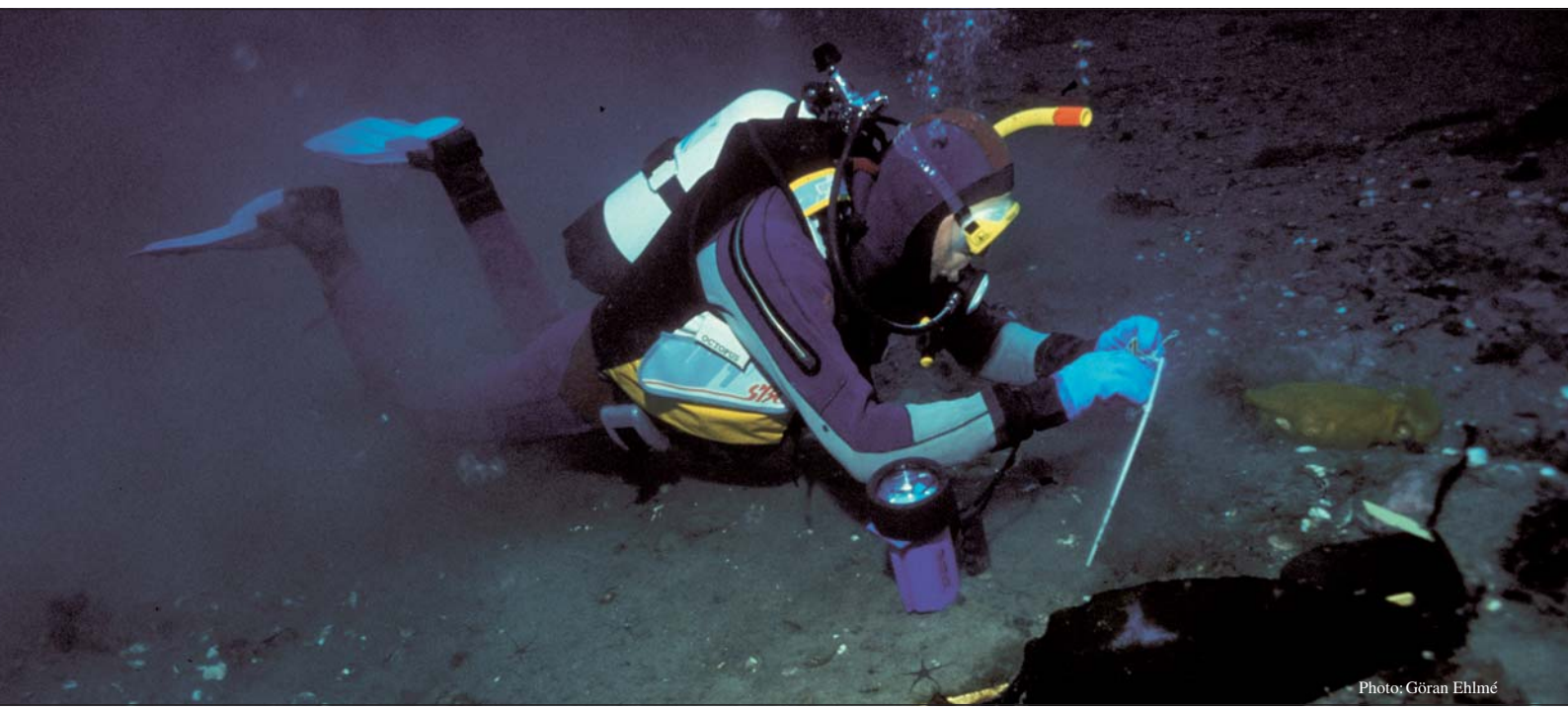

Photo: Göran Ehlmé

9

Benthic primary production in Young Sound, Northeast Greenland

Benthic primary production in Young Sound, Northeast Greenland

Dorte Krause-Jensen[1], Michael Kühl[2], Peter B. Christensen[1] and Jens Borum[3]

[1]National Environmental Research Institute, Dept. of Marine Ecology, Vejlsøvej 25, DK-8600 Silkeborg, Denmark
[2]Marine Biological Laboratory, University of Copenhagen, Strandpromenaden 5, DK-3000 Helsingør, Denmark
[3]Freshwater Biological Laboratory, University of Copenhagen, Helsingørsgade 51, DK-3400 Hillerød, Denmark

Cite as: Krause-Jensen, D., Kühl, M., Christensen, P. B. & Borum, J. 2007. Benthic primary production in Young Sound, Northeast Greenland. In: Rysgaard, S. & Glud, R. N. (Eds.), Carbon cycling in Arctic marine ecosystems: Case study Young Sound. Meddr. Grønland, Bioscience 58: 160-173.

Abstract

The extreme and variable light climate of polar marine environments imposes a substantial limitation on benthic primary production and demands efficient adaptive capacities of the primary producers. This chapter reviews the composition, abundance, primary production and adaptive strategies of benthic primary producers in Young Sound. Benthic primary producers occurred in the 0-50 m depth range and the relative importance of microalgae, crustose coralline macroalgae and foliose macroalgae varied systematically with depth. On a summer day with optimal light conditions benthic primary production showed a maximum of c. 70 mmol O_2 m^{-2} d^{-1} in shallow water. Production rates declined gradually to c. 20 mmol O_2 m^{-2} d^{-1} at 10–20 m depth and to 2.5 mmol O_2 m^{-2} d^{-1} at 30 m depth. Foliose macroalgae contributed markedly to primary production in shallow water but became insignificant at water depths >15 m, while benthic diatoms contributed most to primary production at intermediate water depths (5-30 m). At water depths greater than 30 m only coralline algae occurred, but their production was low because of their low abundance, low P_{max} and the low ambient irradiance at those depths. All algal groups were well adapted to the ambient irradiance and could, within minutes, acclimate their photosynthetic performance to changing light conditions. The benthic primary production in Young Sound markedly surpassed the pelagic primary production down to water depths of 20 m and the results thereby underline the potential importance of benthic primary production in shallow-water Arctic ecosystems.

9.1 Introduction

Benthic primary producers can contribute significantly to the production of shallow-water ecosystems in temperate and tropical regions (e.g. Mann, 1973; Borum & Sand-Jensen, 1996; Cahoon, 1999), but their importance for ecosystem primary production in the Arctic is only sparsely explored.

Annual primary production of Arctic phytoplankton can be surprisingly high despite the harsh conditions (Sambrotto et al., 1984; Subbarao & Platt, 1984), but the extent to which benthic production matches planktonic production is unknown. The few previous studies on benthic microalgal produc-

tion show contrasting results; microalgae range from playing an insignificant role in primary production (Horner & Schrader, 1982) to being the most important contributors (Matheke & Horner, 1974). Existing information on area production of polar macroalgae is also sparce, although several studies have evaluated photosynthesis and growth of macroalgae on an individual basis (e.g. Chapman & Lindley, 1980; Dunton, 1985; Dunton, 1990). The work in Young Sound provides the first estimates of the area production of coralline macroalgae (Roberts et al., 2002) and hence, in combination with area production estimates of foliose macroalgae (Borum et al., 2002), contributes to the very limited database on area production of Arctic kelp (e.g. Chapman & Lindley, 1981; Dunton et al., 1982). The studies of benthic primary production in Young Sound also provide the first estimate of total benthic production in the Arctic.

The extreme and variable light climate of Arctic marine environments, ranging from winter months of permanent darkness to periods of continuous light during summer, and the simultaneous exposure to low temperatures demand a high capacity for physiological adaptation of the plants. Due to their shorter life cycle, benthic and planktonic microalgae can occur in highest abundance during the summer period when light conditions are optimal. The perennial algae, however, need to cope with the seasonal changes in growth conditions and must rely on extreme plasticity of their photosynthetic apparatus and metabolism. They need a low respiration rate to minimise carbon losses during winter darkness, an efficient light capture in the periods of low irradiance under the ice cover in early and late summer, and an ability to profit maximally from the 24-h light period in mid-summer. On the other hand, the perennial life form with its slow, but continuous, production of new biomass ensures that the algae are ready to start photosynthesis as soon as light becomes available. For some species (e.g. Laminarians) this advantage is enhanced by the ability to extend their surface area before the break-up of the surface ice cover (Dunton, 1985) and thereby increase the capacity for light capture. These algae produce a new thin blade during the period of ice cover through allocation of resources stored in the old thallus (Chapman & Lindley, 1980).

Physical disturbance in the shallow depth range constitutes another limitation on benthic primary producers. Ice scouring along the coast may detach the algae from their substrata or destroy the thallus and thus induce a significant loss of biomass (Gutt, 2001). Moreover, intense walrus feeding in some depth intervals (Born et al., 2003; Chapter 10) may seriously affect the abundance of benthic micro- and macroalgae in Young Sound.

In spite of these limitations, the benthic algal community likely contributes significantly to the primary production of Young Sound, as the annual primary production of phytoplankton and sea-ice algae cannot account for the annual C input required by the benthic secondary producers (See Chapter 4, 5, 7 & 8).

Here we review the importance of benthic micro- and macroalgae for the primary production in Young Sound. We analyse their composition, distribution, abundance and productivity as well as their adaptive strategies. The results are discussed together with the relatively sparse knowledge available of benthic primary production in polar regions. Parts of the results are also included in a comparison of benthic versus pelagic production on an annual basis (Chapter 11).

9.2 Methods

Most of the information compiled in this chapter is based on methods described in the study of Arctic benthic microalgae by Glud et al. (2002), the study of Arctic coralline macroalgae by Roberts et al. (2002), the study on Arctic foliose macroalgae by Borum et al. (2002) and the study of photosynthetic performance of all three algal groups by Kühl et al. (2001). The following paragraphs provide a brief summary of the methodology used, but for details, please refer to the studies above.

All types of benthic primary producers were collected by divers and identified to genus/species in the laboratory. Distribution and cover of diatoms, foliose macroalgae and encrusted algae were estimated from numerous digital photographs and video recordings of the seafloor. Biomass of foliose macroalgae along the depth gradient was assessed through harvest.

Net benthic microalgal photosynthesis was assessed as i) the sum of the upward and downward diffusive O_2 fluxes calculated from oxygen microprofiles measured in darkness and at increasing irradiance (Fig. 9.1a), and ii) the total oxygen or DIC exchange rate of intact sediment cores incubated in darkness and at increasing irradiance under *in situ*

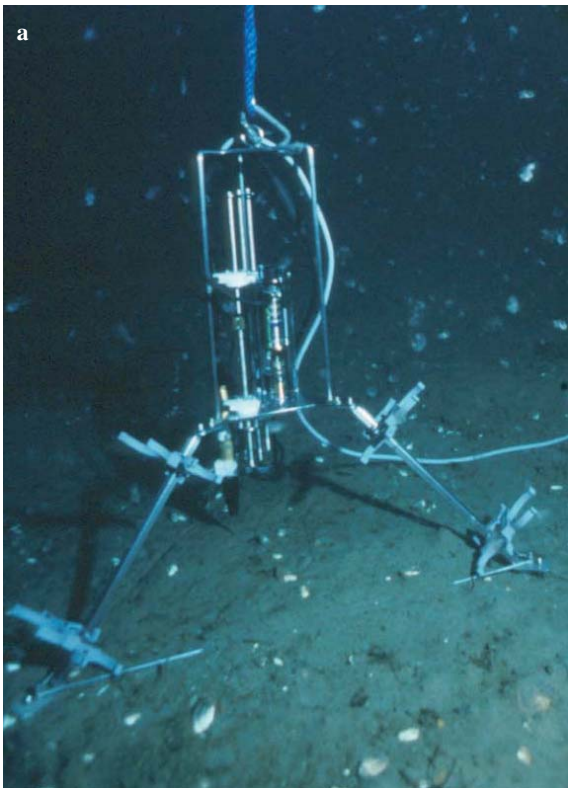

Photo: Jens S. Laursen

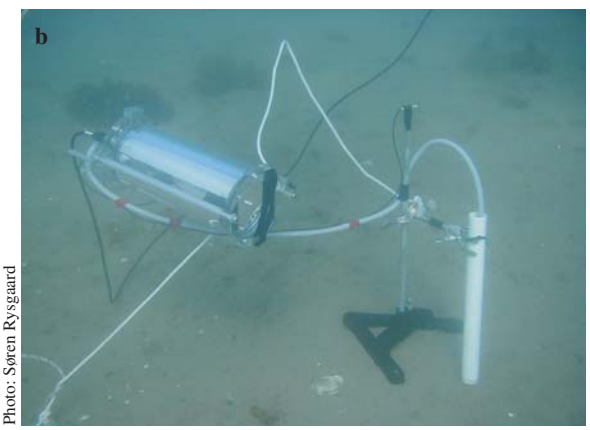

Photo: Søren Rysgaard

Figure 9.1 Illustration of **(a)** the oxygen microsensor technique used to measure production of benthic microalgae and crustose coralline algae and **(b)** of the pulse-amplitude-modulated (PAM) fluorometer.

temperature conditions (Glud et al., 2002). Photosynthesis of crustose coralline algae was assessed based on diffusive O_2 fluxes calculated from oxygen microprofiles measured in the diffusive boundary layer over the coralline surface in darkness and at increasing irradiance (Roberts et al., 2002). Respiration and photosynthesis of thallus discs of *L. saccharina* were measured in a small glass chamber as O_2 consumption in darkness and O_2 production at increasing levels of irradiance (Borum et al., 2002). Data on maximum photosynthetic rate (P_{max}), light utilisation efficiency (α), respiration rate (R), compensation irradiance (E_c) and the irradiance at onset of saturation (E_k) for each algal group were derived from the measured P-E curves. Subsequently, daily rates of area photosynthesis along the depth gradient were assessed for a summer day with optimal light conditions, using the formula of Platt et al. (1980):

$$P=P_{max}[1-\exp(-\alpha E/P_{max})]+R \quad (1)$$

The irradiance (E) at specific depths was calculated based on data on surface irradiance and light attenuation in the water column (Glud et al., 2002). Photosynthetic rates were corrected to represent the actual cover/biomass of the algal groups at each depth. The productivity of *L. saccharina* was also assessed from annual growth rates of the blade at specific water depths.

Relative measures of the photosynthetic activity of all algal groups were obtained both in the laboratory and *in situ* by active fluorescence measurements using an *in situ* measuring device (Diving-PAM, Walz GmbH, Effeltrich Germany) (Kühl et al., 2001; Fig. 9.1b). We used the so-called 'saturation pulse method' (Schreiber et al., 1995) to measure quantum yields of PSII under various actinic light conditions in order to characterise the *in situ* acclimation of the photosynthetic apparatus to irradiance. We measured so-called rapid light curves, (RLC) within 1-2 min or 'light curves (LC)' within longer time periods (30–40 min). In both cases, the light curves, express relative rates of PSII-related electron transport as a function of irradiance (Schreiber et al., 1995). During RLC measurements, the brief (10-20 s) incubation periods at each irradiance level do not allow the phototrophs to acclimate, and these measurements thus provide a snapshot of the photosynthetic capacity at the current ambient irradiance. During LC measurements, the relatively slow increase in irradiance over a 30–40 min period allows the photosynthetic apparatus to acclimate as the experiment is conducted. Consequently, these measurements show the potential short-term photosynthetic capacity of the organisms.

9.3 Results & discussion

9.3.1 Composition and distribution of benthic primary producers

Diatoms were the dominant benthic microalgae in Young Sound and formed a brownish biofilm on the sediment (Fig. 9.2a), while benthic macroalgae included a variety of algal groups. Crustose, coralline species dominated by the red algal genus *Phymatolithon* formed pink crusts on the scattered stones (Fig. 9.2b) while large leathery brown algae of the genera *Fucus* and *Laminaria* dominated the foliose macroalgal community (Fig. 9.2c). Other upright foliose species of brown and red algae, including filamentous brown algae of the genus *Desmarestia* and leathery red algae of the genus *Coccotylus*, were also common (Table 9.1).

Benthic microalgae occurred in the upper sediment layers from shallow depths down to water depths >30 m, while crustose coralline macroalgae covered much of the available rock surface in the depth range 15–50 m. The depth limit at 50 m corresponds to about 0.004% of surface irradiance in the open-water season (Roberts et al., 2002) and the crustose corallines were the deepest-growing macroalgae in Young Sound. The

Table 9.1 Overview of the dominant algal classes and genera/species within the 3 types of benthic primary producers: 1) Microalgae (based on Glud et al., 2002), 2) crustose coralline macroalgae (based on Roberts et al., 2002) and 3) foliose upright macroalgae (based on Borum et al., 2002) and unpublished data).

Algal class	Dominant genera/species
Microalgae	
– Diatoms	*Pinnularia* *Nitzschia* *Navicula*
Macroalgae – crustose coralline	
– Red algae	*Phymatolithon foecundum* *Phymatolithon tenue*
Macroalgae – foliose	
– Brown algae	*Fucus evanescence* *Fucus serratus* *Laminaria saccharina* *Laminaria solidungula* *Desmarestia aculeata* *Desmarestia viridis*
– Red algae	*Coccotylus truncatus*
– Green algae	No dominant species

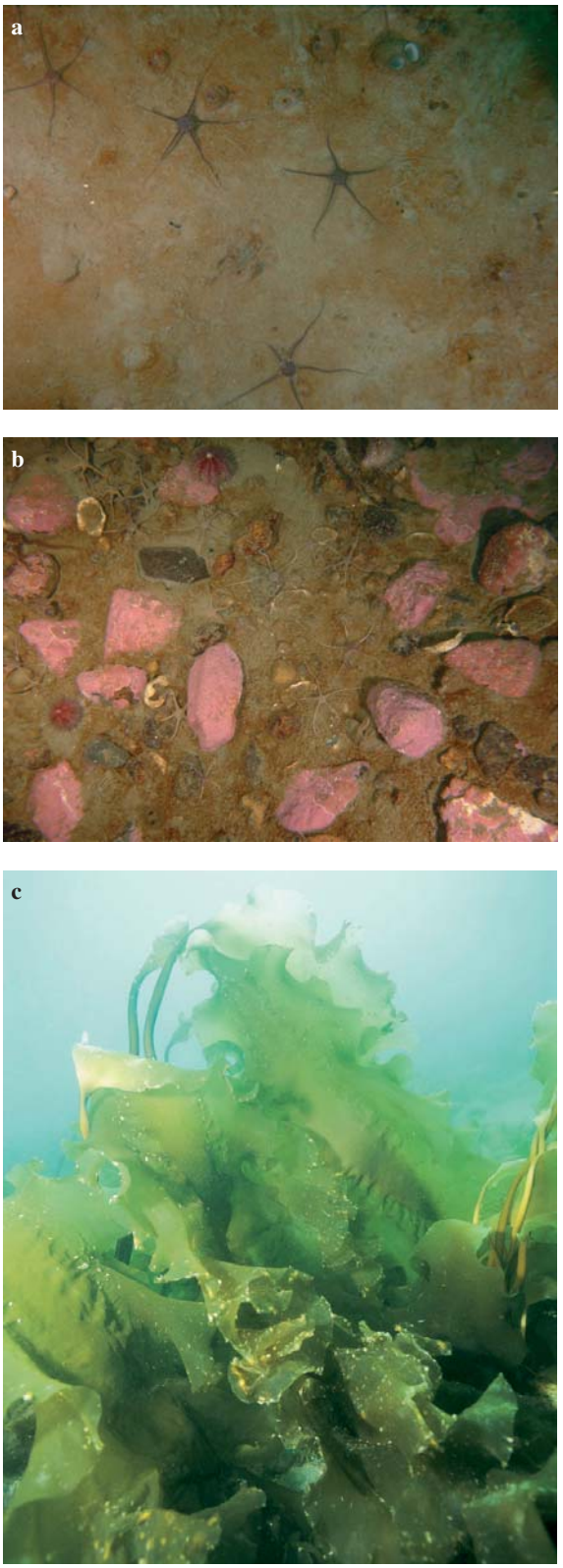

Photo: Peter B. Christensen

Figure 9.2 Photo of **(a)** benthic microalgae, **(b)** crustose, coralline macroalgae of the genus *Phymatolithon* and **(c)** the foliose, upright macroalga *Laminaria saccharina*.

foliose macroalgae occurred on rocks as well as on scattered stones and gravel. In protected, sandy sites of Young Sound, the brown macroalga, *L. saccharina,* grew with its widely branched haptera attached to small-sized gravel. Foliose macroalgae occurred in the depth range 2–25 m. The depth limit of *L. saccharina* was located at about 20 m depth and corresponds to c. 0.7% of surface irradiance (Borum et al., 2002).

The depth penetration of macroalgae seems to be determined largely by light availability, which in turn depends on solar radiation and light attenuation in the water column. Depth limits tend to occur at a smaller percentage of the surface irradiance near the equator where annual solar radiation is high as compared with temperate and polar regions (see Lüning, 1990). Crustose coralline macroalgae are the world's deepest-growing macroalgae and their depth penetration has been reported to range from 15 m, corresponding to 0.05% of surface irradiance in the turbid waters of Helgoland, to 268 m, corresponding to 0.001% of surface irradiance in the clear waters around Bahamas (Lüning & Dring, 1979). Laminarians also generally penetrate to relatively deep waters and the lower depth limit of *L. saccharina* recorded at Young Sound agrees well with the range of minimum light requirements reported for cold-water Laminarians in general (e.g. Lüning & Dring, 1979; Chapman & Lindley, 1980; Dunton, 1990).

The relatively large depth penetration of these species of benthic macroalgae indicates capacity for shade adaptation, which is considered a general feature of polar macroalgae enabling them to cope with the dark winter months (Kirst & Wiencke, 1995). Shade adaptation generally involves slow growth rates that reduce respiration, storage of carbon reserves during periods of favorable growth conditions, long life span and resistance to grazing (Lüning, 1990).

It is remarkable that many of the dominant benthic algae of Young Sound also occur in temperate regions and hence possess a substantial capacity for climatic adaptation, not only to the seasonal variations within the Arctic but also across a wide geographical range. *L. saccharina* thus occurs from Spain in the south to Peary Land at 82°N in North Greenland (Lüning, 1990), and coralline algae also occur from polar regions to the tropics (Johansen, 1981; Steneck, 1986).

9.3.2 Abundance of benthic primary producers in Young Sound

The *in situ* area cover of diatoms and coralline algae was measured by visual analysis of digital images faciliated by the characteristic brownish colour of diatom films and the pink colour of the corallines (Glud et al., 2002; Roberts et al., 2002).

Benthic microalgae covered 23–70% of the sea floor down to water depths of 30 m. Their abundance showed a maximum at 20 m depth before declining towards the deeper, shaded parts (Fig. 9.3; Glud et al., 2002). The horizontal distribution of the microalgae was examined at water depths of 10 m and was found to be very patchy, with marked differences between sites 5–8 m apart, most probably influenced by the intensive feeding activity of walruses in this depth range (Glud et al., 2002).

As the abundance of rocks is very patchy in Young Sound, coralline algae covered only 1–2% and occa-

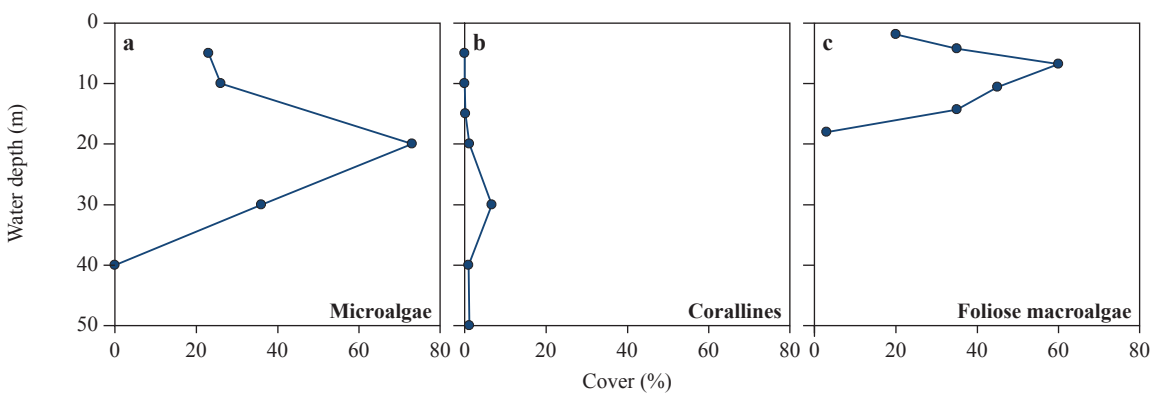

Figure 9.3 Depth distribution of the cover of **(a)** benthic microalgae (from Glud et al., 2002), **(b)** crustose coralline algae (redrawn from Roberts et al., 2002) and **(c)** *Laminaria saccharina* (P.B. Christensen unpublished data, estimated from video recordings).

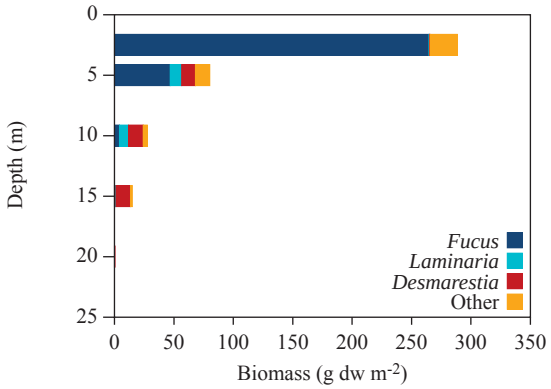

Figure 9.4 Biomass of foliose macroalgae along a depth gradient at Daneborg, Young Sound.

sionally 7% of the sea floor (Fig. 9.3; Roberts et al., 2002). The peak abundance of 7% at 30 m depth was not a consistent feature at this depth in Young Sound but rather resulted from a higher local abundance of rocks at this specific sampling site. The minimum depth range of 15 m was probably due to a combination of ice scouring, walrus feeding disturbance and overgrowth by foliose macroalgae in shallow water, while the maximum depth range of the coralline algae was light regulated.

The cover of foliose macroalgae almost matched that of benthic microalgae, but the macroalgae reached maximum levels at shallower depths (Fig. 9.3). Biomass measurements provided a more precise estimate of the abundance of foliose macroalgae and also showed how different algal species contributed to the total biomass (Fig. 9.4). The total biomass of foliose macroalgae showed a maximum of almost 290 g dw m^{-2} in shallow water and declined towards greater water depths. In shallow water *F. evanescence* dominated the community of foliose macroalgae while *L. saccharina* and the two species of *Desmarestia* were more important at 10–15 m depth. The abundance of foliose macroalgae was probably limited by a combination of lack of suitable substrata, light limitation at greater water depths and intensive feeding activity of walruses from 5–20 m depth. Ice scouring in shallow waters was clearly observed as scouring tracks on the sea floor but apparently did not prevent *F. evanescence* from occurring at a relatively high biomass. At the mouth of Young Sound, where stronger currents created a longer ice-free period, the abundance of kelps was markedly higher (pers. obs.).

9.3.3 Production of benthic primary producers in Young Sound

On a summer day with optimal light conditions, the daily net photosynthetic rate of the total benthic algal community showed a maximum of about 70 mmol O_2 m^{-2} d^{-1} in shallow water (2.5 m), declined gradually down to about 20 mmol O_2 m^{-2} d^{-1} at 10-20 m depth and then declined markedly to 2.5 mmol O_2 m^{-2} d^{-1} at 30 m depth (Fig. 9.5). Foliose macroalgae contributed most to primary production at the shallowest depths with a maximum of about 70 mmol O_2 m^{-2} d^{-1} at 2.5

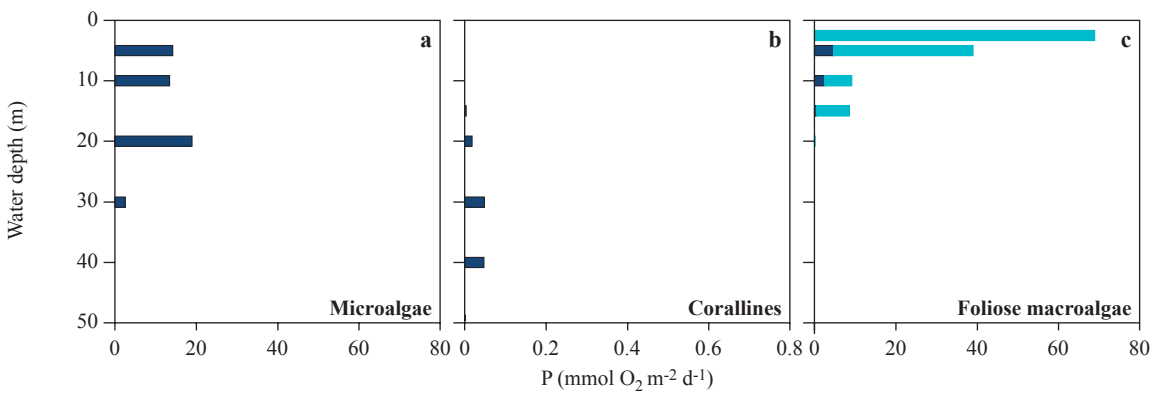

Figure 9.5 Daily rates of area photosynthesis versus depth for **(a)** benthic microalgae, **(b)** corallines and **(c)** foliose macroalgae (dark blue represents *L. saccharina* while light blue bars represent other foliose macroalgae). Based on the equation $P=P_{max}$ [1-exp(-αE/P_{max})]+R (Platt et al., 1980), using photosynthesis parameters from Table 9.3 and data on surface irradiance and light attenuation during a summer day (1 August 1999). Rates were corrected to represent the actual cover/biomass of the algal groups based on Figs. 9.2 and 9.3. We assumed that the group, other foliose macroalgae, shared the same photosynthetic characteristics as *L. saccharina*. Data include only positive net photosynthetic rates.

m depth. Their production rates declined rapidly with depth and became insignificant at water depths >15 m. Benthic diatoms were the dominant primary producers at intermediate water depths. Their production was high from 5 to 20 m depth (13–19 mmol O_2 m^{-2} d^{-1}) and still significant at 30 m depth (2.5 mmol O_2 m^{-2} d^{-1}). At water depths >30 m only coralline algae contributed to the benthic production. Their production was very low, showing a maximum of 0.05 mmol O_2 m^{-2} d^{-1} at 30 m depth. Annual production rates of all primary producers, including phytoplankton and ice algae, are presented and compared in Chapter 11.

The daily production rates of microalgae are within the range reported from the Chukchi Sea by Matheke & Horner (1974), one of the few other Arctic studies on benthic microalgal production. Here the primary production of microalgae ranged between 1.9 and 57 mg C m^{-2} h^{-1} corresponding to about 5–137 mmol O_2 m^{-2} d^{-1} (assuming a photosynthetic quotient of 1.2 and 24 h of production per day). Production rates for crustose coralline algae in the Arctic have not previously been published, but these algae are generally known as the least productive algae in any environment (e.g. Littler & Murray, 1974). We have not been able to find any daily area-based production rates of foliose macroalgae from the Arctic for comparison with the studies in Young Sound.

At water depths down to 20 m, the benthic net production in Young Sound by far surpassed the gross production of phytoplankton which was estimated at c. 40 mg C m^{-2} d^{-1} for water depths <30 m (Glud et al., 2002), corresponding to 4 mmol O_2 m^{-2} d^{-1} (assuming a photosynthetic quotient of 1.2). The remaining group of aquatic primary producers, the ice algae, do not contribute significantly to primary production in Young Sound (Rysgaard et al., 2001). The results from Young Sound thus show that benthic primary production may contribute significantly to the primary production of shallow-water Arctic ecosystems.

On a global scale, however, the rates per unit area of benthic production in Young Sound are quite low. A compilation of 319 literature data on maximum integral gross photosynthesis at high midday irradiance showed a maximum of about 60 mmol O_2 m^{-2} h^{-1} in dense communities of phytoplankton and benthic macrophytes (Krause-Jensen & Sand-Jensen, 1998) and mean rates of 17 mmol O_2 m^{-2} h^{-1} for benthic microalgae, 30 for benthic macroalgae and 22 for phytoplankton (Sand-Jensen & Krause-Jensen, 1997).

9.3.4 Growth measurements of *Laminaria saccharina*

In addition to the photosynthesis measurements described above, production of *L. saccharina* was measured based on leaf growth rates. Every year, *L. saccharina* individuals form a new blade between the stipe and the base of the old blade. The old blade remains attached and a thallus constriction between the old blade and the new one makes it easy to distinguish the two generations of blades (Fig. 9.6). Annual growth of *L. saccharina* can therefore be measured as the total length or biomass of the newest blade when it has reached full length in late summer. As a consequence, annual net growth per m^2 of sea floor can be assessed by harvesting *L. saccharina* in August and measuring the biomass of new blades (Borum et al., 2002). A leaf-tagging technique also provides a direct measure of annual growth rates (Fig. 9.6) and, in addition, allows assessment of growth rates during various periods of the year. Both techniques showed that large *L. saccharina* individuals produced on average 70–90 cm blade per year, corresponding to relative growth rates of approximately 0.5 per year at water depths from 5 to 15 m (Borum et al.,

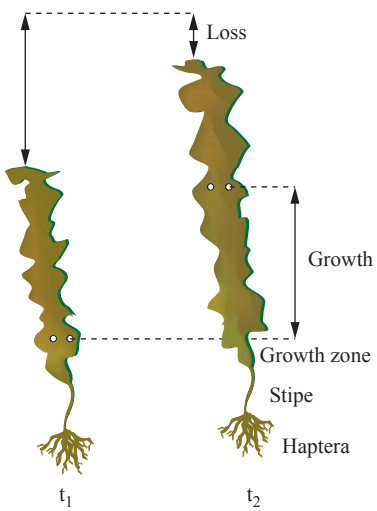

Figure 9.6 Illustration of leaf-tagging technique used to measure growth of *L. saccharina*. The blade is tagged with holes 10 cm above the junction between stipe and blade where the growth zone is located. As the blade grows, the holes are displaced upwards and the distance to the original position of the holes represents new growth. The arrow shows the constriction between the old blade and the new one.

Table 9.2 Mean annual length growth of *L. saccharina* in different sites. All rates were measured by leaf tagging. Most rates have been read and summed from figures showing seasonal changes in growth rate. *Average of 2nd and 3rd growth year. **Located at the lower salinity limit.

Location	Latitude	Depth m	Growth cm yr^{-1}	No. obs.	Reference
NE Greenland, Young Sound	74 18	5	73	>15	Borum et al. (2002)
NE Greenland, Young Sound	74 18	10	71	>15	Borum et al. (2002)
NE Greenland, Young Sound	74 18	15	89	>15	Borum et al. (2002)
Alaska, Beaufort Sea	70 19	6-7	58	13	Dunton (1985)
Iceland	64 20	5	111	17-32	Sjötun & Gunnarsson (1995)
Norway	60 15	5	230*	<40	Sjötun (1993)
Scotland, Loch Creran	56 34	5	239	?	Johnston et al. (1977)
Scotland, St. Andrews sewer st	56 20		160	20	Conolly & Drew (1985)
Scotland, St. Andrews	56 20		124	50	Conolly & Drew (1985)
Scotland, Kings Barn	56 18		73	50	Conolly & Drew (1985)
Scotland, Fifeness	56 17		82	50	Conolly & Drew (1985)
Scotland, Argyll	56 13	1	311	?	Parke (1948)
Denmark, Århus Bay	56 10	7	136	7-70	Thinggaard (2001)
Denmark, Øresund**	55 35		76	2-9	Weile (1996)
Germany, Kiel Bay	54 24	5	129	20	Schaffelke et al. (1996)
Rhode Island, Narragansett Bay	41 29		332	20	Brady-Campbell et al. (1984)
Rhode Island, Narragansett Bay	41 28.5		293	20	Brady-Campbell et al. (1984)
Rhode Island, Rhode Island Sound	41 21		291	20	Brady-Campbell et al. (1984)

2002; Table 9.2). The leaf-tagging technique was also applied for shorter periods of the year (mid-August to mid-June, mid to late June, late June to mid-August) and revealed that rates of length growth were highest around ice-break, i.e. late June to mid-August, when they averaged 6 mm d^{-1} (unpublished data).

Although a mean annual growth of 70–90 cm is impressive considering the 10 months of darkness, much higher growth rates (>3 m per year) of *L. saccharina* have been observed at lower latitudes (Table 9.2). *L. saccharina* is thus able to cope with Arctic conditions but apparently at the cost of reduced growth rates as compared with lower latitudes. We also used the mean biomass of new blades formed per m^2 of sea floor to estimate the annual primary production of *Laminaria saccharina*. The production increased from 0.1 g C m^{-2} yr^{-1} at 2.5 m depth to a maximum of 1.6 g C m^{-2} yr^{-1} at 10 m depth. Probably because of the relatively low biomass of *Laminaria* in Young Sound, these rates are low compared with the few other published production rates of *Laminaria* from Arctic. *L. solidungula* produced 7 C m^{-2} yr^{-1} in the Alaskan Beaufort Sea (Dunton et al., 1982) and 20 g C m^{-2} yr^{-1} in the Canadian high Arctic (Chapman & Lindley 1981) and was the dominant macroalgal species in both locations. There are examples of much higher production rates of *Laminaria* in temperate areas, e.g. 1750 g C m^{-2} yr^{-1} in dense kelp forests in Nova Scotia, Canada (Mann, 1972) and 120 g C m^{-2} yr^{-1} in *L. saccharina* communities in Scotland (Johnston et al., 1977).

9.3.5 Photosynthetic strategy under Arctic conditions

Marine benthic primary production in the Arctic takes place at permanently low temperatures (c. –1.5 to –1.8˚C) except in some shallow-water areas where temperatures may reach slightly above zero in the summer open-water period. Long periods of ice cover in combination with winter months of total darkness result in low irradiance or total darkness for the benthic primary producers during most of the year. In contrast, irradiance levels in shallow water can be high during the open-water period in summer

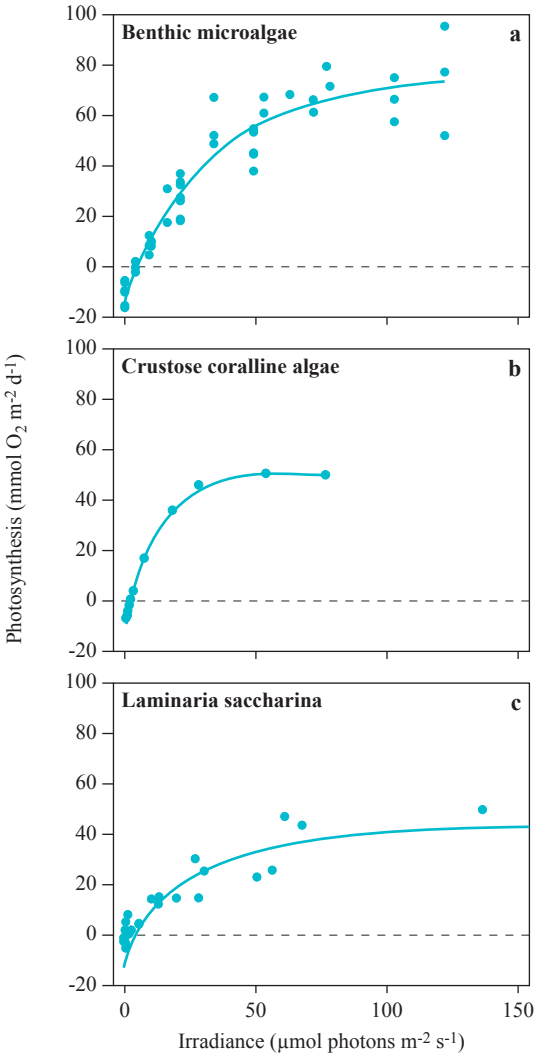

Figure 9.7 P-E curves for **(a)** benthic microalgae (Glud et al., 2002), **(b)** crustose coralline red algae (Roberts et al., 2002) and **(c)** *Laminaria saccharina* (Borum et al., 2002). Data on benthic microalgae and crustose coralline algae are per unit area of algae-covered sediment surface while data on *Laminaria saccharina* are per unit area of thallus surface. Data on *Laminaria saccharina* are recalculated from weight-based values to thallus-area-based values by using a specific weight of 5.84 mg cm^{-2} and recalculated from hourly to daily rates by assuming 24 h of production per day; photosynthesis continued at saturating levels up to irradiance levels of at least 250 µmol photons m^{-2} s^{-1}.

causing enhanced and constant availability of light. The shift from darkness to higher irradiance and vice versa occurs gradually as sun height increases/decreases but also involves more sudden increases in irradiance as the ice cover breaks up or snow-covered ice is re-established.

Our studies followed the performance of various groups of benthic primary producers in Young Sound over the summer season from the last part of the ice-covered period throughout the open-water period, where most production takes place. During this period, photosynthesis/irradiance relationships of benthic microalgae, crustose coralline algae and *L. saccharina* followed normal patterns of saturation with no clear signs of photoinhibition up to irradiances of 120, 80 and 250 µmol photons m^{-2} s^{-1}, respectively (Fig. 9.7). All algal groups measured at Young Sound showed compensation irradiances (E_c) and irradiances at onset of saturation (E_k) in the low end of the range reported for marine algae, thereby indicating adaptation to low light levels (Kirk, 1994; Table 9.3). Crustose coralline algae had the lowest E_c and E_k values and thus demonstrated the most efficient adaptation to low light levels. The other photosynthetic parameters did not show clear differences among algal groups (Table 9.3). Rates of respiration and photosynthesis of *L. saccharina* were quantified on a dry-weight basis (in addition to area-based values) and a comparison of these data with ranges reported for other macroalgae allowed evaluation of the adaptive capacity of *L. saccharina*. Respiration rates were in the low end of the typical range reported for macroalgae (Markager & Sand-Jensen, 1994) and maximum photosynthetic rates were within the reported range for polar macroalgae (Kirsch & Wiencke, 1995); so *L. saccharina* can indeed adapt to the harsh Arctic conditions.

Photosynthesis parameters of benthic diatoms and coralline algae did not vary markedly among water depths (Glud et al., 2002; Roberts et al., 2002). In contrast, the photosynthetic characteristics of *L. saccharina* changed systematically with depth (Borum et al., 2002). Pigment content, respiration rate, light utilisation efficiency and maximum photosynthetic rate all increased significantly with depth while compensation irradiance and irradiance at onset of saturation declined (Fig. 9.8). The larger pigment content and light utilisation efficiency in combination with the reduced compensation and saturation irradiances all

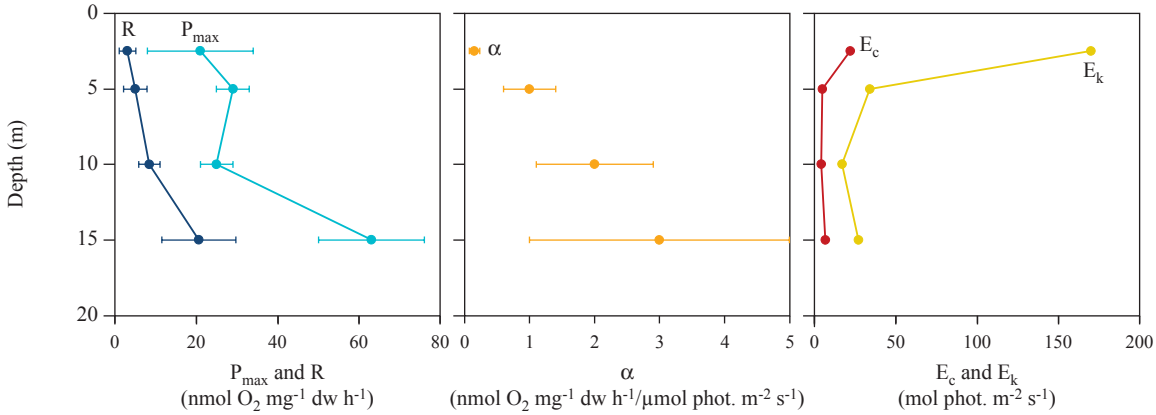

Figure 9.8 Photosynthesis parameters versus depth for *Laminaria saccharina* during the open-water period (August): R (respiration rate), α (photosynthetic efficiency), P_{max} (max. photosynthetic rate), E_c (compensation point), E_k (saturation point).

contribute to more efficient utilisation of the reduced light supplies. A more efficient photosynthetic apparatus requires production and maintenance of higher pigment content and enzymatic activity, which also create higher respiratory costs. In fact, low temperature may be an advantage and a prerequisite for survival in the long dark period, as it keeps respiratory costs low (Borum et al., 2002).

Differences in photosynthetic characteristics between ice-covered and open-water seasons were insignificant in coralline algae but apparent in *L. saccharina*. By the end of the long period of darkness in June, the new leaf blade of *L. saccharina* had low respiration rates, low compensation and saturation irradiances and relatively high maximum photosynthetic rates and was hence well adapted to the low light levels under the ice cover. During the open-water period in August, the compensation irradiance increased, probably in response to the increased ambient irradiance.

Active fluorescence measurements *in situ* using the, saturation pulse method, generated snapshots of the *in situ* acclimation of the photosynthetic apparatus by producing "rapid light curves" (RLC) within 1–2 min or, light curves, (LC) over longer time periods (c. 30 min). RLCs reflected the *in situ* acclima-

Table 9.3 Photosynthetic parameters of benthic diatoms, crustose coralline red algae and *Laminaria saccharina* measured by net O_2 production: R (repiration rate), α (photosynthetic efficiency), P_{max} (max. photosynthetic rate), E_c (compensation point), E_k (saturation point). Data on O_2 production of benthic diatoms and crustose coralline algae are related to the surface of the algal community. For comparability of data, production rates of *L. saccharina* were recalculated from hourly biomass-specific rates (shown in parenthesis) to diurnal rates related to thallus surface area. In this conversion we used the following information on area-specific biomass: June: 5.08 (new thallus), 6.58 (old thallus) and August: 6.17 (new thallus) mg dw cm^{-2} (J. Borum, unpublished data), and multiplied by 24 to obtain diurnal rates. Results from various depths and seasons are represented as averages for benthic diatoms but as ranges for corallines and *Laminaria*.

Algal group/sp.	Depth (m)	Month	R	P_{max}	α	E_c	E_k	Source
			mmol O_2 m^{-2} d^{-1} (nmol O_2 mg^{-1} dw h^{-1})		mmol O_2 m^{-2} d^{-1}/µmol phot m^{-2} s^{-1} (nmol O_2 mg^{-1} dw h^{-1}/µmol phot m^{-2} s^{-1})	µmol phot m^{-2} s^{-1}		
Diatoms	10, 20, 30	Jun, Aug	-10.96	85	2.6	4.5	32.9	Glud et al. (2002)
Corallines	17, 36	Jun, Aug	-4.8	43–67	4.2–6.3	0.7–1.8	7–17	Roberts et al. (2002)
L. saccharina	2.5, 5, 10, 15	Jun, Aug	-4.6–31 (-3–21)	31–180 (21–85)	0.2–13.7 (0.15–5)	2–22	15–170	Borum et al. (2002)

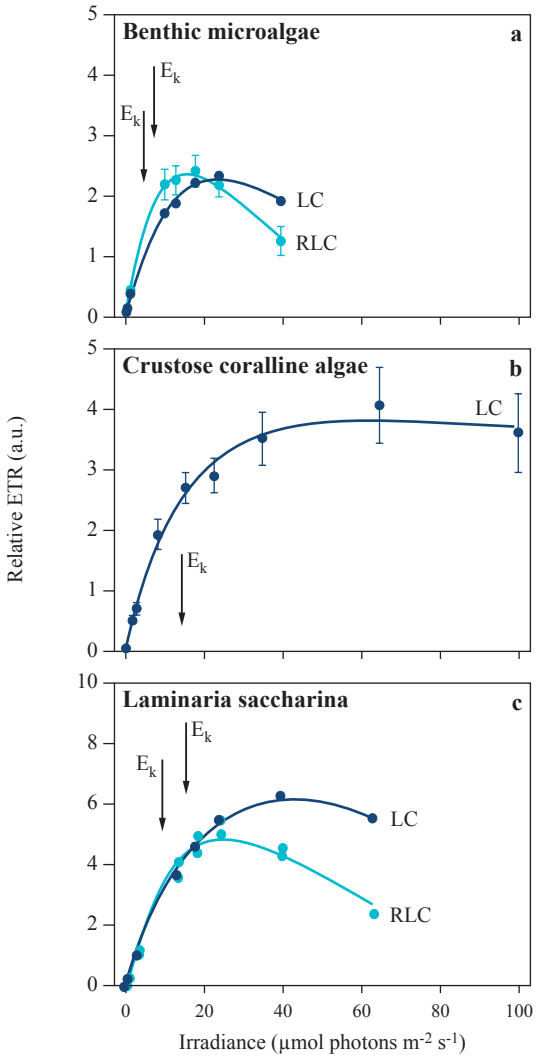

Figure 9.9 Light curves (LC) and rapid light curves (RLC) of **(a)** benthic diatoms (Kühl et al., 2001), **(b)** crustose coralline red algae (Kühl et al., 2001) and **(c)** *Laminaria saccharina* (Kühl et al., 2001).

tion of the phototrophs to ambient light because the short illuminations of each light level (10 s) did not allow any acclimation to the applied light levels during measurement. In contrast, the longer illumination period of each actinic light level used in LCs allowed the photosynthetic apparatus to acclimate during the measurement. Consequently, RLCs and LCs differed markedly within each algal group (Fig. 9.9). RLCs showed lower light saturation points than did LCs, indicating inhibition and/or downregulation of photosynthesis at high light levels while LCs showed no such effect (Fig. 9.9; Table 9.4). The apparent short-

Table 9.4 Light compensation point (E_c) and light saturation point (E_k) for benthic diatoms, crustose coralline red algae and *Laminaria saccharina* measured by net O_2 production, PAM Rapid light curves (RLC) or Light curves (LC). Unit: µmol photons m^{-2} s^{-1}. Data from June 1999 at 10 m depth (diatoms and *L. saccharina*). Based on Kühl et al. (2001).

Algae	E_c	E_k	Method
Diatoms		4.6	RLC
		6.9	LC
Corallines	1.6	17	Net O_2 prod.
		11	RLC
L. saccharina	1.9	12.8	Net O_2 prod.
		7.3	RLC
		12.5	LC

term acclimation to increasing irradiance as measured by LCs reversed to the initial characteristics of the light curve within 15–20 min after irradiance returned to ambient intensity. Our results clearly demonstrated that all the phototrophs were able to acclimate reversibly within minutes to moderate changes in light levels. This result also implies that light curves based on longer illumination periods, such as those used for measuring photosynthesis versus irradiance curves via oxygen production, may not reflect the actual photosynthetic capacity under *in situ* conditions but rather the potential to acclimate to the experimental conditions imposed on the organisms.

However, an important consequence of our observations is that all benthic primary producers seem able to optimise their photosynthetic performance during the season. Traditional measurements of light curves using longer exposure times in combination with detailed measurements of *in situ* irradiance are thus still necessary for the study of photosynthetic capacity and calculation of productivity over longer time scales. Last, but not least, although correlations can be made (e.g. Kuhl et al., 2001), active fluorescence measurements are not easily converted to quantitative measures of photosynthesis in terms of oxygen production or carbon fixation. Thus, direct extrapolation from the photosynthetic acclimation patterns observed with active fluorescence techniques to similar patterns in benthic primary production is a risky business.

At higher irradiance levels and/or under higher UV stress, photoinhibition may take place, and this process is not necessarily reversible. Besides studies of

macroalgae, e.g. by Hanelt and co-workers (Hanelt, 1998; Hanelt et al., 1997), photoinhibition and UV effects on benthic primary producers in the Arctic have not, to our knowledge, been published. Future studies should explore the environmental limits for short-term reversible acclimation among benthic primary producers in the Arctic. A more detailed dataset of benthic primary production over a complete year is still lacking. Such a study could address the important question of how the phototrophs cope with the long period of darkness and would help strengthen the estimate of carbon cycling due to benthic phototrophs. The research logistics available makes Young Sound an excellent location for such a study.

Our studies of benthic primary production in Young Sound revealed that the various photosynthetic groups are well adapted to cope with the extreme Arctic environment in terms of low temperature, long periods of darkness or continuous light. Benthic primary production is a major component in the carbon budget of the Young Sound ecosystem (Glud et al., 2002) as will be addressed further in Chapter 11. As part of the studies in Young Sound, new techniques for *in situ* measurements of photosynthetic performance and productivity were developed and applied. With these techniques, it is now possible to undertake a range of detailed *in situ* studies of surface-associated photosynthesis in the Arctic – a research area, which, despite the great importance of benthic primary production in coastal Arctic ecosystems, is severely underexplored.

9.4 Acknowledgements

This work was financially supported by the Danish Natural Science Research Council, the Carsberg Foundation, the Commission for Scientific Research in Greenland and by DANCEA (the Danish Cooperation for the Environment in the Arctic) under the Danish Ministry of the Environment. This work is a contribution to the Zackenberg Basic and Nuuk Basic programs in Greenland. We thank Morten Foldager Pedersen, Rodney D. Roberts, Ronnie Nøhr Glud, Søren Rysgaard, Kurt Nielsen and Frank Wenzhöfer for their contributions to the papers on benthic primary production in Young Sound on which this chapter is based. Finally, we thank three anonymous referees for their valuable comments.

9.5 References

Born, E. W., Rysgaard, S., Ehlmé, G. Sejr, M. K., Acquarone, M. & Levermann, N. 2003. Underwater observations of foraging free-living walruses (*Odobenus rosmarus*) including estimates of their food consumption. Polar Biol. 26: 348-357.

Borum, J., Pedersen, M. F., Krause-Jensen, D., Christensen, P. B. & Nielsen, K. 2002. Biomass, photosynthesis and growth of *Laminaria saccharina* in a High-Arctic fjord, NE Greenland. Mar. Biol. 141: 11-19.

Borum, J. & Sand-Jensen, K. 1996. Is primary production in shallow coastal marine waters stimulated by nitrogen loading. Oikos 76: 406-410.

Brady-Campbell, M. M., Campbell, D. B. & Harlin, M. M. 1984. Productivity of kelp (*Laminaria* spp.) near the southern limit in the northwestern Atlantic ocean. Mar. Ecol. Prog. Ser. 18: 79-88.

Cahoon, L. B. 1999. The role of benthic microalgae in neritic ecosystems. Oceanogr. Mar. Biol. Ann. Rev. 37: 47-86.

Chapman, A. R. O. & Lindley, J. E. 1980. Seasonal growth of *Laminaria solidongula* in the Canadian high Arctic in relation to irradiance and dissolved nutrient concentrations. Mar. Biol. 57: 1-5.

Chapman, A. R. O. & Lindley, J. E. 1981. Productivity of *Laminaria solidongula* in the Canadian high Arctic. Proc. Int. Seaweed Symp. 10: 247-252.

Conolly, N. J. & Drew, E. A. 1985. Physiology of *Laminaria*. III. Effect of a coastal eutrophication gradient on seasonal growth and tissue composition in *L. digitata* Lamour. and *L. saccharina* (L.) Lamour. P.S.Z.N. I: Mar. Ecol. 6: 181-195.

Dunton, K. H. 1985. Growth of dark-exposed *Laminaria saccharina* (L.) Lamour and *Laminaria solidongula* J. Ag. (Laminariales: Phaeophyta) in the Alaskan Beaufort Sea. J. Exp. Mar. Biol. Ecol. 94: 181-189.

Dunton, K. H. 1990. Growth and production in *Laminaria solidongula*: relation to continuous underwater light levels in the Alaskan high arctic. Mar. Biol. 106: 207-304.

Dunton, K. H., Reimnitz, E. & Schonberg, S. 1982. An Arctic kelp community in the Alaskan Beaufort Sea. Arctic 35: 465-484.

Glud, R. N., Kühl, M., Wenzhöfer, F. & Rysgaard, S. 2002. Benthic diatoms in a high Arctic fjord (Young Sound, NE Greenland): importance for ecosystem primary production. Mar. Ecol. Prog. Ser. 238: 15-29.

Gutt, J. 2001. On the direct impact of ice on marine benthic communities, a review. Polar Biol. 24: 553-564.

Hanelt, D. 1998. Capability of dynamic photoinhibition in Arctic macroalgae is related to their depth distribution. Mar. Biol. 131: 361-369.

Hanelt, D., Melchersman, B., Wiencke, C. & Nultsch, W. 1997. Effects of high light stress on photosynthesis of polar macroalgae in relation to depth distribution. Mar. Ecol. Progr. Ser. 149: 255-266.

Horner, R. & Schrader, G. C. 1982. Relative contributions of ice algae, phytoplankton, and benthic microalgae to primary production in the nearshore regions of the Beaufort Sea. Arctic 35: 485-503.

Johnston, C. S., Jones, R.G. & Hunt, R.D. 1977. A seasonal carbon budget for a laminarian population in a Scottish sea-loch. Helgoländer wits. Meeresunters. 30: 327-345.

Johansen, H. W. 1981. Coralline algae, a first synthesis. CRC Press, Boca Raton, FL, 239 pp.

Kirk, J. T. O. 1994. Light and photosynthesis in aquatic ecosystems. 2nd. ed. Cambridge University Press, Cambridge.

Kirst, G. O. & Wiencke, C. 1995. Ecophysiology of polar algae. J. Phycol. 31: 181-199.

Krause-Jensen, D. & Sand-Jensen, K. 1998. Light attenuation and productivity of aquatic plant communities. Limnol. Oceanogr. 43: 396-407.

Kühl, M., Glud, R. N., Borum, J., Roberts, R. & Rysgaard, S. 2001. Photosynthetic performance of surface-associated algae below sea ice as measured with a pulse-amplitude-modulated (PAM) flourometer and O_2 microsensors. Mar. Ecol. Prog. Ser. 223: 1-14.

Littler, M. M. & Murray, S. N. 1974. The primary productivity of marine macrophytes from a rocky intertidal community. Mar. Biol. 27: 131-135.

Lüning, K. & Dring, M. J. 1979. Continuous underwater light measurement near Helgoland (North Sea) and its significance for characteristic light limits in the sublittoral region. Helgoländer wiss. Meeresunters. 32: 403-424.

Lüning, K. 1990. Seaweeds – their environment, biogeography, and ecophysiology. John Wiley & Sons, inc. New York

Mann, K. H. 1972. Ecological energetics of the seaweed zone in a marine bay on the Atlantic coast of Canada. II Productivity of the seaweeds. Mar. Biol. 14: 199-209.

Mann, K. H. 1973. Seaweeds: Their productivity and strategy for growth. Science 182: 975-981.

Markager, S. & Sand-Jensen, K. 1994. The physiology and ecology of light-growth relationships in macroalgae. In: Round, F. E., & Chapman, D.J. (eds). Progress in phycological research, vol 10. Biopress, Bristol.

Matheke, G. E. M. & Horner, R. 1974. Primary productivity of the benthic microalgae in the Chucki Sea near Barrow, Alaska. J. Fish. Res. Board. Can. 31:1779-1786.

Parke, M. 1948. Studies on British Laminariaceae. I. Growth in *Laminaria saccharina* (L.) Lamour. J. Mar. Biol. Ass. U.K. 27: 651-709.

Platt, T., Gallegos, C. L. & Harrison, W. G. 1980. Photoinhibition of photosynthesis in natural assemblages of marine phytoplankton. J. Mar. Res. 38: 687-701.

Roberts, R. D., Kühl, M., Glud, R. N. & Rysgaard, S. 2002. Primary production of crustose coralline red algae in a high arctic fjord. J. Phycol. 38: 273-283.

Rysgaard, S., Kühl, M., Glud, R. N. & Hansen, J. W. 2001. Biomass, production and horizontal patchiness of sea ice algae in a high-Arctic fjord (Young Sound, NE Greenland). Mar. Ecol. Prog. Ser. 223: 15-23.

Sambrotto, R. N., Goering, J. J. & McRoy, C. P. 1984. Large yearly production of phytoplankton in the western Bering Strait. Science 225: 1147-1150.

Sand-Jensen, K. & Krause-Jensen, D. 1997. Broad-scale comparison of photosynthesis in terrestrial and aquatic plant communities. Oikos 80:1: 203-208.

Schaeffelke, B., Peters, A. F. & Reusch, T. B. H. 1996. Factors influencing depth distribution of soft bottom inhabiting *Laminaria saccharina* (L.) Lamour. in Kiel Bay, Western Baltic. Hydrobiologia 326/327: 127-123.

Schreiber, U., Gademann, R., Ralph, P. J. & Larkum, A. W. D. 1995. Assessment of photosynthetic performance of *Prochloron* in *Lissoclinum patella in hospite* by chlorophyll fluorescence measurements. Plant Cell. Physiol. 38: 945-951.

Sjötun, K. 1993. Seasonal lamina growth in two age groups of *Laminaria saccharina* (L.) Lamour. in Western Norway. Bot. Mar. 36: 433-441.

Sjötun, K. & Gunnarson, K. 1995. Seasonal growth of an Islandic *Laminaria* population (section Simplices, Laminariaceae, Phaeophyta) containing solid- and hollow-stiped plants. Eur. J. Phycol. 30: 281-287.

Steneck, R. S. 1986. The ecology of coralline algal crusts: convergent patterns and adaptive strategies. Ann. Rev. Ecol. Syst. 17: 273-303.

Subbarao, D. V. & Platt, T. 1984. Primary production of Arctic waters. Polar Biol. 3: 191-201.

Thinggaard, R. 2001. Vækstdynamik hos *Laminaria saccharina*. M.Sc. thesis. University of Aarhus and National Environmental Research Institute (NERI), Denmark.

Weile, K. 1996. Baseline study of *Laminaria* populations in Øresund. Doc. nr. 95/120/1E. Produced by VRI/Toxicon AB for Øresundskonsortiet, Denmark..

Photo: Göran Ehlmé

10

An estimation of walrus (*Odobenus rosmarus*) predation on bivalves in the Young Sound area (NE Greenland)

An estimation of walrus (*Odobenus rosmarus*) predation on bivalves in the Young Sound area (NE Greenland)

Erik W. Born[1] and Mario Acquarone[2*]

[1]Greenland Institute of Natural Resources, Kivioq 2, Box 570, DK-3900 Nuuk, Greenland
[2]National Environmental Research Institute, P.O. Box 358, DK-4000 Roskilde, Denmark
*Present address: Frue Kirkestræde 5, DK-5000 Odense, Denmark.

Cite as: Born, E.W. & Acquarone, M. 2007. An estimation of walrus (*Odobenus rosmarus*) predation on bivalves in the Young Sound area (NE Greenland). In: Rysgaard, S. & Glud, R. N. (Eds.), Carbon cycling in Arctic marine ecosystems: Case study Young Sound. Meddr. Grønland, Bioscience 58: 176-191.

Abstract

The total consumption of bivalve prey by walruses (*Odobenus rosmarus*) in the important inshore summer feeding area Young Sound (about 74˚ N) in Northeast Greenland was estimated. To determine relative area use, the movement and activity of three adult male walruses carrying satellite transmitters were studied during the open-water season in 1999 and 2001. Because one of the animals was tracked during both years the study covered a total of four "walrus seasons". Overall, the animals spent c. 30% of their time in the water inshore in Young Sound between Sandøen and Zackenberg. The remaining time was spent along the coast north and south of Young Sound and offshore in the Greenland Sea. The total amount of bivalve food consumed in Young Sound by the walruses during a total of 1620 "walrus feeding days" was calculated from information on the total number of walruses using the area (n=60), occupancy in the study area, and estimates obtained from satellite telemetry on the number of daily feeding dives (118-181/24 h at sea). Depending on the applied estimator of number of feeding dives, the estimated consumption by walruses of shell-free (SF) bivalve wet weight (WW) during the open-water period ranged between 111 and 171 tons. Based on estimates of mean total body mass (TBM: 1000 kg) of walruses using the area and daily *per capita* gross food intake (6% of TBM), the corresponding estimate of consumption by walruses is c. 97 tons SF WW. It is suggested that the two lowest estimates of total consumption are the most plausible.

10.1 Introduction

Major climatic changes in the Arctic due to global warming may affect walruses (*Odobenus rosmarus*) in various ways. Kelly (2001) suggested that a decreased extent of summer sea ice might negatively impact the ability of Pacific walruses (*O. r. divergens*) to obtain food in the Beaufort and Chukchi Seas. Born et al. (2003) hypothesized that in areas such as eastern Greenland, Svalbard and the Canadian High Arctic archipelago where Atlantic walruses (*O. r. rosmarus*) feed intensively inshore, a reduced ice cover may positively affect the walruses by allowing them access to their feeding areas for a longer time period. Furthermore, prolonging of the open-water period may enhance marine productivity in general (Rysgaard et al., 1999).

Temperatures have increased in the East Greenland–Svalbard area since the 1960s (Førland et al., 2002; Hanssen-Bauer, 2002). Consequently, the ice cover in the eastern Atlantic Arctic, including the East Greenland and Svalbard areas has decreased

during the last decades in both thickness and extent (Rothrock et al., 1999; Parkinson, 1992; 2000; Comiso, 2002; Comiso & Parkinson, 2004). Furthermore, the dramatic temperature increase and associated reduction in ice cover in the East Greenland area are predicted to continue during this century (Rysgaard et al., 2003).

To evaluate the effects of reduced ice cover on the Arctic marine ecosystems and their productivity, a multi-disciplinary study CAMP (Changes in the Arctic Marine Production) was initiated in 1995 (see Preface). The focal site of this study is Young Sound (c. 74˚ 15´ N) in Northeast Greenland where a small group of walruses feed intensively on the inshore mollusk banks during summer. Because walruses are a component of this ecosystem it was necessary to quantify their trophic role.

The stenophagous walruses are an important component of many High Arctic marine ecosystems where they predate on the benthic invertebrate fauna in coastal waters (e.g. Vibe, 1950; Fay, 1982; Oliver et al., 1983). Although walruses may feed on a variety of bottom-dwelling invertebrates, only a few bivalve species – usually *Mya* sp., *Hiatella* sp. and *Serripes* sp. – make up the bulk of their diet (Vibe, 1950; Fay, 1982; Fay et al., 1984; Sheffield et al., 2001). The Young Sound study area has a rich benthic infauna including abundant quantities of potential walrus food items (Sejr, 2002; Sejr et al., 2000, 2002; Born et al., 2003).

A small group of walruses, genetically distinct from the neighboring Svalbard and West Greenland groups (Andersen et al., 1998; Born et al., 2001) lives all year round in eastern Greenland where they are distributed mainly north of about 72˚ N (Born et al., 1997). Apparently, the walrus sub-population in eastern Greenland was on the verge of extinction around the middle of the 20th century due to over-exploitation by European whalers and sealers. However, since its protection in 1956 this sub-population of walruses has shown signs of a slow increase (Born et al., 1995, 1997; Witting & Born, 2005).

Two main areas are known where East Greenland walruses concentrate to feed inshore during summer: The Dove Bay area (76˚–77˚ N) and the Young Sound area (Fig. 10.1). Two regularly used terrestrial haul-out sites are found in these areas: Lille Snenæs in Dove Bay, and the island of Sandøen in Young Sound. These haul-outs are used mainly by male walruses, while females are distributed along the coast farther north (Born et al., 1997). In recent years, up to 60 (2004) walruses have been observed hauled out simultaneously on Sandøen (ibid., Born & Berg, 1999; M. Acquarone, unpubl. data).

Based on direct underwater observations of feeding walruses and satellite-telemetered information on diving activity, Born et al. (2003) estimated the amount of food ingested per single feeding dive and during a typical feeding excursion from Sandøen.

In the present study we estimate the total predation pressure exerted by walruses on the bivalve population of the Young Sound area during the open-water season. This is done by combining information on (1) movement and diving activity in Young Sound of individual walruses equipped with satellite-linked transmitters (this study), with (2) information on food ingested per dive and daily *per capita* feeding rate (Born et al., 2003), and (3) an estimate of number of walruses frequenting the area during the open-water period (L.W. Andersen & E.W. Born, unpubl. data). The purpose is to quantify the trophic role of walruses in the Young Sound ecosystem.

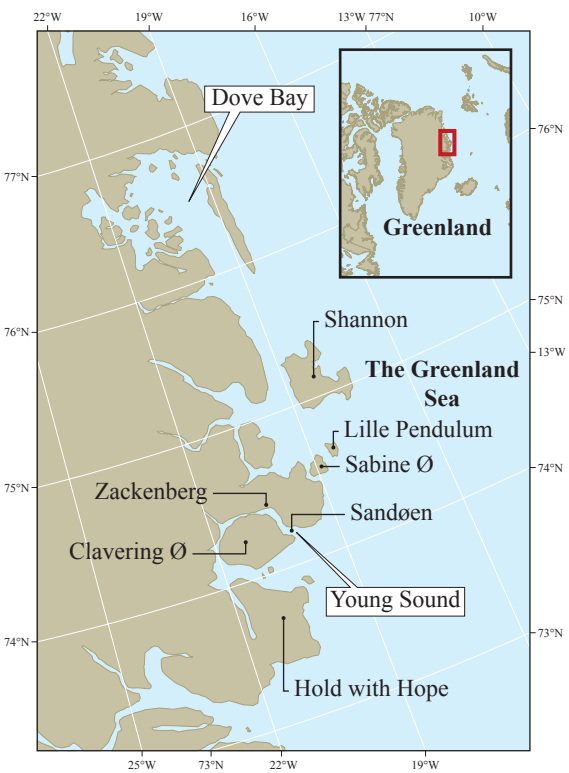

Figure 10.1 Map of the study area in Northeast Greenland.

Table 10.1 Identification code, type of satellite transmitter, date of instrumentation and last re-location, estimate of total body mass (TBM) and approximate age of three different adult male walruses tracked in the Young Sound area (NE Greenland) in 1999 and 2001.

ID	Transmitter type	Output (Watt)	Depth range (m)	Date of instrumentation	Last location Day-month-year	TBM[2)] (kg)	Age[3)] (year)
6481	ST-10	0.25	250	23 Aug. 1999	21 Nov. 1999	950	24 (at least 13)
4344[1)]	ST-10	0.25	500	24 Jul. 2001	4 Sep. 2001	1200	26 (at least 15)
11272	SPOT-2	0.50	-	27 Jul. 2001	14 Oct. 2001	1400	26 (at least 14)
6482	SPOT-2	0.50	-	28 Jul. 2001	24 Oct. 2001	1100	29[4)]

[1)] Tracked as no. 6481 in 1999
[2)] TBM = Total body mass estimated from body dimensions (Knutsen & Born, 1994)
[3)] Age estimated from a "tusk-circumference-at-age" relationship (cf. Materials and methods)
[4)] In 2002, this animal was killed by hunters at the entrance to Scoresby Sound and therefore molar teeth for estimation of age became available. Age was estimated from counting of growth layer groups in tooth cementum following the method of Mansfield (1958).

10.2 Materials and methods

10.2.1 The study animals

During August 1999 and July 2001 three individual adult male Atlantic walruses hauled out among other male walruses on the beach of Sandøen ("The Sand Island"; 74˚15´30´´N, 20˚18´00´´W) in Young Sound (NE Greenland) were immobilized with etorphine (Born & Knutsen, 1990a, Griffiths et al., 1993; Table 10.1). Estimates of total body mass (TBM) of these animals were obtained from equations on TBM versus standard body length and girth in Knutsen & Born (1994) (Table 10.1). Their approximate age was estimated from a "tusk-circumference-at-age" relationship obtained from 51 walruses sampled in NW Greenland (Circumference in cm at basis = 3.0 (SE: 0.94) + 20.5 (SE: 2.57) × (1-exp[-0.068(SE:0.02) × age in years])).

10.2.2 Tracking of movement

After immobilization of the animal, a satellite-linked radio transmitter was attached to one of its tusks as described in Born & Knutsen (1992) and Gjertz et al. (2001). Two different types of satellite transmitters were used. In 1999 and 2001, respectively, a ST-10 transmitter was attached to an individual that was tracked in both years. In 2001, SPOT-2 transmitters were fitted to the tusks of two other walruses (Table 10.1). All transmitters (Wildlife Computers, Redmond, Washington, USA) were able to provide data on location, but their sampling protocols for collection of sensor data were different (cf. section 10.2.3).

The GIS software ArcView 3.2a was used for mapping the movement of the walruses. For analyses of movement and area use (cf. Harris et al., 1990) all position data of all quality classes was run through the PC-SAS®ARGOS-filter, which chooses the most plausible location between the ARGOS primary and alternate locations based on minimum distance from the previous chosen location irrespective of the class (V.5.0, D.Douglas USGS, Alaska Science Center, 100 Savikko Road, PO Box 240009, Douglas, AK 99824, USA, unpubl. method).

Animal 6481 was tracked in 1999 and 2001 (4344; Table 10.1). Because its movements and diving activity differed in the two seasons it is treated as two different "cases" in the analyses of activity. Hence, a total of four individual "walrus seasons" were included in the study.

10.2.3 Activity data

Feeding by walruses was quantified in Young Sound for the areas between Sandøen and Zackenberg, and north of 74˚14´ N (i.e. on the northern coast of Clavering Ø due south of Sandøen). For each animal the approximate time spent inside (i.e. "total time spent inshore") and outside the study area during the open-water season was inferred from the satellite-telemetered locations. Time spent inshore for an animal was defined as fraction of days at locations in Young Sound west of Sandøen of all days monitored during the open-water period. The animals were tracked for different periods of time (Table 10.1) but their feeding activity was only described and quantified for the open-water season (for periods monitored see Table 10.2).

Table 10.2 Estimates of time spent at the inshore feeding banks in Young Sound (NE Greenland) by three adult male walruses tracked by use of satellite telemetry in 1999 and 2001.

ID	Period monitored	Total[1] hours monitored	Hours[2] inshore	% time spent inshore	% of total time spent in the water inshore[3]
6481	24 Aug.[4]–2 Oct. 1999	960	419	43.7	33.0
4344	24 Jul.–2 Aug. 2001[5]	228	228	100.0	34.4
11271	27 Jul.–2 Oct. 2001	1620	357	22.0	10.9
6482	28 Jul.–5 Oct. 2001	1668	948	56.8	44.9
All	All months, both years	4476	1952	43.6	29.5

[1] Period until formation of ice cover in Young Sound
[2] At Sandøen and west of this island
[3] Haul-out time subtracted (cf. Table 10.3)
[4] Day of instrumentation not included
[5] Location received until 4 Sep. but after filtering last validated location was from 2 August 2001

The ST-10 transmitter used in 1999 was able to collect diving data to a depth of 250 m, whereas the one deployed in 2001 had a maximum depth range of 500 m (Table 10.1). Maximum dive depth of the SPOT-2 transmitters was not specified. For the ST-10 units, information on haul-out time (duration of individual haul-outs and % of time hauled out) was collected via "timelines" (TIM) that stored data on the status of the salt-water switch (SWS; i.e. dry versus wet) in the course of 24 h (Born et al., 2002, 2003). The SPOT-2 transmitters were not able to collect dive data or information on the activity of the SWS. For these transmitters, the haul-out time was inferred from temperature data and locations. These units transmitted temperature information summed in 6-h blocks. The temperature histograms were stored in 14 user-defined intervals. For the present purpose, all 6-h blocks in which the temperature was 4˚C or higher were assumed to represent a period where the animal hauled out and exposed the sensor to its own or another walrus' body-heat or ambient air temperatures. Mean temperatures in Young Sound are below freezing 9 months of the year and only the months June to August have a positive mean air temperature of up to 4˚C (Rysgaard et al., 2003; Chapter 3). When a 6-h histogram contained values both below and above 4˚C, the walrus was assumed to be hauled out if ≥75% of the time was spent at ≥4˚C (only <3% of all 6-h blocks were categorized as representing a haul-out period based on this criterion). The reception during the same periods of good quality locations (location class 3 or 2; cf. Harris et al. 1990) was regarded as a confirmation of the fact that the animal was actually hauled out. Percentage of time spent in water inshore was determined as "total time spent in the study area minus percentage of time hauled out".

The ST-10 transmitters sampled time and pressure (depth) every 10 seconds. This data was stored in 6-hour blocks and then relayed to the satellite during the following 24 hours. Three types of dive data were used in the present study: (1) Number of dives per unit time, (2) duration of individual dives, (3) daily maximum dive depth (MDD), and (4) time at depth (TAD). Dive data was stored in 14 user-defined intervals, which were later organized in the following intervals for analysis: 0–6 m, >6 m. For analyses of diving activity (i.e. number of dives to different depths), haul-out time was extracted from the dive data.

Heavy floes of multi-year ice occasionally enter Young Sound from the Greenland Sea during summer. Scouring of the sea floor by this ice and in some cases by icebergs has resulted in relatively low densities of bivalve infauna at depths shallower than c. 6 m along the shores (Sejr et al., 2000; Chapter 7). Dives shallower than 6 m depth were therefore assumed to represent traveling and social activity, whereas all dives deeper than 6 m depth were categorized as feeding dives.

The number of feeding dives per 24 h was determined in two ways: (1) the number of dives exceeding 6 m was extracted from the ST-10 satellite transmitters and the number of dives below 6 m/24 h in water was calculated. In this analysis, which only included days spent inshore, all 6-h blocks with no dives were omitted; (2) the number of dives of between 5 and 7 min duration (i.e. typical feeding dives; Born et al., 2003 and references therein) were summed for

all inshore days and the average number of 5–7-min dives per 24 h at sea ("wet h") was calculated omitting 6-h blocks where the animal was hauled out.

10.2.4 Number, age composition and TBM of walruses

The group of walruses using the Young Sound study area during any summer was assumed to number 60 individuals on average. This estimate was based on (1) genetic identification using 11 nuclear markers (i.e. micro-satellites) of 38 individuals among 84 biopsies taken from walruses at Sandøen during August 2002, and 81 individuals among 185 biopsies collected there in 2004 (L. W. Andersen & E. W. Born, unpublished data), and (2) maximum day counts of 47 in 1991 (Born et al., 1997), 48 in 1994 (Born & Berg, 1999) and 60 in 2004 (M. Acquarone, unpublished data).

We estimated the average TBM of the walruses in Young Sound from ID photos taken at Sandøen in 2002 and 2003. The following method was used: The tusks of male walruses grow throughout life (Mansfield, 1958) and may therefore serve as a proxy for age, and hence TBM (cf. Knutsen & Born, 1994). Individual tusk length was estimated for 27 male walruses individually identified from ID photos taken on Sandøen during August 2002. Furthermore, individual tusk length was estimated from ID photos taken of 36 males among a record of 37 walruses hauled out in one group on Sandøen on 1 and 2 August 2003 (L. Ø. Knutsen & E.W. Born, unpublished data). On good "en face" and/or "profile" photos the length of an individual's tusk (from lip to tip) was estimated by comparing tusk length with the width of the eye (4–5 cm). A TBM vs. tusk length (measured from gum to tip, i.e. "clinical crown") relationship was established based on information on TBM and tusk length in 20 individual Atlantic male walruses from Hudson Bay (Loughrey 1959, n = 8), NW Greenland (E. W. Born & L. Ø. Knutsen, unpublished data; n = 9), and NE Greenland (E. W. Born & M. Acquarone, unpubl.; n = 3). Tusk lengths ranged from 0 to 47 cm, and TBM from 93 to 1629 kg. A quadratic hyperbola ($Y = Y_0 + ax + bx^2$) gave the best fit ($r^2 = 0.84$) to these TBM vs. tusk length data. TBM (kg) = 193.18 (SE: 95.53) + (16.86 (SE: 9.16) × tusk length (cm)) + (0.188 (SE: 0.20) × tusk length^2). To make our lip-to-tip lengths comparable with gum-to-tip lengths, 15% was added to our lip-to-tip estimates to account for the part of the tusk concealed by the lip during photography (i.e. an estimated 4 to 7 cm of the upper tusk was covered by the lip). These corrected tusk lengths in walruses at Sandøen and the TBM vs. tusk length relationship were then used to calculate individual TBM of walruses photographed on Sandøen in 2002 and 2003.

Estimates of shell-free (SF) bivalve wet weight (WW) biomass and dry matter (DM) obtained during single feeding dives were obtained from Born et al. (2003).

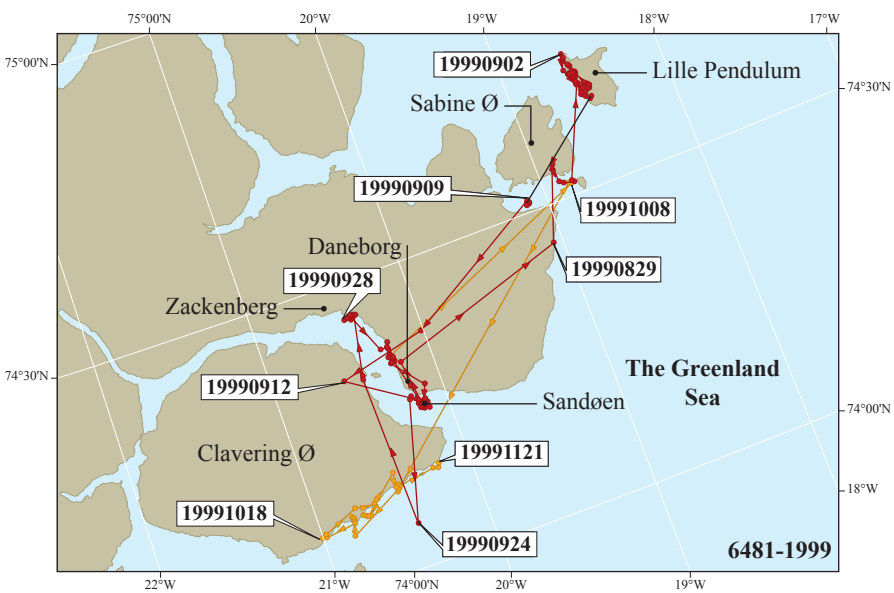

Figure 10.2 Movement of an adult male walrus (no. 6481) in Young Sound and adjacent areas in NE Greenland between 23 August and 21 November 1999. Red tracks = locations received during the open-water period until 3 October when a dense layer of fast ice had formed west of Sandøen. Orange tracks = locations received after formation of fast ice.

The duration of the open-water season (i.e. time from break-up of the fast ice in spring until formation of fast ice in the fall), in which walruses have access to the inshore mollusk banks in Young Sound, was 76 d in 1999 and 108 d in 2001 (Chapter 4). For simplicity, an open-water period of 90 d was used in the calculations.

Data on the total area of suitable walrus feeding habitat in Young Sound between Sandøen and Zackenberg (Fig. 10.2) from the coast to 60 m depth was extracted from Rysgaard et al. (2003, Regions 1, 2 and 3). This area amounted to 50.96 km^2 of which 24.13 km^2 were found between Sandøen and Basalt Ø situated halfway to Zackenberg.

Information on biomass and production of important bivalve prey in Young Sound was obtained from Chapter 7.

10.2.5 Estimation of walrus consumption of bivalves in Young Sound

The total amount of bivalves consumed by the walruses in Young Sound during the open-water season was estimated by two methods:

(1) Information was combined on (a) relative time spent in the Young Sound study area during four "walrus seasons" by three walruses tracked by use of satellite telemetry, (b) satellite-telemetered information on diving activity, (c) estimates of food ingested during single dives, (d) total number of walruses hauled out on Sandøen in Young Sound, and (e) total duration of the open-water period.
(2) Information was combined on (a) the average TBM of walruses using Young Sound, (b) food consumed (6.0% of TBM/walrus/24 wet h, 95% CI: 4.2-7.5; Born et al. 2002), (c) total number of walruses in Young Sound, and (d) total duration of the open-water period.

10.3 Results

10.3.1 The study area

The Young Sound study area has previously been described in Rysgaard et al. (2003) and Born et al. (2003). For the purpose of this study it is important to notice that a sill across the fjord at Sandøen divides Young Sound into an offshore and an inshore area. Inshore, along the coast west of Sandøen up to Zackenberg (Fig. 10.2) there is an abundance of shallow-water banks rich in walrus food items (e.g. Sejr, 2002; Chapter 7). Further inshore (i.e. west of Zackenberg) the fjord is much deeper with steep slopes. Walruses are not seen in this area and as the study animals did not enter this part of the fjord it is probably not a favorable walrus feeding habitat. Hence, for the quantification of bivalve food consumed by walruses in Young Sound only the areas around and west of Sandøen (Fig. 10.2) up to Zackenberg are considered.

10.3.2 The study animals

The estimated TBM and individual age of the three adult male walruses tracked by use of satellite telemetry during 1999 and 2001 ranged between c. 950 and c. 1400 kg and c. 24 and c. 29 years, respectively (Table 10.1).

10.3.3 Movement and area use

Animal no. 6481 was tracked from instrumentation on 23 August on Sandøen until 21 November 1999. During this period it used Young Sound but also moved north and south along the coast (Fig. 10.2). The reception of several high-quality locations (location class = 3) on the southwestern coast of Sabine Ø and from the southeastern coast of Clavering Ø indicated that no. 6481 also hauled out on land in these places. In 1999, this walrus spent about 44% of the time inshore in Young Sound either hauled out on Sandøen or in the water (Table 10.2).

The same individual was tracked in 2001 as no. 4344 from 24 July until 4 September (Table 10.1). However, after filtering of the locations its movements could only be reliably described until 2 August (Fig. 10.3), until which date it remained inshore (Table 10.2).

Animal no. 11272 was tracked from 27 July until 14 October 2001, during which time it made excursions offshore in the Greenland Sea as well as north and south of Young Sound (Fig. 10.4). Judging from the locations, no. 11272 spent about 22% of the time before formation of fast ice in the study area (Table 10.2).

Walrus no. 6482, which was tracked between 28 July and 24 October 2001 also made trips from Sandøen north to the Sabine Ø area and south to the south coast of Clavering Ø (Fig. 10.5). This animal about 57% of the open-water period inside the Young Sound study area (Table 10.2).

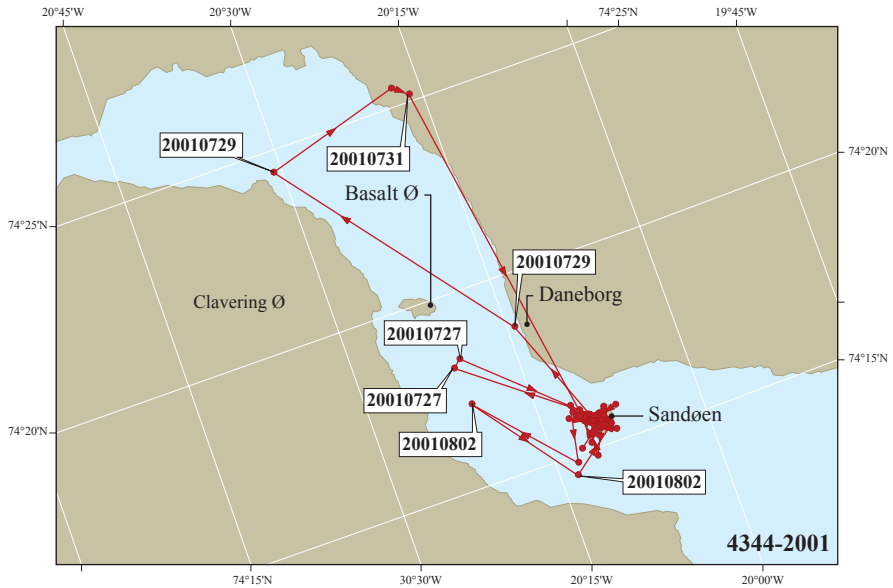

Figure 10.3 Movement of an adult male walrus (no. 4344) in the Young Sound area (NE Greenland) between 24 July and 2 August 2001. This animal was tracked as no. 6481 in 1999 (Table 10.1, Fig. 10.2). Locations were received until 3 September but only locations until 2 August remained after filtering (see Materials and methods).

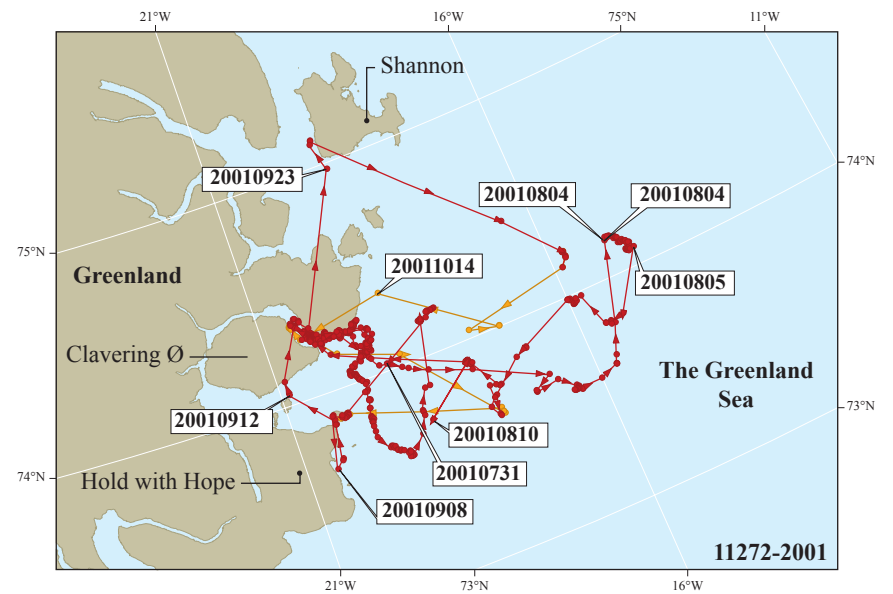

Figure 10.4 Movement of an adult male walrus (no. 11272) in Young Sound and adjacent areas in NE Greenland between 27 July and 14 October 2001. Red tracks = locations received during the open-water period until 3 October when a dense layer of fast ice had formed west of Sandøen. Orange tracks = locations received after formation of fast ice.

Overall, the locations indicated that the four walruses spent a weighted average of about 44% of the time in the Young Sound study area (Table 10.2). When at sea inside Young Sound, the locations indicated a clear preference for the areas in northern parts of the fjord where the waters are shallow (Figs. 10.2 & Fig. 10.5).

10.3.4 Haul-out and diving activity

During the open-water period the four walruses hauled out between c. 21 and 66% of the time. Overall, haul-out time averaged 31.4% (Table 10.3). In total, the walruses spent between c. 11 and 45% of the time in the water inside the study area (Table 10.2). Overall, the satellite-telemetered information indicated that on average the walruses spent about one third (29.5%) of the open-water season in the water in the Young Sound study area (Table 10.2).

Data on diving activity during the open-water season was only available for animal no. 6481/4344. For both years and all months combined, an average of c. 32% of the time at sea was spent between 0 and 6 m depth (about 11% of this time was spent at the surface; i.e. SWS dry), and the remainder of the time was at depths below 6 m (Table 10.4). Less than 1% of the time was spent at depths below c. 40 m.

About 80% of all dives inshore went to depths

Table 10.3 Estimates of haul-out time (%) for four seasons by three adult male walruses during time spent inshore in the Young Sound area (NE Greenland) in 1999 and 2001.

ID no.	Period monitored	% of time hauled out	Total days monitored	No. of 6-h blocks monitored
6481	25 Aug.–29 Sep. 1999	24.3	16	-
4344	24 Jul.–2 Aug. 2001	65.6	10	-
11271	1 Aug.–23 Aug. 2001	50.5	26	97
6482	28 Jul.–5 Oct. 2001	21.0	70	276
All	All months, both years	31.4	122	-

Table 10.4 Time (%) spent in different depth intervals (TAD, Time-At-Depth) by an adult male walrus (same individual in both years) inshore in the Young Sound area (NE Greenland) in 1999 and 2001.

ID no.	Month	Year	% time at different depths			Days monitored	No. of 6-h blocks
			At surface[1)]	0–6 m[2)]	>6 m		
6481	Aug.	1999	9.2	39.8	60.2	9	30
	Sep.	1999	11.8	29.8	70.2	29	88
	Oct.	1999	7.6	25.1	74.9	4	9
4344	Jul	2001	11.1	31.9	68.1	6	22
	Aug.	2001	15.8	37.2	62.8	2	2
	All	99+01	11.0	31.9	68.1	50	151

[1)] Time when the saltwater switch was dry
[2)] Includes time at surface.

Table 10.5 Number of dives and percentage of dives made to different depth intervals by an adult male walrus (same individual in both years) inshore in the Young Sound area (NE Greenland) in 1999 and 2001.

ID no.	Month	Year	% of all dives		No. dives	No. 6-h blocks with dive data[1)]	No. of dives beyond 6 m per 24 h[1)]	Dates
			0–6 m	>6 m				
6481	Aug.	1999	20.1	79.9	1798	29	198	23–31
	Sep.		17.7	82.3	4796	86	184	1–30
4344	Jul.	2001	24.6	75.4	1183	22	162	24–31
	Aug.		40.9	59.1	127	3	100	1–2
	All	99+01	19.7	80.3	7904	140	181	-

[1)] Haul-out periods excluded

of 6 m and deeper. During the different months, the animal made between 100 and 198 dives/24 wet h below 6 m, with an average of 181 dives/24 wet h (Table 10.5). Less than 1% of the dives went deeper than c. 40 m.

The duration of a walrus feeding dive is usually 5–7 min (Born et al. 2003 and references therein). During the inshore period, about 61% of all dives made by no. 6481/4344 lasted between 5 and 7 min (c. 77% of all dives were between 4 and 8 min in duration), Table 10.6. When inshore, the animal made an average of about 118 dives of 5–7 min duration per 24 h. Less than 2% of the dives lasted more than 8 min.

On days when no. 6481/4344 was inshore, the daily maximum depth readings averaged 35.4 m in 1999 (sd = 24.6, range: 14 – 86 m, n = 7 days with maximum dive depth data), and 26.5 m in 2001 (sd = 7.1, range: 20 – 36 m, n = 8), which is in accordance with direct observations (S. Rysgaard & G. Ehlmé, pers. comm.) that walruses in Young Sound mainly feed on the shallow-water bank along the shores. In none of the years did the maximum dive depths differ between inshore and offshore days (unpaired t-tests; $P > 0.05$). Walrus no. 6481/4344 dived to a maximum depth of 136 m on 30 August 1999 at 74˚40´ N and 18˚ 34´ W (i.e. outside Young Sound).

Table 10.6 Number of dives and percentage of dives made in different intervals of dive duration by an adult male walrus (same individual in both years) inshore in the Young Sound area (NE Greenland) in 1999 and 2001.

ID no.	Period	Year	% of dives		Total no. of dives[1)]	No. of 6-h blocks monitored	No. of 5–7 min long dives per 24 wet h	No. of days monitored
			5–7 min	4–8 min				
6481	27 Aug.–2.Oct.	1999	58.3	76.1	1335	27	115	10
4344	25 Jul.–2 Aug.	2001	66.0	78.2	565	12	124	4
	All	99+01	60.6	76.7	1900	39	118	14

[1)] Haul-out periods excluded

Table 10.7 Estimates of bivalves, dry matter (DM) and shell-free (SF), wet weight (WW) consumed per dive, total number of walruses using Young Sound, and estimates of total amount of bivalves, DM and WW eaten in the study area by walruses during the open-water season. During the open-water period, a total of 60 walruses spent about 30% of the time inshore for a total of 1620 "walrus feeding days".

	Parameter	Mean/estimated value	95% CI	Comments
A	Number of bivalves ingested/dive	53.2	43.0–64.4	Estimated from 10 feeding dives in Young Sound (Born et al., 2003)
B	DM/dive (g)	149.0	112.0–186.0	(Born et al., 2003)
C	WM/dive (g)	583.0	444.0–722.0	(Born et al., 2003)
D	Total number of walruses	60	-	Genetically identified (cf. Materials and methods)
E	Walrus feeding days	1620	-	Duration of open-water season, 90 d, *% occupancy * 60 walrus
F	Number of dives/day	118–181	-	Based on Tables 10.5 & 10.6
G	Total number of bivalves eaten	$10.2 * 10^6$–15.6×10^6	-	(A * E * F)
H	Total DM eaten ($\times 10^3$ kg)	28.5–43.7	-	(B * E * F)
I	Total WW eaten ($\times 10^3$ kg)	111–171	-	(C * E * F)
J	Total WW eaten ($\times 10^3$ kg)	97	68–122	Based on mean TBM and a daily food consumption of 6% (95% CI: 4.2–7.5%) of TBM when in water (Born et al., 2003).

DM = Dry Matter; WW = Wet Weight, or wet matter

10.3.5 The number of walruses in Young Sound

The number of animals hauled out on Sandøen likely reflects the number using Young Sound and adjacent areas for feeding during summer. Mainly adult males haul out on Sandøen, and observations of females or immature individuals are rare. However, during the summers of 2001–2004 the occurrence on Sandøen of females and young became more frequent (Born et al., 1997; Born et al., 2000; E. W. Born, unpublished data).

Opportunistic and systematic observations (Born & Berg, 1999; E. W. Born, unpublished data) of the number of walruses hauled out at Sandøen have been carried out since 1983. The daily maximum number of hauled out individuals ranged between 3 and 60. The highest numbers were recorded in 1991 (47), 1994 (48) and 2004 (60) (Born et al., 1997; Born & Berg, 1999; M. Acquarone, unpublished data). The maximum numbers seen on one occasion in the period late July through August 1998–2004 varied markedly (1998: 28, 1999: 9, 2000: 22, 2001: 19, 2002: 19, 2003: 37, 2004: 60; Born & Berg, 1999; Born et al., 2000; Acquarone et al., 2001; M. Acquarone, unpublished data). In 1999, when the lowest number was observed, unusually much pack ice entered Young Sound from the Greenland Sea. Sometimes this ice blocked the beach at the walrus haul-out, probably precluding access to the area. However, during all seasons it was clear from observations of individually recognizable animals (cf. Born et al. 1997) that the number of walruses frequenting the haul-out during August was higher than the highest number seen on any single occasion. This was confirmed in 2002 and 2003 when the daily maximum count during the period late July to late August was 19 and 37, respectively, whereas genetic identification *post*

hoc revealed that a total of 38 and 81 different animals used the haul-out during the same period (L. W. Andersen & E. W. Born, unpublished data).

10.3.6 Average TBM of walruses in Young Sound

Based on photos of 27 male walruses individually identified in 2002, the estimate of the average TBM of walruses at Sandøen was 1068 kg (sd = 295; range: 595–1571 kg). The corresponding estimate for 2003 was 970 kg (sd = 341; range: 296–1656 kg). However, for convenience, we use an average TBM of 1000 kg for the calculations of food consumption in Young Sound.

10.3.7 Estimation of the walrus consumption of bivalves in Young Sound

For the calculation of bivalve biomass consumption by walruses inshore in Young Sound we assume that a group of 60 walruses have access to the mollusk banks west of Sandøen during an open-water season usually lasting about 90 days. Given the average fraction of the total time spent by the walruses "at sea" inside this study area (ca. 30%), an estimated total of 1620 "walrus feeding days" are spent inshore in Young Sound (Table 10.7).

Method I

Based on the estimates of the daily mean number of dives to 6 m and deeper, and number of dives lasting between 5 and 7 min, the walruses make a total of c. 191×10^3 to 293×10^3 feeding dives in Young Sound between Sandøen and Zackenberg during the open-water season.

Using the estimates on number of bivalves – SF dry matter and wet weight – consumed per feeding dive (Table 10.7), the estimates (two methods of determining number of feeding dives, Tables 10.5 and 10.6) of the total number of bivalves consumed inshore in Young Sound during the open-water season ranged from ca. 10×10^6 to ca. 16×10^6 (Table 10.7). The estimate of the corresponding amounts of bivalve DM was c. 29 to 44 tons while WW amounted to c. 111 to 171 tons, respectively (Table 10.7).

Method II

The daily mean gross food consumption was c. 60 kg/walrus/24 wet h (95% CI: 42–75 kg/walrus/24 h) and the corresponding estimate of the total amount of SF bivalve WW consumed by walruses during the open water season equaled c. 97 tons (i.e. c. 25 tons DM) (Table 10.7).

10.3.8 Estimation of the impact of walrus predation on the bivalves

Daily feeding rates in walruses of 6% of TBM (Born et al., 2003; Acquarone, 2004) indicate that the estimates of 111 tons (*Method I*) and 97 tons (*Method II*) are the most plausible. An estimate of the total consumption by walruses during the open-water season of ca. 100 tons wet matter (i.e. 111 and 97

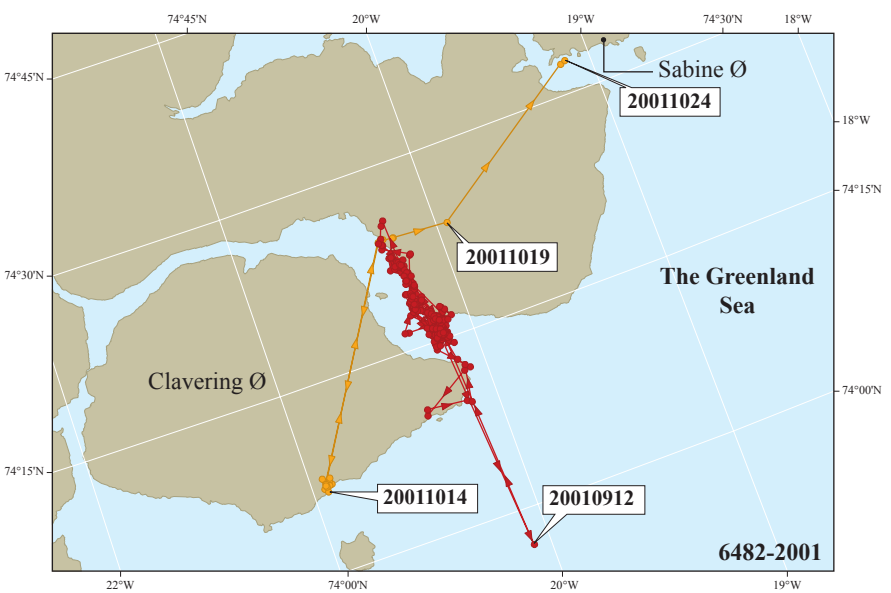

Figure 10.5 Movement of an adult male walrus (no. 6482) in Young Sound and adjacent areas in NE Greenland between 28 July and 24 October 2001. Red tracks = locations received during the open-water period until 6 October when a dense layer of fast ice had formed west of Sandøen. Orange tracks = locations received after formation of fast ice.

Photo: Erik W. Born

An adult male walrus fitted with a ST-10 satellite transmitter monitoring walrus activity in Young Sound.

tons, respectively; Table 10.7, I and J) corresponds to the removal of c. 1.96 g/m^2 SF bivalve WW down to 60 m depth in the areas of Young Sound (total area: 50.96 km^2) that we extrapolate to.

The standing biomass and annual production down to 60 m depth of the two important walrus food items *Mya* sp. and *Hiatella* sp. were determined in the areas between Sandøen and the Basalt Ø (biomass and production of *Serripes* sp. were not determined). In that area (24.13 km^2, <60 m depth), the SF WW biomass and annual production of *Mya* and *Hiatella* taken together are c. 78 g m^{-2} yr^{-1} and 7.9 g m^{-2} yr^{-1} × year, respectively (Chapter 7). Hence, our estimate of walrus predation per m^2 amounts to c. 2.5% of the standing biomass of *Mya* sp. and *Hiatella* sp., and c. 25% of the annual production of these bivalves. However, one must keep in mind that in Young Sound the walruses also forage on other bivalves and benthic invertebrates (Born et al., 1997, 2003).

10.4 Discussion

10.4.1 Numbers and TBM

The estimate of average TBM in this study was 1000 kg. The estimate of average TBM differed slightly between 2002 and 2003. However, because the 27 individually identified walruses in 2002 likely were a non-representative part of the group (ID characters such as scars, knobs and cracked tusks are typical in old walruses; cf. Born et al. 1997), we believe the estimate of average TBM based on all animals in the group in 2003 to be more representative. The majority of walruses using Sandøen and Young Sound are adult males. Asymptotic TBM in males from NW Greenland was 1114 kg (Knutsen & Born, 1994). This indicates that the average TBM used in the present study is reasonable.

10.4.2 Movement

The area of interest to the multi-disciplinary study of marine productivity has been defined as being the areas between Sandøen and Basalt Ø in particular (Chapter 11). This is also the area in which a variety of marine biological studies have been conducted since 1995 (e.g. Rysgaard et al., 1996, 1998, 1999; Sejr et al., 2000, 2002) and for which an overall carbon/energy flow budget has been calculated (Chapter 11). However, the general scarcity of "at sea" locations received from the walruses tracked in the present study only allowed determination of time in Young Sound west of Sandøen to Zackenberg and not sub-division of the time budget in this area.

The satellite-derived locations indicated that walruses on average spend about 30% of the open-water season inshore in Young Sound with a clear preference for the northern shore west of Zackenberg. However, during the study period, the animals also used other feeding locations south, east and north of Young Sound. The latter area (i.e. the Sabine Ø–Lille Pen-

dulum Ø area) is a well-known walrus foraging habitat (Born et al., 1997). In other studies of movement during summer, the walruses also regularly moved c. 80 km or farther away from the haul-out (Born & Knutsen, 1992; Hills, 1992; Wiig et al., 1996). Clearly, walruses use several alternative feeding grounds in the vicinity of their traditional haul-out.

Usually, the fraction of good-quality locations received from hauled out walrusses is relatively high, whereas fewer locations, usually of lower precision, are received from animals at sea (Born & Knutsen, 1992; Jay et al., 2001). Walruses spend proportionally much time submerged (*e.g*. Wiig et al., 1992; Born & Knutsen, 1997; Born et al., 2003) and do not always get the salt-water switch of the transmitter out of the water when ventilating (E.W. Born, unpubl. data), resulting in no or too few signals being transmitted. This may imply that relatively few locations are transmitted from areas where walruses are at sea and actively foraging. This fact obviously will influence the ability to proportionate time in different areas based on locations.

10.4.3 Haul-out and diving activity

We tracked relatively few animals during two open-water seasons. However, the activity of the animals monitored via satellite telemetry was typical of walruses in general. The animals hauled out for an average of about 31% of the time, which is in close agreement with haul-out times obtained during August–September in other studies of walrus activity involving satellite telemetry (Hills, 1992; Born & Knutsen, 1992).

We defined dives deeper than 6 m as feeding dives. The proportions of the number of dives to these depths were within the range observed in walruses studied in Dove Bay in August 2001. Here, six adult male walruses equipped with MK-7 dive recorders (Wildlife Computers) hauled out for an average of 34% of the time and made an average of 165 dives to >6 m/24 "wet" h (range: 108–208 dives/24 h) (Acquarone, 2004).

Visual observations of walruses feeding along the northern coast of Young Sound indicate that they feed between c. 8 and 34 m (Born et al., 2003). The vast majority of dives were between 6 and 42 m, which is typical of walruses that are thought to be feeding (Gjertz et al., 2001; Jay et al., 2001). Hence, our assumption that activity between 0 and 6 m was mainly associated with traveling, breathing and resting at the surface, and social interactions with other walruses seems sound.

We also quantified foraging from the number of dives of 5–7 min duration, which is the duration of typical feeding dives in walruses (Wiig et al., 1992; Gjertz et al., 2001; Jay et al., 2001).

In the present study, the walruses made an average of 118–181 presumed feeding dives/24 h in water. If "at surface" intervals of c. 1 min between feeding dives (Born & Knutsen, 1997; Born et al., 2003) are added it follows that the walruses were engaged in diving for food for between 57% ("dive duration") and 88% ("dives at depth") of their "in water" time. Six adult male walruses tracked by use of satellite transmitters in Dove Bay in 1989 were diving for an average of 72% of their "at sea" time (range: 65%–77%; Born & Knutsen, 1990b). Similarly, six males studied with MK-7 dive recorders in the same area were submerged for an average of 66% of the time (range: 34%–84%; Acquarone, 2004). This indicates that (1) the activity seen in the present study is typical of walruses when feeding inshore, and (2) that the estimate of total food consumption based on number of 5–7-min dives/24 wet h is a reasonable approach.

However, some dives deeper than 6 m and 5–7 min long could have been unsuccessful feeding dives. If so, the amount of food consumed by the walruses is overestimated to an unknown extent.

10.4.4 Estimates of number of walruses, TBM and food consumption

In the calculations of the number of "walrus feeding days" we assumed that the total group using the area is about 60. This was based on the genetic identification of individuals in 2002 and 2003. Clearly, the number using the area can vary widely between years. The fact that 2003 and 2004 were years with very little ice in the area probably caused the walruses to use Sandøen intensively as a haul-out. Consequently, many walruses used the haul-out during those years, and we cannot exclude that this inflated our estimate of the average number of walruses using the Young Sound area.

Based on the tracking of admittedly few animals we estimated that at any given time about 20 walruses are foraging in the Young Sound between Sandøen and Zackenberg at depths between 0 and 60 m. In August 2001, Levermann et al. (2004) studied walrus foraging activity through direct observations

Photo: Göran Ehlmé.

As part of this study, walrus feeding during individual dives was determined by collecting shells of recently predated bivalves (c.f. Born et al. 2003).

within a 1.5-km^2 area at the coast c. 5 km north of the island Sandøen. They found that the probability of a walrus being present within the observation area at any given time was 0.47. Hence, provided that the walrus activity in the observation area of Levermann et al. (2004) is representative of the activity in the entire Young Sound walrus foraging habitat considered by us, a simple extrapolation from the observational data indicates that about 16 walruses are foraging in Young Sound at any given time during August ([51/1.5] × 0.47).

We estimated that the average TBM of the walruses in Young Sound is about 1000 kg. This is somewhat higher than the average TBM of 512 kg used by Welch et al. (1992) for calculation of walrus feeding in Lancaster Sound (Canada), and 712 kg used by Fay (1982) in Alaska. However, the walruses that feed in Young Sound are nearly all adult males in contrast to the other two areas where all age classes and both sexes are represented at the summer feeding grounds.

For calculation of food consumption (*Method II*) we assumed that the daily gross food intake of walruses in the water is 6% (Born et al., 2003). Fay (1982) assumed that the daily food consumption of a 1000 kg walrus is 5.7%. Measurement of walrus energy expenditure by use of double-labeled water in NE Greenland in 2001 indicated that daily gross food consumption in adult male walruses is 5–6% of TBM (Acquarone, 2004). Fay (1982) estimated that daily food intake in free-ranging walruses is 4–8% of TBM. We therefore believe that the estimate of 6% used in this study is realistic.

From direct observations, Levermann et al. (2004) estimated that a total of c. 2.5 tons of bivalve SF wet matter was removed in the 1.5-km^2 observation area (ca. 1.67 g/m^2 SF bivalve WW) during the 90-day open-water period. If we apply this estimate to the total foraging area used in the present study, walruses may consume an estimated c. 85 tons of clam meat in Young Sound during the open-water season. However, in Levermann et al. (2004) the study area constituted only c. 3% of the outer region of the fjord and covered a smaller part of the inshore period.

10.4.5 The impact of the walruses on the bivalve community

A high standing stock of bivalves is present in the study area (Sejr et al., 2000; Sejr et al., 2002; Chapter 7), which is representative of other inshore ice-covered Arctic areas (Berthelsen, 1937; Vibe, 1950; Ockelmann, 1958; Thomson et al., 1986; Grebmeier et al., 1989; Welch et al., 1992).

However, the standing stocks and productivity in Young Sound of other walrus food items, for example *S. groenlandicus*, have not been determined. If these are considered as well, the inshore bivalve banks in Young Sound represent a richer food source than accounted for in our calculation of predation, which is based on only two prey species.

The estimates of gross food intake per dive or per TBM used in the present study were adopted from Born et al. (2003) and were based on three bivalve species that constitute the far most important portion of the walrus diet. However, walruses feed on a variety of benthic food (e.g. Fay, 1982) and as pointed

out by Born et al. (2003) it is not unlikely that walruses in Young Sound may also feed on other bivalves (e.g. *Astarte* sp.) and invertebrate benthos (*e.g*. polychaetes, sea cucumbers and gastropods) besides the three species considered. On the other hand, historical observations of the diet of walruses feeding in the vicinity of Young Sound indicate that *M. truncata* and *Hiatella* sp. were principal food items (Peters, 1874; Payer, 1877a,b) as well as being the most abundant species in the area. Hence, the estimates of the present study of walrus ingestion rates inferred from the bivalves studied are likely to be representative.

We conclude that (1) walruses that haul out on Sandøen only use Young Sound as one of several alternative feeding grounds during summer, and (2) that activity data and information on number of walruses and food ingestion rates indicate that walrus predation in Young Sound is below the carrying capacity of this fjord. This latter conclusion is supported by the fact that, historically, walruses were more abundant in the area (Born et al., 1997).

10.5 Acknowledgments

This study was supported financially by The Danish Natural Science Research Council, The Commission for Scientific Research in Greenland (KVUG), The Greenland Institute of Natural Resources (GN) and The Danish National Environmental Research Institute (NERI). Special thanks to Søren Rysgaard and Mikael Sejr (NERI, Silkeborg, Denmark), Liselotte W. Andersen (NERI, Kalø, Denmark), Göran Ehlmé (WaterProof, Partille, Sweden), Nette Levermann (GN, Nuuk, Greenland), Lars Heilmann (GN) and Lars Ø. Knutsen (Cinenature, Löa, Sweden) for inspiring co-operation in the field and during various phases of analyses. Also thanks to David Griffiths (The Norwegian School of Veterinary Science, Oslo, Norway), Torsten Møller (Kolmården Zoological Garden, Kolmården, Sweden), the Danish Military Patrol, Sirius in Northeast Greenland, and the Danish Polar Centre for valuable support during this study. We thank Wildlife Computers (Seattle, USA) for their enthusiastic work on developing the satellite tags for walrus, and Christina Lockyer (Age-Dynamics, Lyngby, Denmark) for ageing walrus no. 6482. R.E.A. Stewart (Department of Fisheries and Oceans, Winnipeg, Canada) and Ian Gjertz (The Research Council of Norway), who acted as referees on the paper, are thanked for offering useful comments that greatly improved it. We also wish to thank Søren Rysgaard and Ronnie Glud for offering comments that improved the paper.

10.6 References

Acquarone, M. 2004. Body composition, field metabolic rate and feeding ecology of walrus (*Odobenus rosmarus*) in Northeast Greenland. PhD Thesis. National Environmental Research Institute and University of Veterinary Science, Denmark, 142 pp.

Acquarone, M., Born, E. W. & Griffiths, D. 2001. Studies of walrus energetics and behaviour. In: Caning, K & Rasch, M. (eds.). Zero Zackenberg Ecological Research Operations 6th Annual Report. Danish Polar Center, Ministry of Research and Information Technology, Copenhagen, Denmark, 80 pp.

Andersen, L. W., Born E. W., Gjertz, I., Wiig, Ø., Holm, L. E. & Bendixen, C. 1998. Population structure and gene flow of the Atlantic walrus (*Odobenus rosmarus rosmarus*) in the eastern Atlantic Arctic based on mitochondrial DNA and microsatellite variation. Mol. Ecol. 7: 1323-1336.

Born. E. W. & Knutsen, L. Ø. 1990a. Immobilization of Atlantic walrus (*Odobenus rosmarus rosmarus*) by use of etorphine hydrochloride reversed by diprenorphine hydrochloride. Technical Report No. 14. Greenland Home Rule. Department of Wildlife Management, Nuuk, Greenland: 1-15.

Born, E. W. & Knutsen, L. Ø. 1990b. Satellite tracking and behavioural observations of Atlantic walrus (*Odobenus rosmarus rosmarus*) in NE Greenland in 1989. Technical Report No. 20. Greenland Home Rule. Department of Wildlife Management, Nuuk, Greenland: 1-68.

Born, E. W. & Knutsen, L. Ø. 1992. Satellite-linked radio tracking of Atlantic walruses (*Odobenus rosmarus rosmarus*) in northeastern Greenland. Z. Saügetierk 57: 275-287.

Born, E. W., Gjertz, I. & Reeves, R. R. 1995. Population assessment of Atlantic walrus (*Odobenus rosmarus rosmarus*). Nor. Polarinst. Medd. 138: 1-100.

Born, E. W. & Knutsen, L. Ø. 1997. Haul-out activity of male Atlantic walruses (*Odobenus rosmarus rosmarus*) in northeastern Greenland. J. Zool. (Lond.) 243: 381-396.

Born, E. W., Dietz, R., Heide-Jørgensen, M. P. & Knutsen, L. Ø. 1997. Historical and present status of the Atlantic walrus (*Odobenus rosmarus rosmarus*) in eastern Greenland. Meddr. Grønland., Biosci. 46: 1-73.

Born, E. W. & Berg, T. B. 1999. A photographic survey of walruses (*Odobenus rosmarus*) at the Sandøen haul-out (Young Sound, eastern Greenland) in 1998. Technical Report no. 26. Greenland Institute of Natural Resources, Nuuk: 1-19.

Born, E. W., Acquarone, M. & Griffiths, D. 2000. Studies of walrus energetics and behaviour. In: Zero Zackenberg Ecological Research Operations 5th Annual Report. Danish Polar Center, Ministry of Research and Information Technology, Copenhagen, Denmark: 72-73.

Born, E. W., Andersen, L. W., Gjertz, I. & Wiig, Ø. 2001. A review of genetic relationships of Atlantic walruses (*Odobenus rosmarus rosmarus*) east and west of Greenland. Polar Biol. 24 (10): 713-718.

Born, E. W., Teilmann, J. & Riget, F. 2002. Haul-out activity of ringed seals (*Phoca hispida*) determined from satellite telemetry. Mar. Mamm. Sci. 18(1): 167-181

Born, E. W. Rysgaard, R., Ehlmé, G., Sejr, M. K., Acquarone, M. & Levermann, N. 2003. Underwater observations of foraging free-living walruses (*Odobenus rosmarus*) including estimates of their food consumption. Polar. Biol. 26: 348-357.

Berthelsen, E. 1937. Contributions to the animal ecology of the fiords of Angmagssalik and Kangerlugssuaq in East Greenland. Meddr. Grønland. 108(3), 58 pp.

Comiso, J. C. 2002. A rapidly declining perennial sea ice cover in the Arctic. Geophys. Res. Lett. 29: 1956.

Comiso, J. C. & Parkinson, C. L. 2004: Satellite-observed changes in the Arctic. Physics Today, August 2004: 38-44.

Fay, F. H. 1982. Ecology and biology of the Pacific walrus, *Odobenus rosmarus divergens* Illiger. U.S. Department of the Interior Fish and Wildlife Service. North American Fauna 74: 1-279.

Fay, F. H., Bukhtiarov, Y. A., Stoker, S. W. & Shults, L. M. 1984. Foods of the Pacific walrus in winter and spring in the Bering Sea. In: Fay F. H. & Fedoseev, G. A. (eds.). Soviet-American Cooperative Research on Marine Mammals. Vol. 1 - Pinnipeds. NOAA Technical Reports NMFS 12. Washington D.C., USA: 81-88.

Førland, E. J., Hanssen-Bauer, I., Jónsson, T., Kern-Hansen, C., Nordli, P. Ø., Tveito, O. E. & Vaarby Laursen, E. 2002. Twentieth-century variations in temperature and precipitation in the Nordic Arctic. Polar. Rec. 38(206): 203-210.

Gjertz, I., Griffiths, D., Krafft, B. A., Lydersen, C. & Wiig, Ø. 2001. Diving and haul-out patterns of walruses *Odobenus rosmarus* on Svalbard. Polar. Biol. 24: 314-319.

Griffiths, D., Wiig, Ø., Gjertz, I. 1993. Immobilization of walrus with etorphine HCl hydrochloride and Zoletil®. Mar. Mamm. Sci. 9: 250-257.

Grebmeier, J. M., Feder, H. M. & McRoy, P. 1989. Pelagic-benthic coupling on the shelf of the northern Bering and Chuckchi Seas. II. Benthic community structure. Mar. Ecol. Prog. Ser. 51: 253-268.

Hanssen-Bauer, I. 2002. Temperature and precipitation in Svalbard 1912-2050: measurements and scenarios. Polar. Rec. 38(206): 225-232.

Harris, R. B., Fancy, S. G., Douglas, D. C., Garner, G. W., Amstrup, S. C., McCabe, T. R. & Pank, L. F. 1990. Tracking wildlife by satellite: current systems and performance. United States Department of the interior fish and wildlife service, Washington, D.C., USA: 1-52.

Hills, S. 1992. The effect of spatial and temporal variability on population assessment of Pacific walruses. PhD-thesis, University of Maine, Orono, U.S.A.

Jay, C., Farley, S. D. & Garner, G. W. 2001. Summer diving behaviour of male walruses in Bristol Bay, Alaska. Mar. Mam. Sci. 17: 617-631.

Kelly, B.P. 2001. Climate change and ice breeding pinnipeds. In: Walther, G-R., Burga C.A. & Edwards, P.J. (eds.). Fingerprints of climate changes, adapted behaviour and shifting species range. Kluwer Academic/ Plenum Publishers, New York 2001: 43-55.

Knutsen, L. Ø. & Born, E. W. 1994. Body growth in Atlantic walruses (*Odobenus rosmarus rosmarus*) from Greenland. J. Zool. (Lond.) 234: 371-385.

Levermann, N., Sejr, M. K., Rysgaard, S. & Born, E. W. 2004. Walrus foraging ecology and area use in a Northeast Greenlandic fiord. In preparation for Mar Ecol Prog Ser. Chapter II. In: Levermann, N.: Waltzing with walruses. M. Sc. thesis, November 2004, University of Copenhagen: 141 pp.

Loughrey, A. G. 1959. Preliminary investigation of the Atlantic walrus *Odobenus rosmarus rosmarus* (Linnaeus). Can. Wildl. Serv., Wildl. Manage. Bull. Ser. 1 No. 14: 123 pp.

Mansfield, A. W. 1958. The biology of the Atlantic walrus, *Odobenus rosmarus rosmarus* (Linnaeus) in the eastern Canadian arctic. Fisheries Research Board of Canada Manuscr. Rep. Ser. (Biol.) No. 653: 1-146.

Ockelmann, K. 1958. Marine Lamellibranchiata. Meddr. Grønland. 122(4), 256 pp.

Oliver, J. S., Slattery, P. N., O´Connor, E. F. & Lowry, L. F. 1983. Walrus, *Odobenus rosmarus*, feeding in the Bering Sea; a benthic perspective. Fish. Bull. 81: 501-512.

Parkinson, C. L. 1992. Spatial patterns of increases and decreases in the length of the sea ice season in the North Polar Region, 1979-1986. J. Geophys. Res. 97: 14377-14388.

Parkinson, C. L. 2000. Variability of Arctic Sea ice: The view from the space, an 18-year record. Arctic 53: 341-358.

Payer, J. 1877a. Upptäcktsresor i Norra Polarhafvet [Discoveries in the northern Polar Sea]. Albert Bonniers Förlag, Stockholm (In Swedish).

Payer, J. 1877b. Den østrisk-ungarnske Nordpol-Ekspedition i Aarene 1872-1874 [The Austrian-Hungarian North Pole Expedition in the Years 1872-1874]. København (In Danish).

Peters, W. 1874. Die zweite deutsche Nordpolfärht in den Jahren 1869 und 1870 unter Führung des Kapitän Karl Koldewey [The second German North Pole Expedition in the Years 1869 and 1870 under the Command of Captain Karl Koldewey]. F.A. Brockhaus, Leipzig (In German).

Rothrock, D. A., Yu, Y. & Maykut, G. A. 1999. Thinning of the Arctic sea-ice cover. Geophys. Res. Lett. 26: 3469-3472.

Rysgaard, S., Dahlgaard, H. & Finster, K.1996. Primary production, nutrient dynamics and mineralization in a northeastern Greenland fjord during the summer thaw. Polar. Biol. 16: 497-506.

Rysgaard, S., Thamdrup, B., Risgaard-Petersen, N., Fossing, H., Berg, P., Christensen, P. B. & Dalsgaard, T. 1998. Seasonal carbon and nitrogen mineralization in a high-Arctic coastal marine sediment, Young Sound, Northeast Greenland. Mar. Ecol. Prog. Ser. 175: 261-276.

Rysgaard, S., Nielsen, T. G. & Hansen, B. 1999. Seasonal variation in nutrients, pelagic primary production and grazing in a high-Arctic coastal marine ecosystem, Young Sound, Northeast Greenland. Mar. Ecol. Prog. Ser. 179: 13-25.

Rysgaard, S., Vang, T., Stjernholm, M., Rasmussen, B., Windelin, A. & Kiilsholm, S. 2003. Physical conditions, carbon transport and climate change impacts in a NE Greenland fjord. Arct. Antarct. Alp. Res. 35(3): 301-312.

Rysgaard, S., Frandsen, E., Sejr, M. K., Dalsgaard, T., Blicher, M. E. & Christensen, P. B. 2005. Zackenberg Basic: The MarineBasic Programme. In: Rasch, M & Caning, K. (eds.) Zackenberg Ecological Research Operations, 10th Annual report, 2004. Danish Polar Center, Ministry of Science, Technology and Innovation. Copenhagen. 85 pp.

Sejr, M. K., Jensen, K. T. & Rysgaard, S. 2000. Macrozoobenthos in a Northeast Greenland Fjord: Structure and Diversity. Polar Biol. 23: 792-801.

Sejr, M. K., Sand, M. K., Jensen, K. T., Petersen, J. K., Christensen, P. B. & Rysgaard, S. 2002. Growth and production of *Hiatella arctica* (Bivalvia) in a high-arctic fjord (Young Sound Northeast Greenland) Mar. Ecol. Prog. Ser. 244: 163-169.

Sejr, M. K. 2002. Functional importance of macrozoobenthos in Young Sound, NE Greenland. PhD-thesis, University of Aarhus, Denmark, 159 pp.

Sheffield, G., Fay, F. H., Feder, H. & Kelly, B. P. 2001. Laboratory digestion of prey and interpretation of walrus stomach contents. Mar. Mamm. Sci. 17: 310-330.

Thomson, D. H., Martin, C. M. & Cross, W. E. 1986. Identification and characterization of arctic nearshore benthic habitats. Technical Report 1434. Can. Fish. Aquat. Sci., 70 pp.

Vibe, C. 1950. The marine mammals and the marine fauna in the Thule district (Northwest Greenland) with observations on the ice conditions in 1939-41. Meddr. Grønland. 150, 115 pp.

Welch, H. E., Bergmann, M. A., Siferd, T. D., Martin, K. A., Curtis, M. F., Crawford, R. E., Conover, R. J. & Hop, H. 1992. Energy flow through the marine ecosystem of the Lancaster Sound region, Arctic Canada. Arctic 45: 343-357.

Wiig, Ø., Gjertz, I., Griffiths, D. & Lydersen, C. 1992. Diving patterns of an Atlantic walrus *Odobenus rosmarus rosmarus* near Svalbard. Polar. Biol. 13: 71-72.

Wiig, Ø., Gjertz, I. & Griffiths, D. 1996. Migration of walruses (*Odobenus rosmarus*) in the Svalbard and Franz Josef Land area. J. Zool. (Lond.) 238: 769-784.

Witting, L. & Born, E. W. 2005. An assessment of Greenland walrus populations. ICES J. Mar. Sci. 62: 266-284.

Photo: Søren Rysgaard

11

The annual organic carbon budget of Young Sound, NE Greenland

The annual organic carbon budget of Young Sound, NE Greenland

Ronnie N. Glud[1] and Søren Rysgaard[2]

[1]Marine Biological Laboratory, University of Copenhagen, Strandpromenaden 5, DK-3000 Helsingør, Denmark
[2]Greenland Institute of Natural Resources, Kivioq 2, DK-3900 Nuuk, Greenland

Cite as: Glud, R. N. & Rysgaard, S. 2007: The annual organic carbon budget of Young Sound, NE Greenland. In: Rysgaard, S. & Glud, R. N. (Eds.), Carbon cycling in Arctic marine ecosystems: Case study Young Sound. Meddr. Grønland, Bioscience 58: 194-203.

Abstract

On the basis of data presented in the previous chapters a carbon budget for the respective compartments of the outer region of Young Sound (76 km^2) was established. The average and maximum water depth of the region was 76 m and 177 m, respectively. Primary production was mainly related to the activity of phytoplankton (65%), benthic macrophytes (21%) and benthic microphytes (13%), while the contribution sea-ice algae and corallines was negligible (<1%). The pelagic grazing community was completely dominated by copepods, which were capable of consuming 87% of the pelagic primary production.

The benthic carbon demand was almost balanced by the measured sedimentation of POC and the benthic primary production. The organic carbon collected in the sediment traps was estimated to consist of 40% terrestrial carbon, 20% fecal pellets, while the rest was poorly defined marine detritus. The benthic sink for settling organic material was dominated by microbial respiration (59%) and only to a minor extent related to macrofauna respiration (15%) and carbon preservation (26%).

The total primary production in the region (1119 t C yr^{-1}) only sustained c. 40% the estimated organic carbon demand (2850 t C yr^{-1}). Thus, the independently determined input of TOC (990 t C yr^{-1}) imported to Region 1 from land via freshwater runoff and the TOC import of 1446 t C yr^{-1} from the Greenland Sea are required to balance the carbon sinks of the net heterotrophic region. A complete balance between the respective compartments cannot be expected, as the various components of the carbon budget are determined independently. The microbial and viral loops remain poorly constrained, as does the carbon demand of the top-predators. Only the importance of walrus was quantitatively assessed.

11.1 Introduction

Only very few interdisciplinary studies exist that quantitatively assess annual carbon flow through entire marine ecosystems (Walsh et al., 1989; Jørgensen, 1996; Nixon, 1995). The obvious reason is the massive effort required to measure all relevant biogeochemical and hydrographic processes during a seasonal cycle. Nevertheless, to gain fundamental quantitative insight into the functioning of ecosystems, and to evaluate how they will respond to changes in environmental controls like climate or

anthropogenic inputs, such integrated efforts are essential. Performing ecosystem studies in remote areas like the high Arctic is especially challenging – and performing all measurements simultaneously is almost impossible.

To fulfill the original ambition of resolving and investigating the carbon flow through a representative High Arctic ecosystem, various components had to be investigated in successive years. The results of those efforts are summarized in the previous chapters. The present chapter will compile the insights obtained and will establish a carbon budget for a well-defined region of outer Young Sound (Region 1, see Chapter 3). The budget is used to evaluate the importance of various processes and the link between the respective compartments of the system. Specific questions include:

- What is the relative importance of the different organic carbon sources?
- What is the relative importance of the different organic carbon sinks?
- Is the region net heterotrophic or net autotrophic?
- And which central aspects are missing in our present understanding of the system?

To perform this evaluation it was necessary to interpolate and extrapolate measurements performed at different points in time over a 10-year period and to upscale measurements performed at single sites or along depth transects. We chose to extrapolate the findings of the respective stations to the bathymetry of Region 1, which encloses a total area of 76 km^2 and a water volume of 5.8 km^3 (Chapter 3). The average water depth in Region 1 is 76 m and the maximum depth of 177 m is reached along the Northwestern boundary. Twenty one percent of the seafloor area lies at water depths from 0 to 40 m, which roughly defines the depth interval of the photic zone, while 25% of the area lies at depths below 100 m (Fig 11.1).

The data presented in the preceding chapters was collected during a period with large interannual variations in sea-ice cover, downwelling irradiance, precipitation and freshwater input. To constrain the present task and to combine investigations from different years we defined a standard year. This year has an open-water period of 86 days (i.e. 18 July–12 October), which represents the average conditions for the period 1990–2000. In order to define a representative irradiance, we chose to use the light data com-

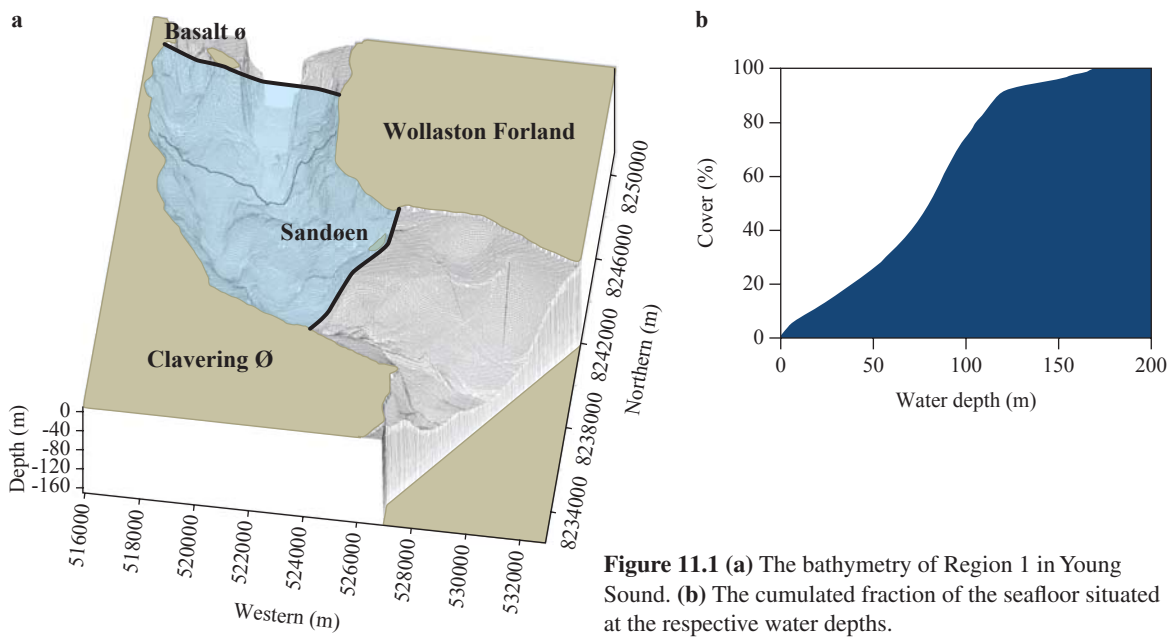

Figure 11.1 (a) The bathymetry of Region 1 in Young Sound. **(b)** The cumulated fraction of the seafloor situated at the respective water depths.

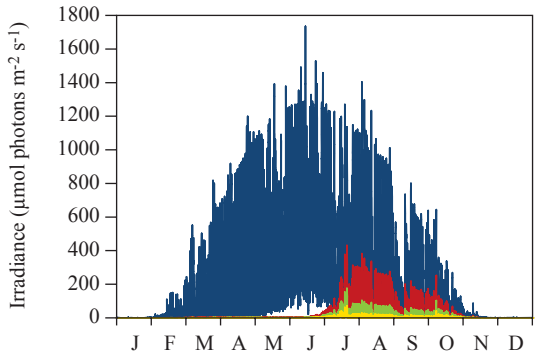

Figure 11.2 Downwelling irradiance measured during 1999 (blue), and the inferred light availability at 10 m (red), 20 m (green) and 30 m (yellow) water depth, taking into account the measured light extinction in the snow and sea-ice cover and in the water column during the same year.

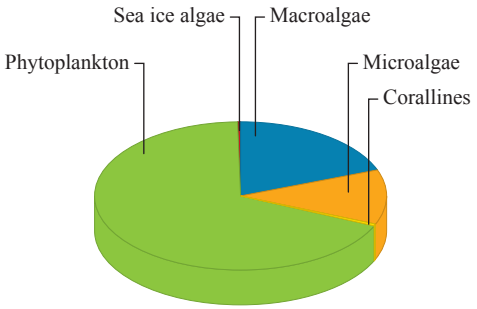

Figure 11.3 The relative contribution of the respective primary producers to the ecosystem production in Region 1 of Young Sound. Phytoplankton 65%, benthic macroalgae 21%, benhic microphytes 13%, sea-ice algae and benthic corallines < 1%. Total primary production in Region 1 is 1119 t C yr^{-1}.

piled during 1999, the snow and sea-ice thickness, and the light extinction coefficients for snow, sea ice and water measured during the same year (Chapter 4). We thereby calculated the irradiance available within the water column and at the sediment surface at the respective water depths (Fig 11.2). These data are used to estimate the annual carbon production of the respective primary producers.

Collecting CTD data from the deeper inner part of the fjord.

Photo: Søren Rysgaard

11.2 Results & discussion

11.2.1 Primary production

The net primary production of benthic microalgae, corallines and *Laminaria saccharina* in Region 1 during a standard year as defined above can be calculated from the information provided in Fig. 9.3 & Table 9.3, Chapter 9. *Laminaria saccharina* only accounts for a few percent of the macroalgae biomass in Region 1, but assuming that the remaining foliose biomass (*Fucus*, *desmarestia*) has a P-E relation similar to that of *Laminaria*, the total benthic net primary production amounts to 391 t C yr^{-1} (Fig 11.3). The corresponding gross primary production of the pelagic community and the sea-ice algae as measured by ^{14}C incubations equals 728 t C yr^{-1} as calculated on the basis of information provided in Chapters 4 and 5 (Fig 11.3).

It is remarkable that, despite the average water depth of 76 m the benthic community is responsible for 35% of the ecosystem production of 1119 t C yr^{-1} in Region 1 (Fig. 11.3). This calculation even compares the net activity of the benthic community with the gross activity of the pelagic community. There is no simple way to convert the net production of the benthic community to gross production, but a number of microsensor studies have concluded that the gross rates of benthic microphytes are 3–6 times higher than the net production (Fenchel & Glud, 2000 and references therein). One might argue that the benthic microphytic contribution should be increased correspondingly. Most of the labile organic

material is, however, quickly recycled through a close autotrophic-heterotrophic coupling within the diatom cover. Likewise, the net production of the macrophytes only represents a minor fraction of the gross production, but, again, most of this difference is respired within the plant itself. Nevertheless, the data strongly emphasize the relative importance of benthic primary production for the carbon flow in Arctic fjord systems. Given the low inclination of the topographic relief surrounding Greenland, one may speculate that benthic primary production is also quantitatively important for the carbon cycling in the coastal waters outside the fjord systems. Considering the high sea-ice algae productivity measured in other locations (e.g. Horner & Schrader, 1982; McMinn et al., 2000) it is surprising that the contribution of sea-ice algae is negligible, an observation confirmed by several investigations performed in successive years. We ascribe this to light impedance by the snow cover during early spring, and the dynamic nature of the sea-ice matrix during late spring due to massive freshwater intrusion, which inhibits sea-ice algal blooms.

11.2.2 A carbon budget for the pelagic food web

The annual pelagic gross primary production in Region 1 as derived from measurements performed during the ice-covered period, 11–27 June 1999, and the open-water period of 87 days in 1996 amounts to 728 t C yr^{-1} (Fig. 11.4; see also Chapter 5). Any contributions during the rest of the season can be ignored due to the fjord being covered by snow and sea-ice in the remaining period. The pelagic primary production is primarily related to the activity of diatoms (Chapter 5). This production can either be grazed by the metazoan or the protozoan communities, but it

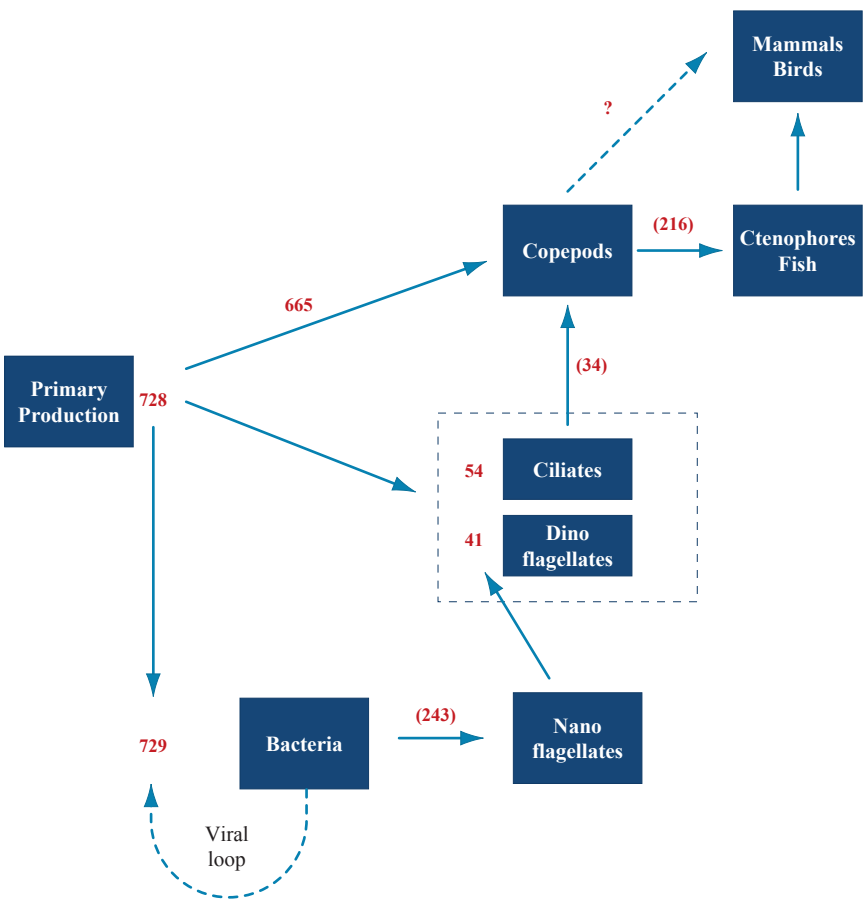

Figure 11.4 The pelagic food web of Young Sound extrapolated from information provided in Chapter 5. The carbon requirement of the respective compartments are written next to the boxes and values next to the arrow represent the amount of organic carbon that potentially can be transferred to the next trophic level. See text for details on the calculations. Units: t C yr^{-1}.

Photo: Morten Frederiksen

Midnight at Sandøen – an evening off.

also supports the bacterial production through leakage of photosynthetates and sloppy feeding. Finally, a fraction of the phytoplankton production could also sink ungrazed to the sea floor and contribute to covering the benthic carbon demand.

The grazing community of Region 1 is dominated by the copepods *Calanus glacialis* and *C. hyperboreus*. When the metazoan grazing potential estimated for Station A (Chapter 5, Table 5.6) is extrapolated to Region 1, their annual carbon requirement amounts to 665 t C yr^{-1}, accounting for 90% of the pelagic primary production (Chapter 5; Rysgaard et al. 1999). The copepods could, however, also complement their carbon demand by grazing on the protozoan grazers. Assuming that the entire protozoan production (Chapter 5, Table 5.6) is grazed by copepods, this corresponds to a potential food source of 34 t C yr^{-1} (Fig 11.4). Sustaining the observed biomass of protozoan grazers represented by ciliates and heterotrophic dinoflagellates (Chapter 5) requirs a basin-wide carbon source of 54 and 41 t C yr^{-1}, respectively (Fig 11.4). The estimated copepod production (Chapter 5, Table 5.6) represents the main food supply for the higher trophic levels and represents a basin-wide carbon supply of 216 t C yr^{-1}. Minor carbon pools and turnover by larvae plankton and *appendicularia* accounting for 4% of the zooplankton biomass were ignored in the present budget.

The lower trophic levels and the microbial loop of Young Sound are very poorly constrained. However, when the estimated annual prokaryotic carbon demand at Station A (Chapter 5) is extrapolated to Region 1, it corresponds to a carbon request of 729 t C yr^{-1}. Given that the pelagic primary producers in Young Sound are dominated by larger specimens, bacteria in principle represent the only food source for nanoflagellates, which in turn are grazed by the larger protozoan zooplankton (Fig. 11.4). If the nanoflagellates consume the entire bacteria production (Chapter 5, Table 5.6) it corresponds to a carbon food source of 243 t C yr^{-1}, which is channeled further up through the trophic system (Fig 11.4). However, a significant fraction of the bacterial production could represent internal DOC cycling mediated by viral lysis. It is generally assumed that 10–40% of the bacterial carbon demand in pelagic environments is covered by virus-induced bacterial lysis (Wilhelm & Suttle, 1999; Middelboe, 2007). However, the viral loop of Young Sound still remains to be investigated, and to give a quantitative estimate of this pathway would be pure guesswork. Resolving the importance of the lower trophic grazing levels and the microbial and viral loops has high priority in the future research plans for Young Sound.

The pelagic primary production of Region 1 (728 t C yr^{-1}) balanced the carbon demand of the meta-

and protozoan grazing communities (665 + 54 + 41 - 34 = 726 t C yr^{-1}) (Fig 11.4). This leaves very little room for the poorly investigated microbial loop (or a direct vertical export of algae material from the photic zone), and the water column thus appears to be net heterotrophic. However, as discussed in Chapter 6, 2436 t TOC yr^{-1} is imported to Region 1, of which 990 t TOC yr^{-1} is of terrestrial origin, while 1446 t TOC yr^{-1} originates from the Greenland Sea. This material more than balances the carbon demand of the net heterotrophic water column and contributes to the vertical transport of organic material required by the benthic community (see below).

11.2.3 Vertical export of organic material and potential sources of sedimenting POC

The net import of particulate material to Region 1 that is not recycled in the water column, ultimately settles at the sediment surface where it is mineralized by benthic animals or microbes, or buried in the sediment record. A sediment trap placed at 65 m water depth in Region 1 revealed vertical POC fluxes of 17, 19 and 25 g C m^{-2} yr^{-1} during the years 2003, 2004 and 2005, respectively (Chapter 6; Rysgaard et al., unpub). Assuming that these values represent the average benthic sedimentation rate of organic material, they correspond to an annual POC sedimentation of 1548 ± 317 t C yr^{-1}. Isotopic analysis of the material collected in the sediment traps suggested that roughly 40% of the material was of terrestrial origin and discharged into the sound via freshwater runoff (Chapter 6). Based on the sediment trap data, this corresponds to an import of 517 t POC yr^{-1} to Region 1 from terrestrial sources during 2003, very close to the independent mass balance studies of 495 t POC yr^{-1} (Chapter 6; Rysgaard et al., 2003). When the average POC sedimentation rate measured during 2003–2005 is applied, this fraction amounts to 619 t C yr^{-1}. The material presumably represents a relatively refractory carbon pool and the POC contribution from land almost balances the benthic carbon preservation (see below). The net import of DOC to Region 1 from land-based sources was estimated at 503 t C yr^{-1} and is in principle available to the planktonic food web, even though it presumably represents a relatively refractory carbon pool (Chapter 6). The remaining POC collected in the sediment traps (1548 - 619 = 929 t C yr^{-1}), must either be produced within the region, be advected into the system from the Greenland Sea, or represent resettling of resuspended material (the latter can presumably be ignored due to the position of the sediment trap c. 40 m above the sediment; Chapter 6). Visual inspection of the trap material revealed intact algae cells (mainly diatoms), but copepod pellets represented an important and distinct fraction of the collected material. Assuming that an average of 40% of the carbon ingested by copepods is released as fecal pellets (Møller et al., 2003), the pellet production in Region 1 can be estimated at 266 t C yr^{-1}. The remaining material in the traps (929 - 266 = 663 t C yr^{-1}) must represent other sources of marine detritus, of which a significant fraction presumably is advected into the region from the Greenland Sea. This can be especially important during late spring prior to sea-ice break-up when a productive polynya develops off the fjord and probably feeds the outer regions of Young Sound with labile organic carbon via estuarine and tidal circulation (Chapters 3 & 5). The total TOC import to Region 1 from the Greenland Sea was estimated at 1446 t C yr^{-1}; Chapter 6), but, unfortunately, the relative fractions of DOC and POC remain unknown.

11.2.4 Benthic carbon demand

The POC settling at the seafloor is either preserved in the sediment record or mineralized by fauna and microbes. Based on the information in Table 8.2, Chapter 8, the annual benthic carbon preservation of Region 1 can be calculated at 564 t C yr^{-1}, while the microbial carbon mineralization (including polychaetes, see below) equaled 1320 t C yr^{-1} (Fig. 11.5). The latter value was derived from core incubations excluding most of the benthic macro and megafauna. The carbon requirement of the most prominent macrofauna groups i.e. brittle stars, bivalves and sea urchins was calculated at 53, 151 and 2 t C yr^{-1}, respectively, using the recommendations in Chapter 7 & 8. A recent study does, however, suggest that the carbon requirement of the sea-urchin community in Region 1 may be as high as 36 t C yr^{-1} (Blicher et al., *in press*). Polychaetes were presumably reasonably well represented during the core incubations and their carbon demand has previously been estimated at 72 t C yr^{-1} (Glud et al., 2000). Hence, microbial respiration accounted for 1248 t C yr^{-1} (1320 - 72 t C yr^{-1}) and benthic animals for 312 t C yr^{-1} (53 + 151 + 36 + 72 t C yr^{-1}) of the degradation in the sediment. For bivalves it has been estimated that 20% of the

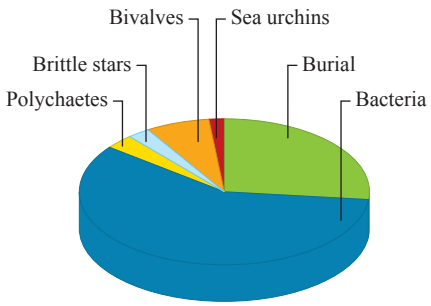

Figure 11.5 The relative contribution to the benthic carbon requirement in Region 1 of Young Sound. The total requirement is 2124 t C yr^{-1}. Bacteria accounts for 59%, burial for 26%, brittle stars for 3%, bivalves for 7%, sea urchins for 2% and polychaetes for 3% of the requirements.

assimilated organic carbon is excreted and thus made available to the benthic microbial community (Sejr et al., 2004). Assuming that this value is representative of all benthic fauna groups, faunal excreta would sustain 5% (62 t C yr^{-1}) of the microbial carbon demand. When all these values are compiled, the total benthic carbon requirement of Region 1 amounts to 2124 t C yr^{-1} (Fig. 11.5 & Fig. 11.6). The net benthic exchange of DOC is marginal (Chapter 8) and is ignored in the established benthic carbon budget. It follows that the benthic heterotrophic activity (i.e. 1560 t C yr^{-1}) is larger than the entire primary production of the region and that external carbon sources (i.e. from land and the Greenland Sea) are required to balance the budget.

The microbial carbon requirement, dominated by the oxygen and sulfate respiring bacteria, accounts

Photo: Søren Rysgaard

for 59% of the annual benthic carbon demand. This value is extrapolated from 79 sediment core incubations performed in 1994 (6), 1996 (67) and 1997 (6) (numbers in brackets represent the respective number of incubations). The extent to which the value represents average conditions in Young Sound is open to discussion, and we have no means of directly evaluating the interannual variability of the benthic microbial carbon mineralization. However, 1996 had an open-water period of 87 days, which is similar to the value for the standard year defined above, and the precipitation of 223 mm during 1996 was close to the annual mean of 198 mm for the period 1996–2003, (Rasch & Caning, 2005). Thus, the light availability in, and the freshwater input to Young Sound during 1996 presumably reflect the average conditions reasonably well. The remaining components of the benthic carbon demand all integrate time scales greater than one year, and as such they presumably provide a relatively robust average value for the area.

The enhanced O_2 uptake following settling of the summer bloom only represents c. 10% of the annual respiration, and on an annual basis most of the benthic activity is presumably sustained by a slowly-degrading carbon pool with a decay rate constant of 76 yr^{-1} (Chapter 8). The benthic macro- and megafauna only accounts for 15% of the total benthic carbon requirement and 25% of the microbial activity (Fig. 11.5). This confirms the general observation that fauna metabolism on its own only has a minor role in carbon mineralization in marine environments (e.g. Glud et al., 1998, 2003). The impact of benthic fauna on benthic mineralization is mainly indirect through bioturbation and bioirrigation activities that stimulate microbial

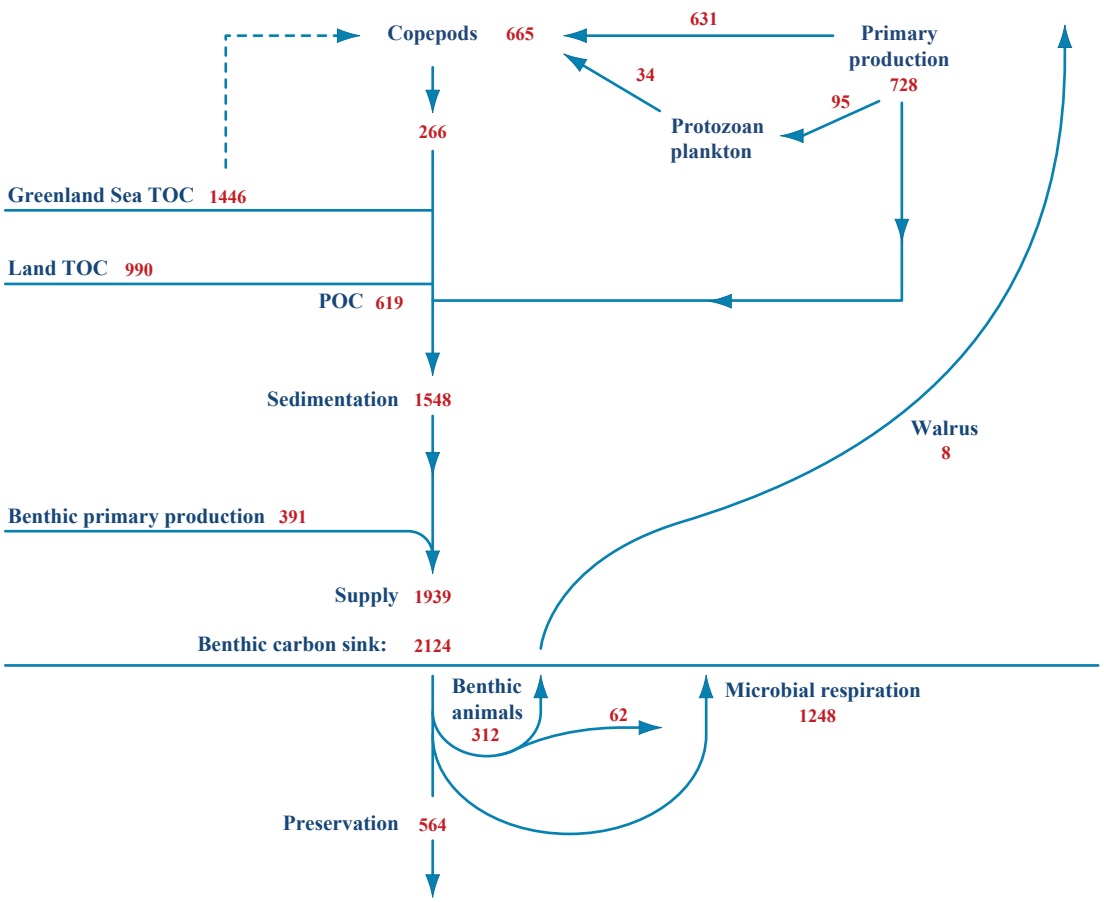

Figure 11.6 Annual carbon budget for Region 1 in Young Sound, Units: t C yr^{-1}. See text for details on the calculations.

and chemical oxidation processes. In total, 26% of the benthic POC demand is preserved in the sediment.

The benthic carbon requirement must be balanced by the POC flux from the overlying water column. Taken together, the annual vertical POC transport measured during 2003–2005, and the benthic primary production as estimated for a normalized standard year (see above), sustained 92 ± 16% (1949 ± 317 t C yr^{-1}) of the benthic carbon requirement. Thus, a good agreement between the supply and demand of organic material for the benthic community can be observed when all the independent measurements are considered (Fig. 11.6).

11.2.5 Higher trophic levels

Most of the higher trophic levels in Region 1 have not been studied in any detail. No reliable estimates exist of the biomass or carbon requirement of fish, seals, birds or whales that occasionally visit the sound. Likewise, we have no information on the quantitative importance of ctenophores and euphausiids that occasionally exhibit mass occurrence within the sound and thus could represent an important grazing potential.

The only top predator to receive attention is the walrus, which has colonized the island Sandøen, and it was concluded that the population consums 85 tons of shell-free bivalves, corresponding to 25 t C yr^{-1} in outer Young Sound (Regions 0, 1, 2 & 3) (Born et al., 2003; Chapter 10). Assuming that the foraging of walruses is evenly distributed, this leads to carbon consumption in Region 1 of 8 t C yr^{-1} (Fig. 11.6), representing a negligible amount of the standing stock of bivalves (Chapters 7 & 10)

11.2.6 Concluding remarks

Young Sound represents one of numerous High Arctic sill fjords, and the interdisciplinary study summarized in the previous chapter offers a unique opportunity to establish a carbon budget for Region 1 in this generally rarely studied type of ecosystem (Fig 11.6). The exercise of establishing such a budget does, however, also reveal that several components are poorly constrained, especially the microbial and viral loops, which could potentially represent a significant sink for organic material in the system. Likewise, the coupling from the invertebrate fauna to the top consumers (fish, seals, whales, birds) – with the exception of the walrus – remains unresolved. The microbial loops and the top consumers deserve more attention in the future (see Chapter 12).

Nevertheless, the present understanding of the system allows us to draw some general conclusions. Even excluding the microbial loop, it follows that the total carbon demand of the benthos and the pelagic grazing community (i.e. 2850 t C yr^{-1}) by far exceeds the primary production of the system (i.e. 1119 t C yr^{-1}) i.e. the net heterotrophic system is in deficit of 1731 t C yr^{-1}. Independent measurements coupled to a hydrodynamic model estimated that the region has a net import of organic material amounting to 2436 t C yr^{-1} with 60% being delivered from the Greenland Sea and the rest from land. This material thus supports the carbon demand of the region. A full balance between these two components cannot be expected, as the advective carbon import is very dependent on the estimated freshwater input. A sensitivity analysis revealed an estimated net import bracketed by a minimum and maximum value of 1300 and 4400 t C yr^{-1}, respectively. The annual freshwater input varied by a factor of 2.5 during 1996–2004 (from 132 to 338 10^6 m^3) (Rasch & Caning, 2005; Chapter 2), and is an important factor in regulating the net carbon import to the region.

11.3 Acknowledgments

This work was supported by the Danish Natural Science Research Council, by DANCEA (the Danish Cooperation for Environment in the Arctic) under the Danish Ministry of the Environment, by the Carlsberg Foundation and by the Commission of Scientific Research in Greenland. This work is a contribution to the Zackenberg Basic and Nuuk Basic Programs in Greenland. Aage V. Jensen Charity Foundation is thanked for providing financial support for research facilities in Young Sound. Bo Thamdrup and Anna Haxen are acknowledged for their comments on this chapter.

11.4 References

Born, E. W., Rysgaard, S., Ehlmé, G., Sejr, M., Acquarone, M. & Levermann, N. 2003. Underwater observations of foraging free-living Atlantic walruses (*Odobenus rosmarcus rosmarcus*) and estimates of their food consumption. Polar Biol. 26: 348-357.

Blicher, M. E., Rysgaard, S. & Sejr M. K. *in press*. Growth and production of the sea urchin, *Strongylocentrotus droebachiensis*, in a high-arctic fjord, and growth along a climatic gradient (64-77°N). Mar. Ecol. Prog. Ser.

Fenchel, T. & Glud, R. N. 2000. Benthic Primary production and O_2-CO_2 dynamics in a shallow water sediment: Spatial and temporal heterogeneity. Ophelia 53: 159-171.

Glud, R.N., Holby, O., Hofmann, F. & Canfield D. E. 1998. Benthic mineralization in Arctic sediments (Svalbard). Mar. Ecol. Prog. Ser. 173: 237-251.

Glud, R. N., Risgaard-Petersen, N., Thamdrup, B., Fossing, H. & Rysgaard S. 2000. Benthic carbon mineralization in a high-arctic sound. Mar. Ecol. Prog. Ser. 206: 59-71.

Hansen, P. J., Hansen, B. W. & Bjørnsen, P. K. 1997. Zooplankton grazing and growth: Scaling within the size range 2 µm to 2000 µm. Limnol. Oceanogr. 42: 687-704.

Horner, R. A. & Schrader, G. C. 1982. Relative contribution of ice algae, phytoplankton, and benthic microalgae to primary production in nearshore regions of the Beaufort Sea. Arctic 35: 485-503.

Jørgensen, B. B. 1996. Case study - Aarhus Bay. In: Jørgensen, B. B. & Richardson, K (eds.). Eutrophication in Coastal Marine Ecosystems. Coastal and Estuarine Studies. American Geophysical Union, Washington: 137-154.

McMinn, A., Ashworth, C. & Ryan, K. -G. 2000. *In situ* net primary productivity of an Antarctic fast ice bottom algal community. Aquat. Microb. Ecol. 21: 177-185.

Middelboe, M. (2007): Microbial disease in the sea: Effects of viruses on marine carbon and nutrient cycling". In Eviner, V. et al. (eds.). Ecology of infectious diseases: Interactions between disease and ecosystem. Princeton University Press.

Møller E. F., Thor, P. & Nielsen, T. G. 2003. Production of DOC by *Calanus finmarchicus*, *C. glacialis* and *C. hyperboreus* through sloppy feeding and leakage from fecal pellets. Mar. Ecol. Prog. Ser. 262: 185-191.

Nixon, S. W., Granger, S. L. & Nowicki, B. L. 1995. An assessment of the annual mass balance of carbon, nitrogen, and phosphorous in Narragansett Bay. Biogeochemistry 31: 15-61.

Rasch, M. & Caning, K. (eds.) 2004. ZERO - Zackenberg Ecological Research Operations. 10th Annual Report, 2005. Danish Polar Center, Ministry of Science, technology and Innovation. Copenhagen, 85 pp.

Rysgaard, S., Nielsen, T. G. & Hansen, B. W. 1999. Seasonal variation in nutrients, pelagic primary production and grazing in a high-Arctic coastal marine ecosystem, Young Sound, Northeast Greenland. Mar. Ecol. Prog. Ser. 179: 13-25.

Rysgaard, S., Glud, R. N., Sejr, M. K., Bendtsen, J. & Christensen, P. B. in press. Inorganic carbon transport during sea ice growth and decay: A carbon pump in polar seas. Journal of Geophysical research Ocean. 2006JC003572

Sejr, M. K., Petersen, J. K., Jensen K. T. & Rysgaard, S. 2004. Effect of foodconcentration on clearance rate and energy budget of the Arctic bivalve *Hiatella arctica* (L) at subzero temperature. J. Exp. Mar. Biol. Ecol. 311: 171-183.

Walsh, J. J., McRoy, C. P., Coachman, L. K., Goering, J. J., Nihoul, J. J., Whitledge, T. E., Blackburn, T. H., Parker, P. L., Wirick, C. D. Shuert, P. G., Grebmeier J. M., Springer, A. M., Tripp R. D., Hansell, D. A., Djenidi, S., Deleersnijder, E., Henriksen, K., Lund, B. A., Andersen P., Müller-Krager, F. E. & Dean, K. 1989. Carbon and nitrogen cycling within the Bering/Chukchi Seas: Sources regions for organic matter effecting AOU demands of the Arctic Ocean. Prog. Oceanogr. 22. 277-359.

Wilhelm, S. W & Suttle, C. R. 1999. Viruses and nutrient cycles in the sea. Bioscience 49: 781-788.

Photo: Peter B. Christensen

12

Carbon cycling and climate change: Predictions for a High Arctic marine ecosystem (Young Sound, NE Greenland)

Carbon cycling and climate change: Predictions for a High Arctic marine ecosystem (Young Sound, NE Greenland)

Søren Rysgaard[1] and Ronnie N. Glud[2]

[1]Greenland Institute of Natural Resources, Kivioq 2, DK-3900 Nuuk, Greenland.
[2]Marine Biological Laboratory, University of Copenhagen, Strandpromenaden 5, DK-3000 Helsingør, Denmark.

Cite as: Rysgaard, S. & Glud R. N. 2007. Carbon cycling and climate change: Predictions for a High Arctic marine ecosystem (Young Sound, NE Greenland). In: Rysgaard, S. & Glud, R. N. (Eds.), Carbon cycling in Arctic marine ecosystems: Case study Young Sound. Meddr. Grønland, Bioscience 58: 206-214.

Abstract

This chapter reviews current predictions of future changes in the High Arctic marine ecosystem Young Sound, NE Greenland. A high-resolution regional atmosphere-ocean model predicts an increase in atmospheric temperature of 6–8°C and in precipitation of 20–30% by the end of this century (2071–2100), leading to increased freshwater runoff, thinning of sea ice, and an increase in open-water period from 2.5 months to 4.7–5.3 months. Evaluation of the consequences of enhanced freshwater runoff to the fjord revealed that the mixed layer thickness of the water column will change only marginally, whereas the transport of saltwater from the Greenland Sea to Young Sound below the halocline is predicted to increase considerably due to stimulated estuarine circulation. The thinning of sea ice and the increase in the open-water period is expected to enhance primary productivity in the area due to a c. 50% increase in light availability. The phytoplankton bloom will continue to occur in a sub-surface layer, but as the exchange between the fjord and the Greenland Sea increases, production will benefit from increased import of nutrients. We estimate that primary productivity in the area will have tripled by the end of the century compared with present-day levels. The longer ice-free period will induce a shift in the pelagic food web structure, from a copepod-dominated grazer community to a situation with growing influence of protozooplankton. The increased pelagic production will enhance sedimentation and thus intensify bacterial mineralization at the sea floor along with carbon burial. This will reduce oxygen availability in the sediment and the relative importance of anaerobic degradation will increase. The rise in sedimentation will also improve food availability for the benthic animals and thus stimulate growth and production until a certain threshold, where sulphide released from anaerobic sulphate reduction may become inhibitory. Finally, an increase in the ice-free period will prolong the period in which birds and marine mammals – e.g. walruses – have access to the food-rich coastal area, and thus improve their foraging conditions. All in all, conditions in Young Sound in 2071–2100 are predicted to resemble present-day conditions c. 450 km further south, e.g. Scoresby Sound.

12.1 Introduction

In the previous chapters, details have been provided on various aspects of the High Arctic marine ecosystem in Young Sound, NE Greenland. This has formed the basis for establishing a carbon budget in the outer part of the fjord under present-day conditions with low temperatures and thick sea-ice cover most of the year (Chapter 11). The question is how this system will develop in response to rising temperatures. Evidence of global climate change is increasing (IPCC 2001) and the changes are expected to be amplified in Arctic

and subarctic regions (ACIA 2005). Surface air temperature observations reveal that the largest increase in recent decades has occurred over the Northern Hemisphere land areas from about 40 to 70°N (Serrenze et al., 2000). Due to warming of the world oceans (Levitus et al., 2000) the sea ice cover in the Arctic has decreased by c. 14% since the 1970s (Johannessen et al., 1999). This decrease has led to prolongation of the ice-free period off the north coast of Russia, in the Greenland Sea, the Barents Sea, and in the Sea of Okhotsk (Parkinson, 1992, 2000). In addition, a general increase in precipitation in the 55–85°N latitude band was observed during the last century (Serreze et al., 2000). In the present chapter, we attempt to forecast the response of a High Arctic ecosystem to the climate changes taking place during this century. The forecast will be based on previously published material and on a synthesis of the knowledge presented in the preceding chapters of this book.

12.2 Results & discussion

12.2.1 Physical conditions in Young Sound, 2071–2100

The HIRHAM regional model (Christensen & Christensen, 2003; Christensen & Kuhry, 2000; Christensen et al., 1998) has previously been used to predict changes in wind, temperature, and precipitation minus evaporation conditions in East Greenland (Kiilsholm & Christensen, 2003; Rysgaard et al., 2003). The model has a 50-km horizontal resolution and has been shown to realistically simulate present-day Arctic conditions (Christensen & Kuhry, 2000; Dethloff et al., 1996). The two emission scenarios, A2 and B2, which are in the middle of the range of the scenarios provided by the Intergovernmental Panel of Climate Change (IPCC), were used in the regional simulations. Small (<5%) changes were predicted in the average 30-year wind conditions in the Northeast Greenland region by the end of this century (2071–2100), as compared to present-day conditions (1961–1990). In contrast, the model predicted a dramatic increase in the average 30-year atmospheric temperatures of up to 6–8°C in NE Greenland by the end of this century (Fig. 12.1a). In addition, the average 30-year precipitation minus evaporation in the region is expected to increase 20–30% during the same time period (Fig. 12.1b). The effect of increased temperatures, precipitation and freshwater runoff can be expected to cause dramatic changes in future sea-ice conditions in Young Sound. Today, sea ice covers the fjord for 9–10 months of the year and grows to a thickness of c. 1.5 m (Chapter 4). Given the increase in air temperature of 9.3°C ± 1.5 during December–February; 4.7°C ± 1.3 during March–May; 0.4°C ± 0.3 during June–August, and 8.6°C ± 2.1 during September–November predicted by HIRHAM (scenario

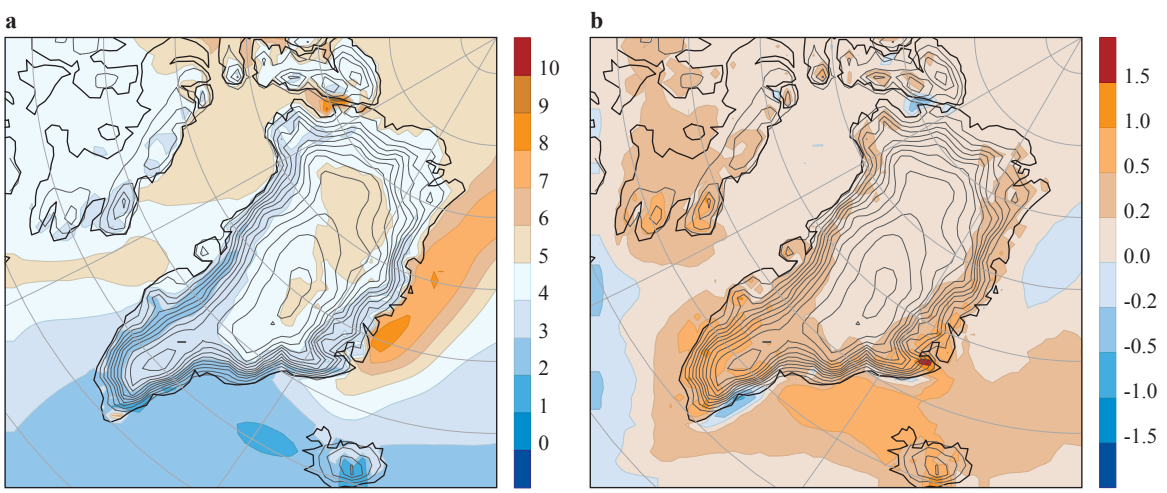

Figure 12.1 Change in **(a)** temperatures at 2 m (°C), and **(b)** precipitation-evaporation (mm d^{-1}) during 2071-2100 relative to 1961-1990, as predicted by HIRHAM4 scenario B2 simulations. Contour interval shown for every 500 m. Redrawn from Rysgaard et al. (2003).

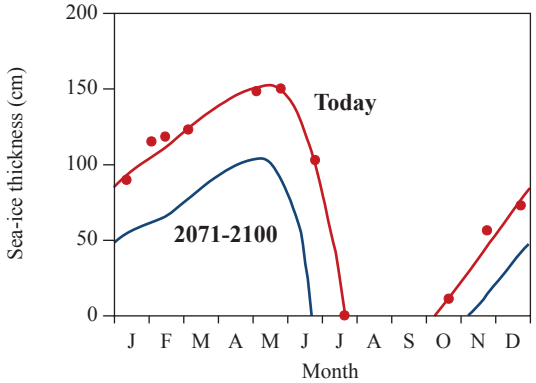

Figure 12.2 Sea ice conditions today and in 2071-2100 as predicted by HIRHAM4 scenario B2 simulations and additional sea ice modelling (see main text for details). Data points represent direct ice thickness measurements and line represents model output. Data from Rysgaard et al. (2003).

B2) in 2071-2100, Rysgaard et al. (2003) estimated that the winter fast-ice thickness in Young Sound would decline from c. 1.5 m to c. 0.8 m, and the open-water season increase from 2.5 months today to 4.7 months by the end of the century (Fig. 12.2). Application of the scenario A2 data would lead to a further decrease in sea-ice thickness and an increase in the sea-ice-free season to 5.3 month.

12.2.2 Primary production in 2071-2100

The reduced sea ice thickness and increased open-water period will alter the light regime in the fjord in the course of this century. By applying the attenuation coefficients for snow and sea ice (Chapter 4), the future sea ice thickness and 20% increase in snow cover (Fig. 12.2), and assuming unchanged downwelling irradiance, future sea ice conditions can be estimated to lead to a c. 50% increase in light availability for primary producers (Fig. 12.3). During the sea-ice-cover period the interception of light by sea ice and snow cover would still limit primary production. However, following the break-up of sea ice the immediate increase in light availability would increase pelagic and benthic primary production (Chapter 5; Chapter 9). Thus, the earlier break-up of sea ice in the future will stimulate both pelagic and benthic primary producers, which are severely light-limited today (See former chapters). The annual pelagic primary production versus the productive open-water period from various Arctic areas has been compiled previously (Rysgaard et al., 1999) and is presented in Fig. 12.4. The increasing trend is presumably a combined effect of increasing light and intensified upwelling during open-water periods enhancing nutrient supply to the photic zone. The scatter around the curve most likely reflects different hydrographical regimes with respect to wind, temperature, salinity and current conditions induced by local upwelling and downwelling. Areas with intense upwelling such as the Bering Strait and Nares Strait (Sambrotto et al., 1984; Springer et al., 1996; Tremblay et al., 2006) are obviously out of range and therefore not included. Based on the relationship in

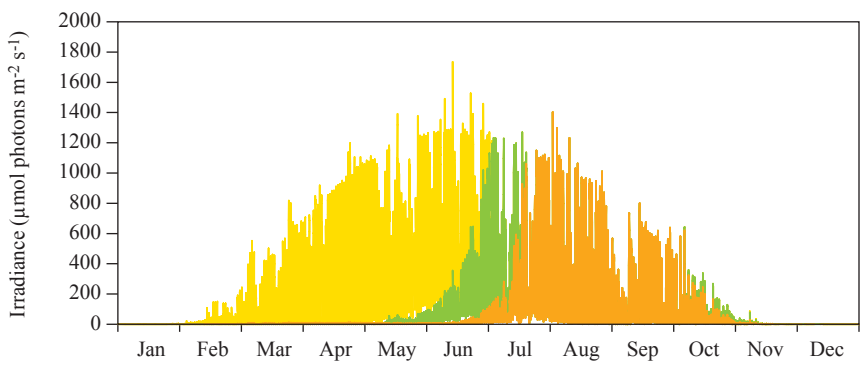

Figure 12.3 Incoming irradiance (PAR) to the surface of Young Sound (yellow + green + orange), below sea ice and during the open-water period under present conditions (orange), and in 2071-2100 (green + orange). PAR data from present time (1999) are from the Zackenberg Basic monitoring programme. PAR data in 2071-2100 are predicted from Fig. 12.2 by applying the attenuation coefficients for snow and sea ice (Chapter 4).

Fig. 12.4, predictions of the sea ice (Fig. 12.2) and light conditions in 2071–2100 (Fig. 12.3), we estimate that primary productivity in the area will have increased from present-day values of c. 10 to c. 35 g C m^{-2} yr^{-1} by the end of the century. Furthermore, the increase in precipitation and melting of the Greenland Ice Sheet will increase freshwater runoff, and model evaluations (Rysgaard et al., 2003; Chapter 3) predict that the transport of saltwater from the Greenland Sea to Young Sound below the halocline will increase considerably due to increased estuarine circulation (Fig. 12.5). Because the mixed layer thickness will change only marginally in the course of this century, the phytoplankton bloom will continue to occur in a subsurface layer, but as net transport increases, production will benefit from increased import of nutrients from the Greenland Sea.

12.2.3 Grazing, vertical flux and mineralization in 2071–2100

It has been shown that zooplankton normally becomes food limited in stratified water columns following a phytoplankton bloom (Kiørboe & Nielsen, 1994; Chapter 5). Thus, a prolonged open-water period is expected to increase primary production and thus zooplankton growth and production in Young Sound. Today, a single phytoplankton bloom is restricted to the short ice-free period and far exceeds that of sea-ice algal production on an annual basis (Chapter 4; Chapter 5). The classical food web dominates the

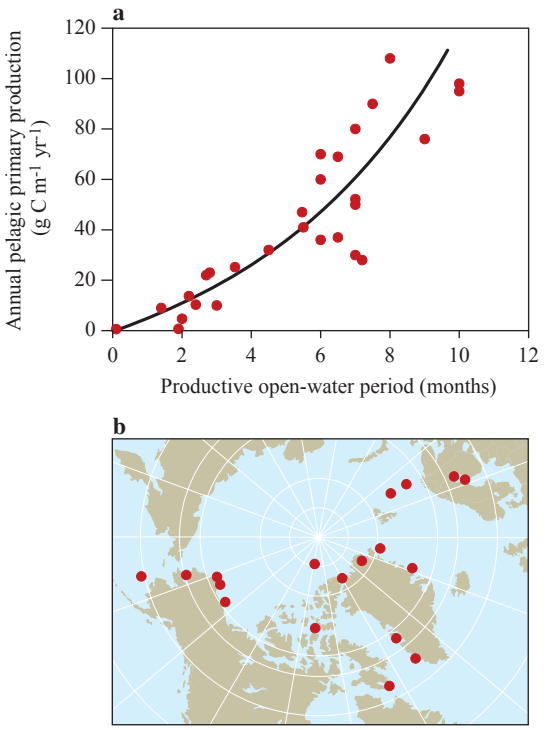

Figure 12.4 (a) Annual pelagic primary production versus the length of the productive open-water period. **(b)** Data compiled from various Arctic regions. The figure is redrawn from Rysgaard et al. (1999) with addition of a dataset from Hegseth (1999).

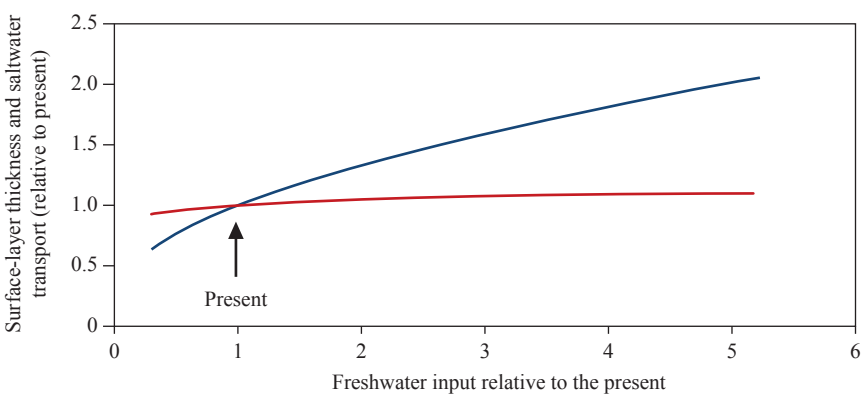

Figure 12.5 Expected changes relative to present conditions in the surface layer thickness (low salinity layer in the upper water layers; red curve) and saltwater transport (blue curve) in the outer parts of Young Sound as a function of freshwater input.

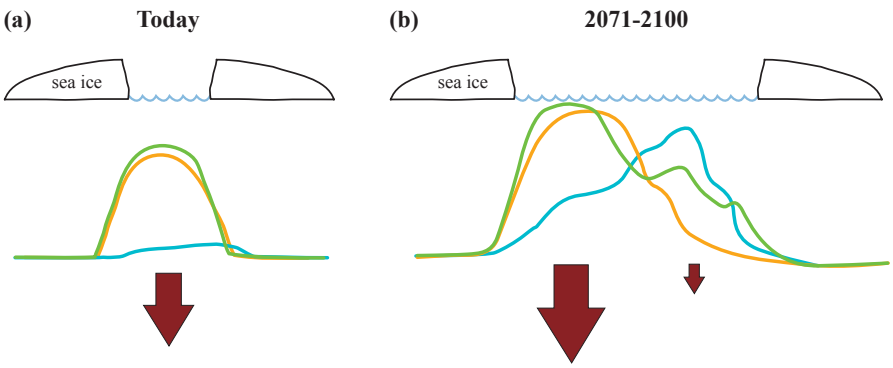

Figure 12.6 Conceptual model of **(a)** present and **(b)** future conditions in sea ice cover, primary production (green curve), copepod grazing (orange curve), protozooplankton (blue curve) as well as vertical export to the sea floor (arrows).

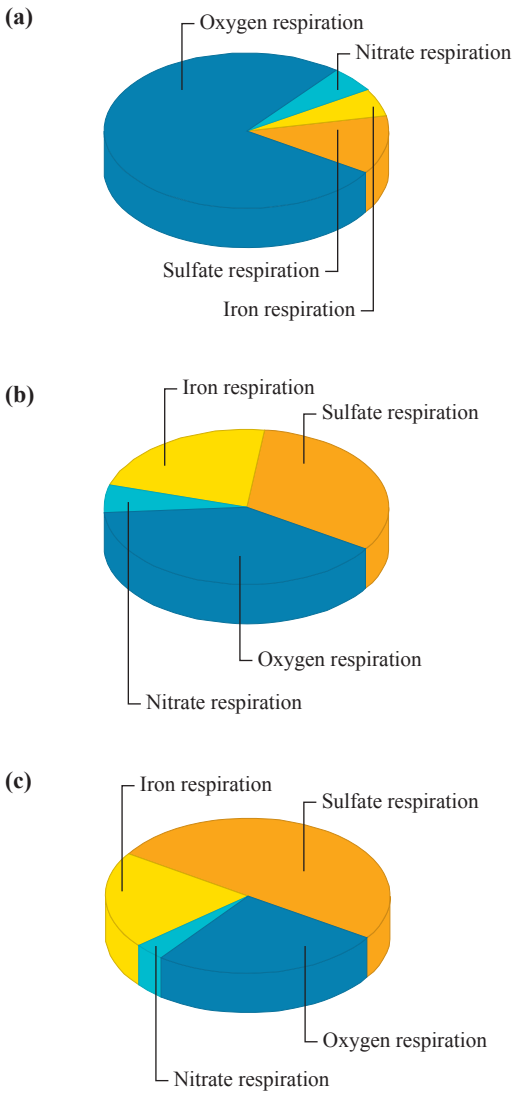

Figure 12.7 Importance of different carbon oxidation pathways in the sediment of Young Sound. **(a)** if the organic matter input is reduced by 50% of present conditions, **(b)** present conditions, and **(c)** if the organic matter input is increased by 100%. Predictions are based on model simulations (Berg et al. 2003).

fjord, i.e. copepods are responsible for >80% of the grazing pressure upon phytoplankton, and >90% of the annual vertical export of organic matter occurs around the short open-water period (Fig 12.6a). In the future, the longer open-water period is expected to induce a shift in the pelagic food web structure from a copepod-dominated grazer community to a situation where smaller protozooplankton play a greater role as observed in subarctic Greenlandic waters at present-day conditions (Levinsen et al., 2000; Levinsen & Nielsen, 2002). Furthermore, a more extensive bloom is likely to occur in the future as observed further south today (Smidt, 1979; Nielsen, 2005). This will affect the vertical flux of organic matter, and result in a high vertical export of organic matter during the spring bloom due to copepod grazing and fecal pellet export, and a second, smaller, vertical export event in autumn. The rising temperature will presumably affect the fraction of assimilated carbon respired by the microbial community, as a larger fraction is respired at low than at high latitudes under present-day conditions (Rivkin & Legendre, 2000). During mid-summer, more nutrients (and organic material) will be recycled in the photic zone, as more of this matter will be retained in the water column due to protozooplankton grazing and bacterial mineralization (Fig. 12.6b) as observed in subarctic ecosystems today (Levinsen et al., 2000; Madsen et al., 2001). An increase in vertical export to the sediment is expected, to the benefit of the food-limited benthos (Sejr et al., 2004; Chapter 7). Furthermore, an increase in the open-water period will prolong the period in which birds and marine mammals such as walruses have access to the plentiful inshore bivalve banks and thus improve their foraging conditions (Chapter 10; Born et al., 2003).

The increase in sedimentation will stimulate organic matter degradation and carbon preservation in the sea bottom. Today, oxygen respiration in sediments at 35 m water depth accounts for 38% of the total oxidation of organic carbon, denitrification 4%, iron reduction 25%, and sulfate reduction 33% (Fig. 12.7; Rysgaard et al., 1998; Chapter 8). To evaluate potential impacts of changes in organic carbon sedimentation, dynamic modeling of organic carbon degradation in the sea bottom was performed (Berg et al., 2003). It was predicted that a 50% reduction in organic material input to the sediment would increase the proportion of organic matter being mineralized through oxygen consumption to 77%, whereas a 100% increase in organic input would reduce the importance of oxygen respiration to 26% (Rysgaard & Berg, unpub.). In the latter scenario, sulfate reduction will be responsible for half of the degradation when the input of organic matter is doubled (Fig. 12.7). Furthermore, a doubling of the organic matter input will reduce the oxygen zone in the sediment with 45% compared with present conditions. One consequence of increasing organic loading is reduction of oxygen availability, less oxidized iron and thus increasing sulfide concentrations in the sediment. This will potentially affect the distribution and composition of the benthic fauna, as sulfide is toxic to most animals.

12.2.4 Monitoring activities and future research

A long-term marine monitoring program (MarineBasic) was initiated in 2002 in order to follow and evaluate the system changes in Young Sound. MarineBasic will provide long-term data:

- Necessary for modeling the coupling between physical oceanography and biological production and consumption
- For use in modeling the regulation of pelagic-benthic coupling (vertical flux)
- To quantify and improve understanding of the lateral coupling (land/fjord/sea)
- To quantify the effect of changing freshwater input, sea-ice cover and hydrographical conditions on biological production and consumption
- To improve current understanding of the effects of climate on species composition and adaptation in the Arctic marine environment

The conceptual design, geographical positions and sampling procedures of the marine monitoring program can be downloaded at www.zackenberg.dk. The site also contains information on the ClimateBasic, GeoBasic and BioBasic monitoring programs, which collect data on the climate and terrestrial environment.

Despite the fact that several integrated research projects have been conducted in Young Sound (see previous chapters) information on certain aspects are still poorly resolved. More knowledge is needed about the physical forces in Young Sound, including brine drainage during sea ice formation and its effect on the circulation in the fjord and the water exchange with the Greenland Sea. Furthermore, model simulations are required on the extent and duration of upwelling events inside the fjord and to quantify the physical coupling to the biological production on an annual scale.

The pelagic microbial and viral loops also need further attention, as these evidently can turn over a large fraction of the organic matter in the water column (Chapter 11). Except for the walruses in the fjord, higher trophic levels have not been studied in any detail. Further work will address the impact of the fish, seals, whales and birds present in the region. A well-established population of the anadromous Arctic charr (*Salvelinus alpinus*) is present in the area, where it feeds in the fjord during summer and winters in the lakes in the valley Zackenbergdalen inside the fjord (Kunnerup, 2001). Furthermore, recent years' trial fishery has revealed occasional large populations of polar cod (*Boreogadus saida*) in the fjord. Seals such as harp seal (*Phoca groenlandica*), ringed seal (*Phoca hispida*), bearded seal (*Erignathus babatus*) and hooded seal (*Cystophora cristata*) have frequently been observed within the area. Occasionally, whales such as bowhead whale (*Balaena mysticetus*), narwhale (*Monodon monoceros*) and killer whale (*Orcinus orca*) enter the fjord. In the outer part of the fjord a small island "Sandøen" houses various birds, for example common eider (*Somateria mollissima*), Arctic tern (*Sterna paradisaea*) and Sabine gull (*Larus sabibi*). They feed in the area, and their impact needs further attention. Finally, we have no information on the quantitative importance of ctenophores and euphausiids that occasionally exhibit mass-occurrence in the fjord and in periods thus represent an important grazing potential.

12.2.5 New perspectives and recommendations

The predicted changes in temperature, ice-free conditions, and precipitation in the area during the course of this century suggest that the physical conditions in Young Sound will develop gradually towards present-day conditions c. 450 km further south, e.g. at Scoresby Sound (Fig. 12.8). Thus, the distance extending from Young Sound and a few hundred km south represents the expected temporal changes that will occur in Young Sound. Furthermore, similar climatic gradients exist on the west coast of Greenland, including subarctic and High Arctic areas. We suggest that evaluation of north-to-south transects in this region would be a highly valuable tool for evaluating shifts in ecosystem structure and element cycling due to climate change.

If sea ice conditions in the future decrease as predicted, humans will have easier access to this remote region. Today, the fishing and hunting taking place in the area belonging to the Northeast Greenland National Park is limited to a few hunters from Scoresby Sound. Due to the heavy sea ice conditions off East Greenland, no trawling has occurred and, hence, undisturbed and very old benthic communities have developed. Bivalves more than 100 years old are common here. In contrast, trawling is very intense and widespread on the west coast of Greenland and one may speculate that the well-developed and undisturbed benthic communities existing in East Greenland act as a spawning site and thus seed the heavily disturbed sea floor in West Greenland through larval drift via the East Greenland Current and the Irminger Current. Furthermore, hunting of walrus, narwhales, other marine mammals and birds in the area may increase in the future due to easier access, and it is important, therefore, that plans for exploitation of the area off the coast are implemented to preserve this unique area, which, at present, has impacts well beyond the borders of the National Park.

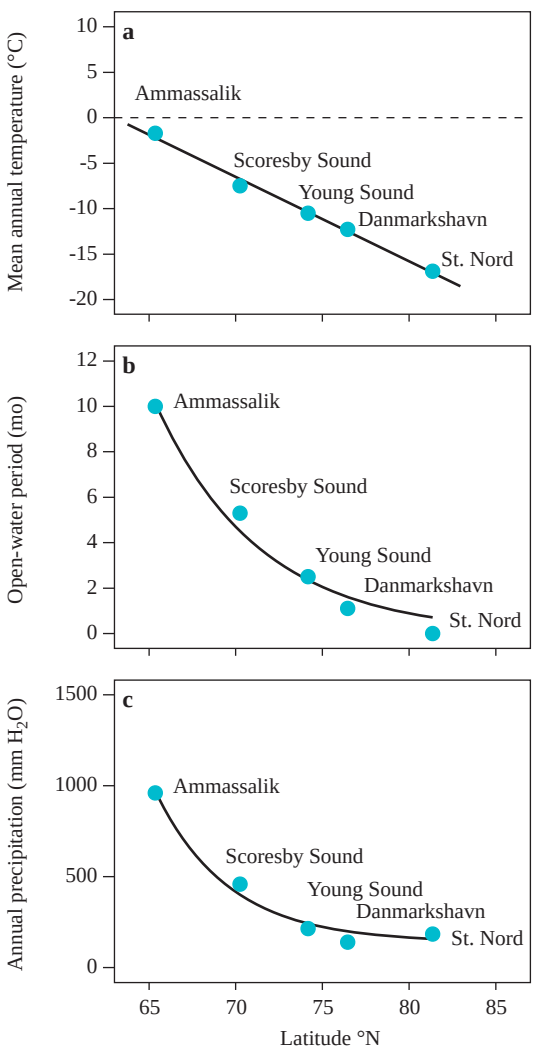

Figure 12.8 (a) Mean annual temperature in East Greenland versus latitude. **(b)** Annual open-water period versus latitude. **(c)** Mean annual precipitation versus latitude. Redrawn from Rysgaard et al. (2003).

12.3 Acknowledgements

This work was supported by the Danish Natural Science Research Council, by DANCEA (the Danish Cooperation for the Environment in the Arctic) under the Danish Ministry of the Environment, by the Carlsberg Foundation and by the Commission of Scientific Research in Greenland. This work is a contribution to the Zackenberg Basic and Nuuk Basic Programs in Greenland. The Aage V. Jensen Chatity Foundation are thanked for providing financial support for research facilities in Young Sound. Bo Thamdrup and Anna Haxen are acknowledge for their comments on this chapter and Peter Berg for providing model simulations of the sediment response to changing organic carbon input.

12.4 References

ACIA 2005. Arctic Climate Impact Assessment. Cambridge University Press, 1042 pp.

Berg, P., Rysgaard, S. & Thamdrup, B. 2003. General dynamic modeling of early diagenesis and nutrient cycling; Applied to an Arctic marine sediment. J. Am. Science 303: 905-955.

Born, E. W., Rysgaard, S., Ehlmé, G., Sejr, M., Acquarone, M. & Levermann, N. 2003. Underwater observations of foraging free-living walruses (*Odobenus rosmarus*) including estimates of their food consumption. Polar Biol. 26: 348-357.

Christensen, J. H. & Christensen O. B. 2003. Severe summertime flooding in Europe. Nature 421: 805-806.

Christensen, O. B., Christensen, J. H., Machenhauer, B., & Botzet, M. 1998. Very-high-resolution regional climate simulations over Scandinavia: present climate. J. Climate 11: 3204–3229.

Christensen, J. H. & Kuhry, P. 2000. High resolution regional climate model validation and permafrost simulation for the East-European Russian Arctic. J. Geophys. Res. 105: 29647–29658.

Dethloff, K., Rinke, A., Lehmann, R., Christensen, J. H., Botzet, M. & Machenhauer, B. 1996. Regional climate model of the arctic atmosphere. J. Geophys. Res. 101: 23401–23422.

IPCC 2001. Climate change 2001: Impact, adaptation, and vulnerability, Contribution of working group 1 to the third assessment report of the Intergovernmental Panel of Climate Change. In: McCarthy, J. J., Canziani, O.F., Lary, N.A., Dokken, D.J. & White, K. S. (eds.). Cambridge University Press, 1032 pp.

Hegseth, E. 1999. Primary production of the northern Barents Sea. Polar Res. 17: 113-123.

Kiilsholm, S., Christensen, J. H., Dethloff, K. & Rinke, A. 2003. Net accumulation of the Greenland Ice Sheet; Modelling arctic regional climate change. Geophys. Res. Lett. 30: 1485, doi:10.1029/2002GL015742.

Kiørboe, T. & Nielsen, T. G. 1984. Regolation of zooplankton biomass and production in a temperate, coastal ecosystem. 1. Copepods. Limnol. Oceanogr. 39: 493-507.

Kunnerup, O. F. 2001. Food growth and migration of an anadromous stock of arctic charr (Salvelinus alpinus L.) in a NE-Greenland fjord. Master thesis. University of Aarhus, Denmark, 50 pp.

Levinsen, H. & Nielsen, T. G. 2002. The trophic role of marine pelagic ciliates and heterotrophic dinoflagellates in arctic and temperate coastal ecosystems: A cross-latitude comparison. Limnol. Oceanogr. 47: 427-439.

Levinsen, H., Nielsen, T. G. & Hansen, B. W. 2000. Annual succession of marine pelagic protozoans in Disko Bay, West Greenland, with emphasis on winter dynamics. Mar. Ecol. Prog. Ser. 206: 119-134.

Levitus, S., Antonov, J. I., Boyer, T. P. & Stephens, C. 2000. Warming of the world ocean. Science 287: 2225–2229.

Madsen, S. D., Nielsen, T. G. & Hansen, B. W. 2001. Annual population development and production by *Calanus finmarchicus*, *C. glacialis* and *C. hyperboreus* in Disko Bay, western Greenland. Mar. Biol. 139: 75-93.

Middelboe, M. (2007): Microbial disease in the sea: Effects of viruses on marine carbon and nutrient cycling". In Eviner, V. et al. (eds.). Ecology of infectious diseases: Interactions between disease and ecosystem. Princeton University Press.

Nielsen, T. G. 2005 Struktur og funktion af fødenettet i havets frie vandmasser. Doktor disputas. Danmarks Miljøundersøgelser, Denmark, 71 pp. (in Danish).

Parkinson, C. L. 1992. Spatial patterns of increases and decreases in the length of the sea ice season in the North Pole Region, 1979–1986. J. Geophys. Res. 97: 14377–14388.

Parkinson, C. L. 2000. Variability of arctic sea ice: The view from space, an 18-year record. Arctic 53: 341-348.

Rivkin, R. B. & Legendre, L. 2000. Biogenic carbon cycling in the upper ocean: Effects of microbial respiration. Science 291: 2398-2400.

Rysgaard, S., Nielsen, T.G. & Hansen, B. 1999. Seasonal variation in nutrients, pelagic primary production and grazing in a High Arctic coastal marine ecosystem, Young Sound, northeast Greenland. Mar. Ecol. Prog. Ser. 179: 13-25.

Rysgaard, S., Thamdrup, B., Risgaard-Petersen N,, Berg, P., Fossing, H., Christensen, P. B. & Dalsgaard, T. 1998. Seasonal carbon and nitrogen mineralization in the sediment of Young Sound, Northeast Greenland. Mar. Ecol. Prog. Ser. 175: 261-276.

Rysgaard, S., Vang, T., Stjernholm, M., Rasmussen, B., Windelin, A.& Kiilsholm, S. 2003. Physical conditions, carbon transport and climate change impacts in a NE Greenland fjord. Arct. Antarct. Alp. Res. 35: 301-312.

Sambrotto, R. N., Goering, J. J. & McRoy, C. P. 1984. Large yearly production of phytoplankton in the Western Bering Strait. Science 325: 1147-1150.

Sejr, M. K., Petersen, J. K., Jensen, K. T. & Rysgaard, S. 2004. Effect of food concentration on clearance rate and energy budget of the Arctic bivalve *Hiatella arctica* (L) at sub-zero temperature. J. Exp. Mar. Biol. Ecol. 311: 171-183.

Serreze, M. C., Walsh, J. E., Chapin, F. S., III, Osterkamp, T., Dyurgerov, M., Romanovsky, V., Oechiel, W. C., Morison, J., Xhang, T. & Barry, R. G. 2000. Observational evidence of recent changes in the northern high-latitude environment. Clim. Change, 46: 159–207.

Smidt, E. 1979. Annual cycles of primary production and of zooplankton at Southwest Greenland. Meddr. Grønland, Bioscience 1: 3-53.

Springer, A. M., McRoy, P. & Flint, M.V. 1996. The Bering Sea green belt: shelf-edge processes and ecosystem production. Fish. Oceanogr. 5: 205-223.

Tremblay, J-E., Michel, C., Hobson, K. A., Gosselin, M. & Price, N. M. 2006. Bloom dynamics in early opening waters of the Arctic Ocean. Limnol. Oceanogr. 51: 900-912.

Wilhelm, S. W. & Suttle, C. R. 1999. Viruses and nutrient cycles in the sea. Bioscience 49: 781-788.

MONOGRAPHS ON GREENLAND

This volume synthesizes the marine research conducted in Young Sound, a High Arctic fjord in Northeast Greenland, since 1994. Several physical, chemical and biological aspects of this ecosystem are presented in individual chapters and used to construct a present-day carbon budget for the area. Finally, predictions are made of future changes to the ecosystem due to climate warming.

Søren Rysgaard is professor at the Greenland Institute of Natural Resources, Nuuk, Greenland. Ronnie N. Glud is associate professor at the Marine Biological Laboratory, University of Copenhagen, Denmark

PUBLISHED BY THE COMMISSION FOR SCIENTIFIC RESEARCH IN GREENLAND